Cysteine Proteases as Therapeutic Targets for Neurodegenerative Diseases

BY

RACHEL KNOPP

B.A. Chemistry, Willamette University, Salem, OR, 2014

THESIS

Submitted in partial fulfillment of the requirements
for the degree of Doctor of Philosophy in Medicinal Chemistry
in the Graduate College of the University of Illinois at Chicago, 2020

Chicago, Illinois

Defense Committee:

Gregory R.J. Thatcher, Ph.D., Chair and Advisor
Leon Tai, Ph.D., T32 Co-Advisor, Anatomy and Cell Biology
Sarah Lutz, Ph.D., Anatomy and Cell Biology
Kiira Ratia, Ph.D.
Alessandra Eustaquio Ph.D.
Terry Moore, Ph.D.

ACKNOWLEDGMENTS

I am extremely grateful for all the support and mentorship I received in my graduate studies. I have received an incredible amount of guidance and encouragement from faculty, staff, and students at the University and have grown tremendously as a researcher over the past five years.

I would first like to thank my advisor Dr. Gregory R. J. Thatcher. I am so grateful for his guidance and support. Dr. Thatcher's overwhelming enthusiasm for science is infectious and inspired me to stay motivated. He helped me grow into the independent, opinionated and diligent researcher I am today and for that I'll always be thankful.

I would also like to thank the T32 director, Dr. Orly Lazarov for supporting me on the ADRD training grant as well as my T32 co-advisor Dr. Leon Tai, for the opportunity to collaborate with his group. As a recipient of this fellowship, I was able to not only expand my skillset, but develop collaborations that brought together drug discovery and basic science that expanded my project and led to the third chapter of this thesis.

Thank you to my committee members Dr. Sarah Lutz, Dr. Kiira Ratia, Dr. Alessandra Eustaquio and Dr. Terry Moore, as well as Dr. Steven DiMagno from my preliminary exam committee. I am so thankful for all of your support, feedback and advice.

I would also like to thank my lab mates for all of their encouragement, guidance and friendship. Many of them contributed to the work represented here: Dr. Sue Lee for her extensive work on the *ALDH2*$^{-/-}$ mice and the mTBI mouse model; Dr. Ammar Jastaniah, Dr. Irina Gaisina and Dr. Bharghava Karumudi for synthesizing all calpain and cathepsin inhibitors; Dr. Emily Pierce for guidance and training me on the enzyme assays; Dr. Oleksii Dubrovskyii for animal handling; Ragda Izar who assisted in Western blot experiments.

ACKNOWLEDGMENTS (continued)

I would also like to thank all of my friends for their support. From coffee buddies, trivia teams, Loomis ladies, gym squad, conference crews, fellow miktators, and more, I was extremely lucky to have made such great friends at UIC. Finally, I would like to thank my family for their unwavering love, particularly my father for providing constant patience and reassurance.

RCK

DECLARATION OF ORIGINALITY

I certify that, to the best of my knowledge, this document does not infringe upon nor violate any copyrighted or proprietary materials. The ideas, techniques, and other materials included in this dissertation, published or otherwise, are fully acknowledged in accordance with standard referencing practices. Efforts of colleagues and collaborators are clearly defined within the acknowledgements section and clarified below.

Chapter 1 represents my own, unpublished work. Dr. Bhargava Karumudi, Dr. Ammar Jastinah and Dr. Irina Gaisina synthesized and purified all inhibitors that were not purchased commercially.

Chapter 2 is partially adapted from a published manuscript (**Knopp, RC** *et al,*. Redox Biology 2020) of which Rachel C. Knopp is a primary author. My co-authors contributed to this work in the following ways: Sue Lee performed all *in vitro* scavenger studies with HNE, developed the mTBI model and analyzed the neuroinflammatory response following neurotrauma. Mike Hollas analyzed the proteomics. Emily Neomuceno and David Gonzalez assisted in all animal studies. David Aamir and Kevin Tam performed immunocytochemistry studies. Yueting Wang performed the proteomics. Emily Pierce performed and analyzed immunoblots. Manel Ben Aissa assisted in manuscript preparation. Greg Thatcher was the mentor for the project and contributed to writing the manuscript. Only data that I directly contributed to or are my own studies was included in this chapter.

Chapter 3 is adapted from a manuscript currently in preparation and represents my own work.

TABLE OF CONTENTS

CHAPTER 1: SMALL MOLECULE INHIBITORS OF CALPAIN-1 AND CATHEPSIN B.....1

1.1 INTRODUCTION 2
1.1.1 Aging and Neurodegeneration 2
1.1.2 Age-Related Dementia: Spotlight on Alzheimer's Disease 3
1.1.3 Alzheimer's Disease and Related Dementia (ADRD) are Multifaceted, Non-linear Diseases 6
1.1.4 AD Drug Discovery Failures: Are we Focusing on the Wrong Thing? 9
1.1.5 Calpain-1 as a Therapeutic Target 11
1.1.6 Calpain-Cathepsin Hypothesis 18
1.1.7 Cathepsin B as a Therapeutic Target 21
1.1.8 Efficacy of Calpain-1 and Cathepsin B Inhibitors in Neurodegeneration 22
1.1.9 Clinical Efficacy of Proteases 23
1.1.10 Objectives 26

1.2 METHODS 27
1.2.1 Enzyme Assays 27
1.2.2 Cell Culture 28
1.2.3 Immunoblots 29
1.2.4 Oxygen Glucose Deprivation 29

1.3 RESULTS AND DISCUSSION 30
1.3.1 Development of Enzyme Screens 30
1.3.2 Identification of Calpain-1 Inhibitors 35
1.3.3 Evaluating Insults that Induce Calpain-1 Activity In Vitro 43
1.3.4 Specific Inhibitory Efficacy of Inhibitors 51
1.3.5 Serendipitous Discovery of Cathepsin K Inhibitors 53

1.4 CONCLUSIONS 55

CHAPTER 2 *:* EARLY CONTRIBUTORS TO ADRD: *IN VITRO* AND *IN VIVO* MODELS OF OXIDATIVE STRESS AND MTBI 59

2.1 INTRODUCTION 60
2.1.1 The Complexity of ADRD 60
2.1.2 Brain Ischemia 62
2.1.3 Oxidative Stress 63
2.1.4 Traumatic Brain Injury 66
2.1.5 Objectives 70

2.2 METHODS 71
2.2.1 Cell Culture 71
2.2.2 Oxygen-Glucose Deprivation and Reperfusion 72
2.2.3 Cellular Immunofluorescence 72
2.2.4 Real Time qPCR 72
2.2.5 Animals 73
2.2.6 Step Through Passive Avoidance 74
2.2.7 Closed Head mTBI 74
2.2.8 Tissue Preparation 74

2.3 RESULTS AND DISCUSSION 75
2.3.1 OGD-R as an in Vitro Model for Ischemia-Reperfusion Injury 75
2.3.2 Calpain-Cathepsin Inhibitors are Protective against Oxygen Glucose Deprivation 81
2.3.3 Calpain-Cathepsin Inhibitors Attenuate Scopolamine-Induced Cognitive Deficits 84
2.3.4 Inhibition Strategies Mitigate In Vitro TNF-a and LPS-Induced Neuroinflammation 87

TABLE OF CONTENTS (Continued)

2.3.5 Oxidative Stress via Lipid Peroxidation Products Induces Neuronal Cell Death 89
2.3.6 Development of a Novel Murine mTBI model with Underlying Oxidative Stress 95

2.4 CONCLUSION 102

CHAPTER 3: ATTENUATION OF BBB-DYSFUNCTION BY CALPAIN AND CATHEPSIN B INHIBITION STRATEGIES 104

3.1 INTRODUCTION 105
3.1.1 Poor Bioavailability of Calpain Inhibitors: Effect on BBB? 105
3.1.2 The Blood Brain Barrier 105
3.1.3 Age-associated Changes to the Blood-Brain Barrier 110
3.1.4 Cerebrovascular Contributions to Cognitive Impairment 112
3.1.5 Calpain-1 overactivation and BBB-Dysfunction: A Therapeutic Opportunity 115
3.1.6 Objectives 120

3.2 METHODS 121
3.2.1 Primary Culture 121
3.2.2 Immunofluorescence 121
3.2.3 Immunoblots 122
3.2.4 Closed-head mild Traumatic Brain Injury 123
3.2.5 Tissue Harvesting 123
3.2.6 Protein Extraction for Western Blot 123
3.2.7 Sodium Fluorescein Extravasation 123
3.2.8 RNA isolation 125
3.2.9 Reverse Transcription 126
3.2.10 Quantitative PCR 126

3.3 RESULTS AND DISCUSSION 127
3.3.1. Inhibition strategies preserve BEC integrity post-OGD-R 127
3.3.2. Reduced Resilience in ALDH2$^{-/-}$ is Reversed by CCH Inhibitors 134
3.3.3. Exacerbated Damage in ApoE4 vs. ApoE3 female BECs 139
3.3.4 ALDH2$^{-/-}$ mice with mTBI exhibit BBB-Dysfunction 141
3.3.5 Calpain-Cathepsin Inhibition Attenuates BBB-Dysfunction 147

3.4 CONCLUSION 153

4. CONCLUSIONS 155

CITED LITERATURE 161

APPENDICES 192

VITA 210

LIST OF TABLES

TABLE I. TYPES OF DEMENTIA MODIFIED FROM THE ALZHEIMER'S ASSOCIATION 2020 FACTS AND FIGURES REPORT 5

TABLE II. CALPAIN SUBSTRATES INVOLVED IN SYNAPTIC PLASTICITY AND/OR NEURODEGENERATION 17

TABLE III. FDA-APPROVED PROTEASE INHIBITORS 25

TABLE IV. SELECTIVITY PROFILES OF COMPOUNDS 1-5 40

TABLE V. SELECTIVITY PROFILES OF COMPOUNDS SELECTED TO MOVE FORWARD TO *IN VITRO* AND *IN VIVO* STUDIES 57

TABLE VI. *IN VIVO* TBI METHODS AND THEIR ASSOCIATED LEVELS OF SEVERITY 69

TABLE VII. PRIMERS UTILIZED FOR INFLAMMATION STUDIES 73

TABLE VIII. PRIMERS UTILIZED IN RT-QPCR STUDIES 127

LIST OF FIGURES

Figure 1. Variation in cognitive decline accounted for by pathological indices from the ROS and RAMP studies 8

Figure 2. Pathologic states associated with calpain-1 hypo- or hyper-activation. 15

Figure 3 Calpain-cathepsin hypothesis 20

Figure 4. Flow of enzymatic assay. 31

Figure 5. Optimization of the cathepsin K assay 32

Figure 6. Characterization of the cathepsin B enzyme assay 33

Figure 7. Benchmarking known compounds. 35

Figure 8. Enzymatic profiles of calpain-1 inhibitors 37

Figure 9. Dose-response IC_{50} curves for compounds 1-5 38

Figure 10. schematic representation of the reversibility assay 41

Figure 11. Inhibitors *1-5* are reversible against calpain-1 42

Figure 12. Compounds *1-5* are reversible against cathepsin K 43

Figure 13. Spectrin breakdown products as biomarkers of calpain-1 activity 44

Figure 14. Optimization of neuroinsults on SH-SY5Y cells to induce SBDPs 46

Figure 15. Pretreatment of 10μM *5* reduces of SBDP 150/145kDa in SH-SY5Y cells 48

Figure 16. Development of an *in Vitro* insult to monitor spectrin breakdown products. 50

Figure 17. Specific inhibitory efficacy of compounds *in vitro* 52

Figure 18. Chemical structures of cathepsin K inhibitors. 54

Figure 19. Enzyme profiles of cathepsin K inhibitors 54

Figure 20. IC_{50} Values of cathepsin K inhibitors 55

Figure 21. CCH inhibition strategies 56

Figure 22. ADRD as a multifactorial disease 61

Figure 23. Downstream effects of oxidative stress 64

LIST OF FIGURES (Continued)

Figure 24. TBI mechanisms: primary injury and secondary cascade 67

Figure 25. Schematic of the OGD-R assay 75

Figure 26. Dynamic changes in cell viability following varying lengths of OGD and reperfusion on SH-SY5Y cells 76

Figure 27. Sulforaphane as a positive and negative control in the OGD-R assay 78

Figure 28. Cell confluency following sulforaphane treatment 79

Figure 29 Sulforaphane as a positive and negative control after OGD-R on HT22 cells 81

Figure 30. Neuroprotective profiles of inhibition strategies in SH-SY5Y cells. 82

Figure 31. Neuroprotective properties of inhibition strategies in primary human neurons 84

Figure 32 CCH inhibitors attenuate scopolamine-induced cognitive deficits in the STPA fear-conditioning experiment 86

Figure 33. Calpain-cathepsin inhibitors attenuated LPS-stimulated TNFa and NOS2 levels in astrocyte-like CCF-STTG1 cells 88

Figure 34. Inhibition strategies attenuated TNFa-stimulated IL-1β levels in CCF-STTG1 cells 89

Figure 35. Lipid peroxidation products, HNE and ONE, induce time-dependent and concentration-dependent cell death of SH-SY5Y cells 91

Figure 36. ONE has greater neurotoxicity than HNE 92

Figure 37. LPP scavengers reduce neurotoxicity of HNE and ONE *in vitro* 93

Figure 38. HNE exacerbates OGD-R induced cell death in SH-SY5Y cells 94

Figure 39. The mTBI apparatus utilized in our studies 96

Figure 40. Underlying oxidative stress with mTBI induces a significant cytokine surge 24 hours post-injury 97

Figure 41. CCH inhibitors attenuate neuroinflammation in the *ALDH2*$^{-/-}$ mTBI model 98

Figure 42. Inhibitors *5* and *NYC-438* reduced levels of GFAP and GFAP-BDP mediated by mTBI 99

Figure 43. Selective and nonselective calpain-1 inhibitors diminish SBDP145 levels in *ALDH2*$^{-/-}$ mice with mTBI 101

Figure 44. Schematic of the architecture of the BBB. 106

LIST OF FIGURES (Continued)

Figure 45. Representative cartoon of the architecture of tight junctions between BECs 108

Figure 46. BBB transport systems 109

Figure 47. Mechanisms of neurodegeneration from BBB-dysfunction..... 113

Figure 48. WT BECs are susceptible to OGD-R insult. 128

Figure 49. Inhibition strategies ameliorate BECs susceptibility to oxidative stress. 130

Figure 50. WT BECs isolated separately from male and female mice exhibit no significant differences. 131

Figure 51. Inhibition strategies mitigate loss of tight junction proteins. 133

Figure 52. Morphological changes between WT and *ALDH2*$^{-/-}$ BECs 1 hour post-OGD-R..... 135

Figure 53. Reduced resilience in *ALDH2*$^{-/-}$ BECs is reversed by CCH inhibitors..... 136

Figure 54. CCH inhibitors reduce SBDP 150kDa and 145kDa in *ALDH2*$^{-/-}$ BECs. 137

Figure 55. *ALDH2*$^{-/-}$ BECs isolated from male and female mice are equally susceptible to OGD-R injury 139

Figure 56. Exacerbated susceptibility of BECs isolated from APOE4-Tg mice v. APOE3-Tg. 141

Figure 57. Sodium fluorescein is a highly fluorescent tracer 142

Figure 58. Elevated sodium fluorescein extravasation in the right hemisphere of ALDH2$^{-/-}$ mice 24 hours post-mTBI. 143

Figure 59 Underlying oxidative stress exacerbates the loss of BBB-associated proteins post-mTBI. 146

Figure 60. CCH inhibitors attenuate loss of BBB-associated proteins 24 Hours post-mTBI in *ALDH2*$^{-/-}$ mice 148

Figure 61. TJs are substrates of cysteine proteases..... 150

Figure 62. Treatment of NYC-438, not 5, attenuates decreased expression of TJs in *ALDH2*$^{-/-}$ mice with mTBI. 152

Figure 63. Schematic of the drug discovery process 157

Figure 64. Efficacy of calpain-1 inhibitors in *in vitro* and *in vivo* models 158

Figure 65. Neuroprotective profiles of all inhibitors 192

LIST OF FIGURES (Continued)

Figure 66. Optimization of the TBARS assay. 193

Figure 67. HNE and ONE induce concentration-dependent increase in LDH release in BECs. 194

Figure 68. Examining BID (BH3 interacting-domain death agonist) on BECs following OGD-R 195

Figure 69. Changes in UCHL1 following 1 or 2 mTBIs 196

Figure 70. Levels of Aldh2 following one or two mTBIs 197

Figure 71. Gene expression of ALDH2 24 hours following one or two mTBIs 198

Figure 72. *5* and *NYC-438* minimally attenuate mRNA expression of iNOS in *ALDH2*$^{-/-}$ mice following mTBI. 199

Figure 73. CCH inhibitors do not induce HepG2 spheroidal death 200

Figure 74. Cathepsin B inhibitors attenuate LAMP2 levels 201

LIST OF SCHEMES

Scheme 1. Mechanism of Cysteine Proteases 12

LIST OF ABBREVIATIONS

AD ..... Alzheimer's disease
ADRD ..... Alzheimer's disease and related dementias
Aldh2 ..... aldehyde dehydrogenase 2
AMC amino-4-methylcoumarin
APOE ..... apolipoprotein E
APP ..... amyloid precursor protein
BBB ..... blood-brain barrier
BCA ..... bicinchoninic acid
BDP ..... breakdown products
BEC ..... brain endothelial cell
BSA ..... bovine serum albumin
CAA ..... cerebral amyloid angiopathy
CAPN ..... calpain
CCH ..... calpain-cathepsin hypothesis
CCI ..... controlled cortical impact
cDNA ..... complementary DNA
cGMP ..... cyclic guanosine momophosphate
CNS ..... central nervous system
CREB ..... cyclic adenosine monophosphate response element binding protein
CSF ..... cerebral spinal fluid
CTSB ..... cathepsin B
CVD ..... cerebrovascular disease
DI ..... discrimination index
DMEM ..... Dulbecco's Modified Eagle Medium
DMSO ..... dimethyl sulfoxide
DNA ..... deoxyribonucleic acid
DTT ..... dithioerythritol
EC ..... endothelial cell
EDTA ..... ethylenediaminetetraacetic acid
eNOS ..... endothelial nitric oxide synthase (NOS3)

fAD .....familial Alzheimer's disease
FBS .....fetal bovine serum
FDA.....US Food and Drug Administration
GAPDH.....Glyceraldehyde 3-phosphate dehydrogenase
GFAP ..... glial fibrillary acidic protein
GSH..... glutathione
GWAS..... genome-wide association study
HEPES ..... 4-(2-hydroxyethyl)-1-piperazineethanesulfonic acid
HH.....histidinyl hydrazide
Hsp70 ..... Heat shock protein 70
HNE 4-hydroxy-2-nonenal
IL-1β interleukin-1β
IL-6 ..... interleukin
IP ..... intraperitoneal
IS ..... ischemic stroke
KO.....knockout
LBD.....lewy body dementia
LDH .....lactate dehydrogenase
LPP..... lipid peroxidation products
LPS..... lipopolysaccharide
LTP ..... Long-term potentiation
MAP-2.....microtubule-associated protein 2
MCAO.....middle cerebral artery occlusion
MCI .....mild cognitive impairment
MDA ..... Malondialdehyde
MES .....morpholine ethanesulfonic acid
MMP-9.....matrix metalloprotease 9
MRI .....magnetic resonance imaging
mTBI ..... mild traumatic brain injury
MTT .....2,5-diphenyl tetrazolium bromide
NAC .....N-acetylcysteine
ND..... neurodegenerative disease

NFT ..... Neurofibrillary tangles
NMDAR ..... N-methyl D-aspartate receptors
NO ..... nitric oxide
Nrf2 ..... nuclear factor (erthroid-derived 2)-like 2
OGD-R ..... oxygen-glucose deprivation and reperfusion
ONE 2-oxo-nonenal
OS ..... oxidative stress
PBS ..... phosphate buffer saline
PCR ..... Polymerase chain reaction
pCREB ..... phosphorylated cAMP response element binding protein
PET ..... positron emission tomography
PK ..... pharmacokinetics
PUFA ..... polyunsaturated fatty acids
PVDF ..... polyvinylidene fluoride
PSEN1, PSEN2 ..... Presenilin-1 and 2
qRT-PCR ..... quantitative Real Time PCR
ROS ..... reactive oxygen species
ROS-RMAP ..... Religious Orders Study and Rush Memory and Aging Project
RNA ..... ribonucleic acid
sAD ..... sporadic AD
SBDP ..... spectrin breakdown products
SCA ..... spinocerebellar ataxia
SEM ..... standard error of the mean
SD ..... standard deviation
SDS-PAGE ..... sodium dodecyl sulfate – polyacrylamide gel electrophoresis
sGC ..... soluble guanylyl cyclase
STPA ..... step through passive avoidance
TBI ..... Traumatic brain injury
TCEP ..... tris (carbethoxy)phosphine
TEAE ..... Treatment emergent adverse events
TEER ..... Transendothelial electrical resistance
Tg ..... Transgenic

TNFa .....tumor necrosis factor alpha

TJ..... Tight Junction

VEGF .....vascular endothelial growth factor

WHO .....World Health Organization

WT ..... wildtype

SUMMARY

Alzheimer's disease and related dementia (ADRD) is a major global health issue that is steadily rising with the aging population. While it is officially listed as the 5th leading cause of death in the United States, it can cause even more deaths than reported, and patients live through years of increased morbidity with disease progression.[1] Unfortunately, the current landscape of ADRD therapeutics is plagued with clinical failures in lieu of a therapeutic strategy that stops, reverses or prevents disease progression. Many small molecule targeting strategies with pre-clinical efficacy have been discontinued before essential proof-of-concept clinical trials, with preference towards antibodies targeting pathological hallmarks. The work herein aimed to reconsider the calpain-cathepsin hypothesis (CCH) for ADRD therapeutics and characterize its involvement in BBB-dysfunction.

Calpain-1 and cathepsin B are bona fide unexploited targets for neuroprotection. These cysteine proteases are found hyperactivated early in the pathogenesis of AD and are incriminated in a neurodegenerative mechanism (the CCH).[2] This mechanism posits that calpain-1 hyperactivation permeabilizes lysosomes leading to the release of cathepsin B, which then degrades cytoplasmic substrates leading to neuronal death.[3] The CCH has been proposed as an underlying contributor not only to AD, but also to traumatic brain injury (TBI), and ischemic stroke (IS). [4, 5] Inhibitors have displayed significant efficacy in numerous *in vitro* and *in vivo* neurodegenerative models;[6-10] however, literature ambiguously utilizes calpain-1 inhibitors that are often-times nonselective.

The focus of chapter 1 was to develop a toolkit of small molecule inhibitors, with the goal of characterizing their efficacy in in vitro and in vivo models and determining a superior targeting strategy. Enzyme assays allowed us to characterize selectivity profiles, reversibility and potency of numerous peptidomimetic small molecules. We identified a family of alpha-ketoamides

with high potency and selectivity towards calpain-1. *In vitro* specific inhibitory efficacy was confirmed by evaluating the breakdown products of spectrin, a clinical biomarker for calpain-1 activity.

The focus of chapter 2 was to differentiate the efficacy of various inhibition strategies in various in vitro and in vivo models, some of which incorporated the loss of neural resilience. Neuroprotective profiles were established, with all inhibitors exhibiting significant efficacy at various treatment paradigms. Furthermore, we saw that calpain-1 inhibitors were able to attenuate neuroinflammation *in vitro* and restore cognitive deficits in an *in vivo* mouse model.

NYC-438 is an irreversible dual inhibitor of calpain-1 and cathepsin B that was synthesized as an analog of ***E-64c***, a well-known pan-cysteine protease inhibitor. ***NYC-438*** was able to restore cognitive deficits in an AD mouse model; however, these effects were independent of underlying pathophysiological hallmarks of AD. This suggested that CCH inhibition strategies may work in mechanisms of neural resilience.

Studies were expanded to incorporate oxidative stress (OS)-based preclinical models of enhanced neural resilience. Lipid peroxidation products (LPPs) caused *in vitro* dose-dependent neuronal cell death. Furthermore, adding a second stressor, or "hit" exacerbated cell death.

Previous studies in the Thatcher lab found that *ALDH2*$^{-/-}$ mice have enhanced susceptibility to mild TBI (mTBI), evidenced primarily by a sharp neuroinflammatory cytokine surge just 24 hours post-neurotrauma. Intriguingly, increased spectrin breakdown products was also observed suggesting the hyperactivation of calpain-1. We found that a single injection of calpain-1 inhibitors administered in a post-treatment paradigm were able to mitigate the inflammatory cytokine surge. Moreover, we saw a reduction in spectrin breakdown products confirming the effects were specifically due to calpain-1 inhibition.

The focus of chapter 3 was to characterize the effects of calpain/cathepsin inhibitors on blood-brain barrier (BBB)-dysfunction and in particular, brain endothelial cell (BEC)-dysfunction. This was driven by the results of Alicapistat, the first and only selective calpain-1 inhibitor to complete Phase 1 clinical trials targeted at ADRD.[11] Alicapistat was without dose-limiting toxicities. However, while there was sufficient plasma bioavailability, the highest dose administered achieved maximal concentrations of < 20nM in the CSF. This is significantly less than the IC_{50} (56 nM for the active diastereomer). ***NYC-438*** also has poor brain bioavailability which suggested that efficacy is imbued by interactions within the neurovascular unit and, more specifically, BECs.

Primary BECs isolated from wild-type (WT) mice were susceptible to OS-based insults. Furthermore, BECs isolated from *ALDH2*$^{-/-}$ mice exhibited enhanced vulnerability to cell death and loss of tight junction proteins compared to WT BECs. These effects were mitigated by selective and nonselective calpain-1 inhibitors, but not cathepsin B inhibitors. Furthermore, we discovered that the "2-hit" mouse model of *ALDH2*$^{-/-}$ + mTBI exhibits significant BBB-dysfunction, which was mitigated by a single treatment of calpain-1 inhibitors. This work establishes calpain inhibition as a potential prophylactic therapeutic strategy to protect the neurovascular unit.

CHAPTER 1: SMALL MOLECULE INHIBITORS OF CALPAIN-1 AND CATHEPSIN B

1.1 INTRODUCTION

1.1.1 Aging and Neurodegeneration

The connection between aging and neurodegeneration has been reported in the scientific realm as early as 1981, when sociocultural contributions were found to impact the prevalence of Alzheimer's Disease and related dementias (ADRD).[12] Aging is a normal physiological process of becoming older, and represents the culmination of all physiological changes during one's lifetime. It is also associated with a progressive increase in susceptibility to disease and death, and, thus, is the greatest known risk factor for a majority of human diseases.[13] However, as life expectancy increases, so does the societal burden of age-related diseases. The world health organization (WHO) reported global life expectancy improved from 2000 to 2016 by 5.5 years, the largest increase since 1960s. Concurrently, they reported a substantial increase in the incidence and mortality rates of age-related diseases worldwide.

The meaning of the word "neurodegeneration" is assumed to be universally understood, but in practice is much more complex. Generally speaking, neurodegeneration is the age-progressive atrophy and deterioration of neurons that leads to cognitive decline. Thus, it accounts for any pathological condition where the nervous system loses structural or functional integrity. However, clinically the term is much more refined; it represents a wide range of diseases where a particular subtype of neurons are affected. Neurodegenerative diseases (NDs) include Alzheimer's Disease (AD), Huntington Disease, amyotrophic lateral sclerosis, Parkinson's Disease, motor neuron disease, and multiple sclerosis. These diseases are heterogeneous and often hereditary in nature, with clinical presentations of difficulty in movement (ataxias) and/or deterioration of mental functioning (dementia).[14] It is estimated that 25% of global death and disability are caused by NDs.[15] Moreover, they account for over 34% of the universal burden of diseases.[16]

However, while there are a wide range of NDs, there exist common pathogenic and mechanistic features that are prevalent in all.[17] These include abnormal accumulation and/or misfolding of proteins serving as the pathological hallmark,[18] affected neurons exhibiting altered patterns of phosphorylation,[17] early loss of synaptic function[19] and neuronal cell death as a late. secondary event[20]. Moreover, in NDs, symptoms may slowly progress for years after the initial appearance of symptoms.[21] NDs encompass a wide range of disorders, including age-related dementias, which was the focus of this research.

1.1.2 Age-Related Dementia: Spotlight on Alzheimer's Disease

Age-related dementia is an umbrella term that describes a particular group of brain diseases with similar clinical symptoms. These symptoms include difficulty in communication, problem-solving, memory, and other cognitive skills that impact an individual's ability to perform everyday tasks.[22] This class of diseases has been reported on for centuries; one of the earliest known incidence was in the 7th century when the Greek philosopher Pythagoras referenced the last 2 (of 6) phases of lifespan incorporated severe mental and physical decay.[23]

While age-related dementia is strongly associated with age, it is not a normal part of the aging process. Normal, "healthy" age-related decline mostly affects attention control and cognitive processing.[24] These changes are subtle, and are primarily associated with quick-recall and measures of speed processing.[25] Abnormal aging leading to age-related dementia encompasses accelerated neuronal dysfunction, neuronal loss and cognitive decline to the extent that common, everyday functional abilities are impaired.

There are varying types of dementia, with the most prevalent being AD (TABLE I). Currently, reports estimate 5.8 million Americans aged 65 years and older are living with AD.[26] To put that in perspective, out of the total population, one in 10 Americans aged 65 years or older have AD. This number is expected to reach or exceed 13.8 million by 2050.[27] This places a

substantial burden on not just the healthcare system, but family and friends alike. It is estimated that the healthcare system will spend $305 billion in 2020, while family and friends provide $244 billion in unpaid care for dementia.[27]

TABLE I. TYPES OF DEMENTIA MODIFIED FROM THE ALZHEIMER'S ASSOCIATION 2020 FACTS AND FIGURES REPORT

Age Related Dementia	Prevalence of dementia cases	Distinguishing Pathology	Clinical Presentation
Alzheimer's Disease (AD)	60 - 80%	Accumulation of amyloid-beta (Aβ) outside neurons and tau tangles inside neurons, death of neurons and damage to brain tissue	Early: difficulty remembering conversations. Late: impaired communication, poor judgement
Cerebrovascular Disease (CVD)	5 - 10%	damaged blood vessels in brain and/or brain tissue injured from lack of blood, oxygen or nutrients.	Impaired judgement or ability to make decisions, poor motor function
Lewy Body Disease (LBD)	5%	abnormal aggregations of alpha-synuclein in neurons.	Early: sleep disturbances. Common symptoms to Alzheimer's
Fronto-temporal lobar degeneration (FTLD)	3%	Death of nerve cells and atrophy in frontal and temporal lobes, upper layers of cortex become soft and spongy, typically have abnormal protein inclusions (tau or TDP-43)	changes in personality, difficulty with producing/comprehending language
Parkinson's Disease (PD)	Unclear.	alpha-synuclein aggregates in the substantia niagra	Problems with movement
Hippocampal sclerosis (HS)	Unclear. In the "oldest-old" individuals 85 years or older	hardening of tissue in hippocampus, often times accumulation of TDP-43	Memory loss
Mixed Pathologies	50%	overlapping pathological features	Overlapping Clinical Presentations

The two traditional pathological hallmarks of AD are senile plaques and neurofibrillary tangles (NFTs). These were first identified and published by the German psychiatrist Alois Alzheimer in 1909 upon postmortem analysis of his 55-year old patient Auguste Deter.[28] In this report, Dr. Alzheimer observed abnormal senile plaques and clumps of tangles localized in the cerebral cortex. Decades later, researchers identified the abnormal senile plaques containing a "cerebrovascular amyloid protein" that we know classify as amyloid beta (Aβ).[29] These peptides are created when amyloid precursor protein (APP) is cleaved by β-secretase and γ-secretase, with the most abundant plaques formed with $A\beta_{1-40}$ and $A\beta_{1-42}$. These plaques are dense, mostly insoluble and found localized around neurons. NFTs, on the other hand, are found accumulated inside the neurons themselves. Further research identified the NFTs as containing the tau protein that had been hyperphosphorylated.[30] While both senile plaques and NFTs are present in normal aging, they are dramatically increased in AD patients brains, particularly in brain regions associated with cognition and memory. [31]

1.1.3 Alzheimer's Disease and Related Dementia (ADRD) are Multifaceted, Non-linear Diseases

Multiple clinical-pathological studies have exposed the varying susceptibilities between individuals in response to cognitive decline, which has led to the emerging ideas of brain and cognitive resilience.[32-36] One study in particular included 10 cognitively-healthy elderly women who, upon autopsy, were found to have Alzheimer's pathology.[34] It was proposed that their extra reserve, by way of larger brains sizes and higher neuronal content, protected them from developing the cognitive decline associated with Alzheimer's pathology. This "reserve" acts as an intermediary between underlying disease pathology and clinical outcome, and was further classified into two categories: brain reserve and cognitive reserve.

Brain reserve is a quantifiable measurement typically referring to brain size, neuronal count, or synapses,[37] and is supported by studies that found a correlation between larger brain sizes

and decreased incidence of dementia.[34, 38] However, cognitive reserve is un-quantifiable and refers to compensatory mechanisms, and the efficiency of brain reserve.[37] More specifically, brain function rather than brain size is the independent variable. Multiple effects (physical, developmental, environmental, etc.) can impact one's cognitive reserve and heighten their vulnerability towards disease.[39, 40]

Adding to the complexity, the Bennett group from Rush University recently published the results of two longitudinal clinical-pathological studies (the Religious Orders study and the Rush Memory and Aging Project (ROS-RMAP)). These studies were community-based studies of aging that included both clinical assessments and postmortem examinations.[41] In these studies, they found that only 41% of the variation in cognitive decline could be accounted by the pathological indices of AD, CVD and LBD (Figure 1).[42] Thus, ~60% of remaining cognitive decline was completely unaccounted for by pathology. While pathological indices remain critical determinants of cognitive decline, there is an urgent need to identify mechanisms leading to cognitive decline that are independent of pathology.

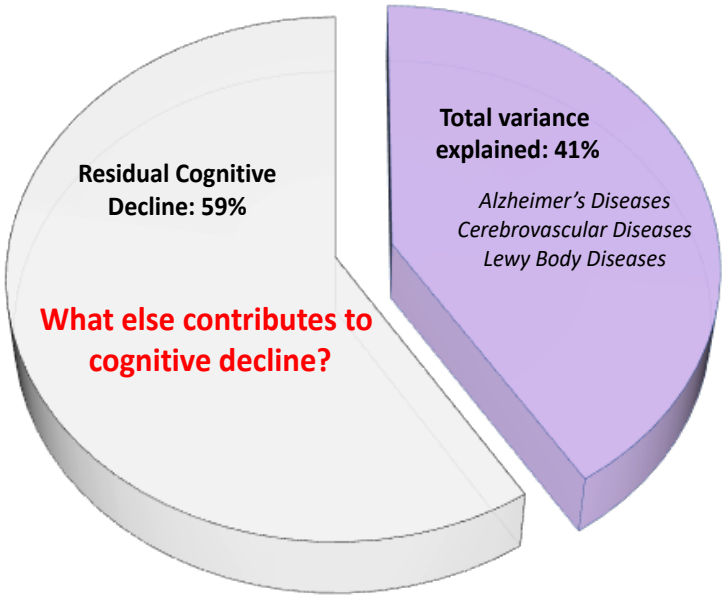

Figure 1. Variation in cognitive decline accounted for by pathological indices from the ROS and RAMP studies
Modified from Boyle, P *et al,* Ann Neurol, **2013**, 73(*3*). Results from two longitudinal clinical-pathologic studies found only 41% of the cognitive decline in age related dementia could be explained by the pathological indices of AD, CVD and LBD.

Furthermore, multiple types of dementia can exist in the same person, a condition referred to as "mixed-dementia" (TABLE I).[43] In fact, the ROS-RMAP studies found the majority of dementia in old age was accounted by mixed pathologies, with AD and cerebral infarcts the most common, followed by AD and Lewy bodies, then all three.[41] This is consistent with numerous other clinical-pathologic studies, and indicates that ADRD can result from the additive and collaborative efforts imposed by numerous pathologies.[44-48] Therefore, ADRD is a highly complex, multifaceted range of diseases.

1.1.4 AD Drug Discovery Failures: Are we Focusing on the Wrong Thing?

Currently, there exist only five US Food and Drug Administration (FDA)-approved therapies for AD; however, these only provide temporary symptomatic relief. Of the five, three are acetylcholinesterase (AChE) inhibitors (rivastigmine, galantamine, and donepezil), one is an N-methyl-D-aspartate receptor (NMDAR)-antagonist (memantine), and the last is a combination of two (donepezil and memantine).

The AChE inhibitors are based off the finding that in AD brains, there was a selective deterioration of cholinergic neurons in the forebrain, accompanied by decreased choline acetyltransferase and AChE.[49, 50] Thus, AChE inhibitors gained traction in large pharmaceutical companies with the development and approval of tacrine, donepezil, rivastigmine and galantamine in 1993, 1996, 2000 and 2001 respectively.[51] Tacrine was discontinued for use in 2013 after reports indicated severe hepatotoxicity side effects. All of these therapeutics were tested for efficacy in delaying disease progression in patients with mild cognitive impairment (MCI), however none showed efficacy.[52-54] Regardless, they are approved for the treatment of mild to moderate AD.

NMDAR-antagonists were developed from the hypothesis that glutamate overstimulation induces excitotoxicity which drives neuronal death.[55] It is proposed that glutamate stimulates NMDARs, which are heavily intertwined with learning and memory, and are severely compromised in AD.[56] Memantine, an NMDAR-antagonist, was developed and approved in 2003 for treatment of moderate to severe AD. Furthermore, the combinatory treatment of memantine and donepezil provided synergistic benefits, and as such the FDA approved the combination therapy in 2008. [57]

However, since 2003, there have been no new FDA-approvals for AD therapeutics. This was not for lack of clinical trials performed; A report from 2014 determined there were 124 Phase I trials, 206 Phase II trials, and 83 Phase III trials conducted between 2002 – 2012. Of all these trials, only one advanced to the clinic (memantine), thus giving an overall success rate of 0.4% (99.6% failure).[58] This clearly demonstrates the difficulty in developing effective and safe ADRD therapeutics, and explains why multiple media reports refer to AD therapeutics as the "holy grail" of drug discovery for large pharmaceutical companies.[59-61]

Drug discovery for AD has been primarily driven by the amyloid hypothesis, which implicates amyloid plaques as the underlying contributor to disease progression. [62] This is supported by the realization that genetic-based (familial) AD cases, which only account for a small percentage of the total incidence, involve mutations of the APP gene or the genes encoding presenilin 1 and 2, the subunits of γ-secretase.[63, 64] Thus, an overwhelming majority of potential disease-modifying treatments that advanced to clinical trials were directed towards inhibiting Aβ, including inhibitors of γ-secretase, β-secretase, Aβ aggregation and anti-amyloid monoclonal antibodies.[65, 66] Conversely, others hypothesize that tau is the primary contributor driving disease progression, which has led to an influx of clinical trials with tau-targeting therapies.[67] Over the past few years, several tau-directed therapies have entered clinical trials but, as of yet, none have succeeded.[68] In fact, the vast majority of scientific efforts for drug discovery was directed towards the pathological indices of AD, cerebrovascular disease (CVD) and Lewy body disease (LBD), the three most common forms of age-related dementia. However, as ADRD as a highly heterogeneous disease, there exists an urgent need for novel targets that are independent of pathological hallmarks.

1.1.5 Calpain-1 as a Therapeutic Target

Proteases are key intracellular regulators that have extensively been looked at as targets for drug development in a wide array of disease states.[69] These proteins represent 1-4% of all genes per genome sequenced to date and are ubiquitously expressed across different life forms. Proteases play a fundamental role in many biological pathways through proteolysis, the mechanism whereby proteins are cleaved into smaller fragments. They can be classified into seven groups dependent on catalytic residue and mechanism: serine (Ser), cysteine (Cys), threonine (Thr), aspartic acid (Asp), glutamic acid (Glu), metalloproteases (Zn) and asparagine peptide lyases. In humans, there are more than 670 proteases, of which 33% are metalloproteases, 31% are serine proteases, 25% are cysteine proteases, and 4% are aspartic proteases. [69]

This research focuses on cysteine proteases as therapeutic targets. Cysteine proteases operate via a catalytic triad of histidine and asparagine with a deprotonated cysteine. Briefly, aspartate orients the imidazole ring of histidine, allowing it to deprotonate cysteine. This cysteine then aims a nucleophilic attack on the carbonyl carbon on the backbone of the peptide substrate, forming an acyl-enzyme intermediate. Subsequently, the N-terminal fragment leaves and is stabilized by the nearby protonated histidine. Water molecules then attack the carbonyl, and the carboxy terminal fragment of the peptide is released from the cysteine. In humans, the two most important cysteine proteases are the cytoplasmic calpains and the lysosomal cathepsins.

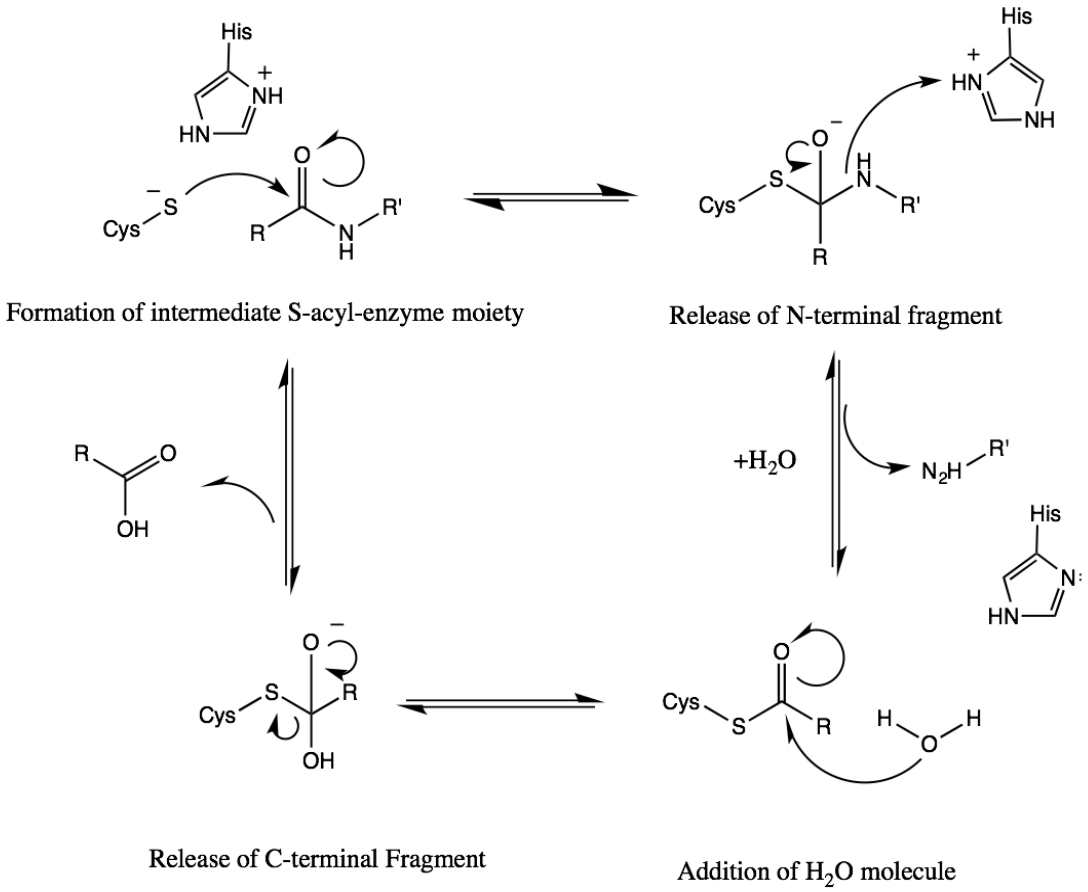

Scheme 1. Mechanism of proteolytic cleavage by cysteine proteases
Cysteine proteases operate via a catalytic triad. For calpain-1, it consists of Cys105, His262 and Asn286. Asn orients His to attack and deprotonate Cys. This prompts Cys to attack the carbonyl atom of the peptide substrate forming an intermediate. Then the N-terminal fragment leaves and is stabilized by His. Water molecules target the carbonyl, provoking the C-terminal fragment to be released from Cys.

Calpains, short for calcium-dependent papain-like cysteine proteases, are calcium-dependent, non-lysosomal cysteine proteases.[70] These enzymes were first discovered in 1964 in humans before being isolated and characterized from human muscle.[71] As its name suggests, calpains are some of the very few proteases and/or proteolytic complexes that are directly activated by calcium (Ca^{2+}). In fact, they were previously referred to as Ca^{2+}-dependent neural proteases prior to the discovery of a wide array of other proteases.[72, 73]

Calpains are ubiquitous proteases in eukaryotes, but exist in some bacteria, few fungi, and no archaea.[74] The human genome contains 15 calpain genes, from *CAPN1 – CAPN16* (excluding *CAPN4)*, which compose an overall superfamily of over 50 different molecular species.[75] Mutations in any one of these human genes are associated with severe disorders or death which are known as calpainopathies. For example, global *CAPN1*$^{-/-}$ results in spastic paraplegia,[76, 77] platelet dysfunction, [59] and spinocerebellar ataxia.[78]

An enzyme's clan denotes homology of the three-dimensional structure and the catalytic site (arrangement of residues and amino acid sequences). Calpains belong to the C02 family of protease clan CA. This family shares common structures with the dyad reactive histidine and cysteine resides at defined positions in the catalytic site. Furthermore, an enzyme's family is determined by statistical significance of the relationship in amino acid sequence to a representative member type. Membership in the C02 family distinguishes these proteases from the papain family (C1), and labels them as having a well-conserved cysteine protease domain called the CysPc motif.[79, 80]

Calpain-1 and calpain-2, the conventional calpains, are the most widely-studied and ubiquitous across the human body, as they exist in all cell types.[81] The variants are distinguished by the concentration of calcium required for activation; calpain-1 requires μM concentrations, while calpain-2 requires mM concentrations. Thus, they are often referred to as μ-calpain and m-

calpain, respectively. The isoforms are heterodimers, with a small similar subunit (26kDa, CAPNS1), and distinct large subunit (~80kDa); thus, they share 55-65% homology. The large subunit contains 4 domains, one of which is the CysPc domain with two protease core (PC) domains. When inactive, the Cys-105 is physically too far from His-262 and Asp-286 to become catalytically active. However, upon Ca^{2+} binding, calpain undergoes a conformational change moving the catalytic triad closer together to become active.[82] While intracellular Ca^{2+} levels indirectly activate calpain activity, calpastatin, an endogenous inhibitor, directly regulates their activity. Calpastatin only operates on calpains that have been activated via autocatalysis through Ca^{2+}.[83]

Calpain-1 (*CAPN1*) has long been studied as a therapeutic target for neurodegeneration. It mediates the proteolysis of many substrates involved in a wide variety of signaling events, including cell adhesion and mobility, cell cycle progression, cytoskeletal remodeling, transcriptional regulation and long-term potentiation (LTP) induction.[84] Regulated by calpastatin, calpain-1 is activated by 2-800μM cytosolic calcium levels. [85] Calpain-1's cleavage of substrates is modulatory, meaning it regulates as opposed to abolishes proteolytic activity. In fact, the partial truncation (non-digestion) of substrates by calpain-1 is considered a form of post-translational modification.[86] Over 200 known substrates of calpain-1 have been reported, but the actual number may exceed over 1000.[87]

The hyper-activation of calpain-1 is heavily intertwined with the calcium hypothesis of AD and brain aging.[88] This hypothesis asserts that dysregulation of intracellular Ca^{2+} underlies neural dysfunction of AD and other chronic age-related brain disorders. This can be in the presence or absence of Aβ pathology; soluble $A\beta_{42}$ can potentiate NMDARs thus triggering excessive Ca^{2+} influx, yet in the absence of Aβ reports have found dysregulated endoplasmic Ca^{2+} homeostasis in

AD and aging.[89, 90] Calpain-1 is activated by Ca^{2+}, and thus this hypothesis could contribute to the proteases' overactivation.

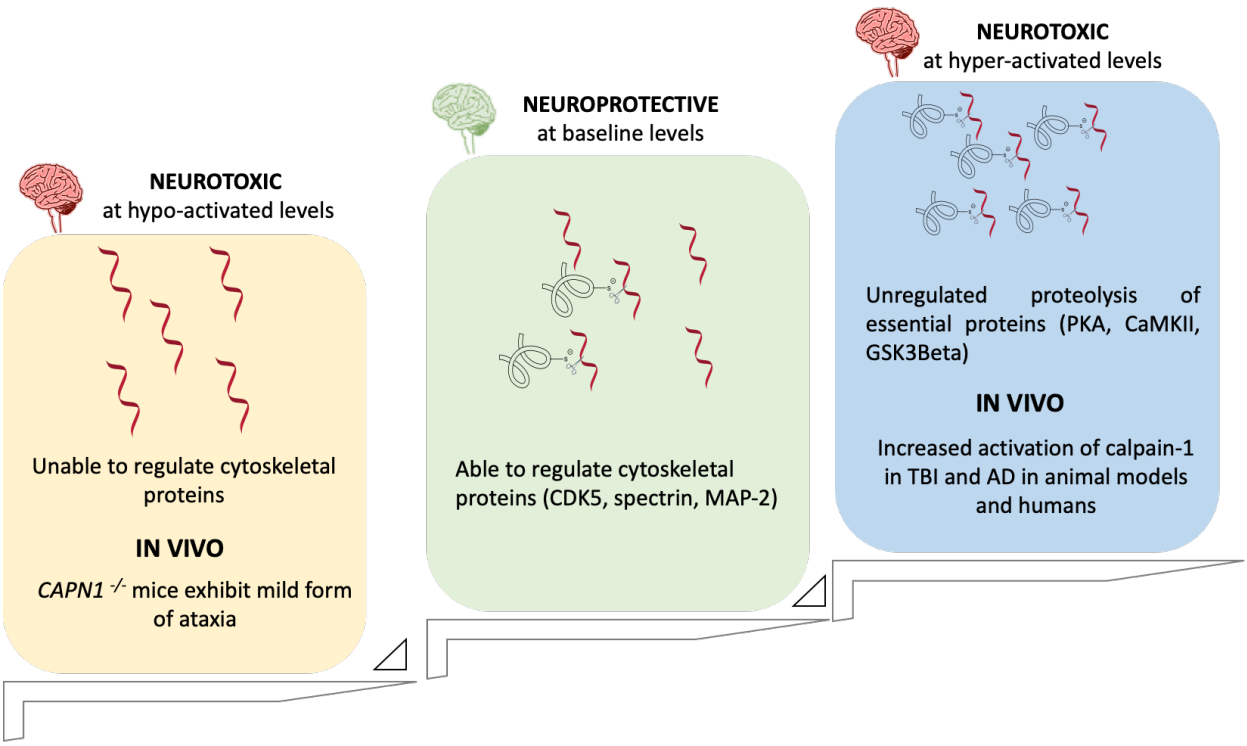

Figure 2. Pathologic states associated with calpain-1 hypo- or hyper-activation.
Proper calpain-1 homeostasis is vital for normal neurological function. Hypo- and hyper-activated calpain-1 are both linked to neurological disorders.

Reports of postmortem brains have shown that calpain-1 is abnormally activated in the AD brain, with calpastatin levels significantly increased.[91] Thus, for decades calpain-1 has been proposed as a target for AD therapeutics.[92] Proper calpain-1 homeostasis and regulation is essential for healthy neurological function (Figure 2): global homozygous or heterozygous human *CAPN1* mutations result in spastic paraplegia,[76, 77] platelet dysfunction, [59] and spinocerebellar ataxia.[78, 93] while hyper-activation of calpain-1 is implicated in the early pathogenesis of AD, TBI, and ischemic stroke. [4]

Alterations in calpain-1 regulation occur relatively early in AD; increases in calpain-1 activity, compared to age-matched controls, were increased in Braak stage III and beyond.[94] [91] This staging is a method to describe the pathological progression of the disease on postmortem brains; Braak stage III indicates early-moderate AD pathology, with neurofibrillary tangles in the entorhinal and transentorhinal layer and amyloid is in the majority of isocortical areas.[95] In fact, one report found the calpain-1 difference to be as high as 7-fold in AD to age-matched controlled brains.[96] Moreover levels of calpastatin, itself a known substrate, were significantly increased.[91, 96] In addition, reports indicate an elevation of cleaved substrates in the postmortem brain.[97] Many of these calpain-1 substrates have physiological roles in synaptic plasticity as well as neurodegeneration (

TABLE II), and may be directly involved with the classical neuropathological hallmarks of AD: amyloid plaques, soluble oligomers of amyloid-β, neurofibrillary tangles, and aggregates of hyper-phosphorylated tau.[98]

TABLE II. CALPAIN SUBSTRATES INVOLVED IN SYNAPTIC PLASTICITY AND/OR NEURODEGENERATION

Protein	Synaptic Plasticity	Neurodegeneration
Calcium/calmodulin-dependent protein kinase II (**CaMKII)**	Associated with LTP induction	Tau kinase[99]
Glycogen synthase kinase 3 beta (**GSK-3 β**)		Increases tau phosphorylation[100]
Microtubule-associated protein 2 (**MAP-2)**	Associated with LTP Induction[101]	
p35-p25 (cyclin dependent kinase 5 (cdk5) regulator)	Associated with LTP induction[98]	Increases tau phosphorylation, disrupts neuronal cytoskeleton
Ras homolog family member A (**RhoA**)	Required for LTP	Inhibits integrin-induced stress fiber assembly and cell spreading[98]
Spectrin	Remodels neuronal structure	Disrupts neuronal structure

Studies quantifying protein levels in postmortem AD brain tissues suggest that an increase in amyloid levels may precede or be concomitant to calpain-1 over-activation, which precedes global elevations in tau phosphorylation and the loss of post-synaptic markers.[94] This is not surprising as calpain-1-mediated proteolysis has been implicated in APP cleavage and thus regulates Aβ production.[97] An abnormal Aβ production alone can hyper-sensitize NMDARs, leading to a surge in cytosolic calcium levels, thereby hyper-activating endogenous calpain-1. This leads to unregulated proteolysis of key tau kinases, GSK-3 and Cdk5 both of which promote tau hyper-phosphorylation and the appearance of neurofibrillary tangles.[100, 102] Furthermore, other calpain-1 substrates (CamKII, MAP-2, GSK-3β) are intrinsically linked with long term potentiation (LTP) induction. Unregulated cleavage of these substrates leads to decreased phosphorylated cAMP response element-binding protein (CREB, an activated transcription factor) and impairment of LTP. Overall these reports suggest that over-activation of calpain-1 has multiple contributing roles to AD pathology and is an important early step in disease progression. Additionally, these findings support ongoing pre-clinical and clinical studies focusing on calpain-1 inhibitors and provide a rationale to investigate novel treatment strategies that prevent or block aberrant activity.

1.1.6 Calpain-Cathepsin Hypothesis

Uncontrolled calpain-1 activity is hypothesized to lead to apoptosis and neuronal loss via release of a second cysteine protease, cathepsin B, a theory known as the 'Calpain-Cathepsin hypothesis' (CCH, Figure 3).[2] First identified in 1998 and supported by experimental observations in the ischemic monkey paradigm, this hypothesis postulates that calpain-1 over-activation ruptures lysosomes, leading to the outflow of cathepsins, one of which is cathepsin B.[2]

While the exact mechanism of lysosomal rupture is unknown, *Yamashima* et al. have suggested that the rupture of lysosomes may be associated with oxidative stress (the concept of

which is discussed more extensively in Chapter 2).[3] They theorize that the lysosomal membrane-associated substrate of calpain is heat shock protein 70.1 (Hsp70.1) after 'priming' by 4-hydroxy-2-nonenal (HNE). More specifically, they theorize HNE primes Hsp70.1 by carbonylating Arg-369 which increases its cleavage efficiency by calpain-1.[2, 103, 104] The cleavage of Hsp70.1 causes disrupted Hsp70.1 binding to bis(monoacylglycerol) phosphate (BMP), a major lysosomal stabilizing complex. [105] This causes lysosomal destabilization and/or rupture seen in multiple neurodegenerative disease states including AD and ischemia injury.

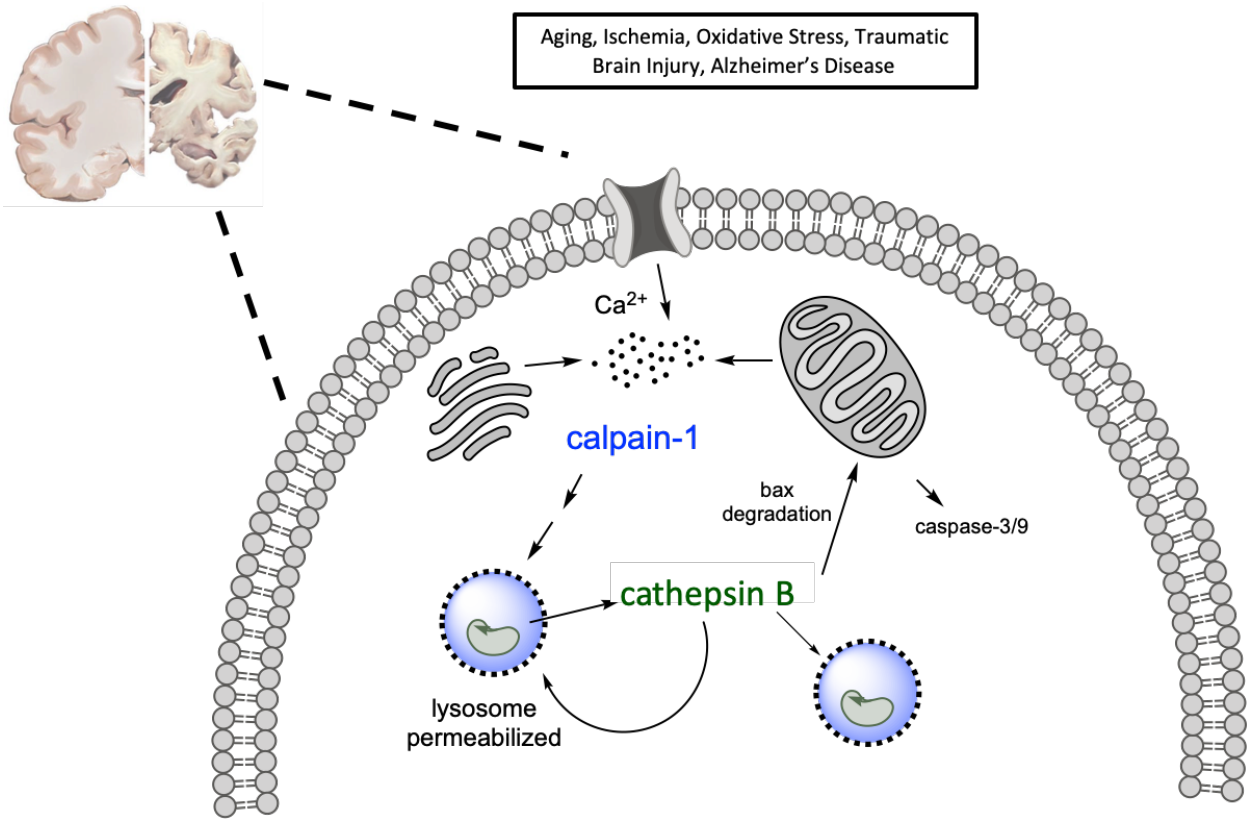

Figure 3 Calpain-cathepsin hypothesis
Schematic representing the calpain-cathepsin hypothesis. Briefly, increased intracellular calcium levels cause hyperactivated calpain-1 levels, which indirectly permeabilize the lysosome. This triggers the release of cathepsin B which further cleaves the lysosomal membrane and attacks the mitochondria releasing apoptotic factors leading to neuronal cell death.

The cathepsins released from the lysosome simultaneously attack it's membrane and damage mitochondria, releasing pro-apoptotic factors including cytochrome c, caspase-9 and caspase-3.[106, 107] In contrast to normal physiology, where localization is restricted to the lysosomes, cathepsin B immunoreactivity was found in neuronal perikarya in post-mortem AD brains. [108] Cathepsin B (and Cathepsin D) were found in senile plaques and reactive astrocytes

demonstrating the distribution of lysosomal proteases is altered in AD brains and suggesting its pathological importance in AD.

1.1.7 Cathepsin B as a Therapeutic Target

Cathepsin B is a lysosomal cysteine protease belonging to the CA clan and C1A family of proteases. "Cathepsin" is derived from the Greek *kathepsin* meaning to digest. This name was given to all proteases active at acidic pH.[109] However, upon further characterization proteases of the cathepsin family were found to have different catalytic types (serine: cathepsin A and G; aspartic: cathepsin D and E and cysteine: B, C, F, H, K, L, O, S, V, X and W).[110] The majority are expressed ubiquitously across human tissue, with overexpression reported in a wide array of diseases including multiple forms of cancer[111-114] As they are localized in the lysosome, cysteine cathepsins have optimal activity at slightly acidic pH, and the majority are unstable at neutral pH, with cathepsins B, S, and D the exceptions.

Cathepsin B was originally identified in beef tissue and is currently the most well-studied cathepsin.[5] Cathepsins are created as zymogens (inactive precursors); intriguingly cathepsin B is activated by both autocatalysis in acidic environments and by other proteases, including cathepsin D.[115] Several endogenous inhibitors exist to regulate cathepsin B activity, with cystatin C the most recognized and potent of the group. Cathepsin B's normal physiological roles include phagocytosis, autophagy, and angiogenesis.[5] However recent reports have found an increase in the levels of cathepsins B and S in human cerebrospinal fluid (CSF) during normal aging. Several groups propose this increase could be due to lysosomal compensatory mechanisms in response to the increase in misfolded and aggregated proteins that occur with age-related disorders.[116, 117]

Cathepsin B has long been investigated as a therapeutic target for neurodegenerative diseases. In TBI animal models and trauma patients, cathepsin B is found upregulated.[118, 119] Furthermore, *Bordi et al*. reported a significant upregulation of both cathepsin B and D in the

hippocampus of AD postmortem patients; they further classified the upregulation of cathepsin B and D to Braak stage III and V, respectively, incriminating cathepsin B as earlier in the disease pathogenesis.[120] Moreover, many reports on neuronal endosomes and lysosomes have implicated the cathepsin system in activation of downstream caspases and initiation of cell death during aging and other pathological states, and have specifically implicated cathepsin B.[121]

While the role of cathepsin B in neurodegeneration is clear, the exact mechanism of cathepsin B is still in debate. It has been reported that at low pH (such as in the lysosome and endosomes during normal conditions), to have exopeptidase activity regulating the turnover of proteins.[122] This activity could be neuroprotective, as in mouse models of AD, where cathepsin B was reported to degrade Aβ in endosomes, where the internalization and processing of APP occurs. [123] This observation was supported by a knockout experiment of cystatin C expression.[124] However, the cystatin C-cathepsin B axis is highly stringent, in that reports suggest that cystatin C overexpression actually leads to lowered Aβ.[125] At higher pH, such as when released into the cytosol in pathological conditions, an occluding loop is opened imbuing cathepsin B with endopeptidase activity. [122] Studies suggest that cathepsin B is involved in IL-1β role maturation by activated microglia, enhancing neuroinflammation in AD.[126] Thus the role of cathepsin B in neurodegeneration may be multifaceted.

1.1.8 Efficacy of Calpain-1 and Cathepsin B Inhibitors in Neurodegeneration

Calpain-1 and cathepsin B have independently and concurrently been investigated as therapeutic targets for decades in numerous models of neurodegeneration. The Arancio group treated APP/PS1 transgenic mice with non-selective calpain-1 inhibitors ***BDA-410*** and ***E64***.[127] Following treatment, synaptic transmission and behavior were similarly re-established to wild-type (WT) levels. Additionally, the LaFerla group used their 3xTgAD mouse model to study a nonselective calpain-1 inhibitor (***A-705253***) that displayed reversal of cognitive deficits in the

Morris water maze, and reduced tau phosphorylation and Cdk5 activation (through p35 to p25 cleavage).[8] In a cerebral ischemia rat model, the Zhang group observed neuroprotection (reduction in cerebral infarct volume) after treatment with ***E64d***.[128] Varying reports suggest cathepsin B inhibition lowers Aβ levels and improves memory deficits in AD models using gene knockout, chemical inhibition, and RNA silencing in cellular and animal models.[129] *CTSB*$^{-/-}$ mice were reported to show reduced TBI-induced deficits in behavior and biomarkers, showing that a simple restoration of aberrant activation of cathepsin B is able to reverse TBI-associated deficits.[5]

Intriguingly, ***NYC-438***, a potent and irreversible inhibitor of calpain-1 and cathepsin B, reversed cognitive deficits and restored long-term potentiation in the APP/PS1 familial Alzheimer's disease (fAD) mouse model; however, efficacy was independent of effects on Aβ neuropathology.[10, 130] This links calpain/cathepsin inhibition to mechanisms of cognitive reserve, and further endorses research into the therapeutic potential of protease inhibitors.

While several *in vitro* and *in vivo* studies support the neuroprotective role of calpain and cathepsin inhibition, these studies used both selective and nonselective calpain-1 inhibitors leading to ambiguity in interpretation.[8-10, 127, 128, 131] Furthermore, nonselective calpain inhibitors generally inhibit cysteine proteases beyond calpain-1 and cathepsin B, some of which, such as multiple caspase isoforms, have been independently proposed as therapeutic targets for neurodegeneration and ADRD.[132-134]

1.1.9 Clinical Efficacy of Proteases

With the assumption that the widespread inhibition of nonselective inhibitors would generate side-effects, the pharmaceutical industry narrowed their focus on developing highly selective inhibitors. Recently, the first clinical trial for a selective calpain-1 inhibitor was completed by AbbVie with the orally active inhibitor Alicapistat (***ABT-957***).[11, 135] This compound was developed as a calpain-1 and -2 inhibitor with high selectivity against cathepsins B, K, L and

S, and displayed promising results in preclinical studies. Unfortunately, the study was terminated.[136] Regardless, Alicapistat demonstrated a good safety profile; AbbVie reported no concerning safety signals, similar treatment-emergent adverse effects (TEAEs) between placebo and alicapistat study groups, and no incidence of deaths or serious TEAEs related to Alicapistat.

A variety of selective or nonselective inhibitors of calpain-1 have previously been developed for therapeutic applications other than neurodegeneration. ***E64d*** (also known as rexostatine, loxistatin, aloxistatin, EST and Estate) entered clinical trials for Duchenne muscular dystrophy.[137] The compound completed Phase III clinical trials before being discontinued, as the therapeutic benefits did not reach the target endpoint. Olesoxime (***TRO19622***), a cholesterol derivative with neuroprotective efficacy, completed phase II clinical trials for spinal muscular atrophy (SMA) supported by Hoffmann-La Roche, and amyotrophic lateral sclerosis (ALS) supported by Trophos (later acquired by Hoffmann-La Roche).[81] However, development was halted for both indications after disappointing clinical trial results. This compound was later found to suppress the effects of calpain.[138]

Small molecule protease inhibitors have established clinical efficacy, with inhibitors approve for HIV infection[139], multiple myeloma cancer[140], and hypertension[141] among others; some have even reached FDA-approval (TABLE III). Thus, with Alicapistat displaying a good safety profile and recognized clinical efficacy of protease inhibitors, development of cysteine protease inhibitors for ADRD remains a validated, and promising therapeutic avenue.

TABLE III. FDA-APPROVED PROTEASE INHIBITORS

Drug Name	Protease Target	Indication	Type	Date on Market
Captopril (Capoten; BMS)	ACE (metallo)	Hypertension	Peptidic	1981
Aliskiren (Tekturna/Rasilez; Novartis/Speedel)	Renin (aspartic)	Hypertension	Non-peptidic	2007
Tipranavir (Aptivus; Pfizer/BI)	HIV protease (aspartic)	HIV/AIDS	Non-peptidic	2005
Bortezomib (Velcade; Millennium)	Proteosome (threonine)	Cancer	Peptidic	2003
Sitagliptin (Januvia; Merck)	DPP4 (serine)	Diabetes	Non-peptidic	2006
Desirudin (Revasc/Iprivask; Novartis)	Thrombine (serine)	Coagulation	Peptidic	1998
Rivaroxaban (Xarelto; Bayer)	Faxtor Xa (serine)	Coagulation	Non-peptidic	2008

Targeting calpain-1 and cathepsin B is clearly beneficial in some diseases. However, the effect of chronic inhibition must be carefully considered. As mentioned previously, *CAPN1*$^{-/-}$ can cause spastic paraplegia, spinocerebellar ataxia (SCA) and platelet dysfunction.[81] Moreover calpain-1 inhibitors have shown detrimental effects on the immune system,[142] uterine implantation,[143] cancer suppression[144, 145] and cardiomyocytes.[125] Furthermore, mutations in *CTSB* have been linked to tropical pancreatitis, a form of chronic pancreatitis. [146] Thus, preclinical research into effects of inhibition is imperative to develop into clinical success for neurodegenerative diseases.

Serendipitously we discovered a family of cathepsin K inhibitors.[147] Cathepsin K is highly expressed in osteoclasts and able to cleave type I collagen, particularly in the acidic pH conditions required to dissolve bone calcium hydroxyapatite.[148] Human deficiencies in cathepsin K are linked to bone disorders like osteopetrosis and pycnodysostosis.[149, 150] In the study, *Dauth et al.* found learning and memory deficits in *CTSK*$^{-/-}$ mice. Furthermore, they observed significant reductions in cathepsin B and L in the cortex and striatum, along with increased cystatin C levels, the endogenous inhibitor, in the striatum and hippocampus. This is the first study that linked cathepsin K with learning and memory mechanisms. Thus, we pursued the development of selective cathepsin K inhibitors in tandem to better understand the role cathepsin K plays in the CNS.

Recently, Merck and Co sponsored the first selective cathepsin K inhibitor to enter phase III clinical trials.[151] Odanacatib is a highly selective reversible peptidomimetic. Unfortunately, the results demonstrated administration of Odanacatib increased the risk of cardiovascular events and stroke. [152] Thus, Merck and Co dropped all further development of Odanacatib.

1.1.10 Objectives

Literature does not provide clarity on a superior targeting strategy, as many reports ambiguously utilizes both selective and nonselective inhibitors. We theorized nonselective

irreversible targeting would offer superior benefits, as inhibiting both calpain-1 and cathepsin B afford efficacy in *in vivo* and *in vitro* models. This hypothesis is contradictory to traditional medicinal chemistry, which favors a selective, reversible inhibitor to potentially mitigate off-target effects. The objective of this chapter was to identify a library of inhibitors to further characterize selective *vs.* nonselective inhibitors and determine a therapeutic targeting approach.

Specific chapter objectives:

1. Develop kinetic assays for calpain-1, cathepsin B, cathepsin K and papain activity
2. Acquire a tool-kit of inhibitors with varying inhibitory profiles
3. Characterize small molecule inhibitors for potency, reversibility and selectivity
4. Develop a model to test *in vitro* specific inhibitor efficacy for calpain-1 inhibitors

1.2 METHODS

1.2.1 Enzyme Assays

Full length human Calpain-1 (210 nM, Sigma) or Papain (Carica papaya, 236 nM, Sigma,) was added to a buffer solution of 100 mM NaCl, 50 mM HEPES, pH 7.6, 1 mM TCEP, and compound, then incubated at 30°C for 10 min prior to the addition of Suc-LLVY-AMC substrate (30 μM, Enzo Life Sciences). Calpain-1 reactions also contained 1 mM $CaCl_2$. Recombinant human Cathepsin B (10 μM, R&D Systems) was added to a buffer solution of 25 mM MES, 5 mM DTT, pH 5.0 and incubated at room temperature for 15 minutes. The activated cathepsin B (11 nM) was diluted with 25 mM MES, pH 5.0, and inhibitor, then incubated at 30°C for 10 min prior to the addition of Z-LR-AMC substrate (10 μM, R&D Systems). Recombinant human cathepsin K (269 pM, Enzo Life Sciences) was added to a solution of 50 mM CH_3COONa, 2.5 mM EDTA, 1 mM DTT, 0.01% Triton X-100, pH 5.5 and inhibitor, then incubated at 30°C for 10 min prior to

the addition of Z-FR-AMC (10 μM). Papain reactions were carried out in microtiter 96-well plates while the cathepsin B, cathepsin K, and calpain-1 reactions were conducted in Corning 384-well low volume plates. All reactions were performed at 30°C and relative fluorescence was monitored over time (excitation and emission of 346 and 444 nm, respectively) on a synergy hybrid H4. The initial rate of all reactions were normalized to the initial rate of each enzyme with no inhibitor present and the data was represented as percent enzyme activity with standard deviation (SD). Compounds were dissolved in DMSO, and kept below 2% in all experiments. All compounds were screened at 1 and 10μM to determine its enzymatic profile for each protein. If a compound showed activity <50% at 1μM, more detailed dose-response curves were performed. IC_{50} curves were determined by varying the concentration of the inhibitor and plotting the percent enzyme activity on Prism 7.0 and compiling non-linear fit regression curves. Reversibility was determined in a dilution assay with a 1:20 fold dilution. Directly following the 10-minute incubation period, and prior to fluorescent reading, 1:20 of the compound-protease complex was diluted in substrate. The non-diluted and diluted reactions were monitored simultaneously. Reactions with similar activity were classified as irreversible, while reactions with increased protease activity, as compared to the undiluted control, were classified as reversible.

1.2.2 Cell Culture

Human neuroblastoma SH-SY5Y cells (ATTC CRL-2266) and Mouse hippocampal HT22 cells (Kind gift from Dr. Dargusch, Salk Institute) were cultured in DMEM/F12 and DME, respectively, and supplemented with 10% fetal bovine serum and 1% penicillin-streptomycin at 37°C in a humidified atmosphere of 5% CO_2. For cytotoxicity studies, cells were seeded at 2 x 10^4 cells per well in a 96-well plate in low serum media (1% fetal bovine serum). After overnight incubation, cells were administered with varying concentrations of compounds for defined periods of time. Cell viability was determined by MTS using CellTilter 96® Aqueous One Solution Cell

Proliferation Assay or MTT (Methylthiazolyldiphenyl-tetrazolium bromide, Millipore Sigma) and LDH release using CytoTox 96® Non-Radioactive Cytotoxicity Assay (Promega) according to the manufacturer's instructions. Untreated cells served as a negative control as DMSO concentrations were below 0.5%. The experiments were performed in triplicate.

1.2.3 Immunoblots

Cells were cultured up to 90% confluence in 6-well plates and treated with varying concentrations of compounds for defined periods of time. At termination of treatment, cells were washed twice with ice-cold PBS and protein was extracted by adding ice-cold RIPA buffer (Sigma) supplemented with protease and phosphatase inhibitors (Calbiochem). Cells were scraped and the cell lysate was centrifuged at 10,000 x rpm for 10 min at 4°C. Protein concentration was determined using the Pierce BCA-200 Protein Assay Kit (ThermoFisher). Lysates were stored at -20°C before use. Equal amounts of protein were prepared with 6X loading buffer (0.375 M Tris (pH=6.8), 12% SDS, 60% glycerol, 0.6 M DTT, 0.06% bromophenol blue)), heated at 95°C for 5 minutes, cooled to RT before loading onto NuPage 4-12% Bis-Tris Protein Gels.

1.2.4 Oxygen Glucose Deprivation

SH-SY5Y cells are plated in a 96-well plate at 4 x 10^4 cells per well and cultured overnight. To trigger 'ischemia', cell media is replaced with glucose-free media and incubated in a hypoxic chamber (95% N_2, 5% CO_2, <0.5% O_2). At OGD termination, cells are reperfused and replenished with glucose-containing media (Figure 25). Compound concentration is kept consistent throughout media changes. Cell viability is monitored after 24 hours of 'reperfusion', quantified by MTS and confirmed via LDH release (Promega, according to manufacturer's instructions). In every experiment, sulforaphane, is used as a control. HT22 cells are plated at 5 x 10^5 density.

1.3 RESULTS AND DISCUSSION

1.3.1 Development of Enzyme Screens

Four enzymatic assays for cathepsin B, cathepsin K, calpain-1 and papain were utilized in our studies. The pH of the respective buffers varies dependent on the pH_{max} of each protease (calpain-1 and papain at 7.6, cathepsin B at 5, cathepsin K at 5.5). These values are indicative of the physiological location of each protease (cytosol or lysosome). The compounds were screened at 1 and 10μM to determine an enzyme profile for each protease. Briefly, the screen was initiated by incubating the inhibitors with the human recombinant enzyme for 10 minutes at 30°C prior to addition of the AMC substrate. Cathepsin B has an additional pre-initiation step, where buffer containing 1,4-Dithiothreitol (DTT) was added to pro-cathepsin B to cleave the 62 kDa region thereby inducing primed cathepsin B. Furthermore, the calpain-1 buffer contained 1mM Ca^{2+} to activate calpain-1. Cleavage of the substrate to form a fluorescent product was monitored on a Synergy Hybrid Plate Reader (H4 or neo2, Figure 4) over 10 minutes. A decrease in fluorescent cleavage compared to the positive control suggests inhibition activity.

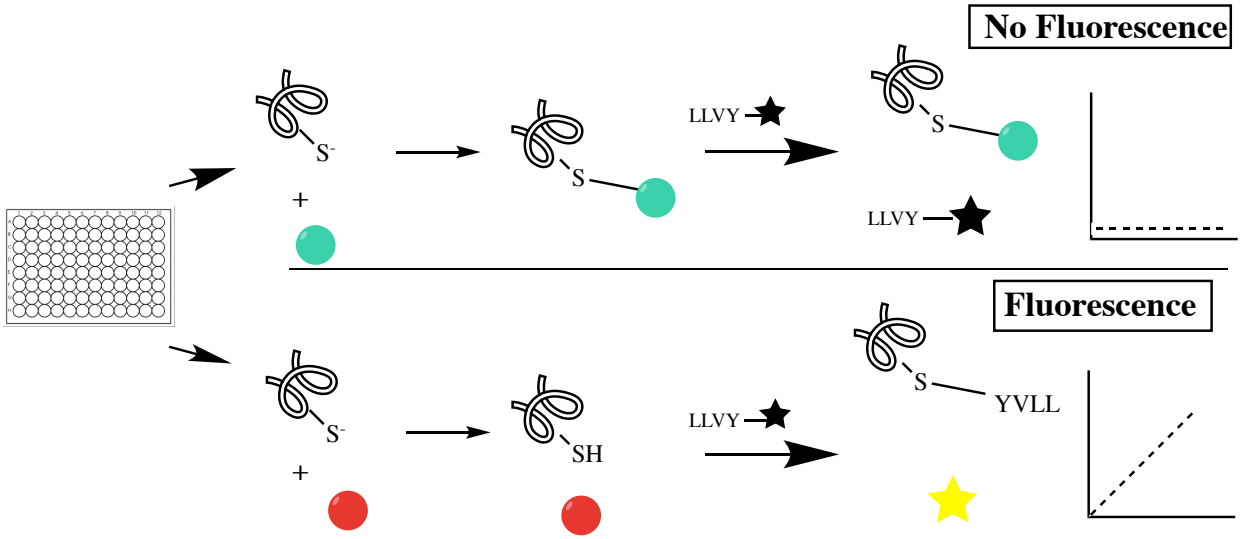

Figure 4. Schematic representation of the enzymatic assay.
Enzyme assays are conducted in a 384-well (calpain-1, cathepsin K, cathepsin B) or a 96-well (papain) plate. Briefly, the compound of interest is incubated with the human recombinant protein prior to addition of an AMC-linked substrate. The mixture is then monitored over a defined time on a fluorescent plate reader. Increased fluorescence over time indicates the enzyme has cleaved the AMC-linked substrate while the absence of fluorescence indicates the proteolytic cysteine on the enzyme is immobilized and bound to the compound of interest.

The cathepsin K assay originally utilized a kit; however, this was modified and adapted to be run in-house. The previous protocol called for a 30 minute incubation period with enzyme and inhibitor. Adjusting this period to 10 minutes had no effect on the enzyme activity alone or with compound (Figure 5). Thus, we proceeded by using a 10 minute incubation for every cathepsin K assay. The compounds used will be discussed later in this chapter.

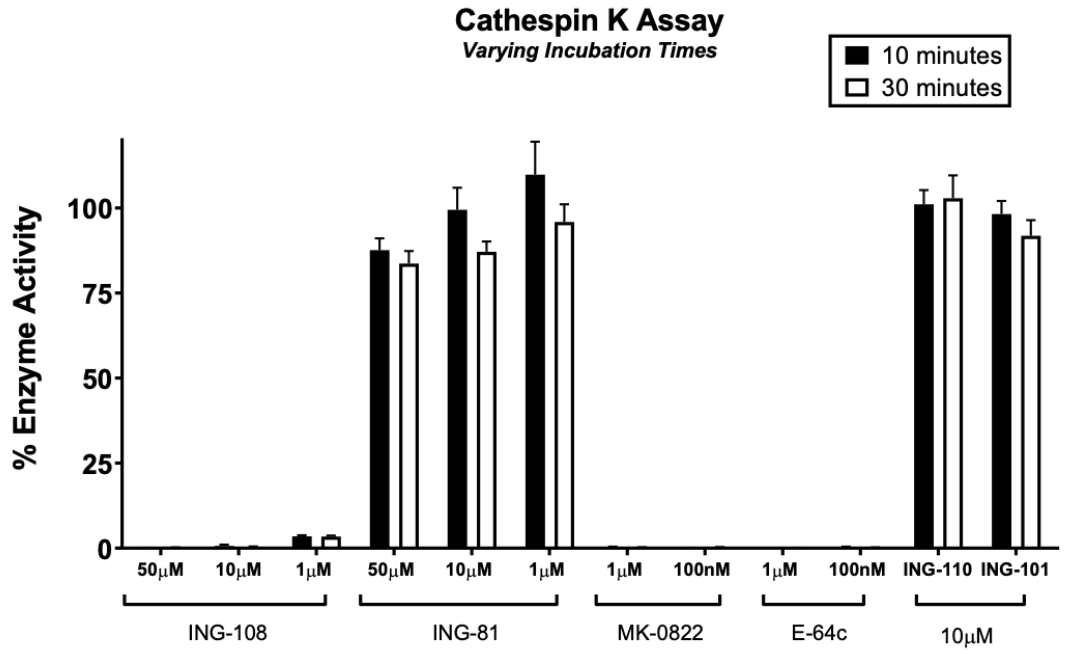

Figure 5. Optimization of the cathepsin K assay
Quantitative analysis of cathepsin K enzyme activity (%) following 10 or 30 minutes of preincubation with various inhibitors determined by AMC cleavage. Data represents mean ± SEM of at least n=6 in three separate experiments.

As the CCH indicates cathepsin B localized outside the lysosome exudes neurotoxic activity, we questioned whether our assay accounted for pH above 5. Using ***CA-074*** as a control,we found that changing the pH to cytosolic concentrations (6.9) abolished all cathepsin B activity (Figure 6). Using a wider range of buffer pH values, we observed ~25% maximal cathepsin B activity at pH 5.5, and completely abolished all activity at pH ranges 6-7.5 (Figure 6).

As extra-lysosomal activity imbues cathepsin B with endopeptidase activity, we wondered if changing the fluorogenic amino-4-methylcoumarin (AMC) substrate to another substrate (LLVY, utilized for calpain-1 and papain assays) would demonstrate cathepsin B activity. However, there was still no activity at any pH value with the LLVY-AMC substrate (Figure 6). Thus, our cathepsin B assay only accounts for lysosomal, endopeptidase conditions.

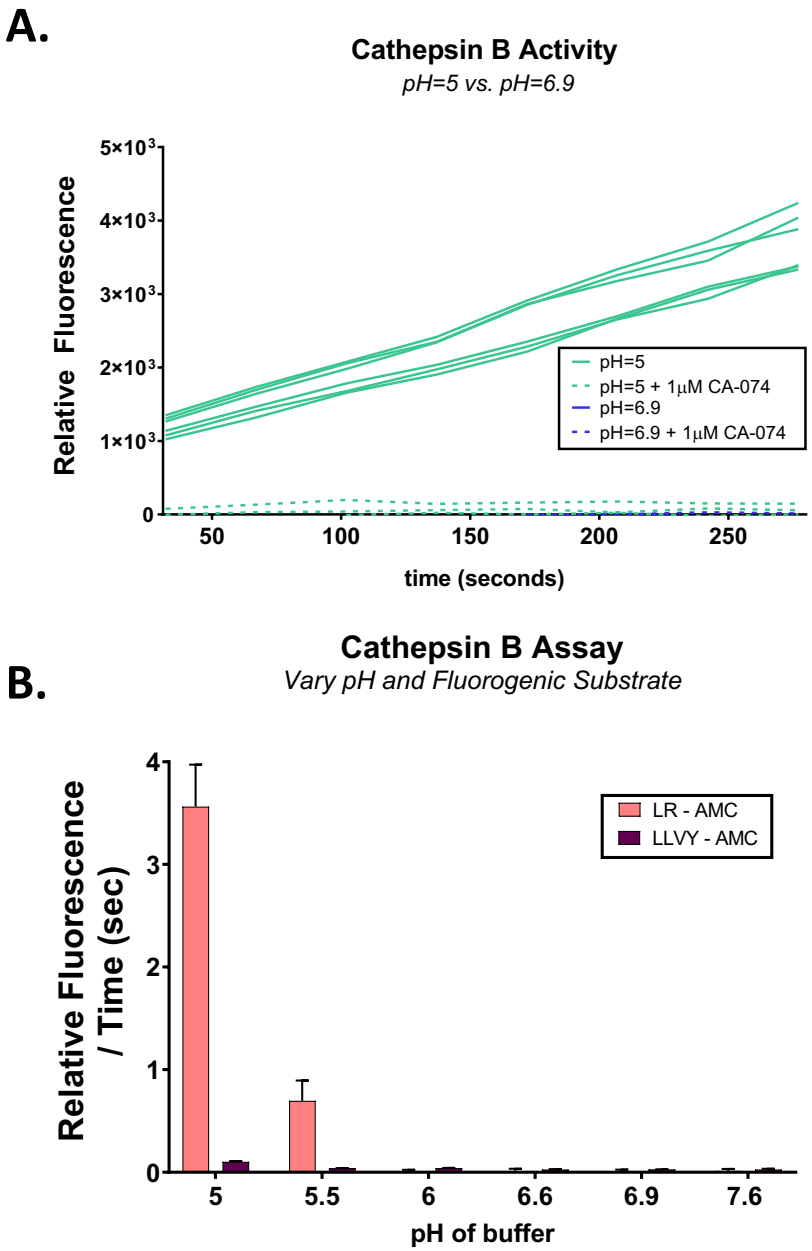

Figure 6. Characterization of the cathepsin B enzyme assay
(A) Fluorogenic activity of cathepsin B incubated in acidic or neutral buffer with or without 1μM CA-074 determined by AMC cleavage over 300 seconds (5 minutes). Each line represents a separate well. (B) Fluorogenic activity per second of cathepsin B at various buffers (pH 5 – 7.6) with either LR-AMC or LLVY-AMC. Data represents mean ± SEM of at least n=6 in 3+ separate experiments.

All kinetic assays had individual, positive controls (Figure 7). These were all screened at 1μM, and tested in every assay performed. Calpain Inhibitor XI (***CAPNXI***) is a cell-permeable, potent (K_i = 140nM) reversible inhibitor against calpain-1, with weak inhibition towards cathepsin B (K_i = 6.9μM). However, our assays reveal this compound has significant activity against cathepsin K at just 1μM and thus, is not as selective as literature suggests. ***CA-074*** is a selective, potent (K_i = 2.24nM) irreversible inhibitor against cathepsin B. ***CA-074 Me*** is a methyl ester prodrug of the carboxylic acid drug and is proposed to be a cell-permeable form. ***E-64c*** is a synthetic analog of ***E-64***, a well-known epoxide isolated from *Aspergillus japonicas.* It is a non-selective, highly potent, irreversible cysteine protease inhibitor. ***E-64d***, the ethyl ester of ***E-64c***, is the pro-drug, cell permeable form. ***NYC-438*** is a non-selective, highly potent (IC_{50}<100nM) epoxide designed in-house.[9] ***NYC-438e*** is the cell-permeable form with an ester replacing the carboxylic acid. Lastly, Odanacatib (***MK-0822***, not shown), developed by Merck, is a selective, highly potent (IC_{50} = 0.2nM) inhibitor of cathepsin K with weak inhibition towards cathepsin B (IC_{50} = 1034nM). ***MK-0822*** recently discontinued phase III clinical trials for osteoporosis in postmenopausal women after analysis revealed an increase in stroke events. The goal was to generate a small library of selective and potent inhibitors of calpain-1 and calpain-1/cathepsin B, using cathepsin K and papain as off-target cysteine proteases.

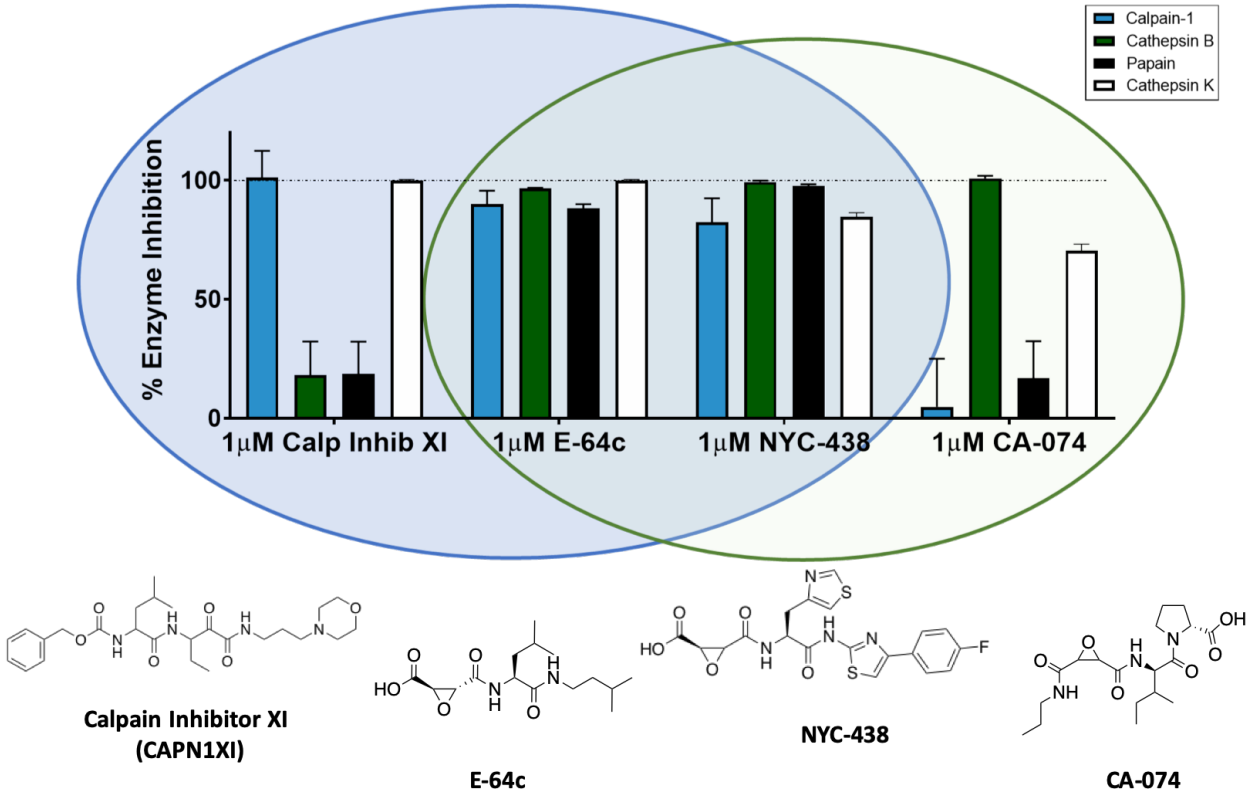

Figure 7. Benchmarking known compounds.
Venn diagram depicting well-known inhibitors with varying degrees of inhibitory efficacy against calpain-1, cathepsin B, Papain and cathepsin K, with chemical structures shown beneath. Data was collected and quantified from enzyme screens monitoring fluorescence induced by AMC substrate cleavage. The blue circle indicates efficacy against calpain-1 while the green circle indicates efficacy against cathepsin B. Data is represented as Mean ± SEM from at least n=6.

1.3.2 Identification of Calpain-1 Inhibitors

Compound ***1***, also known as Alicapistat (***ABT-957***), is a small molecule developed by AbbVie that is highly potent towards calpain-1.[135] Using ***1*** as a lead, compounds ***2*** - ***5*** were further developed (Figure 8). Replacement of the cyclopropyl in the P1' position (R_2) with a methyl or fluorobezene group generated compounds ***2*** and ***3***. An additional fluorine was placed in the P3 position (R_3) to generate compounds ***4*** and ***5***, respectively. This was chosen because of the effect

of fluorine, a vital bioisostere of hydrogen.[153] Fluorine is a small and highly electronegative atom. It's high electronegativity can modify 3D-orientation of a molecule and influence a favored conformation stabilized by dipole-dipole interactions or hydrogen bonding.[154, 155] Moreover it can reduce basicity of nearby amino groups or, due to its electron-withdrawing ability, can increase acidity of alcohols and acids. Bioisosteric replacements play an important role in development of lead series, as selective additions of fluorines on small molecules can enhance pharmacokinetic (PK) and pharmacodynamic (PD) properties, such as improved membrane permeation and metabolic stability.[156]

All were found to be highly selective towards calpain-1 at 1μM with minimal loss of enzyme activity against cathepsin B, papain or cathepsin K (Figure 8). The compounds ***CAPNXI***, ***E64c***, ***NYC-438***, ***CA-074*** were used as controls in each enzyme assay performed.

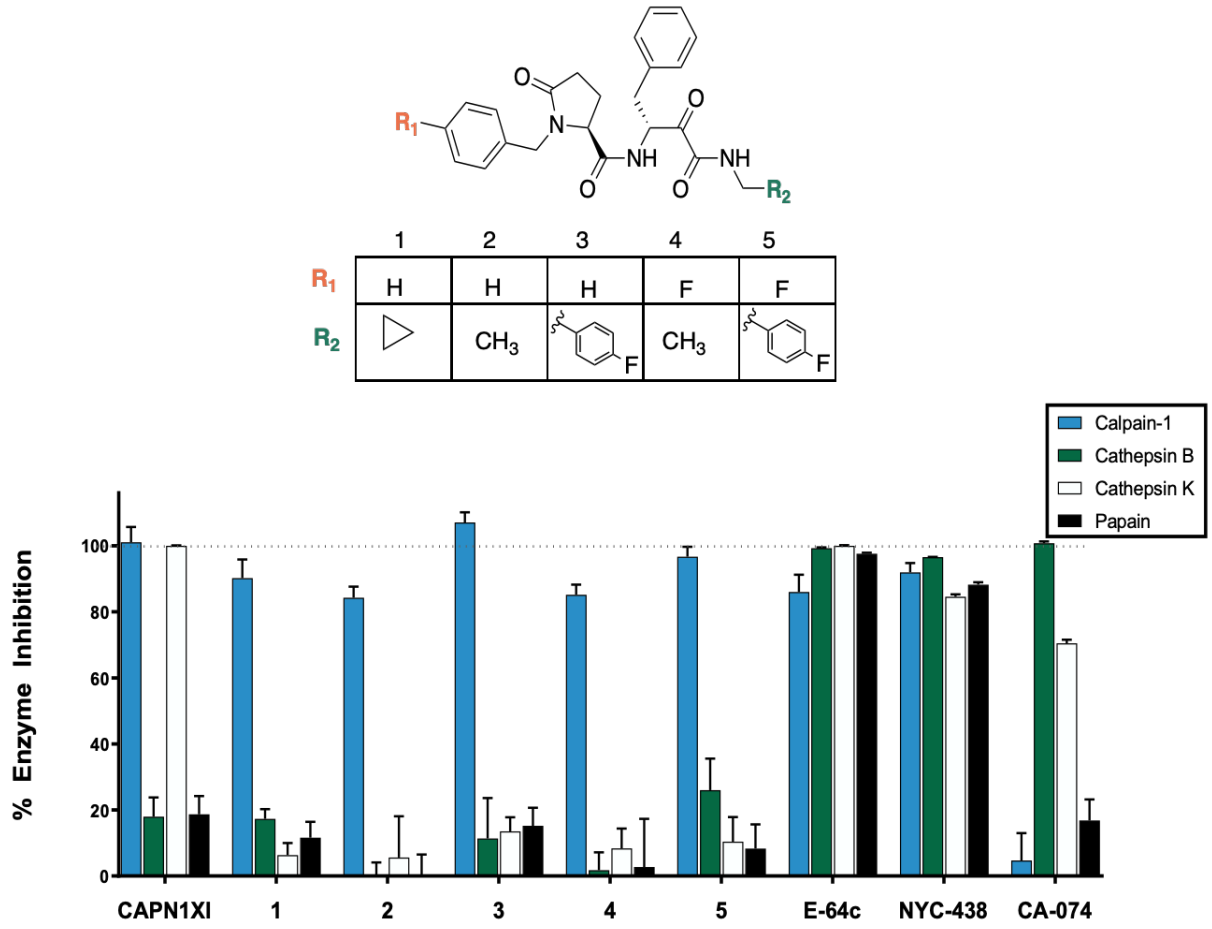

Figure 8. Enzymatic profiles of calpain-1 inhibitors
Chemical structures and selectivity screen of compounds ***1*** **–** ***5*** at 1μM against calpain-1, cathepsin B, cathepsin K and papain. Calpain Inhibitor XI (CAPNXI), CA-074, and E-64c were used as controls for each enzyme screen. Compounds were incubated with inhibitor for 10 minutes prior to addition of substrate. All data are represented as Mean ± SEM from at least n=6 replicates.

More detailed dose-response curves were compiled for compounds ***1-5*** **(**Figure 9**)**. All exhibited IC_{50} values in the nanomolar range. Replacement of the cyclopropyl significantly improved potency, particularly with a benzofluorene which achieved <100nM IC_{50} levels. The addition of a fluorine in the R_1 position had no significant impact on potency (267 ± 26nM *vs.* 378 ± 28nM, and 78.2 ± 10nM *vs.* 128 ± 7.4nM for ***2*** *vs.* ***4*** and ***3*** *vs.* ***5****,* respectively). Overall, ***3*** exhibited the lowest IC_{50} value (78.2 ± 10nM).

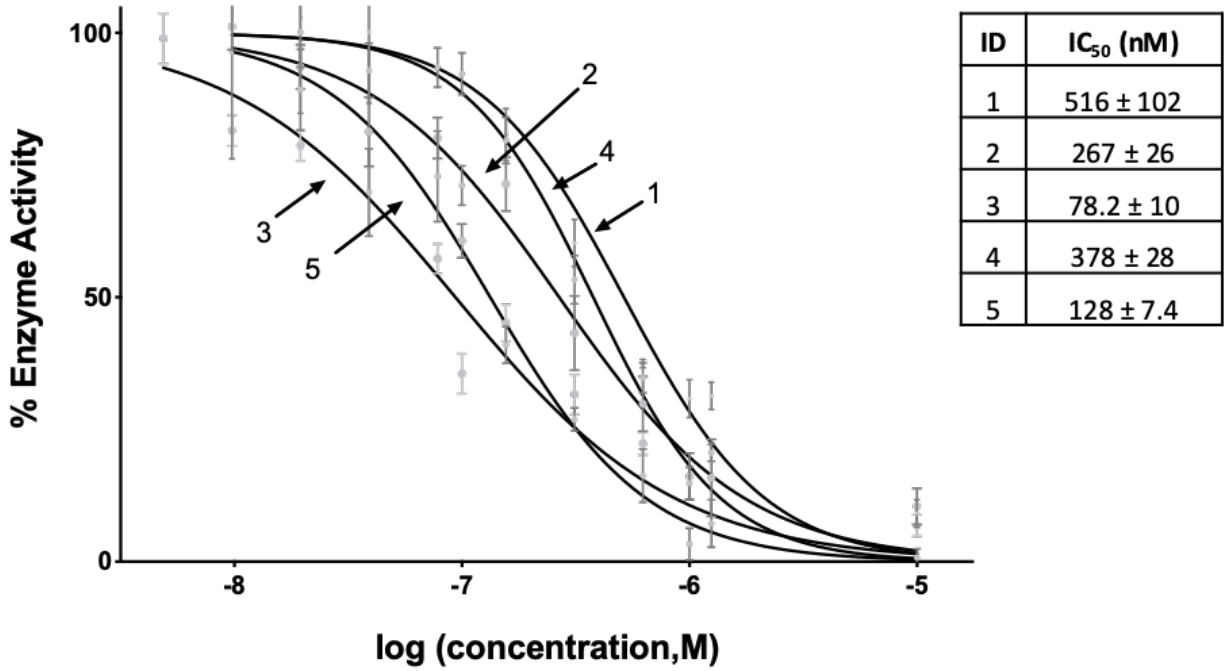

ID	IC_{50} (nM)
1	516 ± 102
2	267 ± 26
3	78.2 ± 10
4	378 ± 28
5	128 ± 7.4

Figure 9. Dose-response IC_{50} curves for compounds 1-5
Enzyme activity determined by AMC cleavage of the substrate LLVY-AMC by calpain-1 after incubation of compounds ***1-5*** at varying concentrations. All data are represented as Mean ± SEM from at least n=6 replicates.

Additional selectivity indexes were performed with compounds screened at 10μM against all proteases (TABLE IV). Addition of a methyl at the R_1 position (***2***) improved inhibitory activity against cathepsin K and papain, which was strengthened after addition of another fluoro in the R_1 position (***4***). While replacement of a benzofluorene (***3***) had no significant effect on selectivity, the additional fluoro slightly improved selectivity (***5***).

TABLE IV. SELECTIVITY PROFILES OF COMPOUNDS 1-5

Selectivity profiles of compounds **1-5** at 1μM and 10μM against calpain-1 (CAPN1), cathepsin B (CTSB), cathepsin K (CTSK) and papain. Data represents Mean ± SEM of at least n=6 replicates.

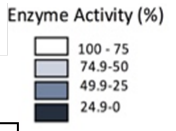

	1	2	3	4	5	
CAPN1	9.8 ± 5.62%	15.73 ± 3.35	-7.1 ± 3.09%	14.8 ± 3.07%	3.3 ± 3.02%	1uM
CTSB	87.6 ± 1.89%	105.6 ± 9.73%	88.6 ± 12.26%	98.2 ± 5.38%	74.0 ± 9.54%	
CTSK	92.6 ± 2.77%	94.4 ± 12.52%	86.5 ± 4.31%	91.7 ± 6.05%	89.6 ± 7.49%	
Papain	97.1 ± 9.58%	100.2 ± 6.68%	84.8 ± 5.45%	97.27 ± 14.6%	91.7 ± 7.30%	
CAPN1	0.78 ± 3.99%	5.8 ± 6.68%	11.2 ± 4.65%	-4.5 ± 2.1%	-5.1 ± 2.93%	10uM
CTSB	41.4 ± 2.30%	44.9 ± 4.8%	34.4 ± 3.14%	62.8 ± 6.05%	34.3 ± 4.18%	
CTSK	48.2 ± 4.68%	71.6 ± 2.80%	45.34 ± 1.19%	76.6 ± 7.03%	50.4 ± 3.03%	
Papain	67.7 ± 5.13%	84.4 ± 15.79%	90.83 ± 16.6%	99.6 ± 7.12%	72.8 ± 3.8%	

Alpha-ketoamides bind to cysteines via a reversible mechanism.[157] Thus, it was proposed these compounds would be reversible. This was confirmed using a 1:20 dilution. Briefly, compounds were incubated with the enzyme for 10 minutes, then 1μL part of the mixture underwent a 1:20 dilution into the substrate mixture while the remainder underwent the non-diluted assay, and fluorescence was read on the synergy H4 hybrid reader. Enzyme activity re-established after dilution indicated dissociated binding of enzyme and inhibitor.

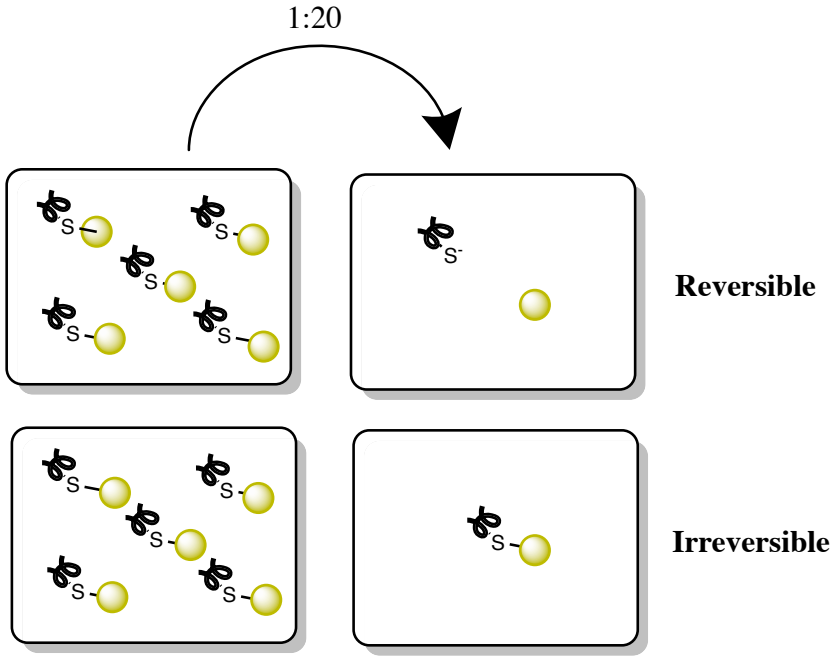

Figure 10. Schematic representation of the 1:20 dilution assay
In this experiment, reversibility is assessed by 1:20 dilution. Compounds are incubated with the enzyme at high concentrations to achieve near-maximal activity. The solution is then diluted 20-fold. Compounds that are reversibly-bound should dissociate from the enzyme, while irreversibly-bound compounds will still be bound.

CAPN1XI, a reversible calpain-1 inhibitor, was used as the positive control in every assay, and compounds were tested at 10μM against calpain-1. Following dilution, calpain-1 activity was re-established back to ~100% activity indicating the binding of compounds ***1 - 5*** to calpain-1 is reversible (Figure 11). However, there was large variability in the enzyme activity due to the sensitivity of the assay. Thus, results were confirmed by characterizing the reversibility of compounds ***1*** – ***5*** to cathepsin K.

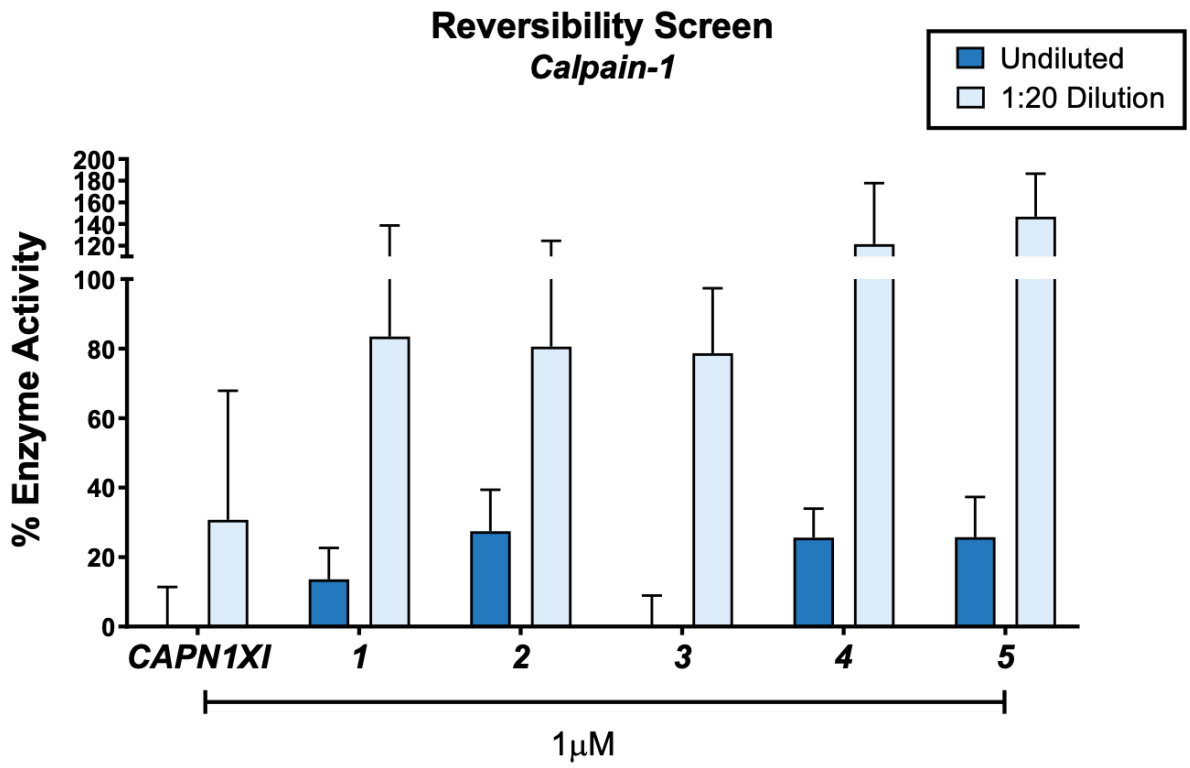

Figure 11. Inhibitors *1-5* are reversible against calpain-1
Compounds 1-5 were analyzed with or without a 1:20 dilution assay against calpain-1. All data are represented as Mean ± SD from at least n=6 replicates.

The 1:20 dilution assay ***1*** – ***5*** was performed using a higher concentration of inhibitor (10μM), as the effect of inhibitors on cathepsin K is less potent than calpain-1. ***MK-0822***, a reversible cathepsin K inhibitor, was used a positive control in every assay. The activity of Cathepsin K was restored following dilution of compounds ***1*** – ***5*** (Figure 12). Thus, these compounds are reversible against cathepsin K and calpain-1.

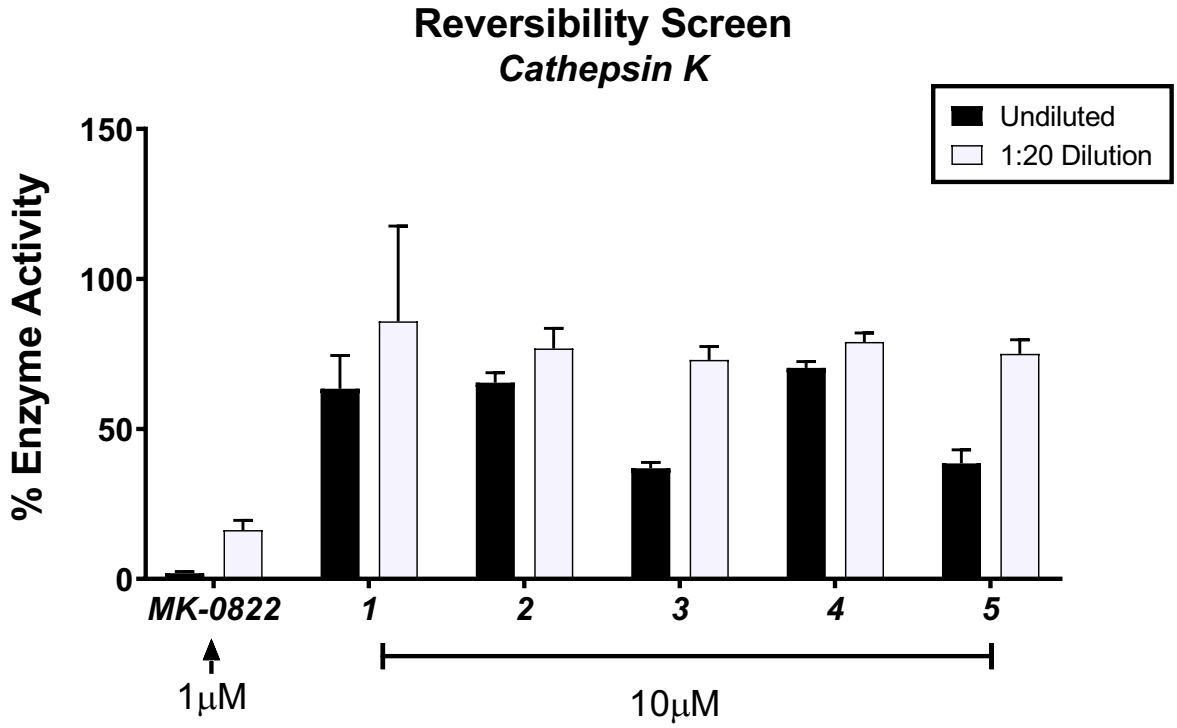

Figure 12. Compounds *1-5* are reversible against cathepsin K
Compounds 1-5 were analyzed with or without a 1:20 dilution assay against calpain-1. All data are represented as Mean ± SEM from at least n=6 replicates.

1.3.3 Evaluating Insults that Induce Calpain-1 Activity In Vitro

After characterizing enzyme inhibitory profiles against pure, human recombinant protein, specific inhibitory efficacy was characterized by monitoring spectrin proteolysis *in vitro.* Spectrin breakdown products (SBDPs) are mediated by calpain-1 and caspase-3, and found in a number of neurodegenerative conditions, both acute and subacute, including stroke, AD, and TBI. [158-160] Spectrin is a major cytoskeletal protein that was initially discovered in human red blood cells, then further characterized as a ubiquitous protein, found in various tissues including the brain. [161-163] In

fact, it was the first protein identified to undergo calpain-mediated cleavage in neuronal cells.[164] [165] Enhanced spectrin proteolysis has been reported during normal brain aging as well as ADRD and other age-related NDs.[166, 167]

Spectrin (250kDa) served as an exemplary substrate, as its BDPs produce 3 fragments mediated by both calpain-1 and caspase-3 (Figure 13).[158, 168] The150kDa fragment is induced by both calpain-1 and caspase-3, while the 145kDa and 120kDa fragments are specifically produced by calpain-1 and caspase-3, respectively. This also provided markers that distinguished between two types of neuronal death: both necrosis and apoptosis which are mediated by calpains and caspases, respectively.[168]

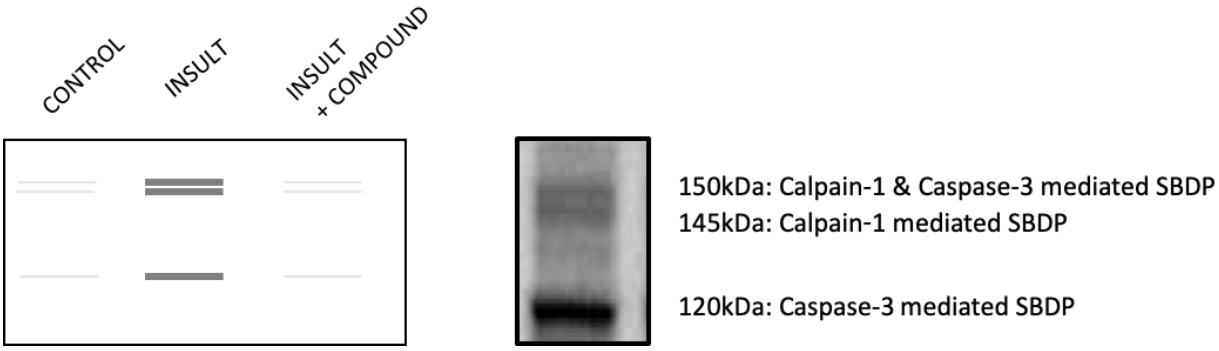

Figure 13. Spectrin breakdown products as biomarkers of calpain-1 activity
Expected results when monitoring spectrin proteolysis *in vitro*. A neuroinsult should induce spectrin breakdown products (SBDPs), which will be mitigated by inhibitors.

Various neuroinsults were tested on SH-SY5Y cells and the appearance of SBDPs were monitored on immunoblots, with particular focus on the 145kDa fragment. SH-SY5Y cells were initially used as they were the proposed model for neuroprotection assays (see Chapter 2). The neuroinsults chosen were selected from previous literature: 1μM Thapsigargin for 24 hours (1), 2 hours oxygen glucose deprivation with 24 hours reperfusion (OGD-R, 2), 5μM 4-hydroxy-2-nonenal (HNE) for 24 hours (3) and 0.5μg/mL Calcium ionophore A23187 for 24 hours (4). Thapsigargin is a competitive inhibitor of the sarco endoplasmic reticulum Ca^{2+} ATPase (SERCA) which raises intracellular calcium levels.[169] OGD-R and HNE, both extensively discussed in Chapter 2, activate calpain and caspase-3.[170] [171] Lastly calcium ionophore A23187 was used to stimulate calpain-1 hyper-activation. The positive control used on every western blot was 500nM of staurosporine treated for 24 hours. Staurosporine is a potent inhibitor of protein kinases that induces quick, robust apoptosis, and produces thick SBDP bands on a western blot.[172] Of note, staurosporine cleaves actin, hence the disappearance of actin bands in lanes treated with staurosporine.

Intriguingly, treatment of thapsigargin changed the morphology of SH-SY5Y cells. The cells became more elongated and thinner. Moreover, SH-SY5Y cells were sensitive to calcium ionophore A23187 treatment. Most cells detached after 1μg/mL treatment; thus, the dose was reduced by 50%.

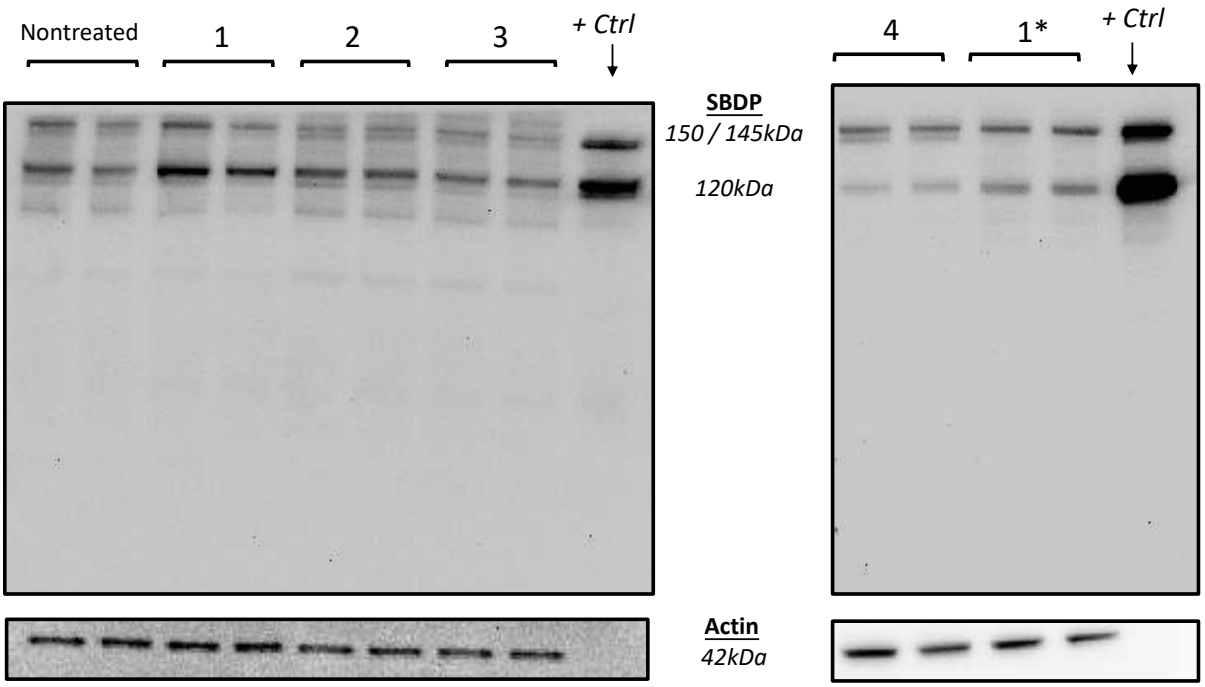

Figure 14. Optimization of neuroinsults on SH-SY5Y cells to induce SBDPs
Representative immunoblots of SH-SY5Y cells with various neuroinsults probed with spectrin and actin antibodies. Only SBDP 150, 145 and 120kDa are shown. Neuroinsults were as follows: 1μM Thapsigargin for 24 hours (1), 2 hours OGD-R (2), 5μM HNE for 24 hours (3), 0.5μg/mL Calcium ionophore A23187 for 24 hours (4). 500nM Staurosporine for 24 hours was used as a positive control.

The treatments were performed in duplicate, run on western blots, and probed with spectrin antibody. Treatment with OGD-R, HNE and calcium ionophore A23187 produced the calpain-specific SBDP 145kDa. However, the bands were very faint.

SH-SY5Y cells were pretreated with 10μM of ***CAPN1XI*** or ***5*** for 2 hours, then stimulated with a neuroinsult (either 2 hours OGD-R or 1μM Thapsigargin for 24 hours), with SBDP analyzed *via* immunoblot (Figure 15). OGD-R treatment increased SBDP 150/145kDa, which was decreased with ***5*** and not ***CAPNXI***, but without significance. Moreover, thapsigargin treatment increased both SBDP 150/145 and 120kDa, which was attenuated by ***5*** and ***CAPNXI,*** without significance. Unfortunately, the SH-SY5Y cells had several problems that were not ideal including producing indistinct SBDP bands that muddled quantitative results and a slow growth rate (Figure 15). Thus, HT22 cells, an immortalized mouse hippocampal cell line was selected because they have a rapid growth rate and can be more predictive for mouse *in vivo* studies (Chapter 2 and 3).

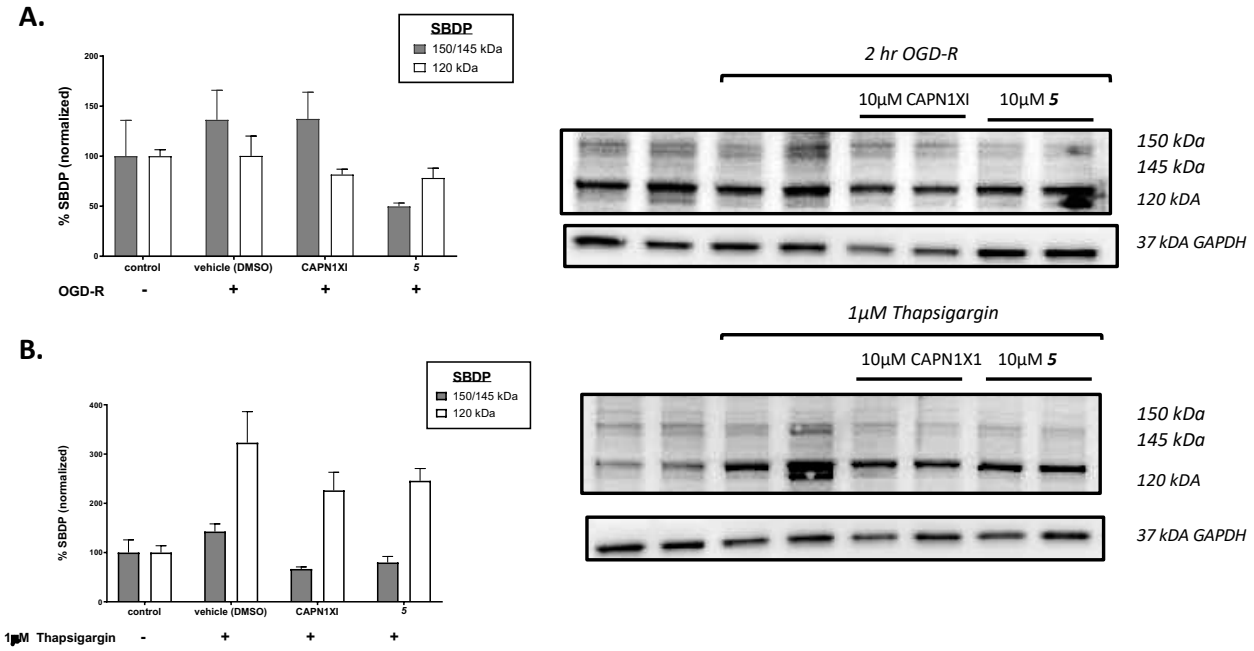

Figure 15. Pretreatment of 10μM *5* reduces of SBDP 150/145kDa in SH-SY5Y cells
(**A** and **B**) Quantitative analysis and representative immunoblots of SH-SY5Y cells pretreated for 2 hours with 10μM ***5*** and ***CAPN1XI*** then stimulated with 2 hours OGD-R (**A**) or 1μM Thapsigargin (**B**) for 24 hours, then probed with spectrin and GAPDH Ab. Quantified data is represented as Mean ± SEM from at least n=3 replicates.

We insulted HT22 cells with both OGD-R, and ionomycin, another calcium ionophore. HT22 cells treated with 20μM ionomycin for 20, 40, and 60 minutes produced profound increases in SBDP 150 and 145kDa (Figure 16A). The SBDP 145kDa was clearly distinct from SBDP 150kDa and ideal for monitoring our compounds' specific efficacy on calpain-1 activity. Moreover, SBDP were monitored in HT22 cells that underwent 2 or 4 hours of OGD with or without 24 hours of reperfusion (OGD vs OGD-R, Figure 16B). A sharp increase in the SBDP 150kDa band directly following OGD was observed, an effect that nearly returns to baseline after reperfusion. This fragment is cleaved by both calpain-1 and caspase-3. However, the SBDP

120kDa fragment (cleaved exclusively by caspase-3) remains at normal levels after OGD, but significantly increases with reperfusion. These studies suggest calpain-1 is a dynamically regulated enzyme, with transient activation following insult.

Microtubule associated protein 2 (MAP2), a reported cleavage product of calpain-1, was also monitored.[173] The immunoblot suggests MAP2 levels minimally decreased by ~50% after OGD and returned back to basal levels with reperfusion. To have an accurate estimation of protein content various housekeeping genes were also monitored, as all are classical loading protein controls, but some (GAPDH and tubulin) have been reported to be cleaved by calpain-1.[173] No change was observed in the control proteins.

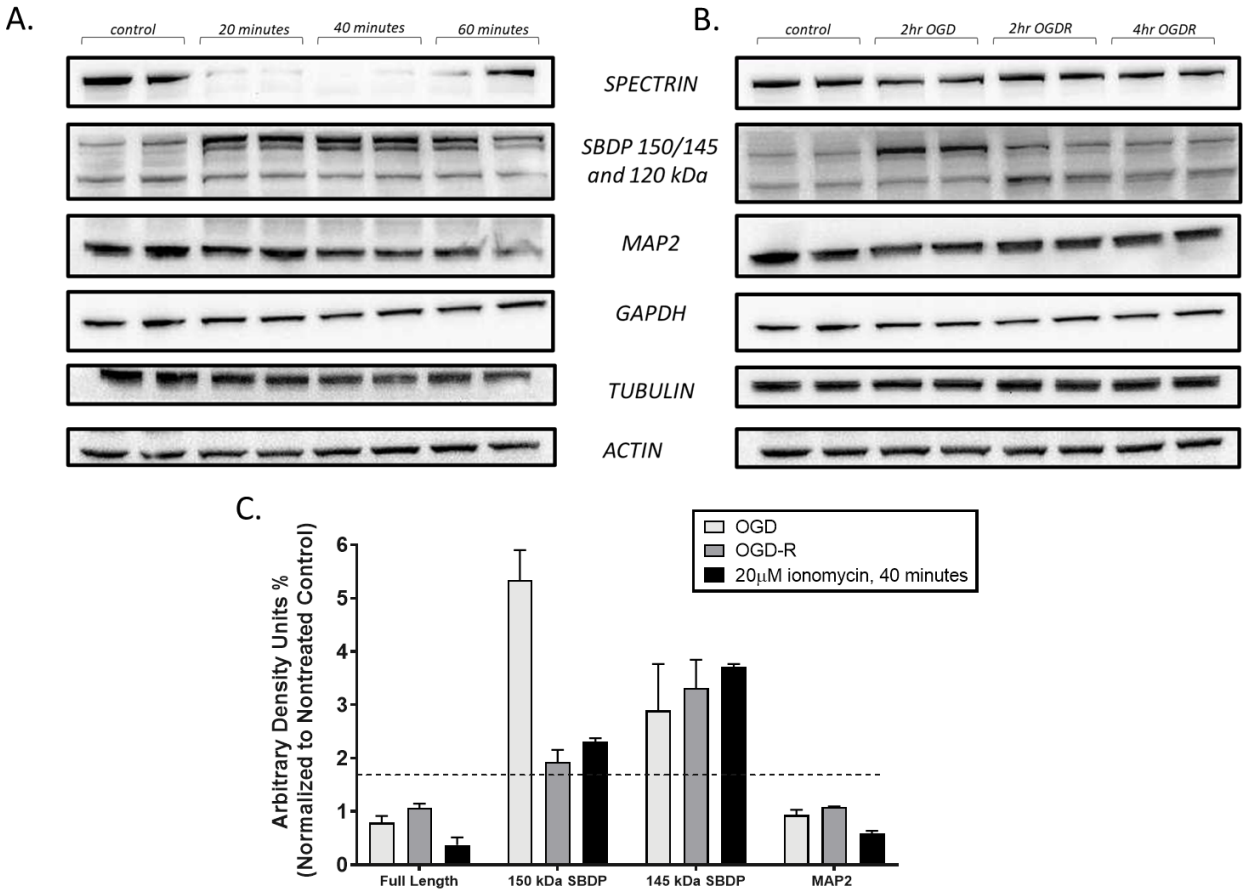

Figure 16. Development of an *in vitro* insult to monitor spectrin breakdown products.
(**A**) Immunoblot of HT22 cells treated with 20μM ionomycin for 0, 20, 40 or 60 minutes and probed with spectrin, microtubule associated protein 2 (MAP2), glyceraldehyde 3-phosphate dehydrogenase (GAPDH), tubulin and actin antibodies. (**B**) Immunoblot of SH-SY5Y cells that underwent 0, 2 or 4 hours of OGD with or without reperfusion and probed with spectrin, MSP2, GAPDH, tubulin and actin antibodies. (**C**). Quantitative analysis of immunoblots with 2 hours OGD, OGD-R and 20μM ionomycin for 40 minutes. Data represents mean ± SEM of at least n=6 biological replicates

1.3.4 Specific Inhibitory Efficacy of Inhibitors

Specific inhibitory efficacy was measured using the treatment of 20μM ionomycin for 40 minutes. These conditions provided the clearest SBDP bands, particularly in separating the nonspecific and specific calpain-1 (SBDP 150 and 145kDa, respectively) bands. Ionomycin-stimulated cells were treated with 10μM of selective (***5***), nonselective (***E64c*** and ***NYC-438***) calpain-1 and selective cathepsin B (***CA-074***) inhibitors in a co-treatment paradigm. The selective calpain inhibitor ***CA-XI*** was used as a positive control. All inhibitors reduced levels of SBDP 150kDa, the calpain-1 and caspase-3 dependent protein, but not significantly (Figure 17). However, for the specific calpain-1 mediated fragment, all selective and nonselective calpain inhibitors significantly reduced levels of SBDP145. ***CA-074*** had no effect on SBD145kDa. This trend was the same for MAP2 degradation, the other substrate mediated by calpain; all selective and nonselective inhibitors ameliorated the decrease in MAP2, but ***CA-074*** had no effect. These results confirmed that the calpain-1 inhibitors had specific efficacy *in vitro.*

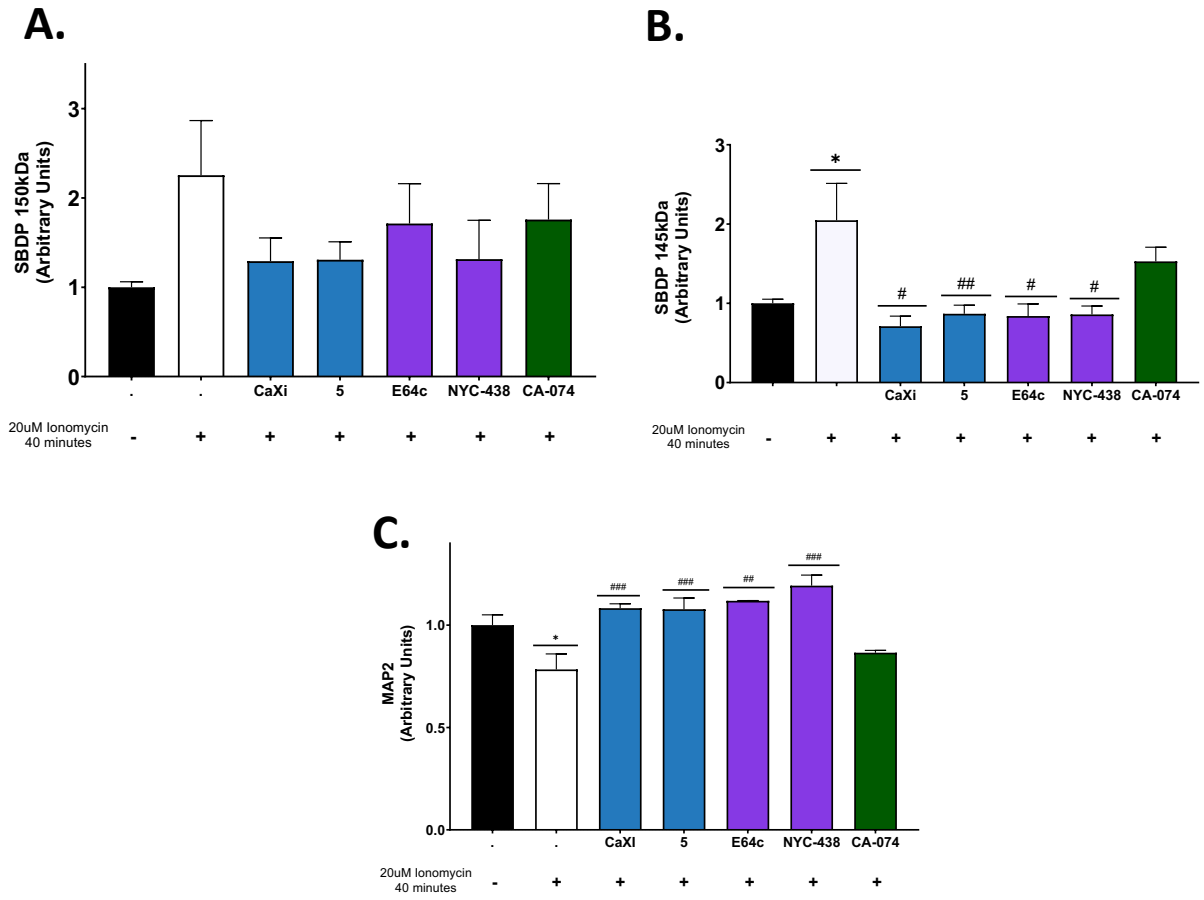

Figure 17. Specific inhibitory efficacy of compounds *in vitro*

(**A**-**C**) Quantification of western blots of HT22 cells co-treated with 10µM inhibitors and 20µM ionomycin for 40 minutes. Proteins quantified were SBDP 150kDa (**A**), SBDP 145kDa (**B**) and MAP2 (**C**). Data represents mean ± SEM of at least n=3 duplicates of cell passages. All protein was normalized to the housekeeping protein, actin. Equal protein amounts were loaded in all lanes of immunoblots. * : compared to nontreated control, # : compared to 20µM ionomycin treated cells. *p<.05, **p<.01, ***p<.001

1.3.5 Serendipitous Discovery of Cathepsin K Inhibitors

The series of cathepsin K inhibitors began with the discovery of ***AJ1-35*** and ***ING-108*** as selective and potent inhibitors (Figure 18). Further chemical development by Drs. Ammar Jastaniah and Irina Gaisina yielded 6 other peptidomimetic compounds that maintained high selectivity against calpain-1, cathepsin B and papain at 1μM (Figure 19). More detailed dose-response curves were performed to collect IC_{50} values and further characterize the compounds (Figure 20).

The addition of a fluoro group on the para position of benzene in the P3/4 position (***AJ1-62***) and the increased flexibility with a CH_2 group in the P3/P4 position reduced potency, but maintained selectivity. Intriguingly, the addition of a CH_2 group between the thiazole and benzene moderately increased inhibition towards calpain-1. When the P2 position was substituted from leucine to a benzyl, regardless of increased flexibility, the potency was completely abolished, with slight inhibition only seen at higher concentrations. The top five inhibitors had IC_{50}s beneath 250nM, with the most potent (***AJ1-135*** and ***ING-108***) at 47.1 ± 1.5 nM and 51.2 nM ± 2.7 nM, respectively (Figure 20). AJ1-0 was found to have no significant inhibition against any cysteine protease screened, indicating the cyanocyclopropyl alone is not enough to induce inhibition.

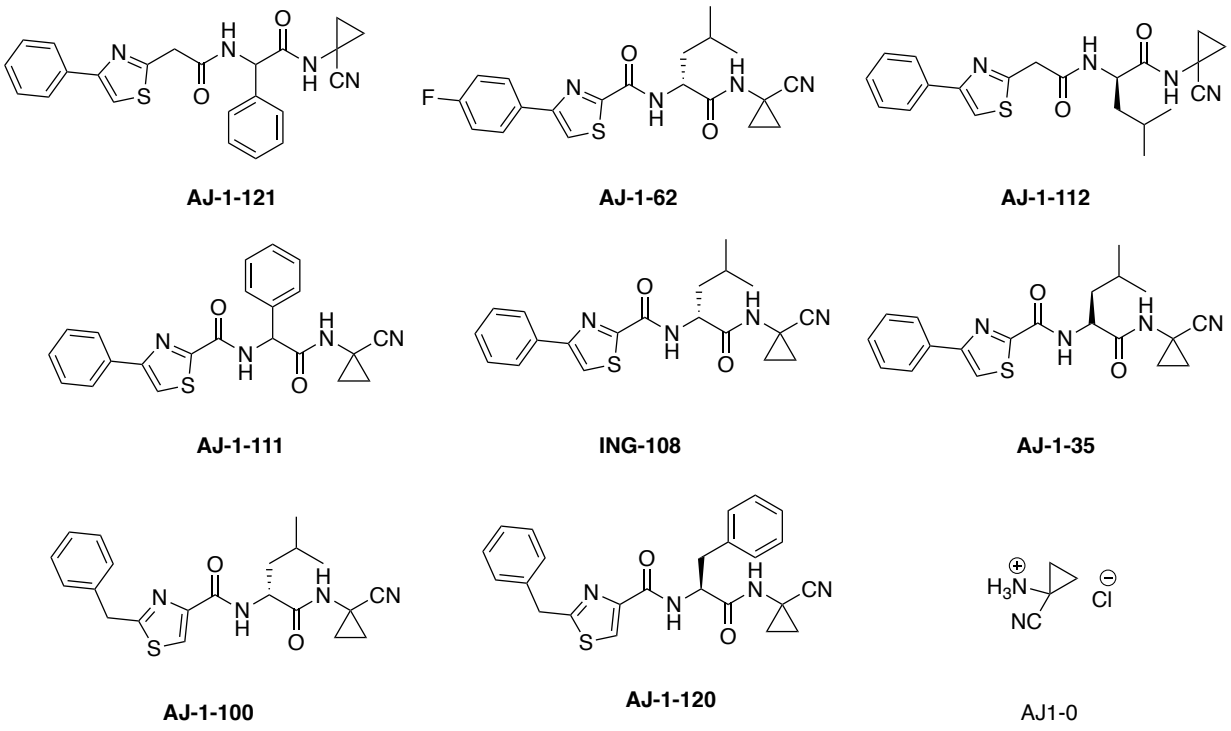

Figure 18. Chemical structures of cathepsin K inhibitors.
Chemical structures of peptidomimetic cyanocyclopropyl small molecule inhibitors of cathepsin K.

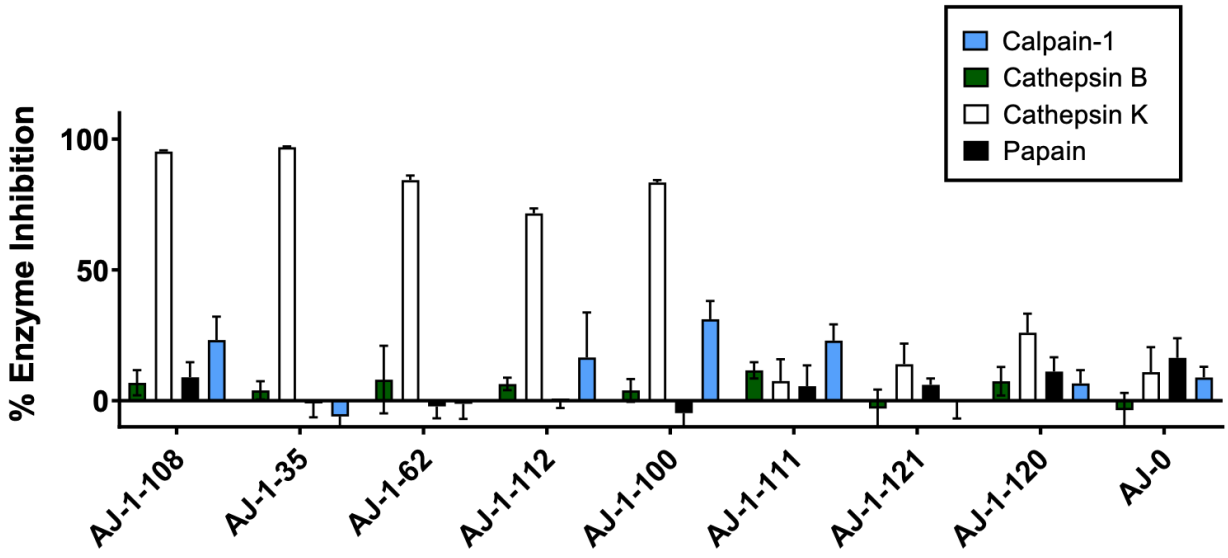

Figure 19. Enzyme profiles of cathepsin K inhibitors
Enzyme inhibition against calpain-1, cathepsin B, cathepsin K and papain. Data represents mean ± SEM of at least n=3 biological replicates

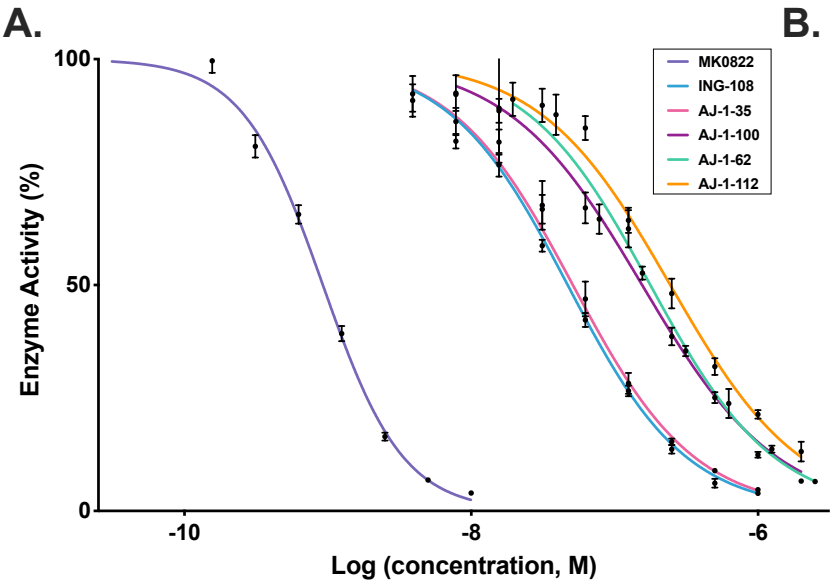

	IC_{50} (nM)
MK0822	.92 ± .03
ING-108	47.1 ± 1.5
AJ-1-35	51.2 ± 2.7
AJ-1-100	156 ± 11.1
AJ-1-62	177 ± 10.3
AJ-1-112	244 ± 15.2

Figure 20. IC_{50} Values of cathepsin K inhibitors
(A) Dose response curves for small molecule inhibitors. (**B**). Calculated IC_{50} values. Data represents mean ± SEM of at least n=3

1.4 CONCLUSIONS

Enzyme assays were developed to establish inhibition profiles of novel peptidomimetic compounds against calpain-1 and cathepsin B. Previous work from the Thatcher group yielded ***NYC-438***, a non-selective irreversible epoxide designed in-house.[9] ***NYC-438*** exhibits high potency against calpain-1 (IC_{50} = 241 ± 34.2nM) and cathepsin B (IC_{50} = 62.2 ± 8.0nM, Figure 21). In our studies, reported selective calpain-1 inhibitors exhibited activity against other proteases at low doses. To this end, we sought to develop a true selective calpain-1 inhibitor.

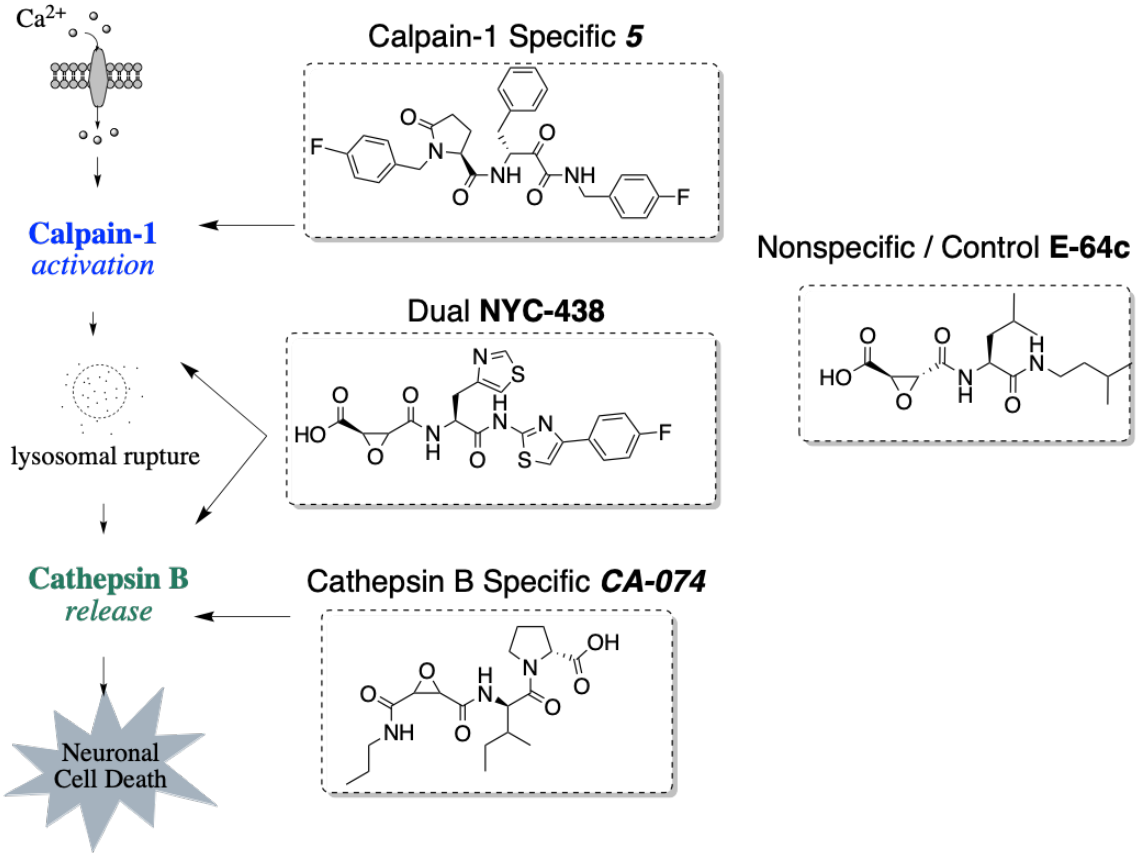

Figure 21. CCH inhibition strategies
The toolkit of inhibitors consisted of ***5***, a calpain-1 specific inhibitor, ***NYC-438***, a dual inhibitor, ***CA-074***, a selective cathepsin B inhibitor and ***E64c***, a nonselective inhibitor control.

A family of α-ketoamide calpain-1 inhibitors (***1-5***) were identified. These compounds displayed high potency against calpain-1, selectivity against all proteases and were reversible. While the enzymatic profiles and IC_{50} values of ***3*** and ***5*** had minimal differences, compound ***5*** was ultimately decided to move forward into *in vitro* and *in vivo* studies (TABLE V). This was because ***5*** contained additional bioisosteres which can enhance PK/PD properties.

Thus, the compounds selected for *in vitro* and *in vivo* studies were ***5*** as the reversible selective calpain-1 inhibitor and ***NYC-438*** as the irreversible dual calpain-1 and cathepsin B

inhibitor (TABLE V). ***CA-074*** was used as a "selective" irreversible cathepsin B inhibitor, with well-reported efficacy in TBI models.[5] Of note, our studies determined ***CA-074*** exhibits moderate activity against cathepsin K, indicating it is not a true "selective" inhibitor. Additionally, ***E-64c*** was selected to be used as a control for an irreversible pan-cysteine protease inhibitor.

TABLE V. SELECTIVITY PROFILES OF COMPOUNDS SELECTED TO MOVE FORWARD TO *IN VITRO* AND *IN VIVO* STUDIES

Selectivity profiles of compounds against Calpain-1, cathepsin B, cathepsin K, and papain

Compound	Inhibitory activity in IC50 (nM) of				(Ir)rev.
	μ-calpain	Cathepsin B	Cathepsin K	Papain	
5	128 ± 7.4	~4000	>10000	>10000	R
NYC-438	241 ± 34.2	62.2 ± 8.0	234 ± 8.2	213 ± 9.6	I
E-64c	247 ± 48.3	5.42 ± 0.7	0.248 ± 15.4	77.8 ± 3.5	I
CA-074	>10000	7.62 ± 7.6	~3000	>10000	I

A major limitation of this study remains the cathepsin B enzymatic assay. This protease is particularly intriguing as its cleavage products alter with pH; at low pH, cathepsin B exhibits exopeptidase activities but at higher pH, such as when its released from the lysosome, it undergoes a conformational change where its occluding loop opens allowing for endopeptidase activity.[122] This extra-lysosomal endopeptidase activity is detected in AD postmortem patients brains and presumed to indirectly exert neurotoxicity. Our enzyme assays do not function at pH higher than 5.5, and thus we may not be correctly determining if our inhibitors are binding to this neurotoxic, endopeptidase, extra-lysosomal form of cathepsin B.

Unfortunately, the cleavage products of the endopeptidase activity are still uncharacterized and thus the exact mechanism of cathepsin B neurotoxicity remains unknown. Some researchers theorize that cathepsin B binds to a complex which has a role in neuroplasticity. This complex, when bound to cathepsin B, cannot function properly, and results in the loss in neuroplasticity leading to cellular death.[5] Other researchers theorize that cathepsin B inhibitors actually hit a different target than cathepsin B. Thus, future studies must incorporate a new kinetic method that accounts for this extracellular activity, or track free cathepsin B intracellularly to determine our cathepsin B inhibitor are binding to conformation of extra-lysosomal cathepsin B.

While this study seeks to develop and characterize selective calpain-1 and dual calpain-1 and cathepsin B inhibitors, we did uncover a series of selective, potent, and reversible cathepsin K inhibitors. Cathepsin K is highly expressed in osteoclasts and able to cleave type I collagen. Intriguingly, a recent report identified a link between cathepsin K and CNS regulation and development.[147] Additionally, Odanacatib, a cathepsin K inhibitor developed for treatment of osteoporosis, was very recently dropped by Merck and Co due to increased risk of cardiovascular events and stroke. [152] Thus, there exists a link between cathepsin K and the CNS. Future research into characterizing the compounds' inhibitory effect on Cathepsin K's collagenase activity through collagenase gels, multiplex cathepsin zymography (*in situ* zymography, gelatin/gel zymograhy*)* and NIR-labelling of collagen for Cath K inhibition would be beneficial for characterization and development of these compounds, followed by studies that carefully analyze their effects in *in vitro* and *in vivo* models of CNS dysfunction.

CHAPTER 2*:* EARLY CONTRIBUTORS TO ADRD: *IN VITRO* AND *IN VIVO* MODELS OF OXIDATIVE STRESS AND MTBI

Partially adapted with permissions from Redox Biology, Interaction of oxidative stress and neurotrauma causes significant and persistent behavioral and pro-inflammatory effects in a tractable model of mild traumatic brain injury. **Knopp, R.**, Lee, S.H., Hollas, M.,, Neomuceno, E., Gonzalez, D., Tam, K.T., Aamir, D., Wang, Y., Pierce, E., BenAissa, M., Thatcher, G.R.J. (2020)

2.1 INTRODUCTION

2.1.1 The Complexity of ADRD

ADRD is a highly complex neurodegenerative disease. Since Dr. Alzheimer's discovery of amyloid plaques and neurofibrillary tangles, scientists have recognized a strong positive correlation between the appearance of these neuropathological hallmarks and clinical signs of late-life dementia. In fact, as examined in Chapter 1, drug discovery for AD has primarily focused on targeting APP fragments, largely driven by theory known as the amyloid cascade hypothesis. This theory implicates amyloid aggregates as the root cause of AD. However, with the increasing number of agents targeting amyloid that have failed clinical trials, researchers have begun to recognize that this model is simply inadequate.[174, 175] This is strongly supported by a plethora of longitudinal clinical-pathological studies that suggest appearance of the neuropathological hallmarks does not definitively correlate with clinical dementia.[176, 177] Furthermore, other longitudinal studies suggest a lot of late-life cognitive decline is driven by factors other than the classical neuropathological hallmarks.[178] Thus, AD must be examined as a highly complex biological and biochemical disease that is multifaceted and cannot exclusively explained by a simple linear model (Figure 22).

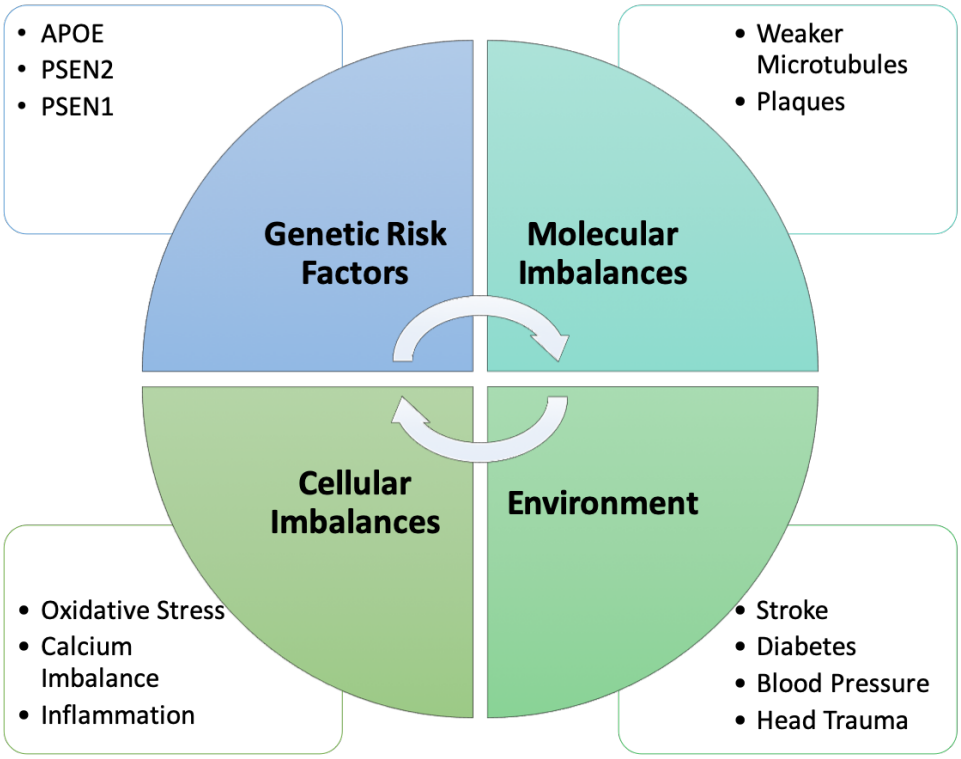

Figure 22. ADRD as a multifactorial disease
Alzheimer's disease and related dementia is a non-linear, multifactorial disease consisting of cellular and molecular imbalances, genetic risk factors and environmental stressors.

The overwhelming majority of AD cases are sporadic (sAD, ~90% of all cases), with the underlying mechanisms and causes unknown.[179] However, the neuropathological and clinical presentations between early-onset familial (fAD) and sAD are often indistinguishable.[180] Since the etiology of sAD is unknown, the overwhelming majority of preclinical models (both *in vitro* and *in vivo*) rely on the known genetic mutations associated with fAD.[179] These models are necessary and valuable as the genetic mutations contribute to AD pathophysiology. However, there is an urgent need to develop non-genetic based preclinical models that rely on other mechanisms associated with loss in cognitive reserve

Adding to the complexity, there is substantial variability amongst individuals in progression of sporadic neurodegenerative diseases, including ADRD.[181, 182] Equally, in neurotrauma, such as stroke and TBI, there is individual variability in secondary sequelae that determines the functional response.[183] This presents a dilemma for development of preclinical models that must demonstrate statistical significance with reasonable sample size, and usually leads to the forfeit of the heterogeneity observed in human patient populations in exchange for a genetically driven homogeneity in the animal model.[184]

2.1.2 Brain Ischemia

Ischemia injury occurs when there is insufficient blood supply to a tissue region, resulting in reduced levels of oxygen, glucose and other essential metabolic substances, which in turn leads to the death of tissue. Ischemia injuries can occur anywhere in the body, but the research presented herein is focused on brain ischemia and its role in neurodegeneration. Brain ischemia is classified as a sub-type of stroke and occurs in two types: focal (confined to a specific region) or global (a wide area of brain tissue).

Multiple cross-sectional studies suggest brain ischemia is a strong risk factor for dementia; patients presenting with post-ischemic brain injury frequently have varying degrees of cognitive deficits.[185] One report found that one fourth of elderly patients three months after ischemic stroke meet the diagnostic criteria for dementia. [185] Furthermore, post-ischemic Alzheimer-type dementia (also known as vascular dementia) is the second most common occurring form of dementia.[186] Patients with post-ischemic brain injury as well as *in vivo* animal models with ischemia-reperfusion injury present with varying degrees of cognitive deficits.[187, 188]

Brain ischemia induces a variety of mechanisms that are present in ADRD including neuronal loss, synaptic dysfunction, accumulation of APP, tau protein dysfunction, white matter

lesions, and neurodegeneration.[189, 190] In fact, some reports propose the production of reactive oxygen species (ROS) is the primary cause of AD-like neurodegeneration following brain injury through increased inflammation, APP accumulation and neuronal energy failure.[191] This, in turn, induces cellular destruction of neurons in the hippocampus and contribute to white matter lesions.[192]

2.1.3 Oxidative Stress

Likely a major contributor to the loss of neural reserve is oxidative stress (OS), which has frequently been linked to neurodegenerative disorders. Oxidative damage mediated by lipid peroxidation products (LPP) has been shown to play a significant role in the early stages and in the progression of mild cognitive impairment (MCI), ADRD and traumatic brain injury (TBI) neuropathy.[193-202] OS appears when cellular free radical-induced damages exceed the amount of endogenous anti-oxidant defenses.[203] The brain is particularly susceptible to the increased production of reactive oxygen species (ROS), likely due to its high oxygen consumption rate, high concentration of polyunsaturated fatty acids (PUFAs), and lower levels of antioxidants. [204]

Many theories of OS in ADRD correlate the increased formation of ROS to the abnormal accumulation of Aβ and tau.[205, 206] One such study by *Butterfield, D.A.* found using *in vitro* and *in* vivo studies that Met-35 of membrane-found $A\beta_{42}$ is critical to OS, as its accelerates free radical formation through allylic H-atom abstraction.[207, 208] Moreover, many studies have reported a positive feedback loop between OS and Aβ and tau; both increased ROS produces aberrant production of Aβ/tau, and increased Aβ/tau accelerates ROS amplification.[205, 206]

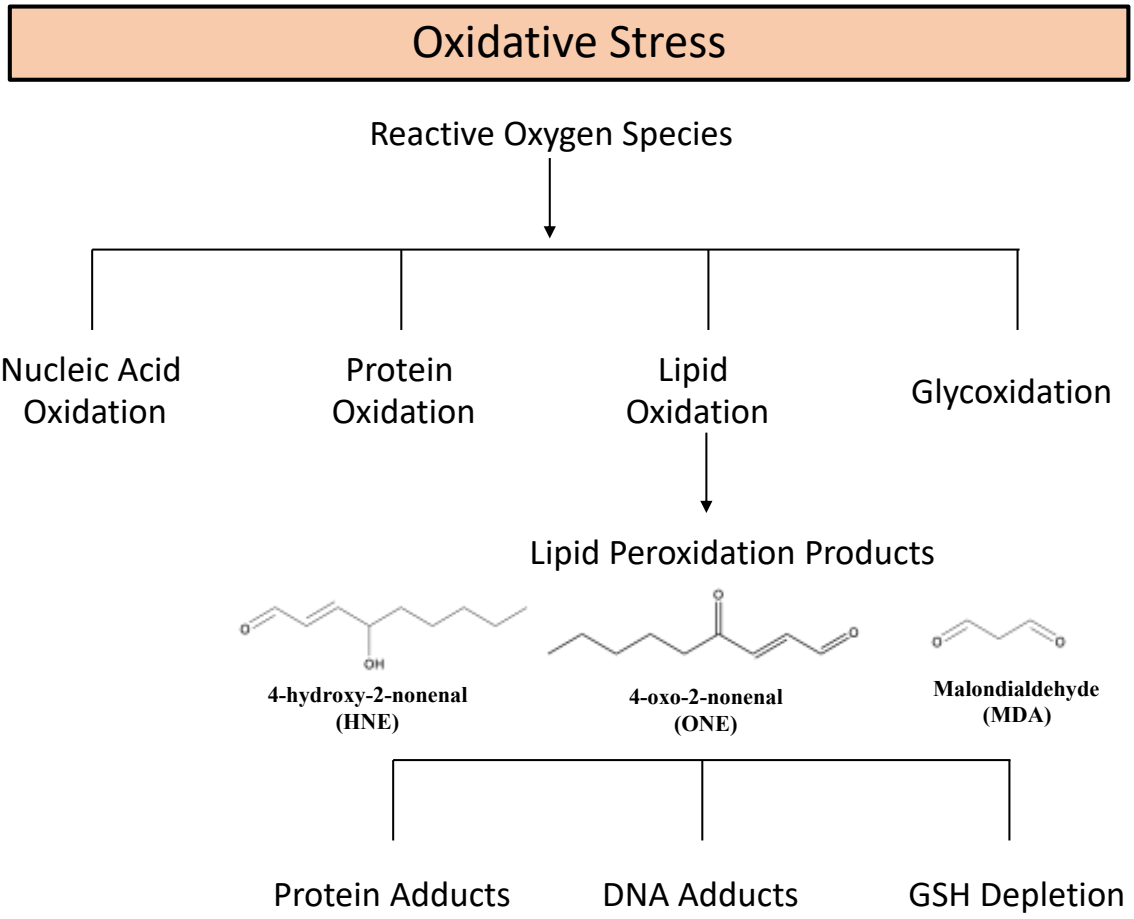

Figure 23. Downstream effects of oxidative stress
Schematic detailing the effects of oxidative stress (via reactive oxygen species, ROS), which induces lipid peroxidation products (LPP), and ultimately protein crosslinking. Chemical structures of various LPPs are shown.

Increased ROS leads to DNA oxidation, protein oxidation, and the appearance of lipid peroxidation products (LPPs, Figure 23). The LPPs, 4-hydroxynonenal (HNE), 4-oxo-2-nonenal (ONE) and malondialdehyde (MDA), among others, are electrophiles that covalently modify and sometimes crosslink proteins and nucleic acids.[209-211] HNE has received most attention because HNE-protein adducts have been shown to be elevated in the amygdala, hippocampus, and parahippocampal gyrus of TBI patients, as well as patients with MCI and early onset AD.[197, 202, 212-218] HNE is a reactive electrophile consisting of an α,β-unsaturated aldehyde produced from peroxidation of the PUFAs linoleic acid and arachidonic acid. It is highly reactive and forms protein adducts via two mechanisms: 1) irreversible Michael addition via the attack of nucleophilic acid at the 3-carbon or 2) reversible Schiff base formation at the free aldehyde.[219] The Michael addition primarily occurs at cysteine residues but can also occur at reactive lysine or histidine residues, while the Schiff base formation occurs almost exclusively with lysine residues.[220]

Amongst pathways of LPP detoxification, the enzyme action of certain glutathione-S-transferases and mitochondrial aldehyde dehydrogenase-2 (Aldh2) are recognized as primary contributors, ablating the reactive, electrophilic alkene and aldehyde groups of HNE, respectively.[221] The *ALDH2*$^{-/-}$ mouse was developed to study Aldh2-mediated metabolism in the liver and is viable and overtly healthy.[222] This mouse was subsequently observed to display a cognitive deficit amenable to pharmacotherapeutic intervention.[223, 224] More widely studied are transgenic mice bearing mutations in *ALDH2.* Loss of function in mitochondrial Aldh2 reduces the capacity of mitochondria and cells to detoxify reactive aldehyde LPPs, such as HNE. Aldh2*2, more commonly referred to as the "Asian allele", is a common loss-of-function mutation in *ALDH2*, proposed to contribute to AD risk in the East Asian population and to *APOE4* risk in AD, and also to risk of Parkinson's disease (PD). [225-229] Twenty percent of transgenic Aldh2*2 mice were reported to develop neurodegeneration after one year which increased to 78% of mice after

1.5 years, without significant defects in motor or sensory functions.[230] The double knockout of *ALDH1A1* and *ALDH2* has been proposed as a model for PD.[231] Preclinical animal models that manifest elevated brain levels of HNE-protein adducts may therefore provide novel and relevant models of the interplay between oxidative stress with attenuated neural reserve.

2.1.4 Traumatic Brain Injury

Traumatic brain injury (TBI) is defined as any disruption of standard brain function provoked by a physical force (jolt, blow, bump, penetrating injury etc.) to the head. TBI has recently been gaining attraction as a risk factor to early onset dementia and ADRD; some researchers even propose TBI is the best-established environmental risk factor. [232, 233] In numerous case-control studies, *Fleminger et al.* found that TBI with sufficient severity to cause loss of consciousness resulted in a 50% increased risk of dementia.[234] Moreover, a longitudinal clinical study by *Plassman et al* evaluated US Navy and Marine veterans with hospitalized cases of TBI or non-TBI injuries during World War II.[235] This study found the veterans with sufficient TBI (loss of consciousness or posttraumatic amnesia that lasted longer than 24 hours) resulted in a 4-fold increase in dementia compared to age-matched controls. Furthermore, those who received a moderate TBI (loss of consciousness or posttraumatic amnesia that lasted between 30 minutes to 24 hours) resulted in a 2-fold increased risk of dementia. Adding to the complexity, repetitive mild TBI (prevalent in contact sports, soldiers, child abuse victims, etc.) has been linked to long-term cognitive dysfunction. [236] Multiple studies have reported increased cellular ADRD markers after repeated TBIs, such as increased tau immunoreactivity in neurons,[237] increased APP, and heightened amyloid levels in a fAD mouse model that was not seen after a single insult.[238]

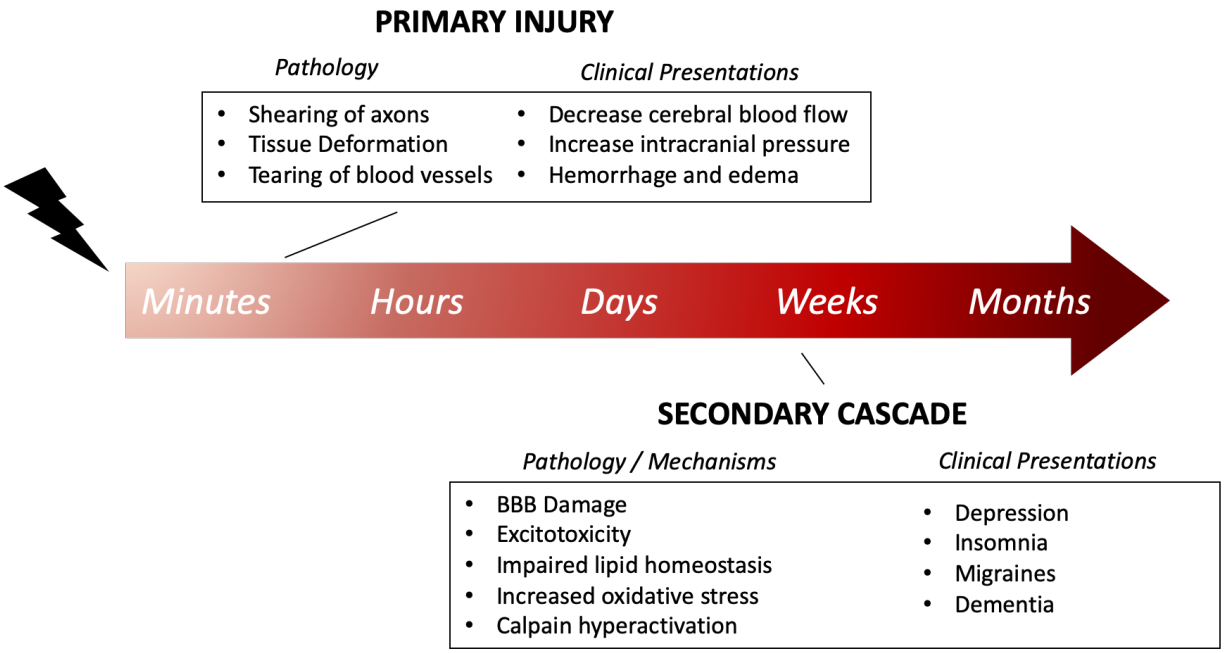

Figure 24. TBI mechanisms: primary injury and secondary cascade
Traumatic brain injury has both primary and secondary mechanisms. The primary injury consists of all damage induced by the blunt insult, i.e. shearing of axons, tissue deformation and tearing of blood vessels. This presents clinically as hemorrhage and increased intracranial pressure, and occurs quickly after injury (minutes to hours). The secondary cascade of events occurs days, weeks and even months following. It comprises dysregulated signaling cascades (calpain hyperactivation, excitotoxicity, impaired lipid homeostasis) can often present clinically with increased migraines, insomnia and early signs of dementia.

Injuries resulting from TBI can be divided into two mechanisms: primary and secondary injury (Figure 24). The primary injury represents the initial blunt physical force of TBI and occurs directly after insult. It includes the shearing of axons and blood vessels, as well as tissue deformation.[239] Clinically it can present as intracranial hematoma, skull fractures, coup and contrecoup contusions, increased intracranial pressure and laceration.[240] Very little can be done to mitigate primary injury except preventative measures (i.e. wearing a helmet). However, secondary

injury can occur hours or days following injury, and is an indirect result of the primary injury that causes long-term detrimental problems. These result from mechanisms initiated from the trauma, and includes ischemia, hypoxia, edema, mitochondrial dysfunction, excitotoxicity, oxidative stress, inflammation and necrosis. As many of these mechanisms can be modulated by therapeutics, the majority of drug discovery for TBI focuses on targeting this secondary cascade.

A variety of *in vivo* TBI models exist, each with varying degree of severity. The most subtle, mild *in vivo* method is the closed-skull free weight-drop model. It inflicts mild TBI (mTBI) by dropping a free weight from a designated height on an intact skull.[241] Other methods of increased severity include the controlled cortical impact (CCI),[242] fluid percussion injury (FPI),[243] blast[244, 245]and ballistic [234] (TABLE VI). All can be classified as moderate or severe dependent on the intensity. CCI delivers an impact *via* a controlled air piston in a defined region on the skull. FPI, the oldest and most commonly used, induces injury through a craniectomy after a fluid pressure pulse. The fluid pulse is generated by the strike of a pendulum hitting the piston of a fluid reservoir. Blast injury results from the primary injury of a blast, while ballistic is caused by the primary injury of a high-velocity projectile.

TABLE VI. *IN VIVO* TBI METHODS AND THEIR ASSOCIATED LEVELS OF SEVERITY

	Mild	Moderate	Severe
Closed Skull	✓		
CCI		✓	✓
Fluid Percussion Injury		✓	✓
Blast		✓	✓
Ballistic		✓	✓

This research utilized the closed-head free weight drop model of mTBI. The main advantage of using this mTBI model, aside from the experimental ease and low cost, is that the severity of insult can be altered by adjusting the mass of the weight and height of impact. However, the largest challenge remains finding the balance where the model translates to clinical presentations of mTBI patients. The first instance of the non-surgical closed-head weight drop model was developed by *Feeny et. al*., and used in rats.[246] Reports indicated the appearance of hemorrhages at the contusion site, and thus *Marmarou et. al*. modified this method by having a heavy weight (450 gram) drop through a Plexiglas guide tube, thus developing a novel model of diffuse brain injury.[247] To prevent skull fracture, a stainless-steel disc was cemented onto the skull; however, many believed this elevated the trauma to moderate or severe. [248]

2.1.5 Objectives

Calpain-1 and cathepsin B have both independently and concurrently been investigated as therapeutic targets in numerous fAD models. ***E-64***, a pan-cysteine protease inhibitor, restored synaptic function in hippocampal slices from *APP/PS1* mice.[127] ***E-64*** was further developed to ***E-64d***, a reported selective cathepsin B inhibitor, and was shown to attenuate cognitive deficits and reduce Aβ levels in transgenic (Tg) mice that incorporated the wild-type, but not Swedish mutant, beta-secretase site of APP.[131] Of note, our kinetic assays revealed that ***E-64d*** maintained its promiscuity towards all proteases. Moreover ***A-705253***, a calpain-1 inhibitor, reversed cognitive deficits and reduced tau phosphorylation in the 3xTgAD mouse model. [10, 130] Lastly ***NYC-438***, a potent and irreversible inhibitor of calpain-1 and cathepsin B, significantly reversed cognitive deficits and restored long-term potentiation in the *APP/PS1* mouse model.[130] Intriguingly, there was no change in Aβ deposition levels, indicating calpain/cathepsin inhibition strategies are involved in mechanisms of cognitive resilience.

The objective of this chapter was to test the tool-kit of inhibitors developed in Chapter 1, and characterize their efficacy in numerous *in vitro* and *in vivo* models. A running theme in this research is the complexity of ADRD. Furthermore, as demonstrated by ***NYC-438***, CCH inhibition strategy may work in mechanisms of resilience. Thus, we sought to test our inhibition strategies in numerous models, either modeling neurodegeneration itself, or incorporating the loss of neural resilience.

Specific chapter objectives:

1. Determine neuroprotection profiles of inhibitors at varying treatment paradigms
2. Differentiate efficacy of treatment strategies in an *in* vivo model of cognitive-deficits
3. Characterize the role of LPP-mediated neurodegeneration
4. Ascertain the effect of inhibition strategies on mitigating neuroinflammation

5. Understand the role of additive "hits" in *in vitro* and *in vivo* assays
6. Establish specific inhibitory efficacy of calpain inhibitors *in vivo*

2.2 METHODS

2.2.1 Cell Culture

Human neuroblastoma SH-SY5Y cells (ATTC CRL-2266), CCF-STTG1 cells (ATTC CRL-1718) were cultured in DMEM/F12 (Gibco) and supplemented with 10% fetal bovine serum (Gemini Bio) and 1% penicillin-streptomycin at 37°C in a humidified atmosphere of 5% CO_2. Mouse hippocampal HT22 cells (Kind gift from Dr. Dargusch, Salk Institute) were cultured in DME and supplemented with 10% fetal bovine serum and 1% penicillin-streptomycin at 37°C in a humidified atmosphere of 5% CO_2. Primary human hippocampal cells (cat # 1540) were purchased from ScienCell Research Laboratories (California, USA), seeded and grown according to manufacturer's instructions. Primary neurons were seeded on a poly-L-lysine coated plate (2 $\mu g/cm^2$), and grown to confluence (2-3 weeks) with media changes every other day. Prior to studies, primary cells were replaced with serum-free media three days prior. For cytotoxicity studies, cells were seeded at 2 x 10^4 cells per well in a 96-well plate in low serum media (1% fetal bovine serum). After overnight incubation, cells were administered with varying concentrations of compounds for defined periods of time. Cell viability was determined by MTS using CellTilter 96® Aqueous One Solution Cell Proliferation Assay or MTT (Methylthiazolyldiphenyl-tetrazolium bromide, Millipore Sigma) and LDH release using CytoTox 96® Non-Radioactive Cytotoxicity Assay (Promega) according to the manufacturer's instructions. Untreated cells served as a negative control as DMSO concentrations were below 0.5%. The experiments were performed in triplicate.

2.2.2 Oxygen-Glucose Deprivation and Reperfusion

SH-SY5Y cells are plated in a 96-well plate at 4 x 10^4 cells per well and cultured overnight. To trigger 'ischemia', cell media is replaced with glucose-free media and incubated in a hypoxic chamber (95% N_2, 5% CO_2, <0.5% O_2). At OGD termination, cells are reperfused and replenished with glucose-containing media (Figure 12). Compound concentration is kept consistent throughout media changes. Cell viability is monitored after 24 hours of 'reperfusion', quantified by MTS and confirmed via LDH release (Promega, according to manufacturer's instructions). In every experiment, sulforaphane, is used as a control. HT22 cells are plated at 5 x 10^5 density

2.2.3 Cellular Immunofluorescence

To measure confluence cells were treated with 5 μM Cell Tracker Red CMTPX (C34552, ThermoFisher) for 30 minutes, then washed and fixed with 4% paraformaldehyde and 0.1% Triton X-100 in PBS for 5 minutes. Cells were then washed and treated with 5uM Hoeschst 33342 (Invitrogen) in Fluorobrite DMEM (A1896701, Fisher). Images were captured on the Celigo microscope or BZ-X700 microscope (Keyence), and confluence was quantified using Keyence software. All OGD-R studies were performed in the absence of fetal bovine serum.

2.2.4 Real Time qPCR

A more detailed protocol is written in Chapter 3. Briefly, RNA was isolated according to the manufacturer's instructions (Qiagen kit) and reconstituted in 30 μL of H_2O. First strand cDNA synthesis was synthesized with 2 ug total RNA using the SuperScript III First-Strand Synthesis System for qRT-PCR (Invitrogen) according to manufacturer's instructions. Inflammation primers were acquired from Applied Biosystems. Each PCR reaction was carried out using the Taqman Gene Expression Master Mix (Applied Biosystems) on the StepOnePlus Real Time PCR system

(Life Technologies). $\Delta\Delta C_T$ values for each gene were normalized to the expression level of β-actin in each sample. Genes used are indicated in TABLE VII.

TABLE VII. PRIMERS UTILIZED FOR INFLAMMATION STUDIES

Gene Symbol	Gene Name	UniGene ID	Product Number	Probe
ACTB	Actin, beta	Mm.328431	Mm01205647_g1	VIC
COX2	Cytochrome c oxidase subunit II	n.s.	Mm03294838_g1	FAM
IL-1β	Interleukin 1 beta	Mm.222830	Mm00434228_m1	FAM
IL-6	Interleukin 6	Mm.1019	Mm00446190_m1	FAM
NOS2	Nitric oxide synthase 2, inducible	Mm.2893	Mm00440502_m1	FAM
TNFα	Tumor Necrosis Factor	Mm.1293	Mm00443258_m1	FAM

2.2.5 Animals

All animal care and procedures were conducted with approved institutional animal care protocols and in accordance with the NIH Guide for the Care and Use of Laboratory Animals. All animal protocols were approved by the University of Illinois at Chicago Institutional Animal Care and Use Committee (ACC#17-029). The experiments use progeny of the *ALDH2*$^{-/-}$ mice originally generated by gene targeting knockout by Kitagawa et al[222], which were then backcrossed with

C57BL/6 mice for more than 10 generations. Wildtype (WT) littermates and knockout mice are generated from mating heterozygotes and genotyping the progeny by PCR analysis of genomic DNA extracted from ear punches. As no sex differences were observed in any of the memory tasks, both male and female mice were combined for all studies. All treatments were via intraperitoneal injection (i.p), unless otherwise noted.

2.2.6 Step Through Passive Avoidance

Step through passive avoidance (STPA) was performed on 8-10 week old C57Bl/6 mice (Charles River's Laboratories) and modified from previous literature.[249, 250] No difference between male and female mice was observed, thus both were used for the study. Scopolamine (1mg/kg) dissolved in saline was administered via *i.p*. injection 30 min prior to training phase, and drugs were administered 20 minutes prior.

2.2.7 Closed Head mTBI

Protocol was modified from previous literature. [251] Mice were anesthetized with isoflurane (5% flow rate) and immediately placed under the vertical 30cm long guide tube and stabilized by a sponge cushion. A 30g weight with a rounded tip (34 x 13mm) was dropped vertically through the tube and directed to the right sagittal plane between the eye and the ear, inducing a unilateral injury on the intact scalp.

2.2.8 *Tissue Preparation*

Mice were sacrificed using CO_2 asphyxiation, perfused with ice-cold PBS, brains extracted and split into 2 hemispheres (ipsilateral vs. contralateral), flash frozen in liquid nitrogen, and stored at -80°C for further protein or RNA extractions. Brains were homogenized in Trizol (Invitrogen) using a hand-held pestle homogenizer and spun at 10,000 x g for 10 min at 4°C to remove cellular debris.

2.3 RESULTS AND DISCUSSION

2.3.1 OGD-R as an in Vitro Model for Ischemia-Reperfusion Injury

Neuroprotection profiles of inhibition strategies were assessed utilizing *in vitro* oxygen-glucose deprivation and reperfusion (OGD-R), a well-characterized model of ischemic stroke that closely mimics *in vivo* models of brain ischemia and reperfusion (Figure 25).[252] This model produces OS, a vital initiator of neuronal injury following ischemia-reperfusion injury.[253] We began by optimizing conditions with the SH-SY5Y cells, a human neuroblastoma cell line.

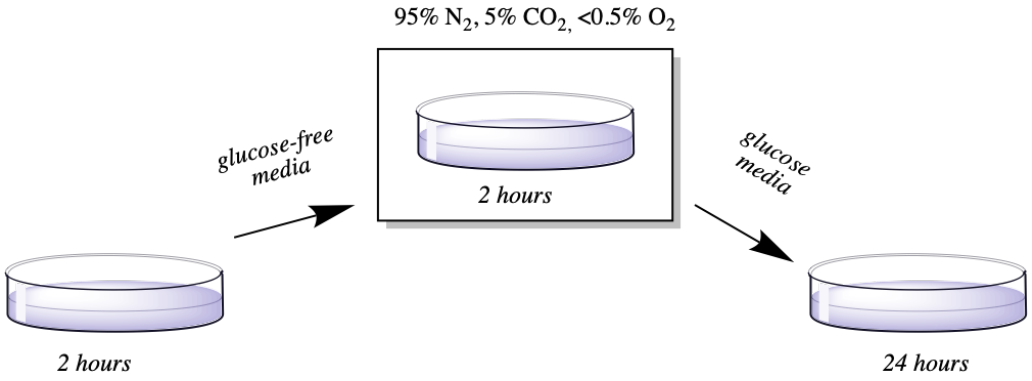

Figure 25. Schematic of the OGD-R assay
Representative diagram of the OGD-R methodology. Briefly, cells are deprived of glucose (via glucose-free media) and oxygen (via a hypoxia chamber) for 2 hours, then restored to normal conditions for 24 hours.

SH-SY5Y cells underwent varying lengths of OGD (0, 1, 2, 4 or 6 hours), and 24 hours of reperfusion, with cell viability monitored using the MTS assay. We observed an inversely proportional relationship between the increasing lengths of OGD-R and remaining cell viability (Figure 26A). This confirmed that the OGD-R model is an *in vitro* model for neurodegeneration. Moreover, we varied the time of reperfusion (0, 1, 2, 3, 24 hours) following 2 hours of OGD (Figure 26B). Cell viability was most affected directly after OGD (~60%), and increased following reperfusion (~80% after 24 hours) suggesting that reperfusion employs some mechanisms of recovery.

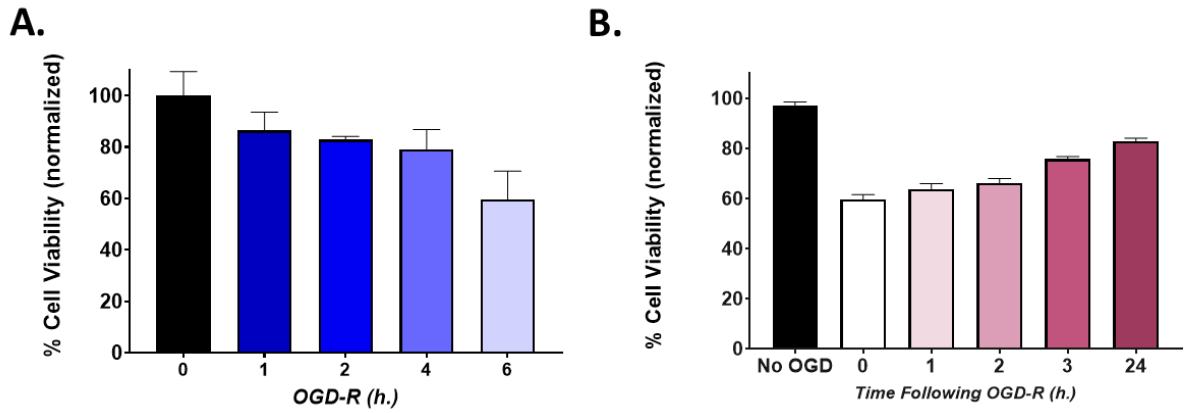

Figure 26. Dynamic changes in cell viability following varying lengths of OGD and reperfusion on SH-SY5Y cells
(**A**) Cell viability following 0, 1, 2, 4 and 6 hours of OGD and 24 hours reperfusion. (**B**) Cell viability remaining after 2 hours OGD and 0, 1, 2, 3 or 24 hours reperfusion. Data represents mean ± SEM of at least n=6 replicates.

We decided to move forward with the OGD-R paradigm of 2 hours OGD and 24 hours reperfusion, as it produces a modest, albeit significant drop in cell viability. In all assays, sulforaphane, a NFE2-related factor2 (Nrf2) activator, was used as both a positive and negative control as prior literature from our lab showed differences with 1 and 10μM against primary neuronal cultures.[254] Our studies found that these results extended to SH-SY5Y cells at three treatment paradigms: pre-treatment (2 hours prior), ischemia (immediately prior), and reperfusion (directly following OGD-R). 1μM sulforaphane was protective at all three paradigms (121.2 ± 4.9%, 113 ± 4.2%, 113.8 ± 3.5%, respectively, Figure 27) compared to nontreated control (Figure 27). Additionally, 10μM sulforaphane was neurodegenerative at all three paradigms (58.2 ± 5.9%, 62.7 ± 3.4%, 87.2 ± 2.5%, respectively) compared to nontreated control.

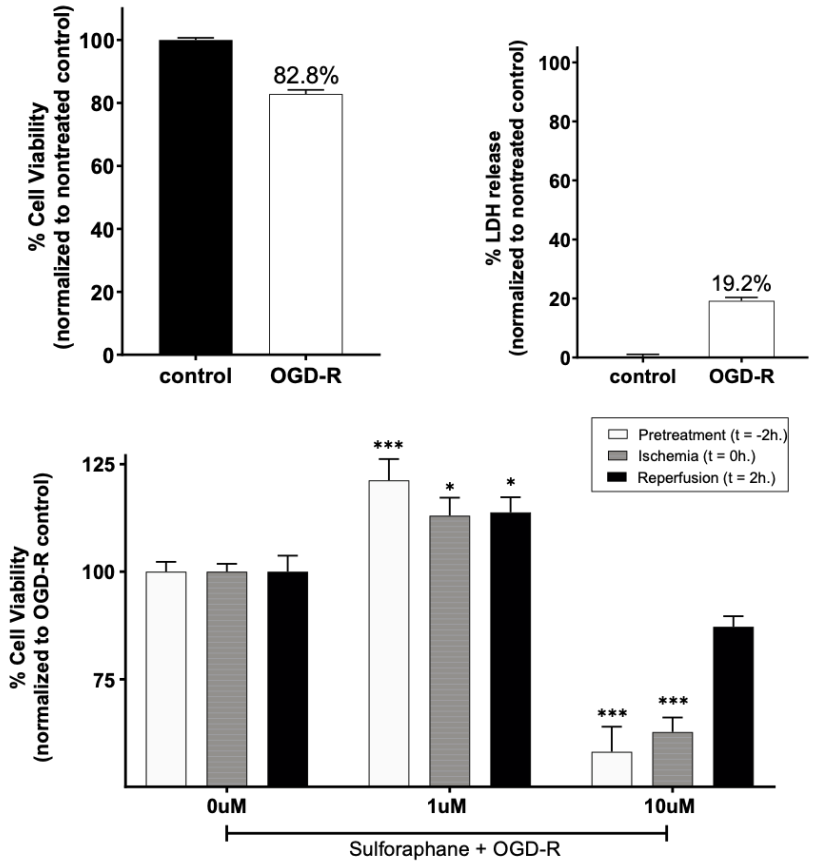

Figure 27. Sulforaphane as a positive and negative control in the OGD-R assay
(**A**) Cell viability quantified MTS of SH-SY5Y cells treated with 2 hours of oxygen-glucose deprivation and 24 hours reperfusion (OGD-R) and nontreated controls. (**B)** LDH release of SH-SY5Y cells treated with OGD-R and nontreated controls. (**C**) OGD-R of SH-SY5Y cells treated with 1 or 10µM at pre-treatment *(t*=-2h.), ischemia (*t*=0h.) or reperfusion (*t*=2) treatment paradigms. Data represents mean ± SEM of at least n=6 replicates analyzed by one-way ANOVA with Dunnett's or Tukey's multi-comparison analysis

Cells were visualized utilizing a cell tracker to qualitatively analyze treatment with sulforaphane (Figure 28). Directly following OGD (*t*=2h.), SHSY-5Y cells visually appear the same with all concentrations of sulforaphane. After 24 hours of reperfusion (*t*=26h.), the well treated with 10µM sulforaphane treatment appeared to have significantly more viable cells, as evidenced by an increase in green fluorescence, while the well treated with 1µM had significantly less fluorescence than the nontreated control.

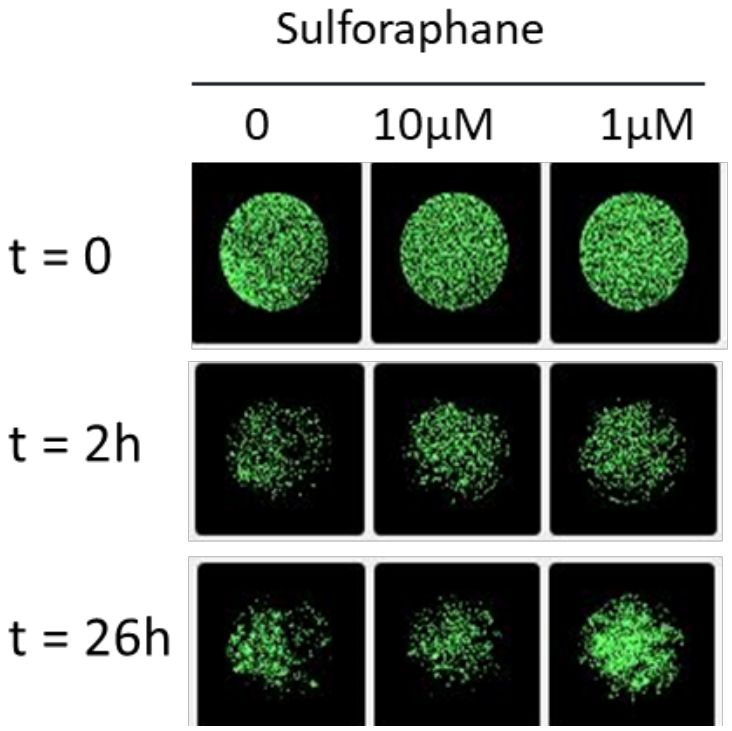

Figure 28. Cell confluency following sulforaphane treatment
SHSY-5Y cells were treated with 0, 1 or 10µM Sulforaphane then underwent OGD-R, with cells fixed, permeabilized then stained with green cell tracker and imaged on the Celigo at 0, 2 or 26 hours.

Results were confirmed using a secondary cell line. OGD-R induces an exacerbated loss in cell viability in the HT22 cells (67.51 ± 4.18 %, Figure 29A). Similar to SH-SY5Y cells, sulforaphane (1 and 10 μM) was both a positive and negative control at all treatment paradigms (Figure 29B). As the effect of OGD-R in SH-SY5Y cells was more subtle, and has more relevance being a human cell line, inhibition strategies were tested in these cells.

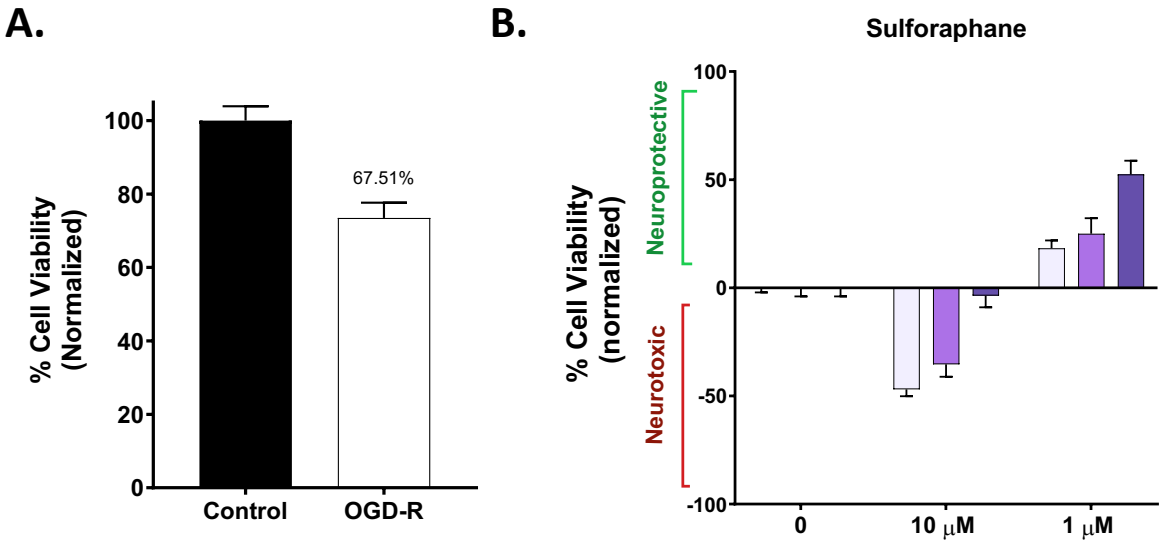

Figure 29. Sulforaphane as a positive and negative control after OGD-R on HT22 cells
(**A**) Cell viability quantified MTS of HT22 cells treated with 2 hours of oxygen-glucose deprivation and 24 hours reperfusion (OGD-R) and nontreated controls. (**B**) OGD-R of HT22 cells treated with 1 or 10μM at pre-treatment *(t*=-2h.), ischemia (*t*=0h.) or reperfusion (*t*=-2) treatment paradigms. Data represents mean ± SEM of at least n=6 replicates analyzed by one-way ANOVA with Dunnett's or Tukey's multi-comparison analysis

2.3.2 Calpain-Cathepsin Inhibitors are Protective against Oxygen Glucose Deprivation

The ability of the inhibitors to protect against OGD-R loss was assessed at three various treatment paradigms. Compounds evaluated were ***5,*** the selective calpain-1 inhibitor, ***NYC-438***, the nonselective inhibitor and ***CA-074***, the selective cathepsin B inhibitor. ***E64c*** was used as the pan-cysteine protease inhibiton control. In our studies, we found all compounds to be neuroprotective at the pre-treatment and ischemia paradigms (Figure 30) when treated at 10μM. Intriguingly, ***CA-074*** was the only CCH inhibitor with significant neuroprotection in the post-treatment paradigm (178.3 ± 68.2%, Figure 30), though all strategies exhibited a moderate level of protection.

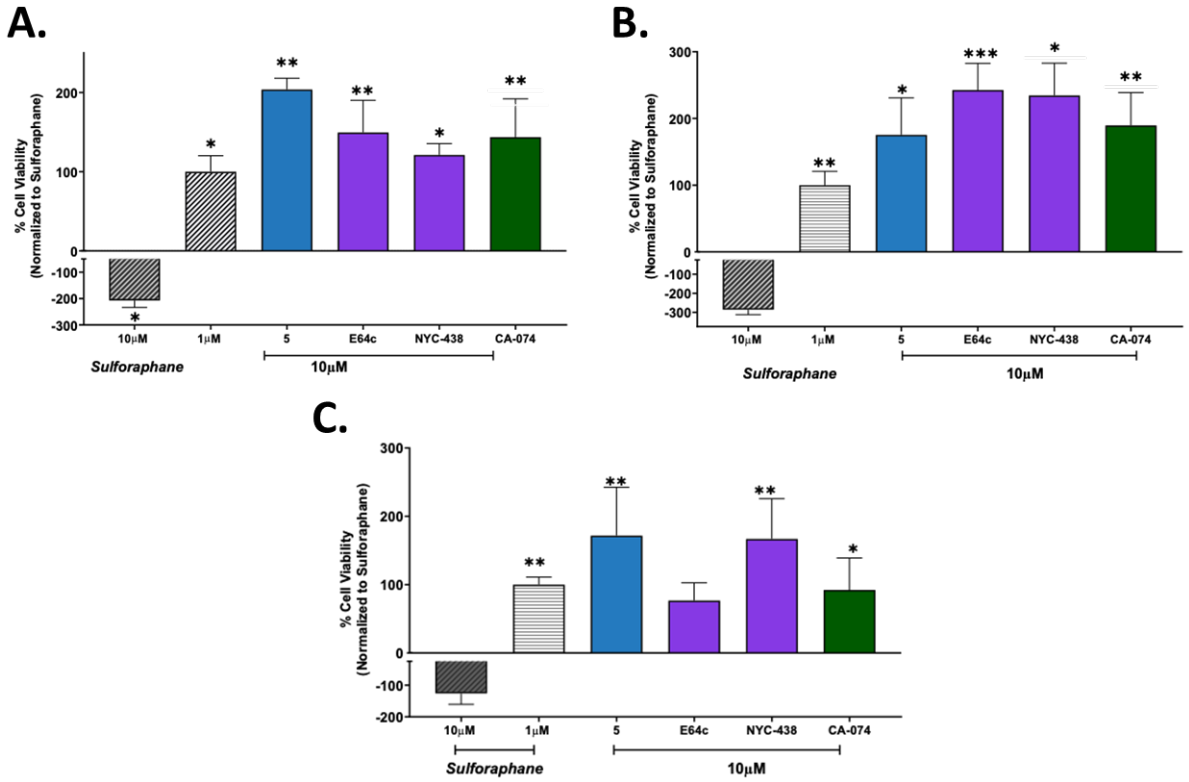

Figure 30. Neuroprotective profiles of 10μM inhibitors against OGD-R in SH-SY5Y cells. (**A-C**). Cell viability quantified by MTS release of SH-SY5Y cells following OGD-R with treatment of sulforaphane or 10μM inhibitors at varying treatment paradigms: pretreatment (*t*=-2h, **A**), ischemia (*t*=0, **B**), or reperfusion (*t*=2h, **C**). Figures were normalized to 1μM sulforaphane treatment at 100% and vehicle control at 0%. Data represents mean ± SEM of at least n=6 replicates analyzed by one-way ANOVA with Dunnett's or Tukey's multi-comparison analysis. *p<.05, **p<.01, **p<.001 *v.* nontreated control.

While neuronal cell lines are a valuable resource, utilizing primary neuronal culture can be more advantageous as they are not transformed and immortalized, thus potentially more characteristic of neuronal cells *in vivo.*[255] However, primary cells are more challenging, time-consuming, expensive, and limited as they are mortal, residing in the non-replicative G0 state. Thus, we only assessed neuroprotection at the ischemia paradigm with select inhibitors in primary neurons. The primary cells exhibited a similar response to OGD-R, with a slight loss of cell death (82.9 ± 3.5%, Figure 31A) and increase in LDH release (17.8 ± 1.5%, Figure 31B).

Administration of the CCH inhibitors at the ischemia paradigm showed dose-dependent neuroprotection of all inhibition strategies (Figure 31C). Significant neuroprotection was seen at the 10μM dose, but not 1μM. Our results concur with previous literature that targeting the CCH, which posits overactivation of these cysteine proteases in neurodegeneration, has therapeutic efficacy in *in vitro* ischemia-reperfusion injury at various treatment paradigms (pre, at, and post).[256, 257]

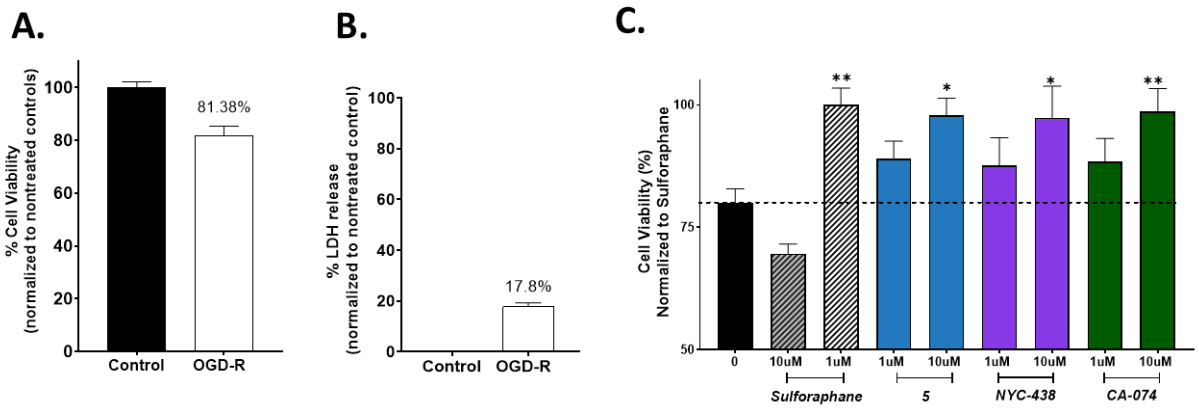

Figure 31. Neuroprotective properties of inhibition strategies in primary human neurons (**A**) Cell viability quantified by MTS of primary human hippocampal neurons treated with OGD-R and nontreated controls. (**B**) LDH release of primary human hippocampal neurons treated with OGD-R and nontreated controls. (**C**) Cell viability quantified by MTS release of primary human hippocampal neurons following OGD-R with treatment of sulforaphane or 10μM inhibitors at the ischemia paradigm (*t*=0). Data represents mean ± SEM of at least n=6 replicates analyzed by one-way ANOVA with Dunnett's or Tukey's multi-comparison analysis. *p<.05, **p<.01, **p<.001 *v.* nontreated control.

2.3.3 Calpain-Cathepsin Inhibitors Attenuate Scopolamine-Induced Cognitive Deficits

A recent report indicated calpain-1 inhibition reverses scopolamine-induced cognitive deficits.[258] This study theorized the effects were due to improved cholinergic function which translated into enhanced behavioral performance. However, this mechanism is ambiguous as calpain/cathepsin inhibitors exhibit poor brain bioavailability (see Chapter 3). Thus, the theoretical basis for this observation is unclear and may be associated with the inhibitor chemotype, or an interaction on brain endothelial cells (BECs). After completing other *in vivo* studies, we propose these results may be due to eNOS, a signaling molecule increased by calpain-1 inhibition (see Chapter 3).

The ability of selective (***3***) and nonselective (***E-64d)*** inhibitors to reverse cognitive deficits was evaluated with the step-through passive avoidance (STPA). This assay exploits the natural tendency of mice to enter dark surroundings. The mice undergo habituation followed by training of the apparatus, which involves numerous sessions to train mice to remain in the illuminated compartment by provoking an electric shock if they migrate to the dark compartment. Scopolamine is an FDA-approved treatment for motion sickness, and is well-known agent to induce amnesia in mice.[249] Scopolamine was administered 30 minutes prior to the testing phase based on literature. Compounds (***3*** and ***E-64d***) were administered 20 minutes prior to the testing phase.

GT-1061 is a NO-mimetic synthesized by our lab. This compound is part of a family of novel nitrates with reported neuroprotection and memory-enhancing properties, and entered Phase 1 clinical studies for AD.[250, 259, 260] ***GT-1061*** has demonstrated efficacy in reversing scopolamine-induced cognitive deficits and was thus used as a positive control in our studies.[261]

Scopolamine administration caused a significant reduction in latency to enter the dark compartment (Nontreated: 256 ± 20.38, Scopolamine: 57.13 ± 20.26, Figure 32). This was significantly attenuated by both selective and nonselective inhibitors (***3***: 193.1 ± 42.77, ***E-64d***: 187.1 ± 27.46). Unfortunately, no superior targeting strategy was observed.

To note, compound ***3*** was used in this experiment, as much of the work presented in this thesis was performed simultaneously. When this experiment was in progress, compound ***5*** had not yet completed chemical synthesis nor enzyme profiling.

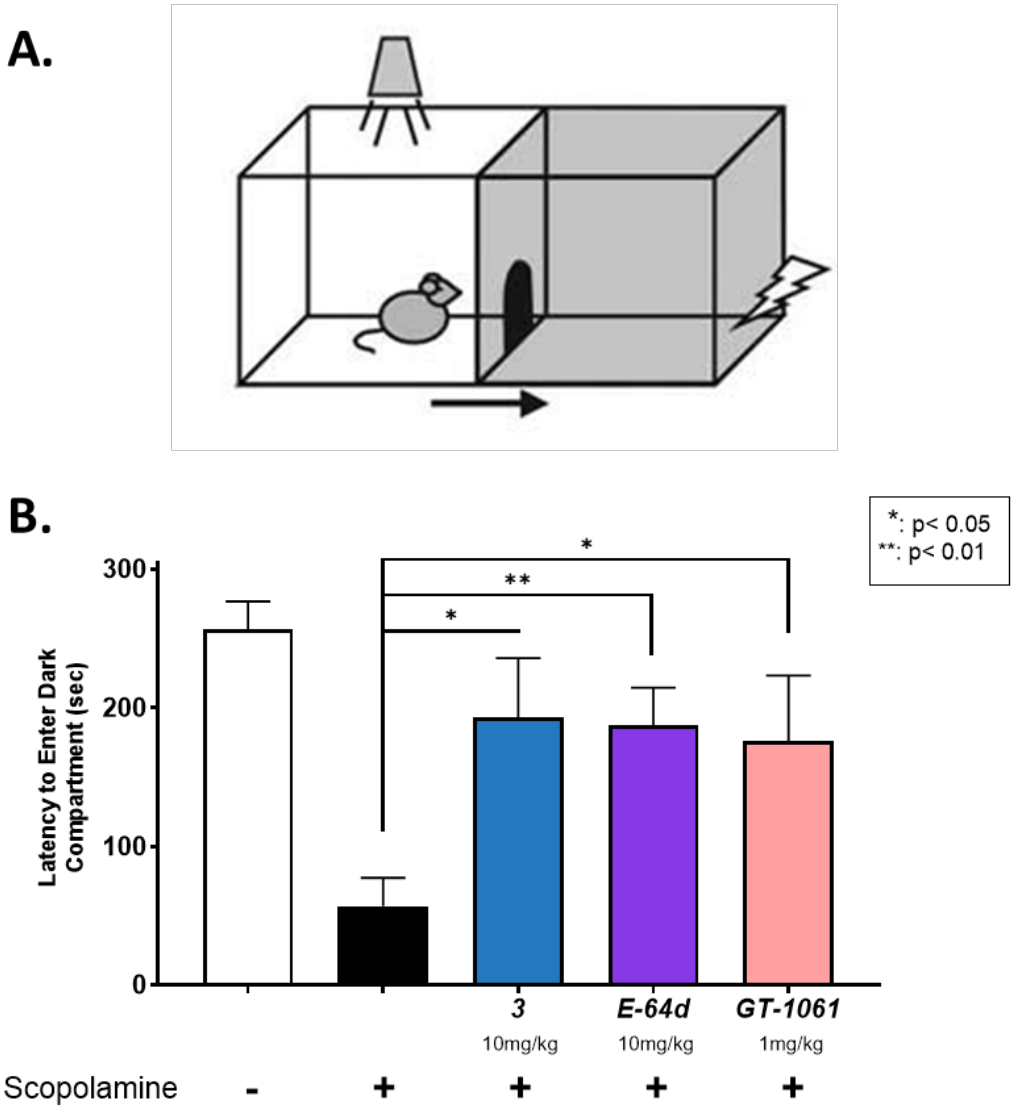

Figure 32 CCH inhibitors attenuate scopolamine-induced cognitive deficits in the STPA fear-conditioning experiment

(A) Schematic representation of the step-through passive avoidance (STPA) chamber. (B) Quantitative analysis of the latency of C57Bl/6 mice to enter the dark compartment of the chamber (sec). Mice were treated with 1mg/kg scopolamine 30 minutes prior to the training phase, then treated with ***3*** (10mg/kg), ***NYC-438***(10mg/kg), and ***GT-1061*** (1mg/kg) were administered 10 minutes prior to the training phase. Data represent mean ± SEM with n=6-9 mice.

2.3.4 Inhibition Strategies Mitigate In Vitro TNF-a and LPS-Induced Neuroinflammation

Reports indicate calpain-1 and cathepsin B mediates neuroinflammatory signaling cascades.[262] In fact, inflammatory agents can induce calpain-1 hyperactivation. To test if CCH inhibitors could attenuate neuroinflammation, CCF-STTG1, a human astrocytoma cell line, was treated with 1μg/mL lipopolysaccharide (LPS) and 1ng/mL TNF-α, both well-characterized inflammatory agents. Concurrently, cells were co-treated with 10μM of ***5***, ***NYC-438***, and **CA-*074***.

F420, a compound synthesized by our lab, is a tissue-selective ATP-binding cassette A1 (ABCA1) agonist with CNS efficacy and minimal peripheral lipogenic activity. Our lab has demonstrated anti-inflammatory efficacy in *in vitro* and *in vivo* models. Thus, it was selected as a positive control for *in vitro* inflammatory studies.

LPS stimulation alone significantly increased TNF-α and NOS2 levels (7.87 ± 0.87 and 15.01 ± .07, respectively, Figure 33). All inhibition strategies attenuated the neuroinflammation levels (TNF-α = ***5***: 1.031 ± 0.31, ***NYC-438***: 3.56 ± 2.2, ***CA-074***: 1.45 ± 0.08; NOS2 = ***5***: 11.21 ± 0.65, ***NYC-438***: 10.82 ± 0.28, ***CA-074***: 10.21 ± 0.56). There was no clear difference in CCH targeting to reduce LPS-stimulated inflammation.

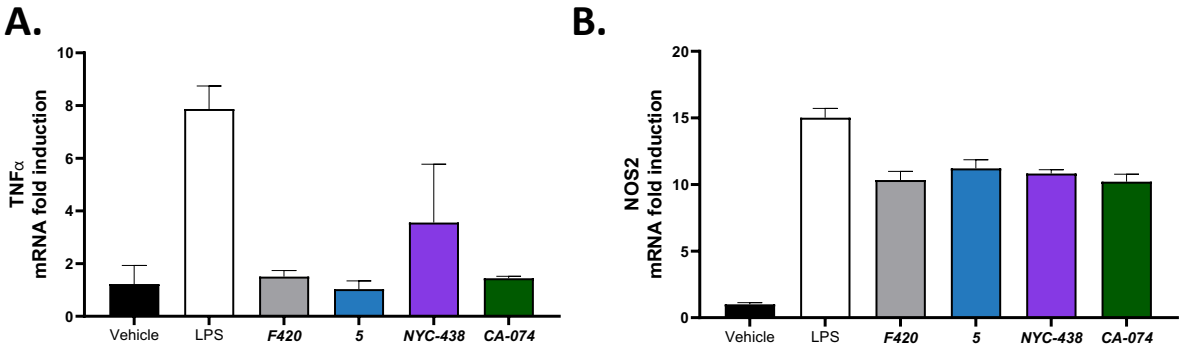

Figure 33. Calpain-cathepsin inhibitors attenuated LPS-stimulated TNFa and NOS2 levels in astrocyte-like CCF-STTG1 cells

(**A** and **B**) "Astrocyte-like" CCF-STTG1 cells were co-treated with 1μg/mL LPS and 10μM ***5***, ***NYC-438***, ***CA-074***, or ***F420*** for 24 hours. mRNA was extracted and levels of TNF-**α** (**A**) and NOS2 (**B**) were quantified by qRT-PCR. All samples were normalized to the housekeeping gene β-actin, then the vehicle control at 1. Data represent mean ± SD of at least n=2 replicates.

Similarly, TNF-α stimulation alone significantly increased IL-1β and IL-6 expression (14.4 ± 0.71 and 6.81 ± 0.49, respectively Figure 34). Inhibition strategies attenuated IL-1β, but not IL-6 levels (IL-1β = ***5***: 6.24 ± 0.57; ***NYC-438***: 6.60 ± 0.14; ***CA-074***: 6.81 ± 0.17; IL-6 = ***5***: 10.04 ± 0.65; ***NYC-438***: 9.57 ± 0.34; ***CA-074***: 12.78 ± 0.82).

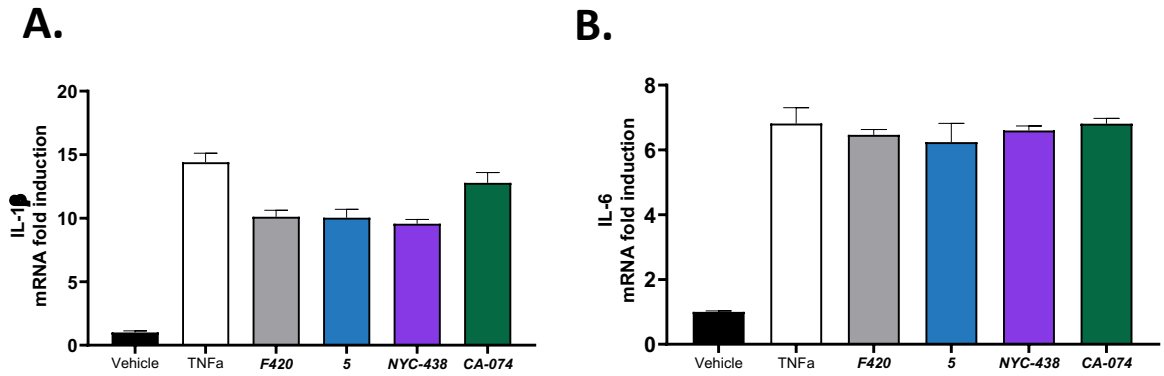

Figure 34. Inhibition strategies attenuated TNFa-stimulated IL-1β levels in CCF-STTG1 cells
(A and **B**) "Astrocyte-like" CCF-STTG1 cells were co-treated with 1ng/mL TNF-α and 10μM ***5***, ***NYC-438***, ***CA-074*** or ***F420*** for 24 hours. mRNA was extracted and levels of IL-1β (**A**) and IL-6 (**B**) were quantified by qRT-PCR. All samples were normalized to the housekeeping gene β-actin, then the vehicle control at 1. Data represent mean ± SD of at least n=2 replicates.

2.3.5 Oxidative Stress via Lipid Peroxidation Products Induces Neuronal Cell Death

An early event in progression of neurodegenerative disease is elevated OS accompanied by increased levels of LPP (specifically HNE) that can form neurotoxic protein and DNA adducts.[193-202] To mimic the effects of OS *in vitro*, neuronal cells were treated with exogenous LPP (HNE and ONE). SH-SY5Y cells were treated with the LPPs, HNE and ONE, and assessed for cell viability (MTS assay) to understand the dose-dependent phenotypic effects of LPPs *in vitro*. Treatment with HNE (1-50 μM) caused a concentration-dependent loss of cell viability, measured at 6 and 24 hours (Figure 35A and B). However, increasing HNE concentration from 10 μM to 50 μM did not significantly increase the observed ~45% cell death, consistent with previous literature.

[263] The effect of 25μM HNE 6-48 hours post-treatment had no significant effect on cell viability (Figure 35C). Unsurprisingly, in part because of its greater reactivity, ONE (0.1-25μM) was more cytotoxic, producing ~15% cell death at 0.1μM and dose-dependent neurotoxicity up to 25μM (~75% cell death, Figure 35D, Figure 36). Results were confirmed using the LDH assay (Figure 36)

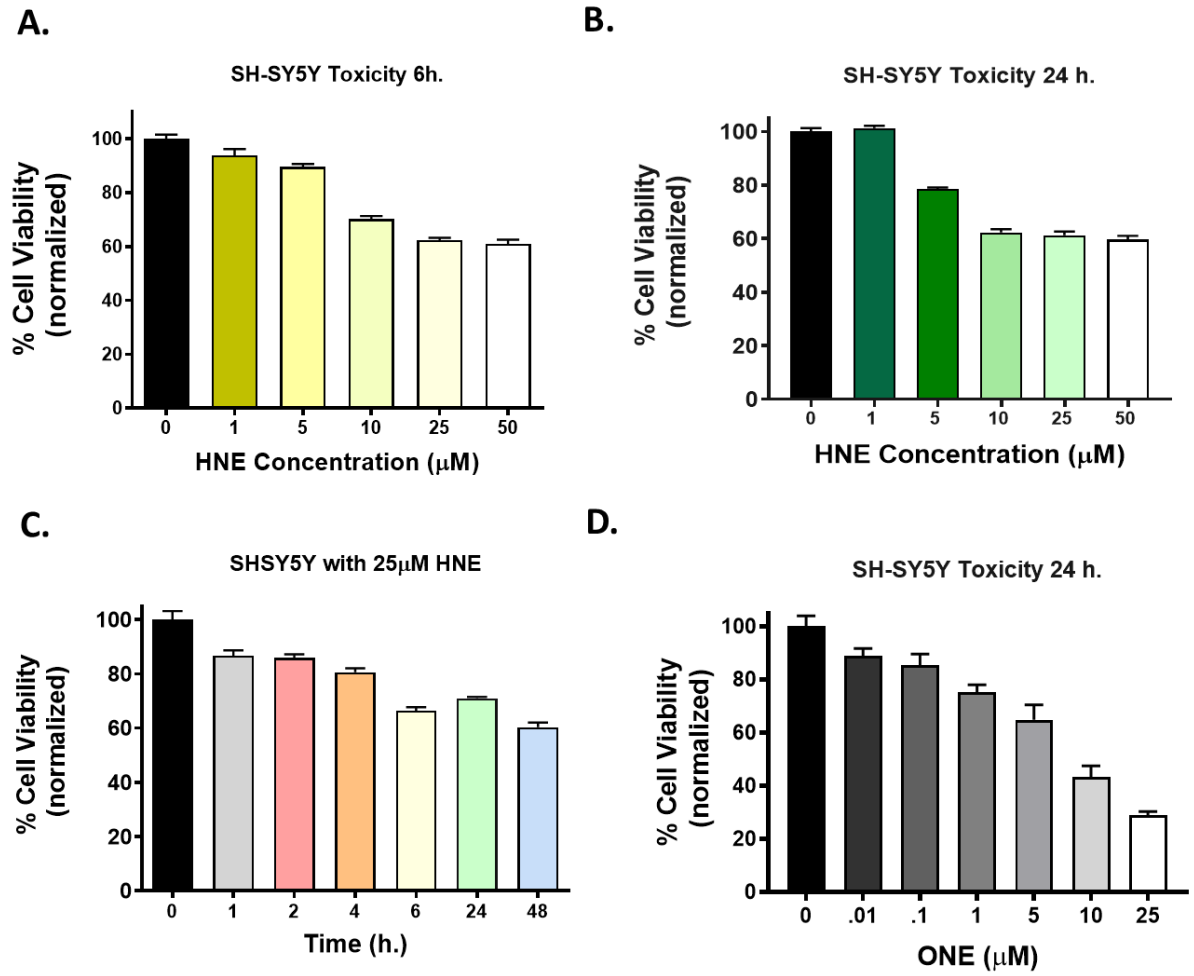

Figure 35. Lipid peroxidation products, HNE and ONE, induce time-dependent and concentration-dependent cell death of SH-SY5Y cells

(**A**-**B**) Quantitative analysis of SH-SY5Y cells treated with 0-50μM HNE for 6 and 24 hours (**A** and **B**, respectively) and analyzed via MTS. (**C**.) Quantitative analysis of SH-SY5Y cells treated with 25μM HNE for 0-48 hours and analyzed via MTS. (**D**) Quantitative analysis of SH-SY5Y cells treated with 0-25μM ONE for 24 hours and analyzed via MTS. Data represent mean ± SEM with n=6.

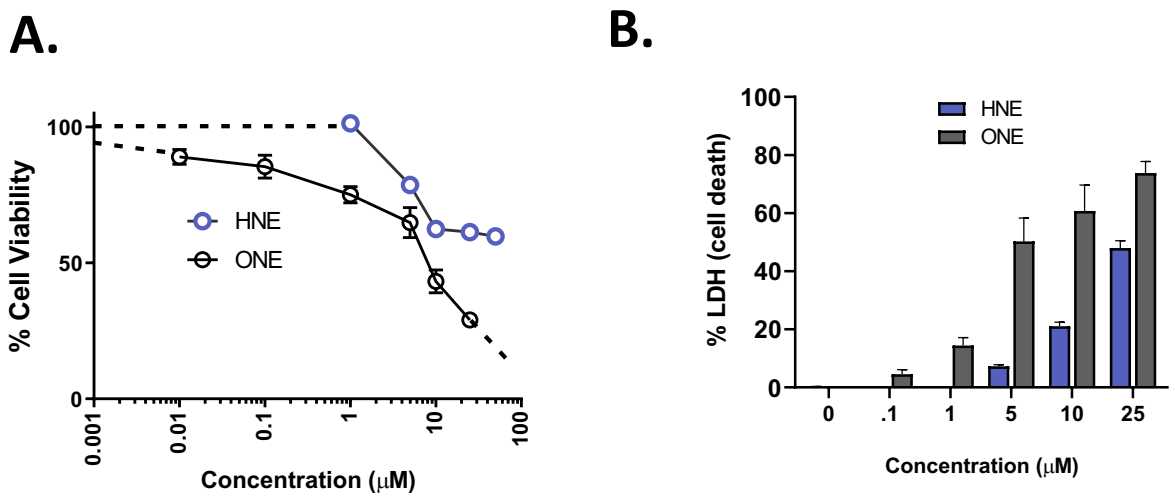

Figure 36. ONE has greater neurotoxicity than HNE
(**A** and **B**) Quantitative analysis of SH-SY5Y cells incubated with either 4-HNE (0-50 μM) or ONE (0-25 μM) for 24 hours with cell viability quantified by MTS **(A)** and LDH (**B**). Data represent mean ± S.E.M. analyzed by one-way ANOVA with Dunnett's or Tukey's multi-comparison analysis from three cell passages (n=6/passage, *p<0.05, **p<0.01, ***p<0.001).

Scavenging agents were compared to determine the relative potential to alleviate the impact of increased LPPs in cell cultures. The agents selected, and their concentrations, were well characterized in the literature. [264-266] Additional control experiments of cells treated with the scavengers alone had no effect on cell viability. SH-SY5Y cells were co-treated with both scavengers (50 μM and 250 μM) and LPPs (HNE: 5 μM and 10 μM; ONE: 1 μM and 5 μM), and cell viability was measured at 24 hours via MTS and LDH. N-acetyl cysteine (NAC) displayed the highest level of neuroprotection at 50 μM (Figure 37). All scavengers, including hydralazine and L-carnosine, showed some neuroprotection. At 250 μM, L-histidyl hydrazide (HH) and NAC were equivalent and superior to other scavengers in their neuroprotective actions.

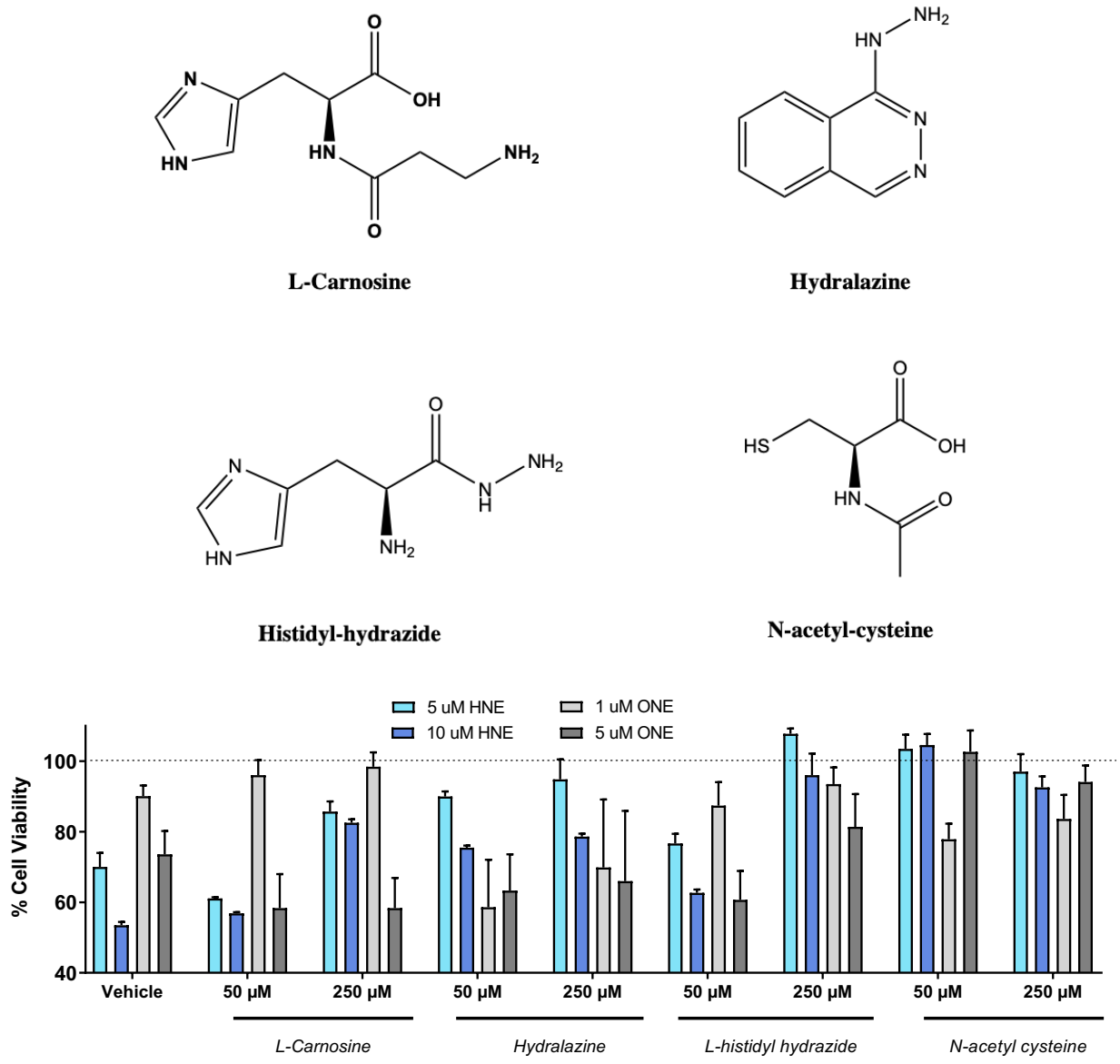

Figure 37. LPP scavengers reduce neurotoxicity of HNE and ONE *in vitro*
Quantitative analysis of SH-SY5Y cells co-treated with well-studied scavengers (50 µM and 250 µM) and either 4-HNE (5 µM and 10 µM) or ONE (1 µM and 5 µM) for 24 hours with cell viability quantified by MTS. Data represent mean ± S.E.M. analyzed by one-way ANOVA with Dunnett's or Tukey's multi-comparison analysis from three cell passages (n=6/passage, *p<0.05, **p<0.01, ***p<0.001).

To mimic the effects of a "2nd hit" *in vitro*, cells were treated with exogenous HNE (1st hit) and OGD-R (2nd hit) to test if an underlying level of oxidative stress, caused by HNE, would exacerbate the neuronal loss subsequent to a second insult. SH-SY5Y cells were treated with 0-50μM HNE then immediately treated with OGD-R. Exacerbated cell death was observed at all concentrations of HNE (Figure 38). These results demonstrated that a secondary neuronal insult against the background of elevated LPP can lead to attenuated neural reserve.

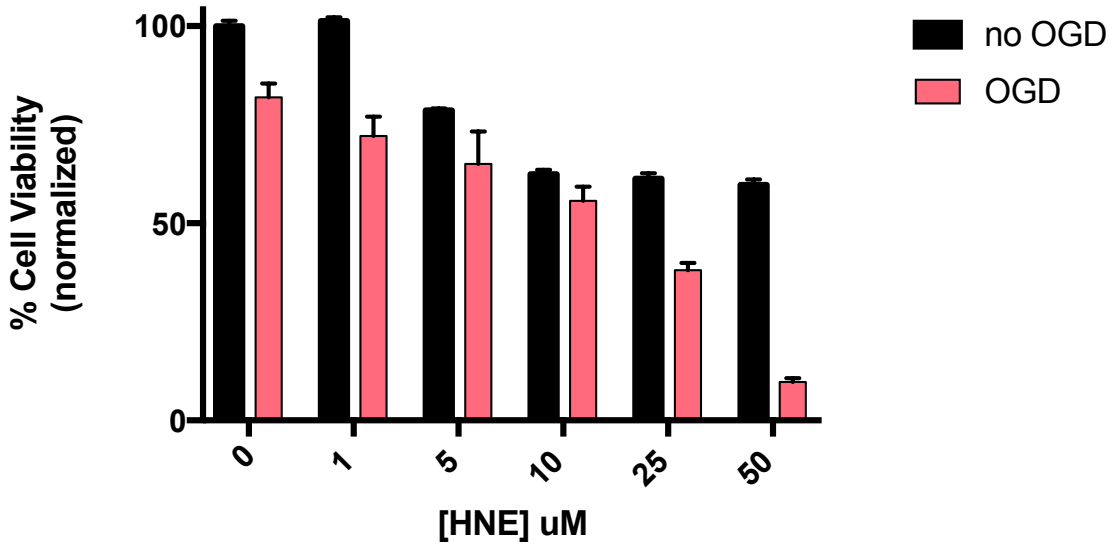

Figure 38. HNE exacerbates OGD-R induced cell death in SH-SY5Y cells.
SH-SY5Y cells treated with OGD-R and 0-50μM HNE for 24 hours and quantified via MTS. Data represent mean ± SEM with n=6.

2.3.6 Development of a Novel Murine mTBI model with Underlying Oxidative Stress

Both oxidative stress and mild neurotrauma contribute to risk of ADRD [193-199] and likely also contribute to the age-related loss of neural reserve that interacts with hallmark AD pathology to cause progression to dementia.[267] Moreover, OS is hypothesized to play a driving role in the secondary cascade of effects following mTBI.[268] Therefore, as a foundation for this approach, we chose to study mTBI, a relatively common and mild neurotrauma, in *ALDH2*$^{-/-}$ mice.

Previous results from our lab showed that the *ALDH2*$^{-/-}$ mice present with elevated HNE adducts accompanied by decreased mitochondrial function but without neuronal loss.[269] This suggests that key mediators of mitochondrial health are impaired in *ALDH2*$^{-/-}$ mice, supporting previous findings that LPP significantly contributes to mitochondrial dysfunction.[263, 270] Moreover, these mice exhibit cognitive impairment, significant beginning at 4 months of age, and is compatible with observed reductions in synaptic proteins essential in learning and memory in the hippocampus. This cognitive decline does not decline from 4 months to 14 months of age. Moreover, the cognitive deficit can be readily reversed at 9 months of age with both acute administration of pro-cognitive, anti-amnestic agents, and an LPP scavenger.

We utilized a closed-head weight drop insult to characterize the effects of underlying LPP in exacerbating secondary injury in mTBI. A 30g bullet was dropped down a 80cm long tube and directed towards the right hemisphere between the ear and the eye (

Figure 39). The skull was intact and the head was free, stabilized in a sponge. This model is non-stereotaxic, reflecting the heterogeneity observed in human TBI populations. No gross pathological changes in infarct damage or contusion were seen in mice that were included in data analysis.

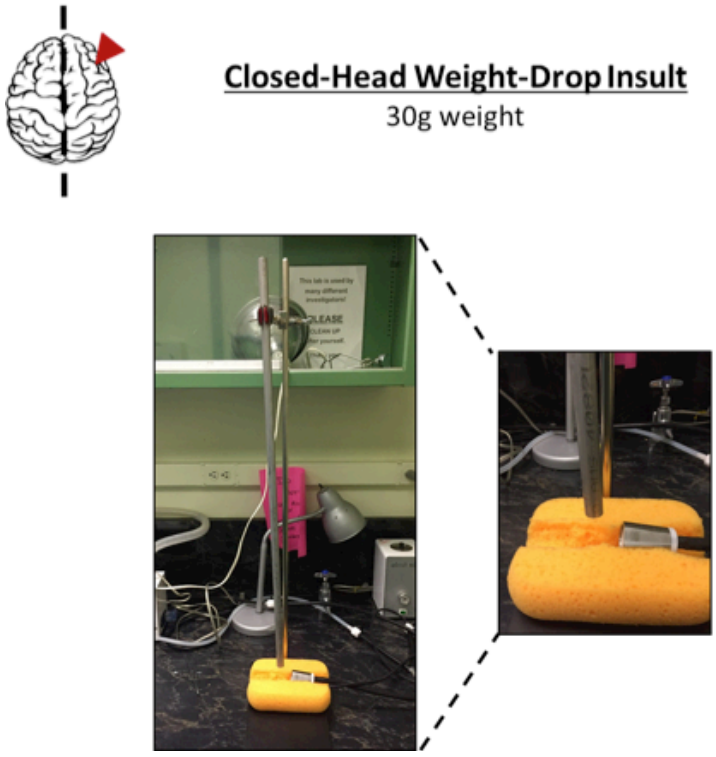

Figure 39. The mTBI apparatus utilized in our studies
A 30g bullet was dropped down an 80cm long tube and directed towards the right hemisphere, between the eye and the ear, of a mouse. All animals were anesthetized throughout the experiment with their heads stabilized by a sponge.

Brain tissues were analyzed for changes in pro-inflammatory cytokine expression. In *ALDH2*$^{-/-}$ mice, pro-inflammatory cytokines were increased 24 hours post-mTBI in the ipsilateral hemisphere, with changes in TNF-α reaching significance (8.7-fold increase, Figure 40). No changes in inflammatory markers in WT mice induced by mTBI reached significance. These observations show that elevated LPP and increased basal oxidative stress amplify the effects of mTBI with diminished cognitive function and elevated pro-inflammatory cytokines.

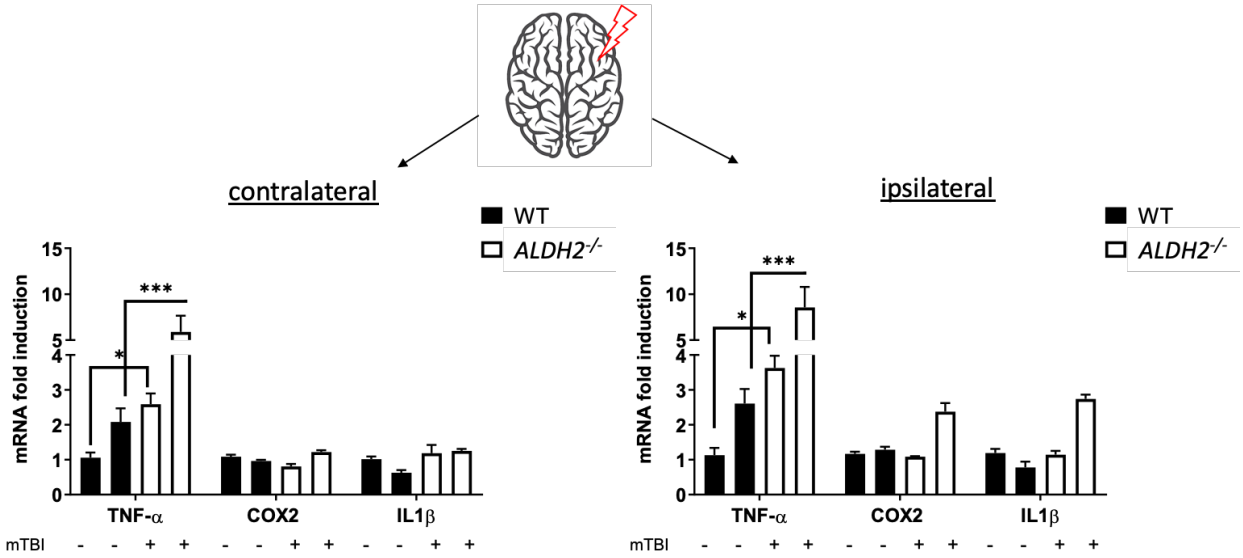

Figure 40. Underlying oxidative stress with mTBI induces a significant cytokine surge 24 hours post-injury

qRT-PCR analysis of TNF-α, COX2 and IL-1β gene expression in the contralateral and ipsilateral hemispheres of WT and *ALDH2*$^{-/-}$ mice 24 hours post-mTBI and null mouse controls. All samples were normalized to the housekeeping gene, β-actin. Data represent mean ± S.E.M analyzed by one-way ANOVA with Dunnett's or Tukey's multi-comparison analysis from (n=6) *p<0.05, **p< 0.01, ***p< 0.001.

Researchers have demonstrated that *CTSB*$^{-/-}$ mice experience significantly reduced TBI-induced CNS inflammation and inflammatory pain.[126, 271] Furthermore, our *in vitro* studies demonstrate the anti-inflammatory properties of CCH inhibitors(Figure 33 and Figure 34).. These findings provided support to test inhibition strategies in the reduced resilience *in vivo* model.

ALDH2$^{-/-}$ mice were administered a single injection of 10mg/kg ***3, 5*** and ***NYC-438*** and ***E-64d*** via *i.p.* one hour post-mTBI. Mice were sacrificed 24 hours post-mTBI, with inflammatory levels of the ipsilateral hemisphere measured. We focused on looking at TNF-α levels, as this was the only cytokine significantly increased in the 2-hit model. Treatment with all inhibitors significantly decreased TNF-α (WT: 1.0 ± 0.14; *ALDH2*$^{-/-}$ + mTBI: 3.61 ± 0.9; ***3***: 0.82 ± 0.22; ***5***:

2.0 ± 0.48; ***NYC-438***: 1.16 ± 0.37; ***E-64d***: 1.24 ± 0.3). We also examined IL-1β and COX2 levels as a second screen for anti-neuroinflammatory properties *in vivo.* As there was no significant difference in selective or nonselective inhibitors, we only examined these additional markers in the ipsilateral hemispheres of mice treated with ***5*** and ***NYC-438***. These displayed no effect on IL-1β or COX2 (Figure 41).

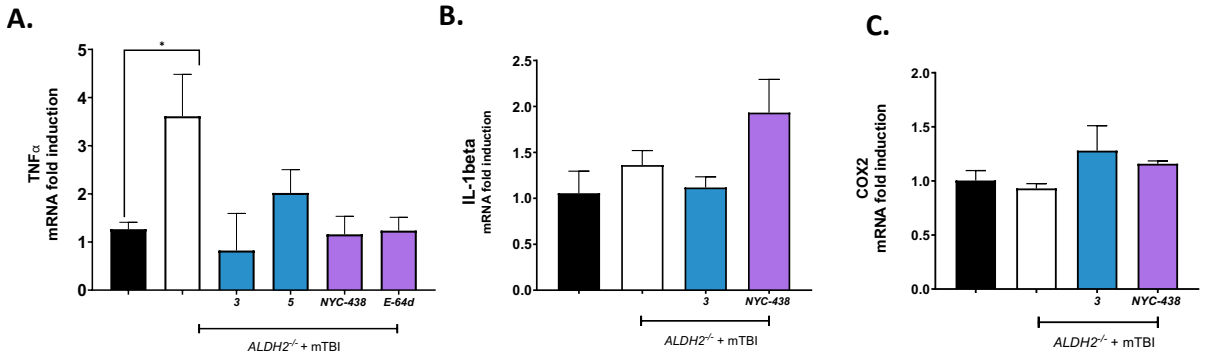

Figure 41. CCH inhibitors attenuate neuroinflammation in the *ALDH2*$^{-/-}$ mTBI model
(A–C) qRT-PCR analysis of TNF-α, (**A**) COX2 (**B**) and IL-1β (**C**) gene expression in the ipsilateral hemispheres of *ALDH2*$^{-/-}$ mice 24 hours post-mTBI and null WT mouse controls (black bar). All samples were normalized to the housekeeping gene, β-actin. Data represent mean ± S.E.M analyzed by one-way ANOVA with Dunnett's or Tukey's multi-comparison analysis from (n=6) *p<0.05, **p< 0.01, ***p< 0.001.

Levels of glial fibrillary acidic protein (GFAP) and associated breakdown products (GFAP-BDP) were also exacerbated in the ipsilateral hemisphere of the *ALDH2*$^{-/-}$ + mTBI mouse model (Figure 42). Calpain-mediated GFAP cleavage produces a range of BDP between 30 and 50kDa;[272, 273] thus, calpain-1 may be hyperactivated in this model. OS alone significantly increased

both GFAP (WT: 1.0 ± 0.06; *ALDH2*$^{-/-}$: 1.29 ± 0.09) and GFAP-BDP (WT: 1.0 ± 0.07; *ALDH2*$^{-/-}$: 1.1 ± 0.1), which was further exacerbated by mTBI (*ALDH2*$^{-/-}$ + mTBI GFAP: 1.44 ± 0.12; *ALDH2*$^{-/-}$ + mTBI GFAP-BDP: 1.64 ± 0.22). The increased GFAP was significantly reduced with a single treatment of ***NYC-438*** (0.99 ± 0.16) but not ***5*** (1.46 ± 0.12), while both significantly increased GFAP-BDP (***5***: 0.75 ± 0.13; ***NYC-438***: 0.49 ± 0.09).

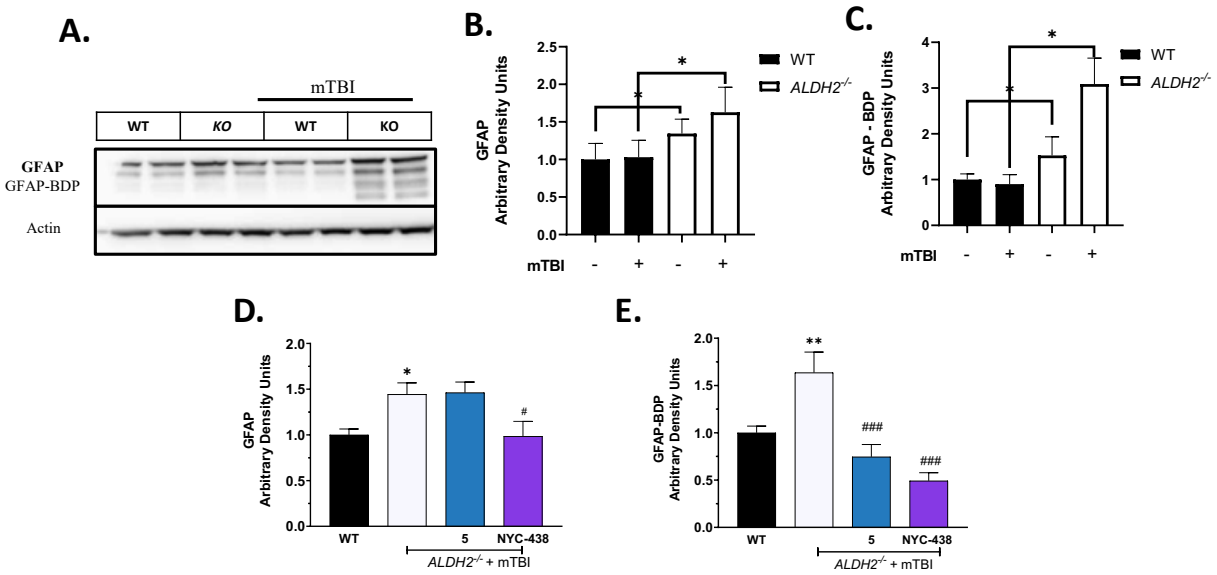

Figure 42. Inhibitors *5* and *NYC-438* reduced levels of GFAP and GFAP-BDP mediated by mTBI

(**A**-**E**) Representitive immunoblots (**A**) and quantitative analysis of immunoblots from the ipsilateral hemisphere of WT and *ALDH2*$^{-/-}$ mice 24 hours post-mTBI and null mouse controls probed with GFAP Ab and quantified for GFAP (**B**) and GFAP-BDP (**C**). Quantitative analysis of immunoblots from WT and *ALDH2*$^{-/-}$ mice treated with 10mg/kg of ***5*** or ***NYC-438*** 1-hour post mTBI and probed with GFAP (**D**) and GFAP-BDP (**E**). All samples were normalized to the housekeeping gene, β-actin. Data represent mean ± S.E.M analyzed by one-way ANOVA with Dunnett's or Tukey's multi-comparison analysis from (n=6) *p <0.05, **p< 0.01, ***p< 0.001.

Similar to confirming specific inhibitory efficacy *in vitro*, target engagement was analyzed in the mTBI mice by analyzing SBDPs (Figure 43). SBDP 150kDa, the calpain-1 and caspase-3 mediated fragment, increased with OS alone and OS + mTBI, (albeit not significantly) and was reduced with selective and nonselective inhibitors. Levels of SBDP 145kDa, the calpain-1 specific fragment, were increased in the OS mice and significantly increased with OS + mTBI (WT: 1.0 ± 0.08; WT + mTBI: 0.98 ± 0.04; *ALDH2*$^{-/-}$: 1.30 ± 0.13; *ALDH2*$^{-/-}$+ mTBI: 1.45 ± 0.15). The increased SBDP 145kDa, and GFAP-BDP provided confirmation for calpain-1 hyperactivated in this model. Furthermore, elevated SBDP 145kDa is associated with heightened clinical severity following stroke and neuronal death.[274] Thus, the mild insult on the background oxidative stress provided an amplified model of neurodegeneration.

Single treatment of selective and nonselective inhibitors significantly reduced levels of SBPD 145kDa back to WT conditions (***3:*** 0.69 ± .09; ***5:*** 0.83 ± 0.10; ***NYC-438***: 0.93 ± 0.20; ***NYC-438e***: 0.76 ± 0.09) confirming inhibitory efficacy in the OS + mTBI mice. Important to note that ***NYC-438e*** was tested in tandem. This compound is structurally identical to ***NYC-438***, except it incorporates an ester in place of the carboxylic acid (P1' position). Previous work from our lab suggests that this compound may have better brain penetration in this pro-drug form.

Lastly, there was no change in levels of SBDP120, the caspase-3 specific fragment in any condition with or without inhibitors. Intriguingly, mTBI alone had no effect on levels of any SBDPs. These results confirm the efficacy of our inhibition strategies *in vivo.*

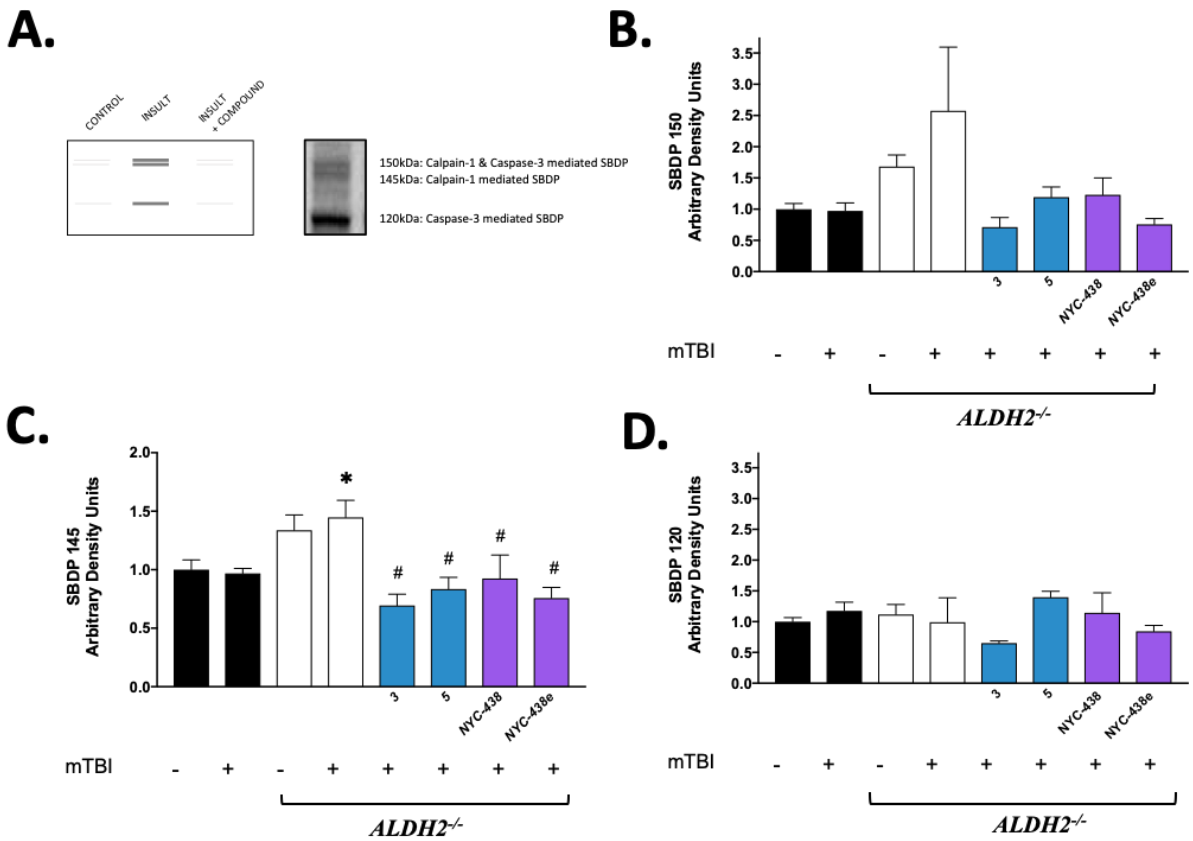

Figure 43. Selective and nonselective calpain-1 inhibitors diminish SBDP145 levels in *ALDH2*$^{-/-}$ mice with mTBI

(**A**) Representative schematic of expected SBDP cleavage fragments. (**B**-**D**) Analysis of immunoblots from the ipsilateral hemisphere of WT and *ALDH2*$^{-/-}$ mice 24 hours post-mTBI and null mouse controls probed with spectrin Ab and quantified for SBDP 150kDa (**B**), 145kDa (**C**) and 120kDa (**D**) monitored. All samples were normalized to the housekeeping gene, β-actin. Data represent mean ± S.E.M analyzed by one-way ANOVA with Dunnett's or Tukey's multi-comparison analysis from (n=6) *p <0.05, **p< 0.01, ***p< 0.001.

2.4 CONCLUSION

Translational scientists are increasingly recognizing ADRD as a multifactorial disease, with multiple contributing factors (environmental, cellular, genetic, etc.). These studies provided convincing support for further pre-clinical development of calpain and cathepsin inhibition strategies as potential ADRD therapeutics. Our inhibition strategies show efficacy in simple *in vitro* models of neurodegeneration (OGD-R) and complex *in vivo* models of reduced neural resilience in lieu of severe phenotypic effects (*ALDH2*$^{-/-}$ + mTBI). Moreover, we saw efficacy at numerous treatment paradigms, whether it be pre-, at- or post-insult.

It's essential that therapies for neurotrauma display efficacy in a post-treatment paradigm, as most neurotraumas occur sporadically (such as military or sports accidents). Two-hit models and multiple mTBI studies show an additive or even multiplying effect of damage both short-term and long-term. Thus, if some of the damage could be restored after a single "hit", it could alleviate the potential aggravated signaling cascades that contribute to behavioral and pathological damage. While longer studies are required (daily dose for 1 week, 1 month), this evidence suggests calpain inhibition strategies can mitigate or prevent further exacerbation of secondary sequalae.

While there exists a plethora of well-established and necessary genetic-based animal models, there exists an urgent need for models with reduced neural resilience and underlying pathologic processes relevant to ADRD and neurodegenerative diseases. The interaction of oxidative stress and neurotrauma in *ALDH2*$^{-/-}$ mice provides a model to explore mechanisms of loss of neural reserve and cognitive resilience, and provides a tractable preclinical model for testing novel therapeutic agents. The closed-skull, weight-drop model of mTBI, used as a 2nd hit in our studies, did not elicit significant or persistent effects in WT mice. In contrast, significant effects were observed in *ALDH2*$^{-/-}$ mice. These effects were most marked with a sharp neuroinflammatory response 24 hours post-trauma, a mechanism hypothesized to drive secondary cascade following

TBI. The increase in GFAP, its proteolytic degradation products (BDP), and SBDP 145kDa suggested the hyper-activation of calpain-1 in this model. Thus, this *in vivo* model was appropriate and relevant to test our inhibition strategies. While a superior targeting strategy has not yet been identified, this supports calpain and cathepsin B as underlying mediators of ADRD, and advocates for further preclinical development.

CHAPTER 3: ATTENUATION OF BBB-DYSFUNCTION BY CALPAIN AND CATHEPSIN B INHIBITION STRATEGIES

3.1 INTRODUCTION

3.1.1 Poor Bioavailability of Calpain Inhibitors: Effect on BBB?

The assumption that off-target drug actions drive side effects led the pharmaceutical industry to focus on developing highly selective calpain-1 inhibitors. These efforts culminated in Alicapistat, an orally active inhibitor of human calpain-1 and calpain-2, which recently completed Phase 1 clinical trials targeted at ADRD.[11] Alicapistat is highly selective against other cysteine proteases, in particular cathepsin B, K, L and S, and exists as a 1:1 mixture of 2 diastereomers (Alicapistat R,S, and Alicapistat R,R). Phase 1 studies demonstrated that Alicapistat was without dose-limiting toxicities, and there was sufficient plasma bioavailability (peak plasma concentrations were approximately 4 μM). [11] However, the concentration achieved in CSF at the highest dose was < 20 nM, less than half that of the IC_{50} (56 nM for the active diastereomer).. Data from our lab also suggests NYC-438 possesses poor brain bioavailability, raising the intriguing possibility that efficacy is driven by interactions with the neurovascular unit and specifically, brain endothelial cells (BEC)s.

3.1.2 The Blood Brain Barrier

The blood-brain barrier (BBB) is a tightly controlled physiochemical border that regulates the transport of molecules in and out of the central nervous system (CNS) and prevents toxins and pathogens from penetrating the neural tissue. This system is vital for supporting neuronal function and maintaining brain health. It is important to note that the BBB is commonly referred to as the vascular boundary between the circulating blood and brain parenchyma.[275] More specialized vascular barriers include the blood-nerve,[276] the blood-retinal,[277] the blood-labyrinth[278] and the blood-cerebrospinal fluid[279] barriers. Despite comprising only ~2% of the body's mass, the human brain consumes roughly 20% of the body's oxygen and glucose under normal, healthy

physiological conditions.[280] Moreover, the brain alone does not contain a storage of fuel, and requires rapid energy from circulating blood.[281] The process of managing the swift changes of energy demands is known as neurovascular coupling, a mechanism which increases the rate of cerebral blood flow and oxygen transport. Some reports have found that the total length of cerebral blood vessels is around 400 miles long to provide transport exchanges; of this, capillaries contribute over 85% of the vessel length.[282] The architecture of the BBB is intricately designed to ensure strict regulation of chemical transport; a continuous endothelial membrane lies within brain capillaries, with pericytes embedded in the capillary basement membrane and astrocytes serving as "end-feet" support (Figure 44).

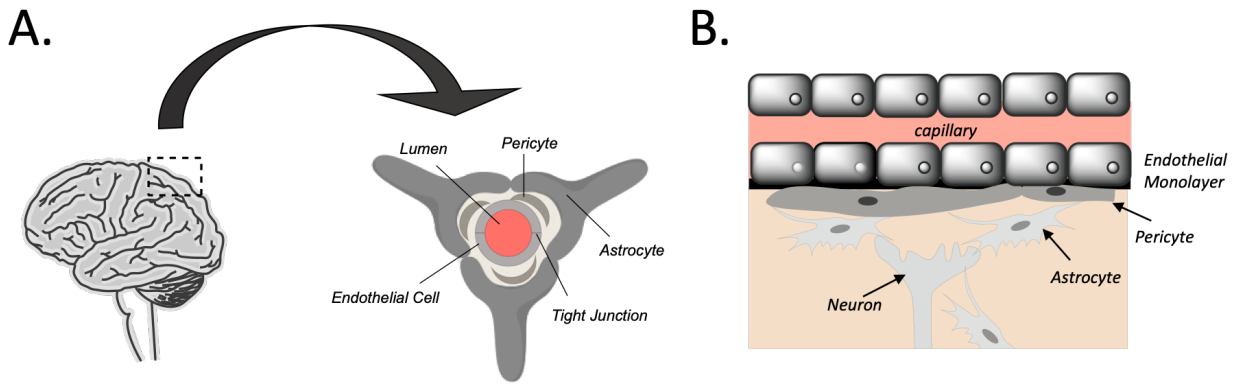

Figure 44. Schematic of the architecture of the BBB.
(**A**) Representative cross-section of a brain capillary (**B**) Representative longitudinal section of a brain capillary

BBB functionality is largely manifested through the brain endothelial cells (BECs)[275] and thus are significantly distinct from other endothelial cells (ECs) found elsewhere in the body. Structurally, BECs are significantly smaller (39% less thick) than muscle ECs, which gives the BBB a highly restricted permeability.[283] It's theorized that this decrease in thickness allows for a faster transport of nutrients through the membrane, cytoplasm, and into the brain parenchyma.[284] In the human brain, capillaries contain ~12 m^2 of endothelial cell surface, and the smaller mass is imperative for quick, efficient transfer of important nutrients from the blood to the brain and vice versa.[285]

The abundance and quantity of tight junctions (TJs) also differentiate BECs from ECs. TJs are proteins that align as a series of sealing strands, with each strand acting independently from the other. Each of these strands are embedded in the plasma membrane of a single EC. The extracellular domain(s) of each strand interacts with extracellular domain(s) of strands embedded in other ECs. There are over 40 different proteins (strands) that make up TJs,[286] with the most common being occludin, claudins, and junction adhesion molecule (JAM) proteins. The TJs are anchored into the actin component of the cytoskeleton by peripheral membrane proteins (e.g. zona occludens, ZO-1) located on the intracellular side of the plasma membrane. While TJs exist and are structurally similar in all tissues, they are found in significantly greater quantities in BECs. In ECs, TJs exist as a series of "buttons", whereas in BECs they form a continuous, closed "zipper" (Figure 45).[283] This tightly sealed barrier results in high transendothelial electrical resistance (TEER) as well as low transcellular and paracellular permeability.[287]

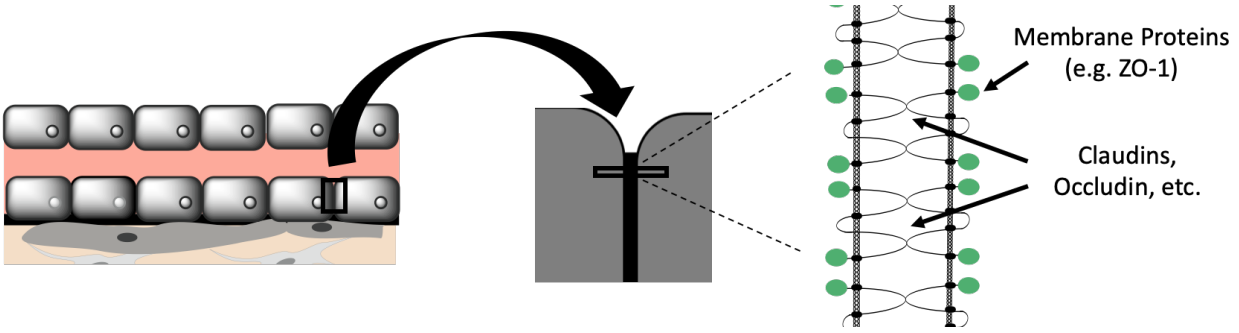

Figure 45. Representative cartoon of the architecture of tight junctions between BECs
Brain endothelial cells are tightly sealed together by tight junction proteins. This results in high transendothelial electrical resistance (TEER) as well as low paracellular and trancellular permeability.

Furthermore, the BBB presents with a reduction in pinocytosis (fluid endocytosis), a feature that is increasingly recognized to be contributed specifically by molecular processes of BECs.[288] One of these is the membrane lipid composition in BECs conferred by the lipid transporter major facilitator superfamily domain containing 2A (Mfsd2a) which prevents the assembly of caveolin-1 vesicles. [289, 290]

Furthermore, the BBB transport system is regulated primarily by BEC transport systems excluding gasses and small lipophilic molecules that are able to diffuse unrestricted across the endothelium (Figure 46).[275, 291] Endothelial carrier-mediate transport (CMT) allows solutes (carbohydrates, amino acids, fatty acids, nucleotides, vitamins, hormones, etc.) to pass through the BBB via substrate-specific transporters. [57] This includes GLUT1 (carbohydrate transporter),[275] large neutral endothelial AA transporter 1 (LAT1/2)[292] and 2 as well as cationic AA transporter 1 and 3 (CAT1/3, amino acids),[293] monocarboxylate transporters (MCT1 and MCT8, monocarboxylates and hormones), [294] fatty acid transport protein 1 and 4 (FATP1/4, fatty

acids),[295] sodium-independent concentrative nucleoside transporter-2 (CNT2, nucleotides)[296] and organic anion transporter-3 (OAT3)[297] and organic cation/carnitine transporter-2 (OCTN2, organic anion and cations).[298]

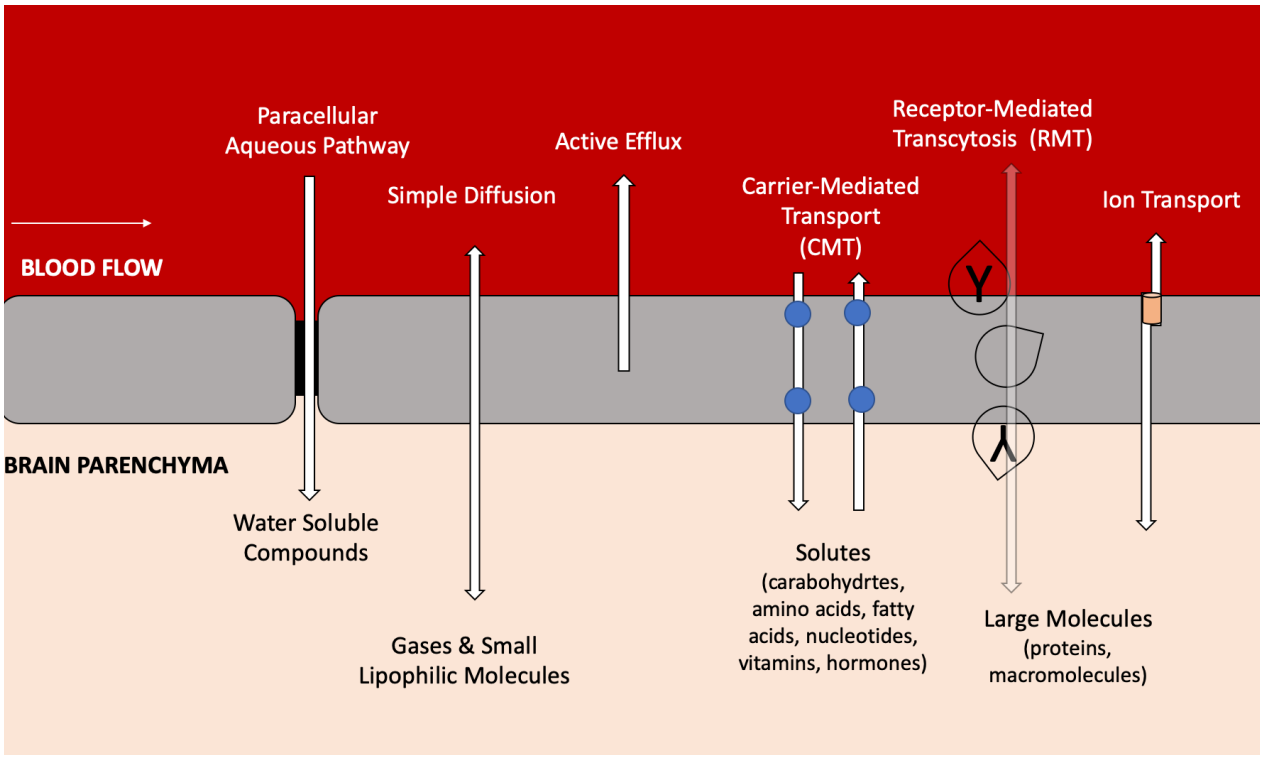

Figure 46. BBB transport systems
The blood-brain barrier has a variety of transport mechanisms to allow passage of substances from the circulating blood into the neural tissue.

Larger molecules, such as proteins and macromolecules (growth factors, albumin, immunoglobulins, etc.) use receptor-mediated transport (RMT) to cross the BBB. These receptors include transferrin and insulin receptors, [299, 300] as well as lipoprotein receptors and receptor for

advanced glycation end products (RAGE, on the abluminal and luminal membrane, respectively).[301, 66] Generally, the rate of peptides to transport through the BBB is slower than nutrient transport.[302] Moreover, endothelial active efflux ATP-binding cassette transporters (ABCs) provide a mode for active transport to prevent brain accumulation of drug conjugates, nucleosides, xenobiotics and drugs.[282] This is vitally important, as ABC transporters have gained traction in the drug discovery realm as important determinants of CNS drug distribution (both to and from the CNS).[303, 304]

BECs also regulate ion transport through sodium pumps (Na^+- K^+-ATPase),[305] calcium transporters (Na^+-Ca^{2+}),[306] potassium channels (voltage-gated K^+ channel),[307] and other ion transporters (NKCC1).[308] These channels, pumps and transporters are especially vital for maintaining proper ion milieu, an essential component of proper CNS functioning.[309]

It is important to note that the supporting cells of the BBB (pericytes and astrocytes) are imperative for proper BEC function. Reports indicate pericyte knockout mouse models have severe impairment of BBB induction and maintenance.[310] Moreover, *Abbott et al* revealed that astrocyte-conditioned media was sufficient to promote BEC functionalities *in vitro*.[311]

3.1.3 Age-associated Changes to the Blood-Brain Barrier

A major limitation to identifying normal physiological BBB changes induced by aging is that many of the techniques require tissues that can only be obtained post-mortem. However, with the recent advances in imaging techniques (PET scan, MRI, etc.), we have been able to gain more insight into potential age-associated changes.

The most straight-forward method to quantitatively determine BBB-functionality in living humans is by measuring the ratio of BBB-impermeable proteins (e.g. immunoglobulin G, albumin) in the cerebrospinal fluid (CSF) *vs.* serum. Unfortunately, this tactic is unreliable as other known

CNS changes with aging can muddle the results; reports have indicated aging affects production and reabsorption of the CSF as well as leakage of the blood-CSF barrier, both of which would dramatically affect the ratio.[312-314] Moreover, the increased inflammation in the serum and CSF that occurs with aging dramatically affects the levels of BBB-impermeable proteins that are typically measured.[314] Intriguingly, *Montagne et al.* utilized an advanced dynamic contrast-enhanced magnetic resonance imaging technique, with gadolinium as a tracer, to visualize leaky areas in normal brains.[315] By using 24 living human subjects with no cognitive impairment (male and females, aged 23 – 91), they studied 12 different CNS regions and found a correlation between BBB-breakdown in the hippocampus and age. Albeit, the BBB-breakdown was quite minimal. Moreover, studies have been performed in young *vs* aged mice which corroborate the finding that slight BBB-dysfunction occurs with age.[316, 317]

In addition to BBB-dysfunction, multiple reports reveal a direct correlation between increasing age and impairment of BEC transport function and signaling. *Bonte et al.* described an age-dependent decrease in metabolism particularly in grey matter of the frontal and temporal lobe.[318] This was measured by monitoring brain glucose uptake of ^{18}F-fludeoxyglucose via PET scans, and corrected for the volume loss. Furthermore, multiple articles report decreased levels of both of LRP-1 and P-gp, both efflux transporters of Aβ, in brain microvessels of older individuals without cognitive impairment.[319-323] Insulin transport may also be affected with aging, as *Sartorius et al.* reported decreased CSF / serum ratios of insulin in older, healthy individuals.[324] Concomitantly, the overall concentration of insulin in brain tissues has also been reported to decrease with human aging.[325]

It is clear that BEC functionality decreases with normal aging. Intriguingly, the levels of many circulating proteins vary with age and directly impact BEC functionality. Notably, concentrations

of enzyme acid sphingomyelinase (ASM) increase in BECs with age and contribute to BBB disruption via caveolae-cytoskeleton mechanisms.[326]

It's imperative to understand that there is no conclusive evidence that BBB-dysfunction definitively leads to brain damage; that is BBB-impairment does not always lead to brain injury. In fact, some CNS therapies rely on transient BBB-opening for delivery of chemotherapeutics.[327] Furthermore, *Lipsman et al.* transiently opened the BBB repeatedly in patients with mild to moderate AD, and saw no clinical nor radiographic adverse events, and no change in cognitive scores.[328] These reports exemplify the complexity of the BBB, and warrant further research into its functionality as a therapeutic target.

3.1.4 Cerebrovascular Contributions to Cognitive Impairment

The breakdown of BBB and associated hyperpermeability is a hallmark feature of various neurodegenerative and neuroinflammatory diseases including AD, TBI and IS.[329, 330] In fact, cerebrovascular dysfunction has been implicated in the early AD pathogenesis and a driver of cognitive dysfunction; many some studies indicate cerebrovascular dysfunction occurs prior to symptomatic onset and is among the first detectable biomarker changes. [315, 331, 332] Furthermore, cerebrovascular diseases as well as vascular risk factors (diabetes, hypertension, hyperlipidemia, pollution and obesity) all increase the risk of ADRD.[329]

Intriguingly, various reports indicate BBB-dysfunction, in particular BEC-dysfunction, can precede neurodegeneration.[285, 315, 333, 334] Early initiation of hyperpermeability is not typically associated with overt, blunt injury, but with subtler alterations that breach endothelial junctions.[335] BEC-degeneration and reduced TJs cause a myriad of factors including faulty transport, increased inflammation and an accumulation of neurotoxic factors which all promote neurodegeneration (Figure 47).

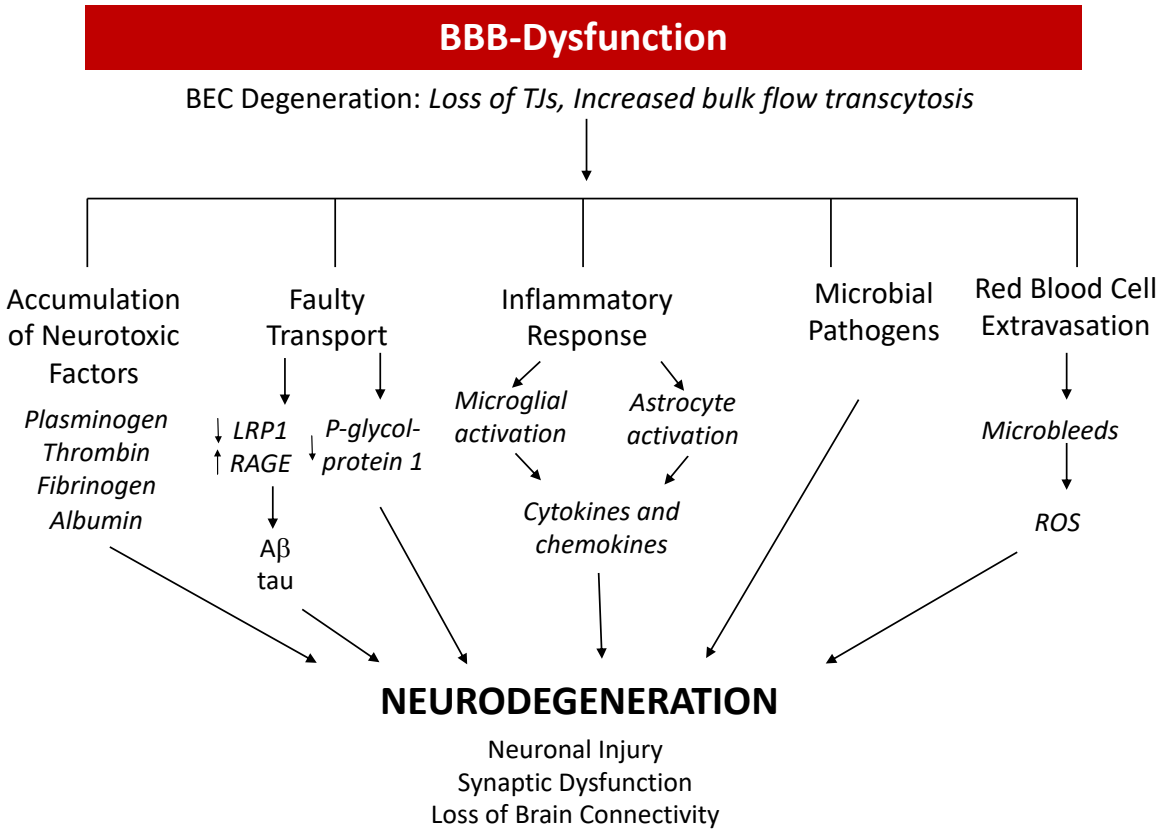

Figure 47. Mechanisms of neurodegeneration from BBB-dysfunction
A variety of mechanisms stemming from blood-brain barrier dysfunction can lead to neurodegeneration

Many genetic mutations known to contribute to ADRD can lead to BBB breakdown and cerebrovascular dysfunction. Mutations in *APP* and *PSEN1/2* genes cause autosomal-dominant AD (ADAD), an inherited form of AD that accounts for ~1% of all AD cases.[336] These mutations are well reported to lead to BBB breakdown, as evidenced in most ADAD cases. [266] Furthermore, multiple genome-wide association studies (GWAS) have identified various genes that are associated with an increased risk for neurodegenerative diseases. *APOE4* is the strongest known genetic risk factor identified for sporadic, late-onset AD. [337] One or two *APOE4* alleles is reported to increase the risk for developing ADRD by ~3.8-fold and ~12-fold respectively, compared to the *APOE3* genotype, with the effect stronger in females.[338, 339] Reports indicate human carriers of *APOE4* have enhanced BBB breakdown, pericyte degeneration, impaired cerebrovascular reactivity and reduced uptake of glucose compared to non-carriers.[340-342] Mutations in phosphatidylinositol binding clathrin assembly protein (*PICALM)* has also been identified in a majority of GWAS studies as a contributor to sporadic late-onset AD. [343] These polymorphisms indicate lower PICALM levels contribute to ADRD risk; similarly studies have shown PICALM, localized in the endothelial of human cerebral vessels, is downregulated in AD patients.[344] *In vivo* fAD models with *Picalm*$^{+/-}$ (lower levels of PICALM in the BBB) present with accelerated amyloid pathology and behavioral deficits.[344]

Sporadic forms of ADRD, without known genetic mutations, are also highly intertwined with BBB dysfunction and vascular pathology. As mentioned previously, *Montagne et al.* reported decreased BBB function in the hippocampus of aged individuals.[315] However, this study also observed a significant decrease in BBB functionality of individuals with MCI and early AD compared to healthy age-matched controls, including the prevalence of gray and white matter lesions before the signs of brain atrophy and dementia. Other studies have reported increased CNS microbleeds in 25% of individuals with MCI and 45-78% of individuals with early AD.[345]

Furthermore, the albumin quotient (Qalb, the ratio of CSF / serum albumin levels) is significantly elevated in MCI and preclinical AD patients.[315, 346] In addition to neuroimaging studies in living individuals, post-mortem studies have identified accumulated blood-derived proteins including fibrinogen, albumin, and immunoglobulin G in the prefrontal and entorhinal cortex and hippocampus of AD patients.[347, 348]

Of particular importance to this study is the impact of the BBB architecture, particularly BECs, in AD progression. Multiple post-mortem studies have reported reduced capillary length and microvascular degeneration with diminished TJ protein expression and BEC degeneration. [340, 349, 350] Loss of claudin-5 as well as ZO-1 is associated with BBB breakdown in acute CNS diseases and neurodegenerative disorders.[285, 287] Mutations in *OCLN*, the gene encoding for occludin, leads the neurological syndrome pseudo-TORCH 1, which is characterized by early-onset seizures, severe microcephaly, and developmental delays.[351] Furthermore, studies have found significantly reduced levels of pericytes and pericyte coverage in the AD cortex and hippocampus compared to age-matched controls, a finding that is exacerbated by the *APOE4* gene.[340]

3.1.5 Calpain-1 overactivation and BBB-Dysfunction: A Therapeutic Opportunity

In normal, healthy physiological conditions, calpain-1 is an important regulator of endothelial cell function. Both calpain-1 and calpain-2 are expressed in endothelial cells and serve to maintain vascular physiological integrity.[352, 353] Activation of calpain-1 is reportedly induced by endothelial growth factors, namely vascular endothelial growth factor (VEGF), and is essential for angiogenesis and wound healing [79, 354-356] *Qui et al* found that the over-expression of calpastatin (calpain's endogenous inhibitor) significantly delayed skin wound healing in mice, an effect specifically provoked by impaired angiogenesis. Moreover *Gonscherowski et al* found that

treatment of un-stimulated human umbilical vein endothelial cells with 12μM calpain inhibitor I (***ALLM***) or 1μM calpastatin reduced vascular endothelial integrity.[353]

However, in pathogenic conditions where there is an overactivation of calpain, endothelial functionality declines. Calpain hyperactivation is found in the pathophysiology of multiple cardiovascular disorders and contributes to endothelial dysfunction.[357-360] Moreover, calpain expression was found elevated in cortical endothelial cells of human patients following TBI. [361] While only a handful of studies have examined the role of calpain inhibition in BECs, it has nevertheless been proposed as a therapeutic remedy to regulate BEC-dysfunction and BBB permeability.

Reports indicate calpain inhibition can attenuate BBB-dysfunction by protecting against loss of TJs. *Alluri et al.* reported calpain inhibition protected against IL-1β-induced loss of ZO-1.[362] Importantly, by using calpain-1 siRNA, calpain III inhibition, and calpastatin treatment, they were able to validate the effects were specifically induced by calpain-1 activity. In other studies, calpain-1 inhibition attenuated ZO-1 activity and endothelial cell barrier disruption induced by particulate matter in human lung endothelial cells.[363] Moreover, calpain inhibition (via ***ALLM***) attenuated occludin levels in Caco-2 cells induced by TPEN, a zinc chelator.[364] In fact, it has been proposed that multiple tight junction proteins (occludin, E-cadherin, and ZO-1) are substrates of calpain.[365] Additionally, a recent report found release of cathepsin B activates NLRP3 (NOD-, LRR-, and pyrin domain-containing protein 3) inflammasomes which in turn disrupts endothelial junctions.[366] Inhibition of cathepsin B (via ***CA-074***) attenuated transendothelial electric resistance (TEER) induced by nicotine in cultured endothelial cells. Intriguingly, the researchers found a loss of ZO-1 after nicotine administration but did not look at (or report on) the effects of ***CA-074*** on ZO-1 levels.

While calpain-1 and cathepsin B inhibition is reported to preserve TJs in multiple cell types, it also protects against BBB-permeability. *Tsubokawa et al.* reported administration of E-64d (5 mg/kg) given 30 minutes prior was found to decrease infarct volume and Evans blue dye penetration 24 hours post-mild cerebral artery occlusion (MCAO).[128] Furthermore, *Alluri et al.* found calpain inhibitor III (10 mg/kg) given immediately prior or post controlled cortical impact (CCI) reduced Evans blue dye perfusion and FITC-dextran fluorescence one hour post-CCI. [362]

One of the most well-studied mechanisms connecting calpain-1 and cathepsin B's association with the BBB involves matrix metalloprotease 9 (MMP-9), a versatile zinc-containing endopeptidase. The hyper-activation of MMP-9 has emerged over the last decade as a key contributor to the disruption of the BBB; MMP-9 has been reported to degrade TJ proteins as well as type IV collagen, laminin and fibronectin, all main elements of the basal lamina.[367-369] OS-based theories of BBB-dysfunction link increased free radicals to hyper-activation of MMP-9 which stimulates their degradation activity that can occur on TJs and disrupts the vital physiological barrier.[370] Additionally, numerous clinical studies have confirmed an increase in MMP-9 activity in the brains of stroke,[367] ADRD,[371, 372] and TBI patients.[373]

Previous results demonstrated that calpain-1 inhibition (via the calpastatin-derived inhibitor ***CP1B***) and cathepsin B inhibition (via global *CTSB*$^{-/-}$) attenuated MMP-9 activation in leukemia and glioblastoma cell lines, respectively.[374, 375] These findings prompted *Tsubokawa et al.* to investigate the inhibition of calpain-1 and cathepsin B on the BBB, where they found a single administration of ***E64d*** (5 mg/kg) 30 minutes prior to MCAO in rats decreased MMP-9 activity in both endothelial cells and neurons.[128] However, the most intriguing part of the study involved the time-course of calpain-1, cathepsin B, and MMP-9 activation. They found that two hours post-MCAO, there was a sharp activation of calpain-1 and cathepsin B without a change in MMP-9 activity. They then studied the brains six hours post-MCAO where they saw an increase in MMP-

9 activity along with activation in calpain-1 and cathepsin B. Moreover, the activation of all three proteins were co-localized in neurons and neurovascular structures, indicating that calpain-1 and cathepsin B regulate MMP-9 activation.

It's important to note that MMP-9 activity is also expressed in astrocytes and pericytes, two important cell types of the neurovascular system.[376, 377] In fact, pericytes have been reported to be the primary source of MMP-9 activity in the BBB.[378] Moreover, the regulation of pericyte contractibility and cellular stiffness is controlled by calpain.[379] Thus, calpain activity regulates BBB functionality in ways other than endothelial functionality.

A vital component to endothelial cell functionality is nitric oxide (NO). NO has multiple roles in brain function including vasodilation, inflammatory mediation and neuromodulation.[380, 381] In endothelial cells, NO is induced by the activation of endothelial nitric oxide synthase (eNOS). Aged mice (14-15 month old) with *eNOS*$^{-/-}$ exhibit an increase in inflammation and decrease in spatial learning and memory.[382] Moreover, the decrease in NO has been shown to promote AD pathology *in vitro* (via NOS inhibitor L-NAME and sGC inhibitor ODQ) and *in vivo* (via *eNOS*$^{-/-}$) by increasing APP and $A\beta_{1\text{-}40}$ in both neurons and endothelial cells.[382] Another study found that even the partial loss of eNOS (*eNOS*$^{+/-}$) increased cerebral amyloid angiopathy (CAA) in the cerebrum and hippocampus of aged mice (18 months), further strengthening the role of eNOS in the amyloidogenic processing of APP and elevation of Aβ peptides.[383] Importantly, these mice also presented with cognitive deficits. Thus, the eNOS/NO/sGC/cGMP/CREB pathway has been proposed as a therapeutic target for ADRD.[384]

Given the significance of eNOS in endothelial dysfunction, it's crucial to understand how calpain-1 modulates eNOS activity; calpain-1 substrates include eNOS associated proteins (caveolin,[385] heat shock protein 90 (hsp90),[385] Akt[386]), interruption of hsp90 as well as Akt binding to eNOS,[386, 387] and eNOS itself.[354, 388] Numerous reports suggest calpain inhibition can attenuate

the decrease in eNOS activity, thus promoting vascular integrity. *Chen et al* found calpain inhibition by ***E64d*** (1μM) attenuated the decrease in eNOS induced by oxidized low-density lipoprotein and protected against cell-loss in human aortic endothelial cells.[389] Moreover, *Yu et al* saw decreased eNOS in the aorta after calpain inhibitor I (5mg/kg/day for 8 days) was administered to rats on a high cholesterol diet.[390]

While numerous studies have correlated calpain-1 inhibition with the attenuation of eNOS levels, there is a lack of literature establishing this connection in BECs of the BBB. Intriguingly, cAMP response element-binding protein (CREB), a downstream target of the eNOS/NO/sGC/cGMP/CREB pathway, is heavily intertwined with calpain activity. CREB is a transcription factor heavily intertwined in ADRD pathology; its dysfunction is reported in *in vivo* models and patients.[391, 392] Activation via phosphorylation on the serine 133 residue regulates intermediate early genes (IEGs) including *BDNF*, *cFOS*, *Nurr-1* and *Zif268 (EGR-1)*, all which are associated with neuronal function.

The Arancio group has long studied the connection between CREB and calpain: *Puzzo et al* reported a reversal in Aβ-induced impairment of CA1 LTP after administration of an NO donor, an sGC stimular, or cGMP analogs.[393] Moreover, *Trinchese et al* reported a restoration in phosphorylation of CREB (pCREB) *in vitro* in cultured hippocampal neurons from APP/PS1 mice after administration of ***E64*** (1μM) or ***BDA-410*** (50nM).[127] Intriguingly, in this study, treatment of ***E64*** or ***BDA-410*** did not affect basal levels of pCREB in non-glutamate stimulated WT or APP/PSI slices. Thus, they theorize that Aβ causes an increase in calpain hyperactivation which hampers phosphorylation of CREB.

3.1.6 Objectives

Cerebrovascular dysfunction is a critical feature in the onset and progression of ADRD. [285, 330, 332, 394, 395] Recently, a specific 'two-hit vascular hypothesis' of ADRD has been introduced suggesting that a primary feature in ADRD pathogenesis is blood-brain barrier (BBB) dysfunction leading to neuronal injury and pathogenic accumulation of toxic proteins (Aβ, tau) as a "second hit".[396] This hypothesis is supported by studies implicating BBB dysfunction as an early feature in the progression of neurodegenerative disease;[330, 397] however it is still debated whether BBB dysfunction is the cause or consequence of neurotrauma. In contrast to studies on neurons and neuronal function, less attention has been paid to the components of the BBB, notably brain endothelial cell (BEC). The goal of this chapter was to characterize the effects of calpain/cathepsin inhibitors on BECs.

Specific chapter objectives:

1. Demonstrate BEC susceptibility to OS-based insults
2. Contrast varying effects of BECs incorporating AD contributors (OS via *ALDH2*$^{-/-}$ and APOE4 via APOE4-Tg)
3. Characterize the efficacy of CCH inhibition strategies on WT and *ALDH2*$^{-/-}$ BECs
4. Distinguish the impact of *mTBI* vs. *ALDH2*$^{-/-}$ on the BBB
5. Analyze BBB functionality in the 2-hit mouse model (*ALDH2*$^{-/-}$ + mTBI)
6. Test inhibition strategies in an *in vivo* model with BBB-dysfunction

3.2 METHODS

3.2.1 Primary Culture

Cortices were dissected from 3-8 week old mice, chopped with a razor blade, and centrifuged in Minimal Essential Media (ThermoFisher) at 1000 x g for 10 minutes at 4°C. The supernatant was removed and the pellet was triturated in papain (17U per brain) and DNase (84U per brain, LK003178 and LK003172, respectively, Worthington Biochemical) using a 19G needle before being placed in a 37°C water bath for 15 minutes. Following incubation, the sample was triturated with a 21G needle, and mixed vigorously with 2 parts 25% BSA (A2153-50G, Sigma, solubilized in HBSS-/-), before centrifugation at 3880 x g for 15 minutes at 4°C. After removing the supernatant, the pellet was resuspended in 1mL endothelial cell medium (M1166, Cell Biologics) with heparin (5.5U/mL, H3149, Sigma) and centrifuged for 5 minutes at 1000 x g at 4°C to remove residual BSA. The pellet was then resuspended in endothelial cell medium + heparin and plated onto plates coated with 0.005% collagen (C8919, Sigma), 1-2ug/mL laminin (L2020, Sigma), and 50 ug/mL fibronectin (F0895, Sigma). The following day, plates were washed 2x with HBSS+/+ and media was replaced with endothelial cell medium and puromycin (4ug/mL) as a selection agent for 72 hours. Cells were used at the second passage for all studies. The APOE3- and APOE-4-Tg BECs were a kind gift from Dr. Leon Tai. The cells were isolated from the EFAD mice which are 5xFAD mice backcrossed to APOE3 or APOE4 homozygous mice.[398]

3.2.2 Immunofluorescence

Cells were treated with 5μM Cell Tracker Red CMTPX (C34552, ThermoFisher) for 30 minutes, then washed and fixed with 4% Paraformaldehyde and 0.1% Triton X-100 in PBS for 5 minutes. Cells were then washed and treated with 5μM Hoeschst 33342 (Invitrogen) in Fluorobrite DMEM (A1896701, Fisher). Images were captured on the BZ-X700 microscope (Keyence), and

confluence was quantified using Keyence software. All OGD-R studies were performed in the absence of fetal bovine serum and endothelial growth supplements.

3.2.3 Immunoblots

Cells were cultured up to 95% confluence in 6-well plates and treated with varying concentrations of compounds for defined periods of time. At termination of treatment, cells were washed twice with ice-cold PBS and protein was extracted by adding ice-cold RIPA buffer (Sigma) supplemented with protease and phosphatase inhibitors (Calbiochem). Cells were scraped and the cell lysate was centrifuged at 10,000 x rpm for 10 min at 4°C. Protein concentration was determined using the Pierce BCA-200 Protein Assay Kit (ThermoFisher). Lysates were stored at -20°C for at least a day, then thawed on ice. Equal amounts of protein (μg) were prepared with 6X loading buffer (0.375 M Tris (pH=6.8), 12% SDS, 60% glycerol, 0.6 M DTT, 0.06% bromophenol blue), heated at 95°C for 5 minutes, cooled to RT before loading onto NuPage 4-12% Bis-Tris Protein Gels. The gels were transferred onto PVDF membranes using the iBLOT2 (ThermoFisher), blocked in 5% non-fat milk for 1 hour, probed overnight with the primary antibody at 4°C, washed with TBS-T 3x, probed with an HRP-linked secondary antibody (1:1000 in blocking buffer) for 1 hour, washed with TBS-T 3x, then visualized using SuperSignal West Fempto Chemiluminescence substrate (ThermoFisher) on the Azure c400 series. Immunoblots were quantified using Azure Biosystems Technology. All values were normalized to expression levels of beta-actin. Antibodies: anti-spectrin (MAB1622, Millipore), anti-ZO-1 (bs-1329R-TR, Bioss), anti-occludin (66378-1-Ig, Proteintech), anti-claudin 5 (4C3C2, ThermoFisher), anti-eNOS (bs-0163R, Bioss), anti-MAP2 (ab5392, Abcam), anti-MMP9 (ab38898, abcam), anti-GFAP (Z0334, Dako) and HRP-conjugated anti-beta actin (HRP-60008, Proteintech).

3.2.4 Closed-head mild Traumatic Brain Injury

Protocol was modified from previous literature.[251] Mice were anesthetized with isoflurane (5% flow rate) and immediately placed under the vertical 30cm long guide tube and stabilized by a sponge cushion. A 30g weight with a rounded tip (34 x 13mm) was dropped vertically through the tube and directed to the right sagittal plane between the eye and the ear, inducing a unilateral injury on the intact scalp. Following injury, the mice were monitored for return of normal gait and no cerebral edema or seizures.

3.2.5 Tissue Harvesting

Mice were sacrificed using CO_2 asphyxiation, perfused with ice-cold PBS, brains extracted and split into two hemispheres (ipsilateral vs. contralateral), flash frozen in liquid nitrogen, and stored at -80°C for further protein or RNA extractions.

3.2.6 Protein Extraction for Western Blot

Brains were removed from the freezer, weighed, and homogenized using a BeadBug microtube homogenizer (Sigma). Briefly, 2x volume of ice-cold lysis buffer (25mM HEPES pH 7.0, 1mM EGTA, 1mM EDTA, 1% Triton X-100, 0.1% SDS supplemented with protease and phosphatase inhibitors [Roche Diagnostics]) was added to a 2mL beat tube with beads (3x tissue mass). Brain samples were homogenized at 3800rpm for 10 seconds 3x with a rest of 1 minute in between. The homogenized brain was then centrifuged at 1000rpm at 4°C for 15 minutes. Each lysate (minus beats) was then moved to another tube and homogenized again at the same speed and time. The samples were stored on ice for the entirety of the protein extraction.

3.2.7 Sodium Fluorescein Extravasation

Mice were injected with 5mg/kg of 2% NaFl in sterile dH_2O via i.p. 30 minutes prior to sacrifice. Mice were sacrificed with CO_2, and 600-800 μL of blood was collected from the right

ventricle of the heart prior to perfusion with ice-cold PBS at a rate of 6 mL per min for 3 min. Plasma was centrifuged at 1500 x g for 15 minutes at 4°C. Following perfusion, the mice were decapitated and brain hemispheres were collected and stored in -80°C prior to biochemical analysis. Plasma was analyzed immediately on a 96-well black plate using the Synergy neo2 plate reader, measuring absorbance at an excitation wavelength of 440nm and emission of 525nm. Each hemisphere was weighed and homogenized in PBS. An equal amount of 60% trichloroacetic acid in deionized water was added to precipitate proteins, and left on ice for 30 minutes, then centrifuged at 18000 x g for 10 minutes at 4°C. Supernatants were measured in a 96-well black plate. The samples were protected from light throughout the entire experiment either by using light-sensitive 1.5mL Eppendorf tubes, covering in aluminum foil, or working in a dark room. Sodium fluorescein extravasation was quantified as follows:

Equation 1. Quantification of sodium fluorescein extravasation

$$Cleared\ volume\ (\frac{\mu L}{mG}) = \frac{\frac{Brain\ Fluorescence\ (AU)}{\left(\frac{Plasma\ Fluorescence\ (AU)}{plasma\ amount\ measured\ (uL)}\right)}}{\left(\frac{Brain\ weight\ (mg) \times\ brain\ amount\ measured(uL)}{total\ supernatant\ (uL)}\right)}$$

3.2.8 RNA isolation

Following perfusion, whole brains were extracted and separated into two hemispheres (ipsilateral and contralateral) and immediately stored in 1.5mL tubes at -80°C for at least one day. Hemispheres were removed from -80°C, thawed on ice for 10-15 minutes and homogenized with 1mL Trizol using a hand-held pestle homogenizer. The tubes were then spun at 10,000 x g for 10 minutes at 4°C to remove debris. Supernatant was removed and placed in a fresh tube with .200 µL chloroform. Samples were vigorously vortexed for 15 seconds then incubated at room temperature for 2 minutes before centrifugation of 12,000 x g for 15 minutes at 4°C. The upper aqueous phase containing RNA was transferred and isolated using the RNeasy Plus Mini Kit (Qiagen) according to the manufacturer's instructions. Briefly, the RNA containing supernatant was transferred to a gDNA Eliminator spin column in a 2 mL collection tube which was spun for 30 seconds at 12,500 rpm. The flow-through was transferred to an RNeasy spin column with 1:1 70% ethanol added and spun for 15 seconds at 12,500 rpm. Flow through was discarded and 700µL Buffer RW1 was added and spun at 12,500 rpm for 15 seconds. The flow through was again discarded and 500µL of Buffer RPE added to column then spun again for 15 seconds at 12,500 rpm. This step occurred twice. The column was then placed into a new 1.5mL collection tube and spun for 1 minute at 12,500 rpm to fully remove any excess liquid. The RNeasy spin column was then placed into a new 1.5mL collection tube and 30µL RNase-free water was added, then spun at 12,500 rpm for 1 minute to elute RNA.

A Biotek Synergy Neo2 was utilized to quantify RNA using the nucleic acid quantification program. A blank of nuclease-free water was used to ensure no contamination before counting. For each sample, 2µL was added in duplicate on the Take3 Multivolume plate and absorbance values quantified. 260/280nm ratio of absorbance validated purity.

3.2.9 Reverse Transcription

Reverse transcription was performed using the SuperScript III First-Strand Synthesis System for RT-PCR (Invitrogen) according to manufacturer's instructions. Briefly 2µg RNA of each sample was added to nuclease-free microcentrifuge tube, along with 12.5µL nuclease-free water, 2.5µL 50uM oligo $(dT)_{12-18}$ and 2.5µL 10mM dNTP. The mixture was heated at 65°C for 5 minutes before cooling at 4°C. A mixture of 10µL 5X first strand buffer, 2.5µL 0.1mM DTT, 11µL nuclease-free water and 2.5µL superscript III (10,000U) was added, vortexed, and centrifuged to condense sample. The mixture was incubated at 50°C for 60 minutes then inactivated at 70°C for 15 minutes and cooled to 4°C. cDNA was stored in -20°C until qPCR.

3.2.10 Quantitative PCR

Quantitative PCR was carried out utilizing the Taqman Gene Expression Master Mix (Applied Biosystems) on the StepOnePlus Real Time PCR system (Life Technologies). 2µL cDNA of each sample was added in duplicate to a 96-well semi-skirted PCR microplate. A mixture of 10µL TaqMan Master Mix, 6µL nuclease-free water, 1µL gene of interest (FAM fluorophore, ThermoFisher) and 1µL housekeeping gene (ACTB-VIC fluorophore or HPRT-VIC fluorophore, ThermoFisher) were added. The plate was centrifuged for 5 minutes at 2,000rpm before analysis. The plate was cycled with a holding stage of 2 minutes at 50°C followed by 95°C for 10 minutes, then 42 cycles of 15 seconds at 95°C followed by 1 minute at 60°C. C_T levels were collected and normalized to housekeeping gene in each sample. Data is represented as $\Delta\Delta C_T$ and normalized to wildtype controls. An average of at least three biological and three analytical duplicates was used. Genes used are indicated in TABLE VIII.

TABLE VIII. PRIMERS UTILIZED IN RT-QPCR STUDIES

Gene Symbol	Gene Name	UniGene ID	Product Number	Probe
ACTB	Actin, beta	Mm.328431	Mm01205647_g1	VIC
Cldn5	Claudin 5	Mm.22768	Mm00727012_s1	FAM
HPRT	Hypoxanthine guanine phosphoribosyl transferase	Mm.299381	Mm03024075_m1	VIC
Nos3	Nitric oxide synthase 3, endothelial cell	Mm.258415	Mm00435217_m1	FAM
Ocln	Occludin	Mm.4807	Mm00500912_m1	FAM
Tjp1	Tight Junction Protein 1 (ZO-1)	Mm.4342	Mm01320638_m1	FAM

3.3 RESULTS AND DISCUSSION

3.3.1. Inhibition strategies preserve BEC integrity post-OGD-R

Cortical BECs were isolated from wild-type (WT) mice following dissection, digestion and selection (Figure 48A). This protocol was developed and extensively characterized by Dr. Leon Tai and his research group. These BECs are not used beyond passage 2 to maintain phenotype, and grown on a fibronectin, laminin and collagen matrix to maintain adhesion and ensure purity. Using the Keyence microscope, it was demonstrated that WT BECs morphology changes after OGD-R induced stress (Figure 48B).

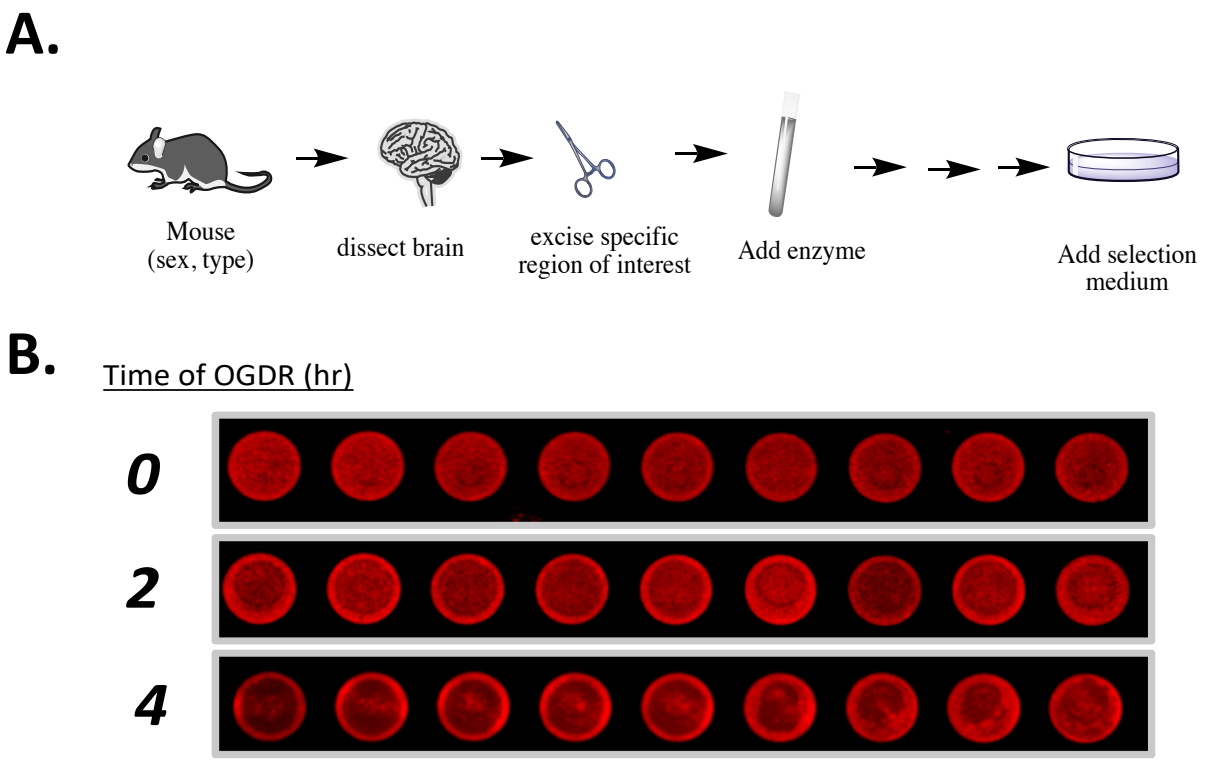

Figure 48. WT BECs are susceptible to OGD-R insult.
(A) Schematic representing the procedure to isolate BECs from WT mice. (B) BECs isolated from WT mice were treated with 0-4 hours of OGD-R, fixed and stained with cell tracker red, and imaged on the Keyence microscope.

Similar to the SH-SY5Y neuronal cells, BECs showed an inversely proportional relationship with cell viability and increasing length of OGD-R (0, 1, 2, 4, and 6 hours of OGD-R, Figure 49A). Significant loss in cell viability was first observed at two hours OGD-R (85.7 ± 2.6%). Moreover, the lipid peroxidation products 4-hydroxynonenal (HNE) and oxo-2-nonenal (ONE) also exerted dose-dependent loss in cell viability validating that the BECs isolated are susceptible to OS (Figure 49B and C). Furthermore, while SH-SY5Y human neuronal cells seemingly plateaued with LPP and OGD treatment, primary WT BECs were exceptionally sensitive to the same insults.

As BECs exhibited similar susceptibility to two hours OGD-R as neuronal cells, it was assumed that if the CCH hypothesis was prevalent, CCH inhibitors would sufficiently attenuate BEC-cell death. Thus, we treated BECs induced with two hours OGD-R with 10μM and 1μM CCH inhibitors at the 'ischemia' treatment paradigm. Using sulforaphane as a control, the selective and nonselective calpain-1 inhibitors were able to dose-dependently mitigate the loss in cellular confluence (Figure 49D). Treatment of 10μM with compound ***5*** or ***NYC-438*** restored BEC confluence to 95.1 ± 2.3% and 93.4 ± 3.1%, respectively, while ***CA-074*** did not.

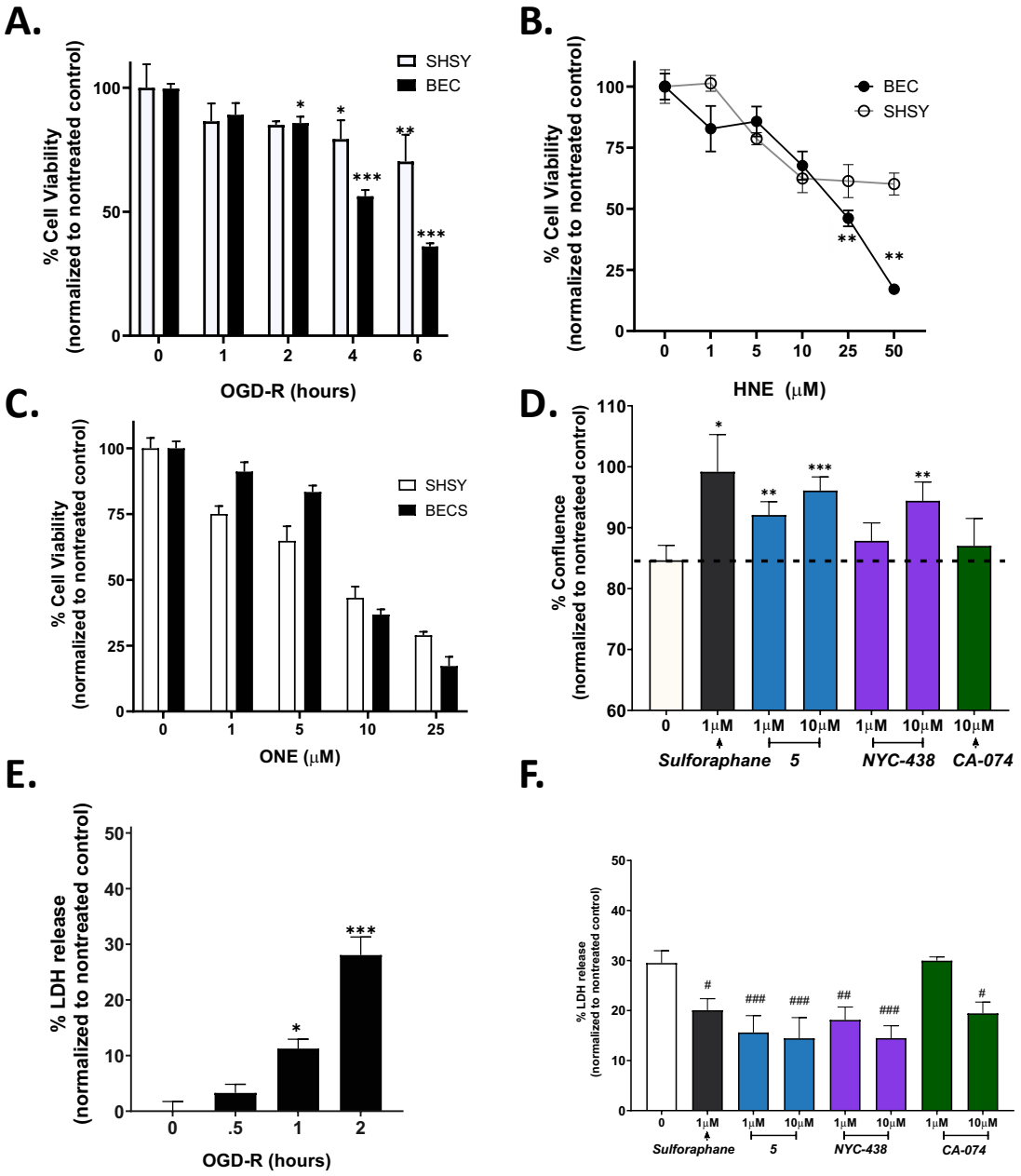

Figure 49. Inhibition strategies ameliorate BECs susceptibility to oxidative stress.
(**A**) Cell viability quantified by immunofluorescence of BECs and SH-SY5Y cells treated with OGD-R for 0, 1, 2, 4 or 6 hours. (**B** and **C**) Cell viability quantified by MTS release of BECs and SH-SY5Y cells after 24 hour treatment of the lipid peroxidation products 4-hydroxy-2-nonenal (HNE, **B**) or 2-oxononenal (ONE, **C**) at various concentrations. (**D**). Cell viability quantified by immunofluorescence of BECs following 2 hours OGD-R with co-treatment of sulforaphane or inhibitors (1 and 10μM). (**E**) LDH release of BECs following 0, 0.5, 1 or 2 hours of OGD-R. (**F**). LDH release of BECs following 2 hours of OGD-R with co-treatment of sulforaphane or inhibitors. Data represents mean ± SEM of at least n=3 in 3 separate isolations analyzed by one-way ANOVA with Dunnett's or Tukey's multi-comparison analysis or one sample t and Wilcoxon test. *p<.05, **p<.01, **p<.001 *v.* nontreated control

We confirmed these results using the LDH assay which utilizes a chemical readout of cell death. This was selected as a less subjective method of qualitative analysis. LDH results showed a similar trend: increasing lengths of OGD-R produced a proportional increase in LDH release (Figure 49E). Treatment of 10μM of all inhibitors significantly reduced the LDH release (nontreated: 28.1 ± 3.3%; ***5***: 14.5 ± 4.1%; ***NYC-438***: 14.5 ± 2.5%; ***CA-074****: 19*.4 ± 2.3%, Figure 49F). However, at 1μM only ***5*** and ***NYC-438*** significantly reduced LDH release.

Previous experiments determined that there were no sex differences between BECs isolated from female versus male mice (Figure 50). Thus, in the previous experiments, BECs were isolated from both male and female mice.

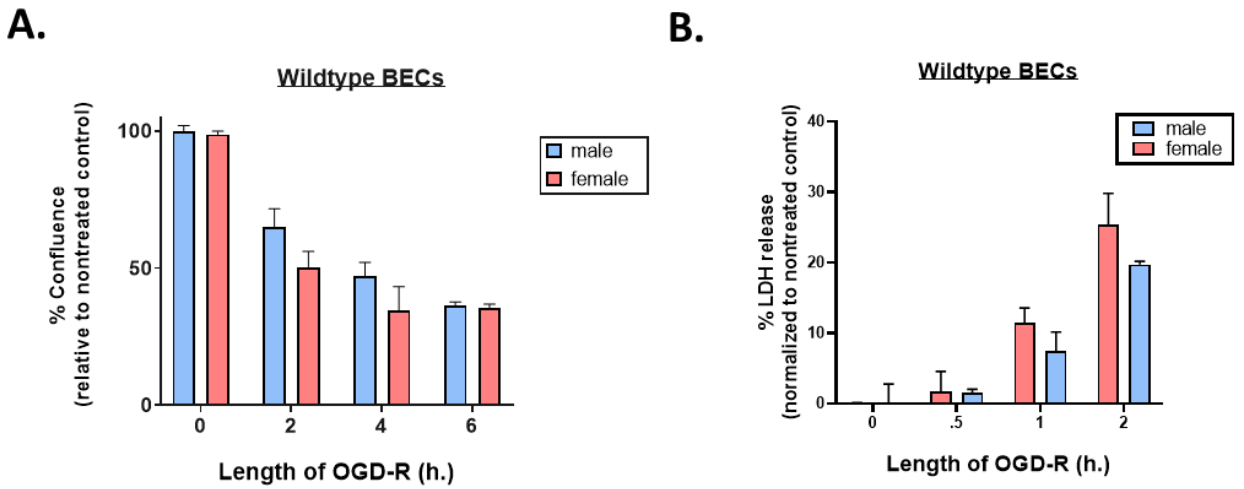

Figure 50. WT BECs isolated separately from male and female mice exhibit no significant differences.
(**A**) Quantification of confluence of WT BECs isolated from male and female mice at varying times of OGD-R determined using Keyence software (**B**) LDH release of WT BECs isolated from male and female mice at varying times of OGD-R. Data represents mean ± SEM of at least n=3 duplicates of cell passages.

Multiple reports have revealed that there is substantial decrease in the expression of tight junction proteins (TJs) in post-mortem brain tissue of ADRD patients.[399, 400] Thus, studies were expanded to determine if CCH inhibitors could protect against this loss. We focused our efforts on two TJs: zona occludens 1 (ZO-1) and occludin. ZO-1 is a scaffold protein that anchors TJs to the actin cytoskeleton while occludin is a plasma-membrane protein. Immunoblots revealed levels of ZO-1 and occludin were significantly reduced after 2 hours OGD-R (88.3 ± 0.02% and 83.2 ± .03% respectively, Figure 51A-D). Co-treatment with 10μM inhibitors ameliorated the loss in ZO-1 and occludin with significance reached with ***5*** and ***NYC-438*** (Figure 51E and F). To ensure the specific inhibitory efficacy in BECs, SBDP 150kDa and 145kDa were examined. All compounds reduced SBDP 150kDa (Figure 51G), but only ***5*** and ***NYC-438***, the calpain-1 inhibitors, significantly reduced SBDP 145kDa levels (Figure 51H).

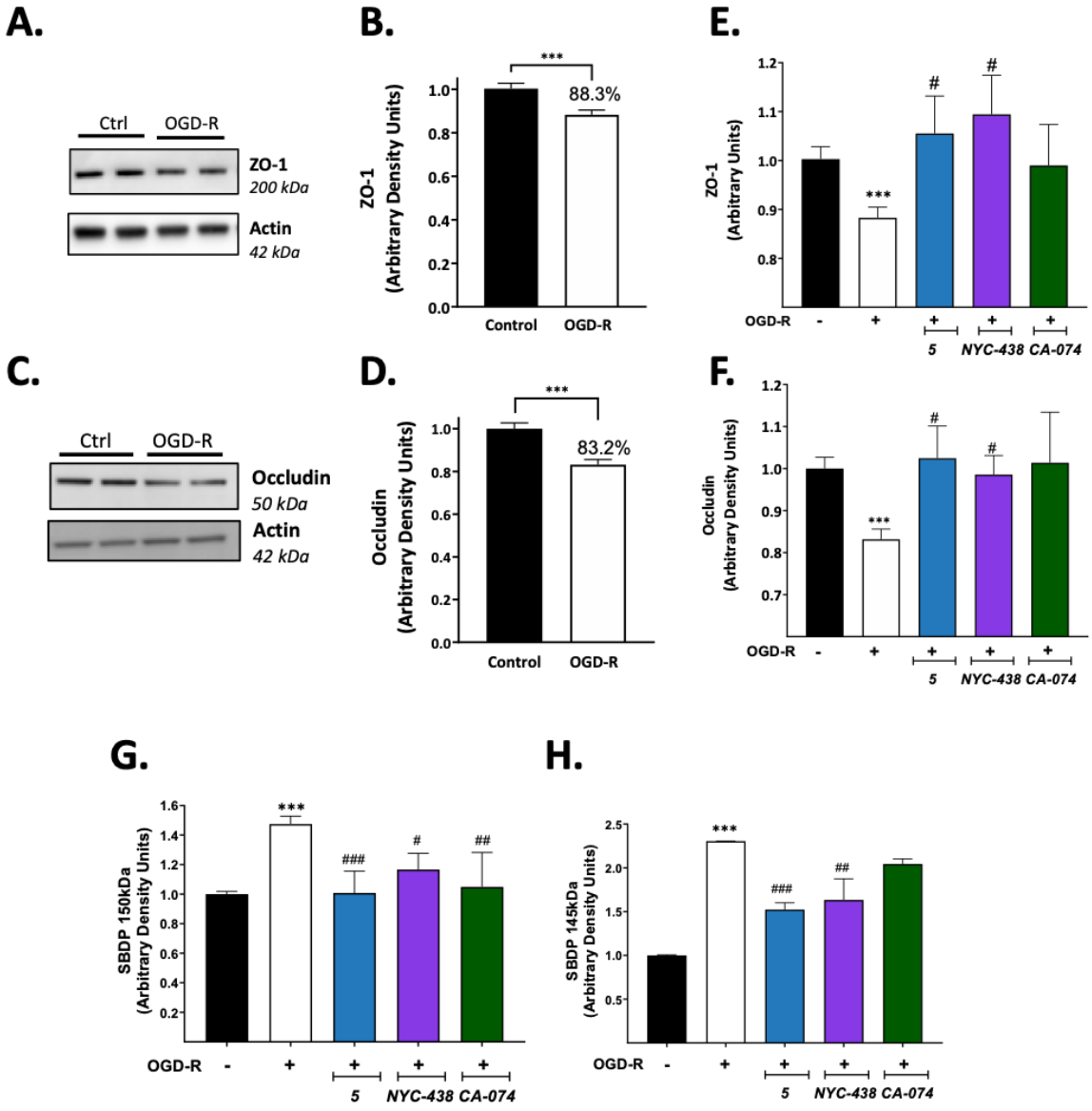

Figure 51. Inhibition strategies mitigate loss of tight junction proteins.
(**A** - **D**) Representative immunoblots of BECs treated with 1 hour OGD-R and nontreated control probed with ZO-1 Ab (**A**) and Occludin Ab (**B**) and associated quantitative analysis (**C** and **D**, respectively). (**E** - **H**) Quantitative analysis of BECs treated with 10μM inhibitors followed by 1 hour OGD-R and nontreated controls probed with ZO-1 (**E**), Occludin (**F**) or Spectrin (SBDP 150kDa and 145 kDa analyzed in **G** and **H**, respectively). All protein was normalized to the housekeeping protein, β-actin. Data represents mean ± SEM of at least n=3 separate isolations analyzed by one sample t and Wilcoxon tests or one-way ANOVA with Dunnett's or Tukey's multi-comparison analysis. Equal protein amounts were loaded in all lanes of immunoblots. ***p<.001 *v.* nontreated control. $^{\#}$p<.05, $^{\#}$p<.01, $^{\#}$p<.001 $^{\#}$p<.05 *v.* OGD-R treated.

3.3.2. Reduced Resilience in ALDH2$^{-/-}$ is Reversed by CCH Inhibitors

Our findings were further enhanced to looking at BECs isolated from the *ALDH2*$^{-/-}$ mouse model to further delineate mechanistic effects of CCH inhibition strategies. Aldehyde dehydrogenase 2 (Aldh2) is a major detoxifier of LPPs in the brain and is heavily implicated in the pathologies of ADRD, ischemia and TBI.[21990] Previous studies found Aβ treatment increased endothelial cell dysfunction, an effect that was reversed with an ALDH2 activator.[401] It was assumed that the *ALDH2*$^{-/-}$ mice would have more susceptible BECs, and therefore a weakened BBB.

We began by testing our compounds' impact on morphology and confluence, not as a measure of functionality, but as a first initial screen before moving to LDH, a qualitative measurement (Figure 52). *ALDH2*$^{-/-}$ BECs appeared to have less coverage than WT BECs after treatment. Moreover, the *ALDH2*$^{-/-}$ BECs looked more elongated post-treatment, while the WT BECs appeared to maintain their morphology despite the loss in coverage.

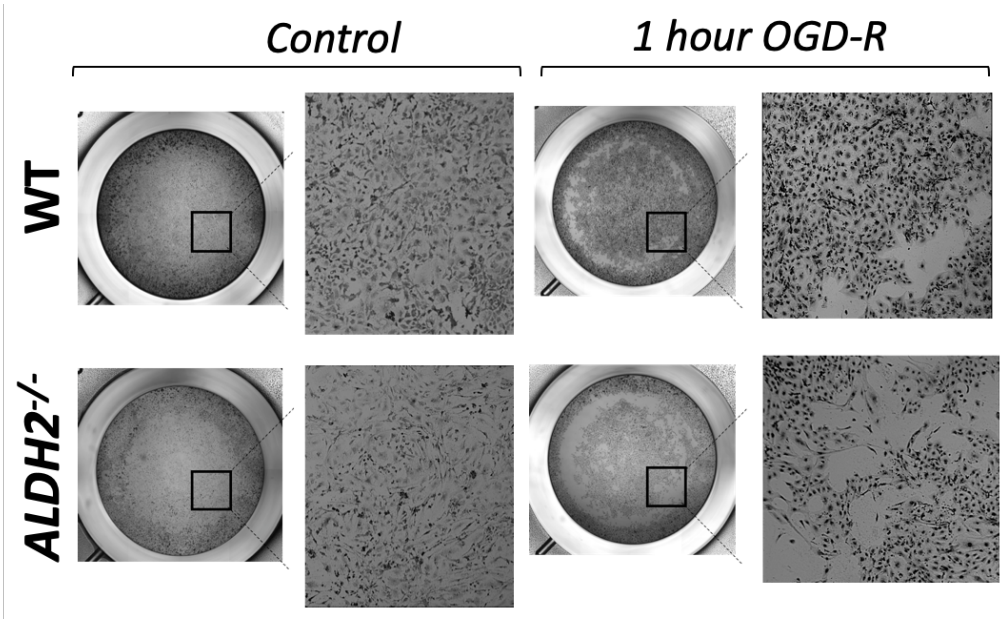

Figure 52. Morphological changes between WT and *ALDH2*$^{-/-}$ BECs 1 hour post-OGD-R
BECs were isolated from WT and *ALDH2*$^{-/-}$ mice, subjected to 1 hour OGD-R, then imaged on the Celligo imager.

Next, we qualitatively compared WT and *ALDH2*$^{-/-}$ BECs after varying lengths of OGD-R, specifically examining confluence and LDH release. *ALDH2*$^{-/-}$ BECs exhibited significantly lower confluence than WT post-OGD-R (1 hour: 72.1 ± 4.0% *v.* 89.1 ± 4.7, Figure 53A and B). The exacerbated response in *ALDH2*$^{-/-}$ BECs was also seen in LDH release (0.5 hours: 16.7 ± 1.0% *v* 3.2 ± 1.6%, 1 hours: 27.9 ± 12.5% *v* 11.3 ± 1.7%, 2 hours: 35.5 ± 3.2% *v.* 28.1 ± 3.3%, Figure 53C). Co-treatment with 10μM inhibitors failed to improve confluence. LDH release was significantly reduced with ***5*** and ***NYC-438*** after 1 hour OGD-R in the *ALDH2*$^{-/-}$ BECs (***5***: 8.6 ± .8%, ***NYC-438***: 9.6 ± .5%, Figure 53D).

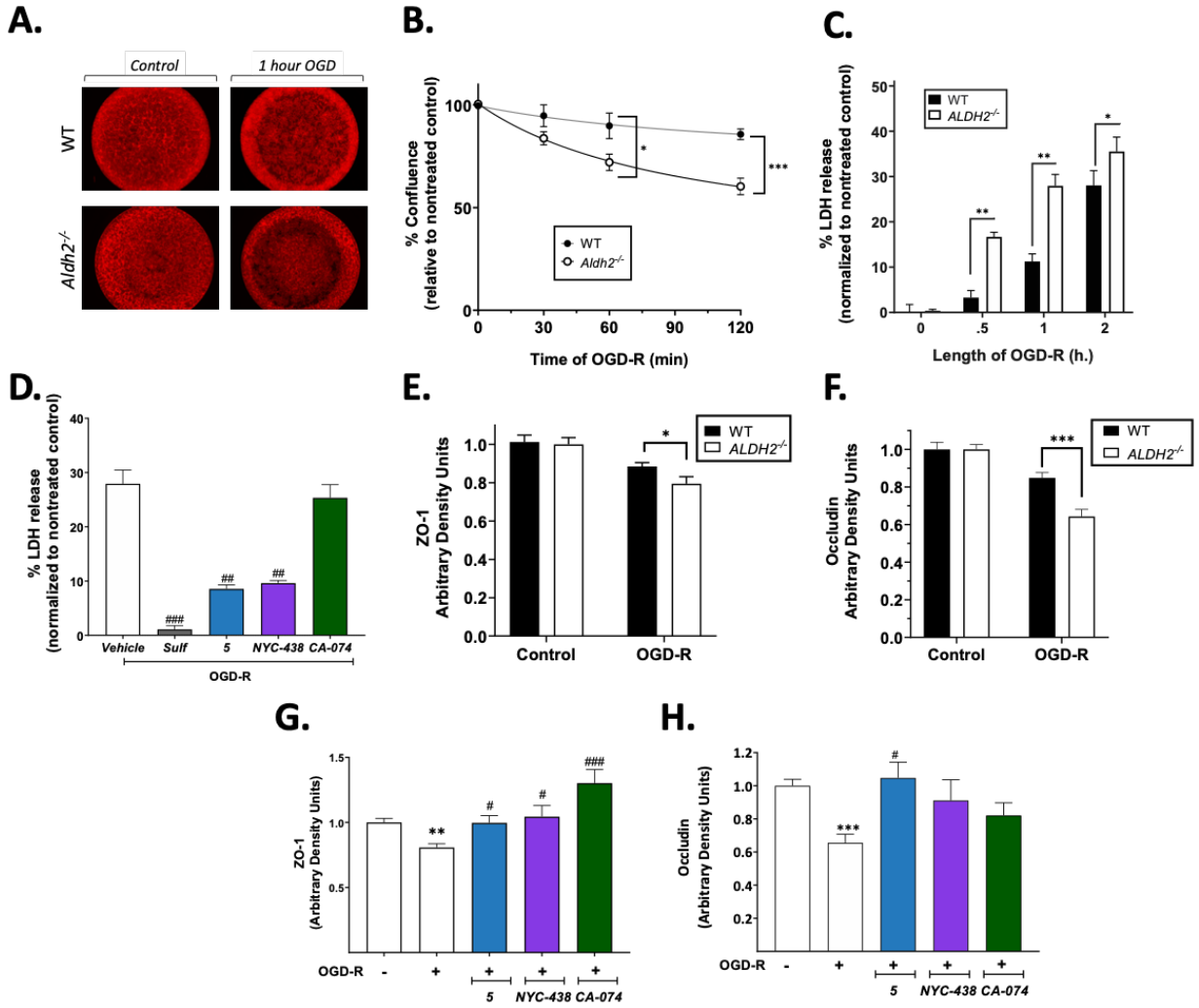

Figure 53. Reduced resilience in *ALDH2*$^{-/-}$ BECs is reversed by CCH inhibitors.
(**A** and **B**) Representative image (**A**) and quantitative analysis of confluence (%, **B**) analyzed by immunofluorescence of WT and *ALDH2*$^{-/-}$ BECs treated with 0, 30, 60 and 120 minutes of OGD-R. (**C**) LDH release of WT and *ALDH2*$^{-/-}$ BECs following 0, .5, 1, 2 hours of OGD-R. (**D**) LDH release of *ALDH2*$^{-/-}$ BECs following 1 hours of OGD-R with co-treatment of 1μM sulforaphane or 10μM inhibitors. (**E** and **F**) Quantitative analysis of *ALDH2*$^{-/-}$ BECs treated with 1 hour OGD-R and nontreated control probed with ZO-1 Ab (**E**) and Occludin Ab (**F**). (**G** – **J**) Quantitative analysis of BECs treated with 10μM inhibitors followed by 1 hour OGD-R and nontreated controls probed with ZO-1 (**E**), Occludin (**F**). Data represents mean ± SEM of at least n=3 separate isolations analyzed by one-way ANOVA with Dunnett's or Tukey's multi-comparison analysis . *p<.05, **p<.01, **p<.001 *v.* nontreated control. $^{\#}$p<.05, $^{\#}$p<.01, $^{\#}$p<.001 $^{\#}$p<.05 *v.* OGD-R treated

Moreover, *ALDH2*$^{-/-}$ BECs exhibited significantly reduced levels in the tight junction proteins ZO-1 (0.79 ± 0.4% *v 0.88* ± 0.2%) and occludin (0.64 ± 0.4% *v 0.83* ± 0.3%) compared to WT following 1 hour OGD-R (Figure 53E and F). Levels of ZO-1 and occludin were improved with co-treatment of ***5*** (1.0 ± 0.6% and 1.1 ± .09%, respectively) and ***NYC-438*** (1.1 ± .08% and .91 ± .12%, Figure 53G and H respectively). Surprisingly, ***CA-074*** significantly improved levels of ZO-1 (1.3 ± 0.1%), but not occludin. Specific inhibitory efficacy of the compounds in the *ALDH2*$^{-/-}$ BECs were confirmed, with ***5*** and ***NYC*-438** significantly reducing SBDP 150kDa, and just ***5*** reducing SBDP 145kDa (Figure 54).

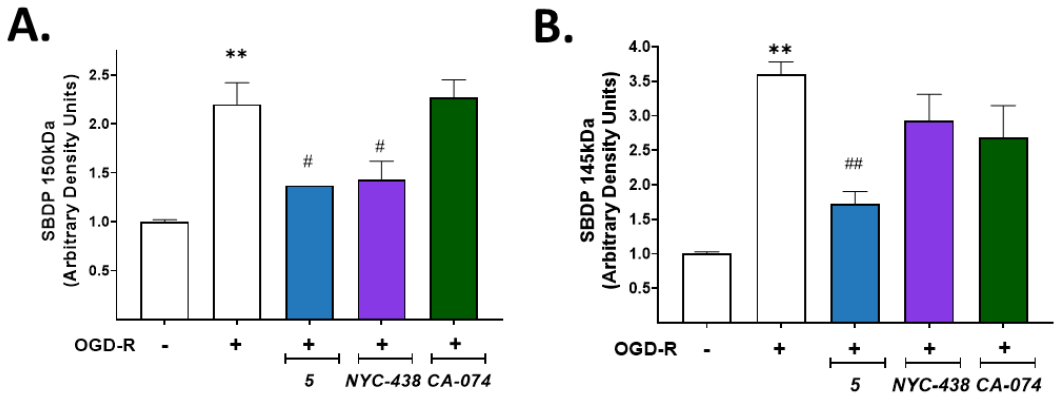

Figure 54. CCH inhibitors reduce SBDP 150kDa and 145kDa in *ALDH2*$^{-/-}$ BECs.
(**A** and **B**) Quantitative analysis of *ALDH2*$^{-/-}$ BECs treated with 1 hour OGD-R and nontreated control probed with Spectrin (SBDP 150 (**A**) or 145kDa (**B**), respectively). Data represents mean ± SEM of at least n=3 separate isolations analyzed by one-way ANOVA with Dunnett's or Tukey's multi-comparison analysis . *p<.05, **p<.01, **p<.001 *v.* nontreated control. $^{\#}$p<.05, $^{\#}$p<.01, $^{\#}$p<.001 $^{\#}$p<.05 *v.* OGD-R treated.

These studies demonstrated the ability of selective and nonselective calpain-1 inhibitors to preserve both WT and *ALDH2*$^{-/-}$ BEC viability and mitigate the loss in TJs following ischemia-reperfusion injury, and support the hypothesis that the CCH extends to BEC-dysfunction. Intriguingly, calpain-1 inhibitors (***5*** and ***NYC-438***) maintained efficacy in all *in vitro* studies, while cathepsin B selective inhibitor displayed variable efficacy. This suggested inhibition of calpain-1 is required for protecting BECs against CCH-mediated damage. Thus, moving into *in vivo* studies, we decided to we characterized selective *v.* nonselective calpain-1 inhibition and forgo cathepsin B inhibitor (***CA*-074**) studies.

Again, studies were performed to ensure no sex differences were observed with the BECs isolated from *ALDH2*$^{-/-}$ mice. There was no difference in susceptibility to OGD-R (Figure 55A and B). Moreover, there were no significant changes in levels of tight junction proteins of male and female for both WT and *ALDH2*$^{-/-}$ BECs (Figure 55C and D).

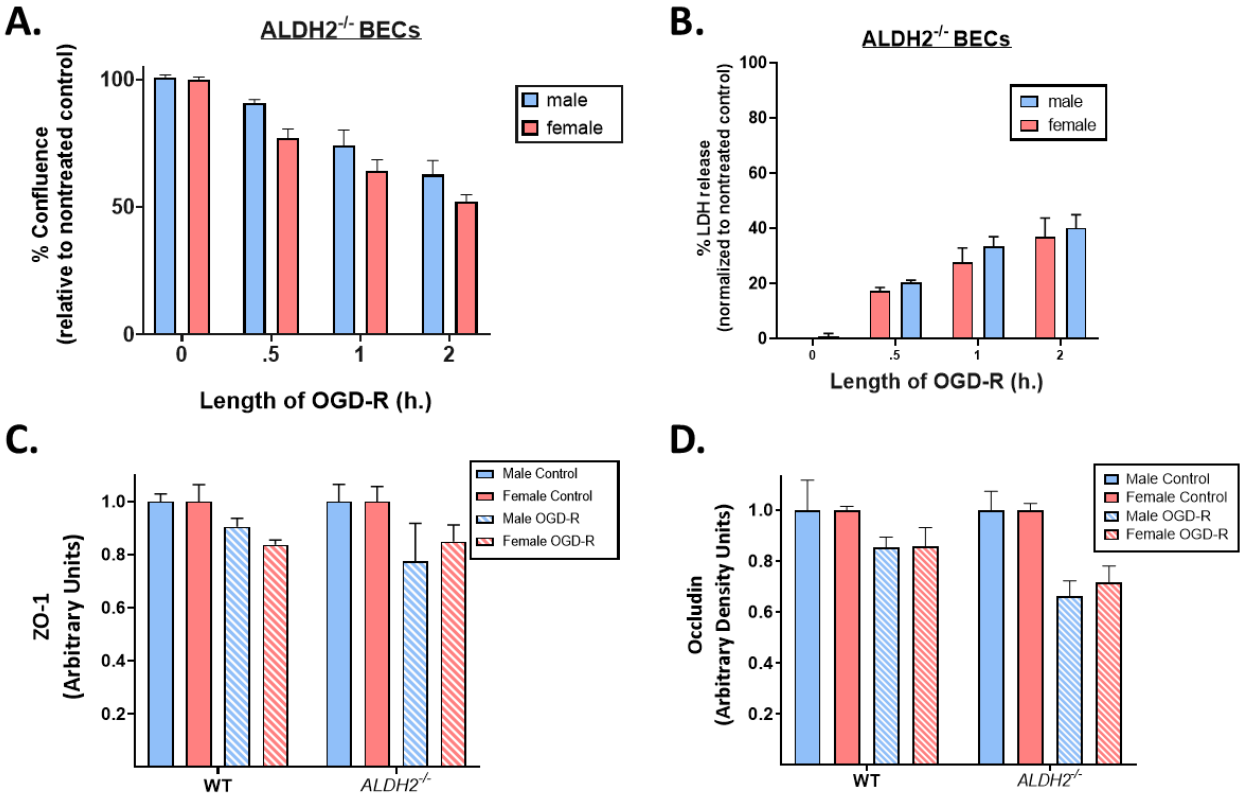

Figure 55. *ALDH2*$^{-/-}$ BECs isolated from male and female mice are equally susceptible to OGD-R injury

(**A**) Quantification of confluence of WT BECs isolated from male and female mice at varying times of OGD-R determined using Keyence software (**B**) LDH release of WT BECs isolated from male and female mice at varying times of OGD-R. (**C** and **D**). Quantification of western blots probed with ZO-1 and Occludin Abs following 1 hour OGD-R. Data represents mean ± SEM of at least n=3 duplicates of cell passages.

3.3.3. Exacerbated Damage in ApoE4 vs. ApoE3 female BECs

We further decided test the susceptibility of BECs in a more relevant genetic-based AD animal model. It is well known that the largest known genetic risk factor for AD is the apolipoprotein E containing the ε4 allele (*APOE4*).[402] The APOE gene is involved in lipid homeostasis by mediating lipid transport.[403] The human APOE gene exists in three alleles: ε2, ε3

and ε4, with has a global frequency of 8.4%, 77.9% and 13.7%, respectively.[404] However, the occurrence of the ε4 allele in AD patients is roughly 40%. APOE ε4 confers an increased risk of AD, as one or both alleles carry a startling 47% and 91% AD frequency, respectively.[338]

Evidence from Dr. Tai's lab suggests that ApoE4-Tg mice have a weakened BBB compared to ApoE3-Tg mice,[405-407] and thus we decided to test their susceptibility to OGD-R induced damage. BECs were isolated from female EFAD mice with either ApoE3-Tg and ApoE4-Tg separately and subjected to varying lengths of OGD-R injury. ApoE3 and Apoe4 BECs exhibited no significant difference in cell viability when subjected to OGDR for 0.5, 1, or 2 hours (Figure 56). However, following 4 hours of OGD-R, ApoE4 BECs were significantly less confluent than ApoE3 BECs. This suggests that the ApoE4 allele, the largest genetic known risk factor for AD, confers reduced resilience against oxidative stress injury.

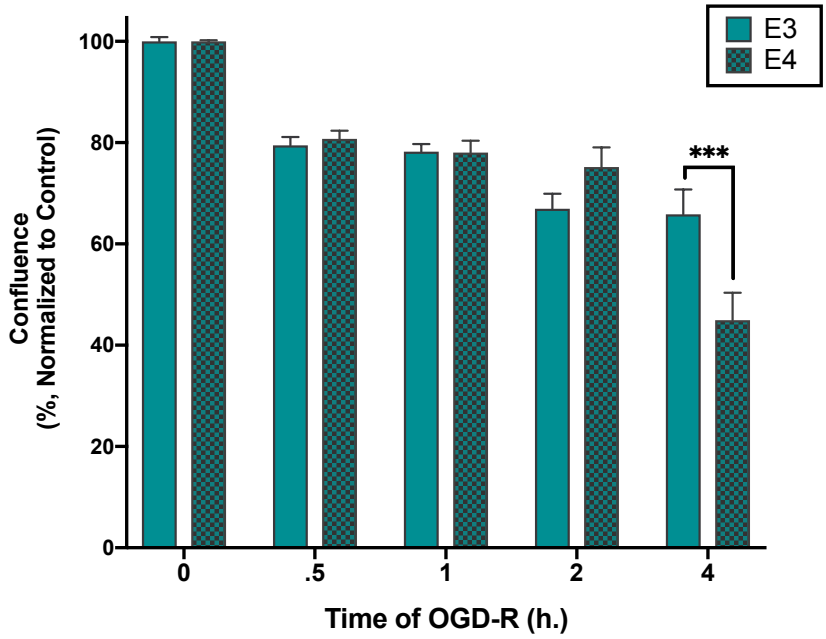

Figure 56. Exacerbated susceptibility of BECs isolated from APOE4-Tg mice v. APOE3-Tg. Confluence of BECs isolated from female APOE4-Tg mice and APOE3-Tg mice at 0-4 hours of OGD-R quantified by Keyence Software. Data represent mean ± SEM of at least n=5 of 2 isolations.

3.3.4 ALDH2$^{-/-}$ mice with mTBI exhibit BBB-Dysfunction

Chapter 2 demonstrated that the *ALDH2*$^{-/-}$ mice exhibit exacerbated damage to mild insult, as evidenced by the sharp cytokine activation and increase in GFAP, GFAP-BDP and SBDP 145kDa.[269] In this chapter, we sought to determine if underlying oxidative stress or mTBI would lead to exacerbated vulnerability to cerebrovascular damage *in vivo*.

Utilizing the mTBI model discussed in chapter 2, WT and *ALDH2*$^{-/-}$ mice underwent a closed-head weight drop on the right hemisphere. Sodium fluorescein (NaFl) was injected via *i.p.* 24 hours post-mTBI and allowed to circulate for 30 minutes before sacrifice, with contralateral and ipsilateral hemispheres collected. NaFl is a commonly used method to determine permeability

of the blood brain barrier.[408] We utilized this method as a first screen to characterize mTBI and OS effect on BBB functionality. Injection of 5 mg/kg of 2% NaFl administered 30 minutes prior to sacrifice is an adequate dose to visibly change the internal milieu of mice to a yellow, highly fluorescent color (Figure 57).

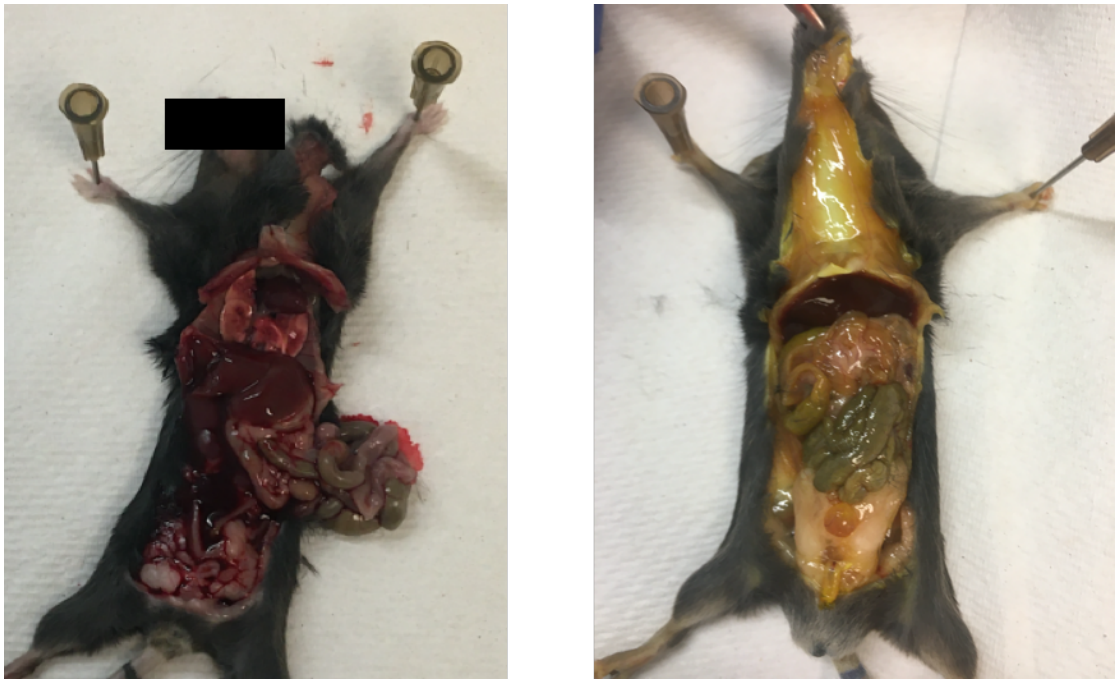

Figure 57. Sodium fluorescein is a highly fluorescent tracer
Photographic representation of the internal milieu of a mouse without (left) or with (right) 5 mg/mL 2% NaFl allowed to sacrifice for 30 minutes prior to sacrifice.

Quantification of NaFl extravasation into the brain revealed a sharp increase induced by mTBI in the WT mice in the ipsilateral hemisphere (*ipsilateral:* WT = 1.0 ± 0.13 µg/uL, WT + mTBI = 1.46 ± 0.20 µg/uL; *contralateral*: WT = 1.0 ± 0.11 µg/uL, WT + mTBI = 0.91 ± 0.11 µg/uL, Figure 58). Moreover, OS alone increased NaFl extravasation (*ALDH2*$^{-/-}$ *ipsilateral*: 1.67 ± 0.33 µg/uL; *ALDH2*$^{-/-}$ *contralateral*: 1.56 ± 0.22 µg/uL). The combination of underlying oxidative stress with mTBI exacerbated the NaFl extravasation in only the right hemisphere, the side of insult (*ALDH2*$^{-/-}$ + mTBI – *ipsilateral*: 2.1 ± 0.21 µg/uL, *contralateral*: 1.47 ± 0.09 µg/uL).

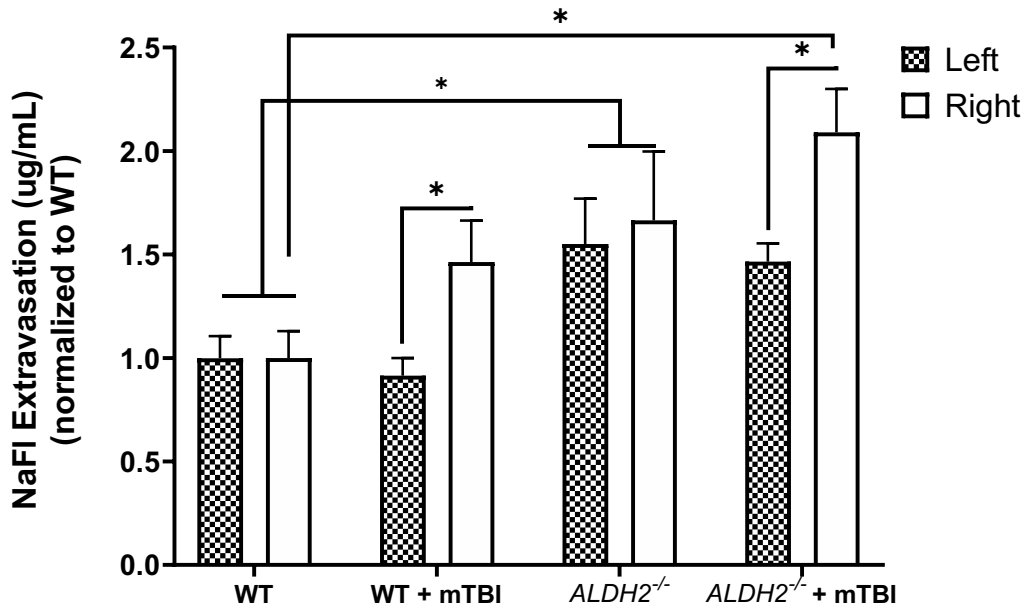

Figure 58. Elevated sodium fluorescein extravasation in the right hemisphere of ALDH2$^{-/-}$ mice 24 hours post-mTBI.
Quantitative analysis of sodium fluorescein (NaFl, 2% in diH_2O) extravasation measured 24 hours post-mTBI in the contralateral and ipsilateral (left and right, respectively) hemisphere. Data

represents mean ± SEM of n=7-10 animals analyzed by One-Way ANOVA with Dunnett's or Tukey's multi-comparison analysis.

As significant changes in NaFl extravasation were only observed in the ipsilateral hemisphere, we continued by observing the changes in proteins associated with BBB breakdown (ZO-1, occludin, claudin-5, MMP-9 and eNOS) in the ipsilateral hemisphere via immunoblot. While mTBI and *ALDH2*$^{-/-}$ alone had no effect on ZO-1 or occludin, the synergy of the two insults produced significantly reduced protein levels 24 hours post-mTBI (ZO-1: WT = 1.0 ± 0.06, WT + mTBI = 0.93 ± 0.08, *ALDH2*$^{-/-}$ = 0.96 ± 0.1, *ALDH2*$^{-/-}$ + mTBI = 0.65 ± .06; Occludin: WT = 1.0 ± 0.05, WT + mTBI = 0.87 ± 0.8, *ALDH2*$^{-/-}$ = 1.06 ± 0.7, *ALDH2*$^{-/-}$+ mTBI = 0.74 ± .04, Figure 59B and C). Levels of claudin-5, an integral membrane protein found significantly decreased in ADRD and other neurodegenerative disorders, remained unchanged in all conditions (Figure 59D).[399] We next looked at MMP-9, a versatile zinc-containing endopeptidase that is suggested to digest tight junctions and basement membrane proteins when significantly increased in TBI and ADRD.[368-370] It was unsurprising that active MMP-9/total MMP-9 levels were significantly increased with mTBI and oxidative stress alone; however, the interaction of *ALDH2*$^{-/-}$ and mTBI did not significantly increase these levels (WT: 1.0 ± 0.1; WT + mTBI: 1.5 ± 0.1; *ALDH2*$^{-/-}$: 1.6 ± 0.2; *ALDH2*$^{-/-}$ + mTBI: 1.6 ± 0.2, Figure 59E).

We next looked at endothelial nitric oxide synthase (eNOS), the catalyst of nitric oxide (NO) in endothelial cells. NO is vital for the regulation of vascular homeostasis and healthy cognitive function in the central nervous system (CNS).[259] However, in NDs like ADRD and TBI, levels of NO are significantly decreased.[409] Indeed, in our model, mTBI alone decreased levels of eNOS (WT: 1.0 ± 0.2, WT + mTBI: 0.82 ± 0.12, Figure 59F). Moreover, heightened OS can significantly decrease eNOS, leading to impaired cerebral blood flow regulation, vascular inflammation and weakened synaptic plasticity.[409] Thus a significant decrease in expression of

eNOS in the *ALDH2*$^{-/-}$ alone was unsurprising (*ALDH2*$^{-/-}$: 0.60 ± 0.23). Interaction of oxidative stress and mTBI considerably exacerbated the loss of expression (*ALDH2*$^{-/-}$ + mTBI: 0.30 ± 0.17).

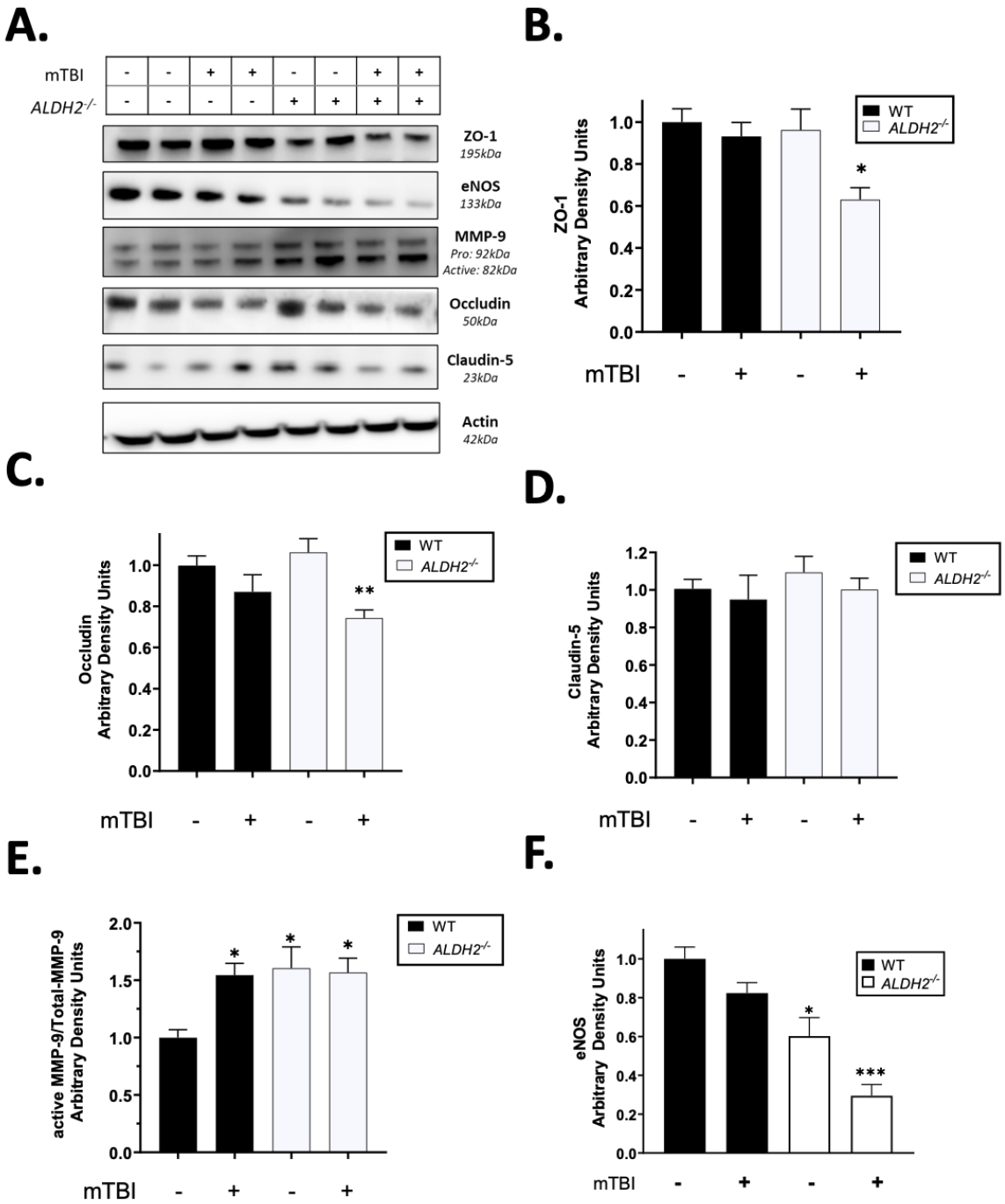

Figure 59 Underlying oxidative stress exacerbates the loss of BBB-associated proteins post-mTBI.

Representative (**A**) and associated quantitative analysis of immunoblots of WT and *ALDH2*$^{-/-}$ 24 hours post-mTBI or null probed with ZO-1 (**B**), Occludin (**C**) Claudin-5 (**D**), MMP-9 (**E**) or eNOS (**F**) Ab 24 hours post-mTBI. Data represents mean ± SEM of n=7-10 animals analyzed by One-Way ANOVA with Dunnett's or Tukey's multi-comparison analysis. All protein was normalized to the housekeeping protein, β-actin. 50µg of protein was loaded in each well. *p<.05, **p<.001 vs. WT null control

3.3.5 Calpain-Cathepsin Inhibition Attenuates BBB-Dysfunction

We focused our efforts on understanding if selective or nonselective calpain-1 inhibition would attenuate the loss in TJs. Utilizing the same post-treatment paradigm as in Chapter 2, *ALDH2*$^{-/-}$ mice were administered 10mg/kg of ***3***, ***5***, ***NYC-438, NYC-438e,*** or vehicle via *i.p*. 1 hour post-TBI, then sacrificed with hemispheres collected 24 hours post-mTBI. Compounds ***5*** and ***NYC-438*** significantly attenuated the loss of ZO-1 (***5***: 1.3 ± 0.1, ***NYC-438***: 1.7 ± 0.3, Figure 60) while ***3*** and ***NYC-438e*** increased but not significantly. Furthermore, ***3, 5***, and ***NYC-438e*** mitigated the loss in occludin (***3***: 1.3 ± 0.3, ***5***:1.3 ± 0.2, ***NYC-438***: 1.4 ± 0.1) levels (Figure 60). Moreover, though claudin-5 levels were unaltered with mTBI, ***5, NYC-438*** , and ***NYC-438e*** unambiguously increased expression of claudin-5 (***5***: 2.5 ± 0.2, ***NYC-438***: 2.0 ± 0.2, ***NYC-438e***: 1.7 ± 0.2). Intriguingly, while all inhibitors reduced MMP-9 activity, only ***5*** mitigated levels with significance (0.7 ± 0.05).

All inhibitors attenuated eNOS-deficiency without evidence for a preferable targeting strategy (***3***: 0.6 ± 0.1, ***5***: 1.25 ± 0.04, ***NYC-438***: 1.23 ± 0.23 ***NYC-438e:*** 1.3 ± 0.03). eNOS operates via the eNOS/NO/sGC/cGMP/CREB pathway.[371] Previous studies from Dr. Arancio Ottavio's lab found nonselective calpain-1 inhibitors (E-64 and BDA-410) significantly restored pCREB levels in hippocampal neurons from APP/PS1 mice.[114] They hypothesized that Aβ increased calpain hyperactivation which in turn hampered phosphorylation of CREB. Our studies suggest that pCREB levels may be increased upstream via restoration of eNOS levels and explain the restoration of scopolamine-induced cognitive deficits observed in Chapter 2 (

Figure 32).

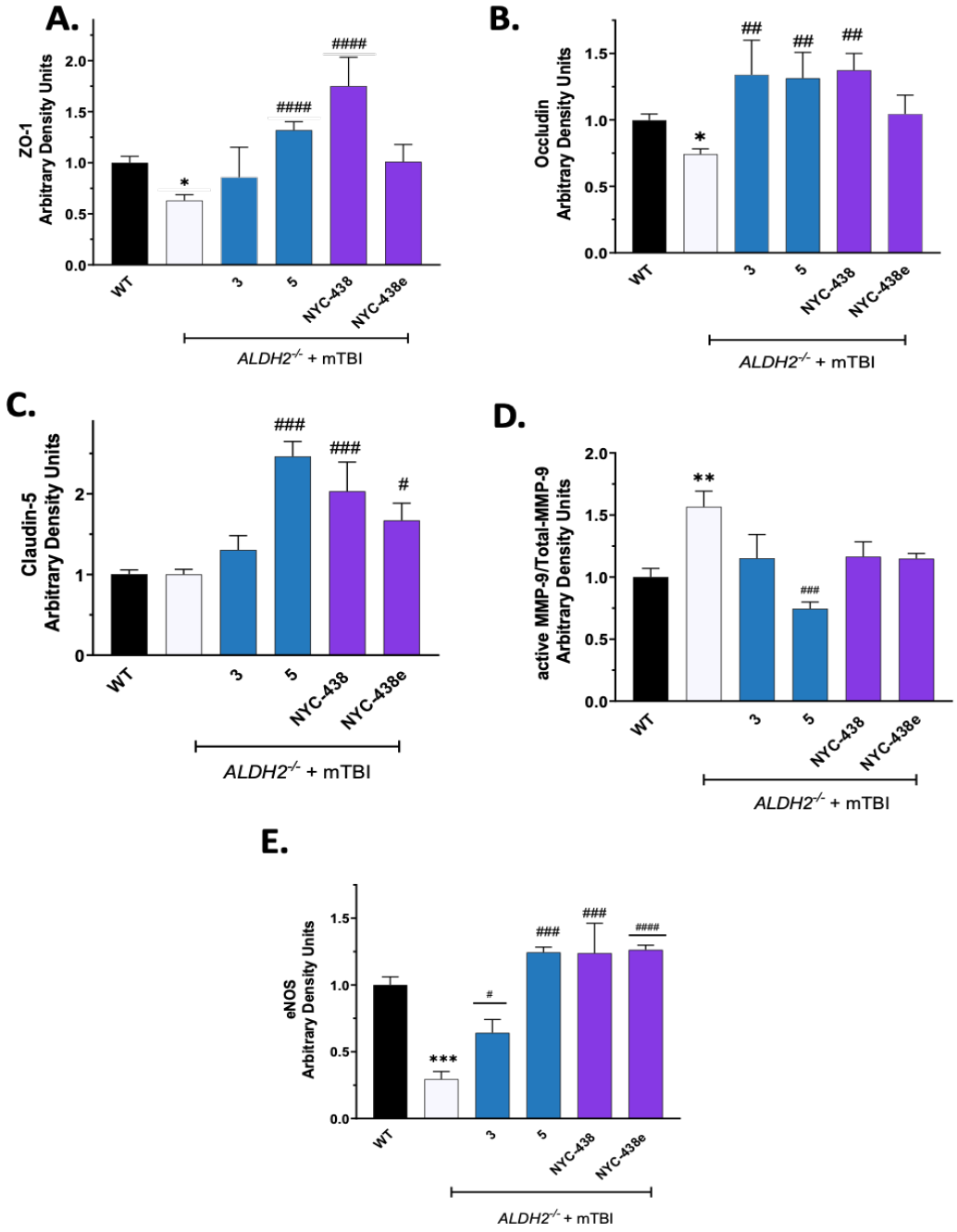

Figure 60. CCH inhibitors attenuate loss of BBB-associated proteins 24 Hours post-mTBI in *ALDH2*$^{-/-}$ mice

(A-D) Quantitative analysis of immunoblots of ipsilateral hemispheres of WT and *ALDH2*$^{-/-}$ 24 hours post-mTBI or null treated with 10mg/kg via i.p of ***5*** or ***NYC-438*** and probed with ZO-1 (**A**), Occludin (**B**), Claudin-5 (**C**), MMP-9 (active/total, **D**) and eNOS (**E**) Ab. Data represents mean ± SEM of n=4-10 animals analyzed by One-Way ANOVA with Dunnett's or Tukey's multi-comparison analysis. All protein was normalized to the housekeeping protein, β-actin. 50µg of protein was loaded in each well. *p<.05, **p<.01, ***p<.001 *v.* WT null control, $^{\#}$p<.05, $^{\#\#}$p<.01, $^{\#\#\#}$p<.001 *v. ALDH2*$^{-/-}$ + mTBI.

As calpain-1 and cathepsin B are vital proteins at normal physiological concentrations, studies were expanded to characterize the effects of inhibition on all mouse models (WT, WT + mTBI, *ALDH2*$^{-/-}$, *ALDH2*$^{-/-}$ + mTBI). All groups were treated with 10mg/kg ***5***, ***NYC-438***, or vehicle control via *i.p.* 1 hour post-mTBI. 24 hours later, mice were sacrificed with ipsilateral hemispheres collected and TJ levels were analyzed via immunoblot. A previous study found calpain inhibitor III, a nonselective calpain/cathepsin B inhibitor, attenuated IL-1β-induced loss of ZO-1; it was unclear if specific inhibition of calpain-1 was exuding the protective effects.[362] Other groups also report cathepsin B inhibition can preserve ZO-1 levels through an indirect mechanism.[366, 410] Our studies found that ***NYC-438*** significantly and profoundly increased ZO-1 levels in all conditions, while ***5*** increased levels but without significance (Figure 61A). This data, along with earlier data showing ***CA-074*** moderately attenuates ZO-1 levels in the WT BECs and significantly attenuates levels in *ALDH2*$^{-/-}$ BECs (Figure 51E and F, respectively), indicate ZO-1 may be a substrate of cathepsin B. Occludin levels did not significantly change in the WT, WT + mTBI, or *ALDH2*$^{-/-}$ groups (Figure 61B). However, it is important to note that ***5*** did moderately reduce levels in all three conditions indicating calpain-1 may be important for regulation of occludin levels. Levels of claudin-5 were significantly increased in most conditions by both ***5*** and ***NYC-438***, indicating protective activity may be specifically due to calpain-1 inhibition (Figure 61C).

As eNOS is well-characterized as a substrate of calpain-1, we examined these levels both as a control and to understand if cathepsin B had a role in eNOS activity. ***5*** significantly increased levels of eNOS in all conditions while ***NYC-438*** significantly increased eNOS levels only in the *ALDH2*$^{-/-}$ groups (Figure 61D). These results confirm that eNOS is indeed a substrate of calpain-1. As ***NYC-438*** treatment was not significantly different than ***5***, it may be suggested that cathepsin B inhibition does not play a role in eNOS activity.

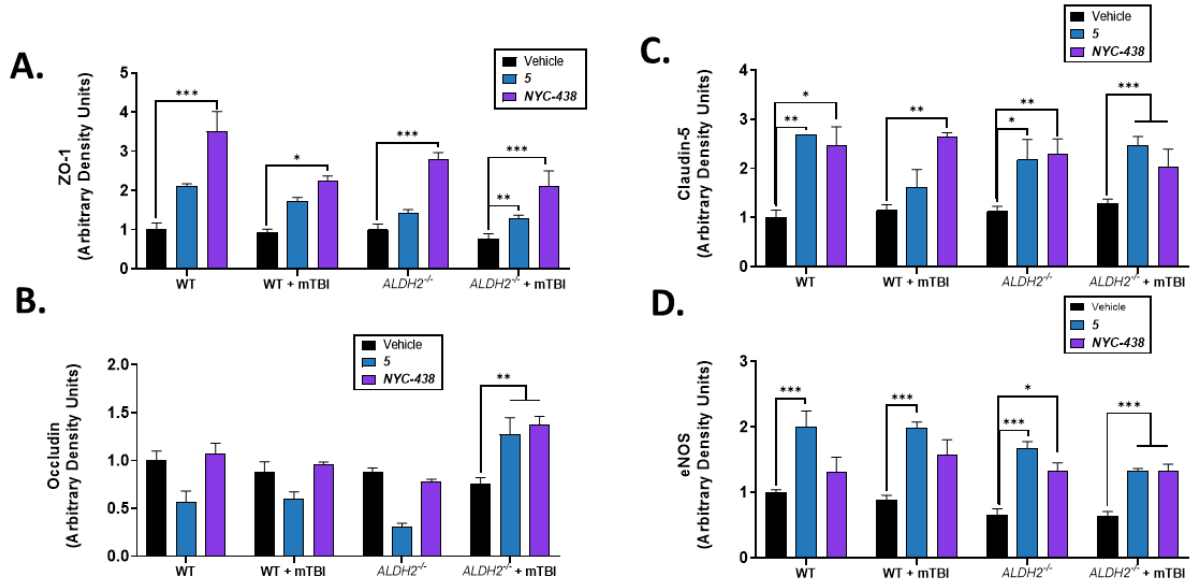

Figure 61. TJs are substrates of cysteine proteases
(A-D) Quantitative analysis of immunoblots of ipsilateral hemispheres of WT and *ALDH2*$^{-/-}$ 24 hours post-mTBI or null treated with 10mg/kg via i.p of *5* or *NYC-438* and probed with ZO- 1 (A), Occludin (B), Claudin-5 (C) and eNOS (D Data represents mean ± SEM of n=7-10 animals analyzed by One-Way ANOVA with or Tukey's multi-comparison analysis. All protein was normalized to the housekeeping protein, β-actin. 50µg of protein was loaded in each well. *p<.05, **p<.01, ***p<.001.

We decided to take it a step further and examine if the changes we observed were also present on a transcriptional level. Intriguingly, ZO-1 was significantly reduced in the *ALDH2*$^{-/-}$ mice with and without mTBI (Figure 62A). ***NYC-438*** was able to significantly attenuate this decrease while ***5*** did not (*ALDH2*$^{-/-}$ + mTBI: 0.67 ± 0.13, ***5***: 0.71 ± 0.1, ***NYC-438***: 0.86 ± 0.06). Moreover, occludin levels were only significantly decreased in the *ALDH2*$^{-/-}$ mice with mTBI indicating oxidative stress alone does not significantly decrease occludin transcription (Figure 62B). ***NYC-438*** and ***5*** both improved levels of occludin mRNA, but only ***NYC-438*** was significant able to restore to baseline levels (*ALDH2*$^{-/-}$ + mTBI: 0.76 ± 0.15, ***5***: 0.86 ± 0.2, ***NYC-438***: 0.96 ± 0.16). Similar to protein levels, claudin-5 mRNA declined non-significantly only in the mice with mTBI (Figure 62C). Again, only ***NYC-438*** was able to significantly attenuate levels of claudin-5 mRNA beyond baseline (*ALDH2*$^{-/-}$ + mTBI: 0.86 ± 0.18, ***5***: 0.84 ± 0.21, ***NYC-438***: 1.14 ± 0.23). Similar to previous literature, eNOS mRNA was significantly reduced in the mTBI animals (Figure 62D)[411]. This decrease was not seen in the *ALDH2*$^{-/-}$ alone indicating underlying oxidative stress does not significantly impact eNOS expression. Intriguingly, both ***5*** and ***NYC-438*** were able to significantly increase expression of eNOS (*ALDH2*$^{-/-}$ + mTBI: 0.83 ± 0.11, ***5***: 1.04 ± 0.2, ***NYC-438***: 1.06 ± 0.18).

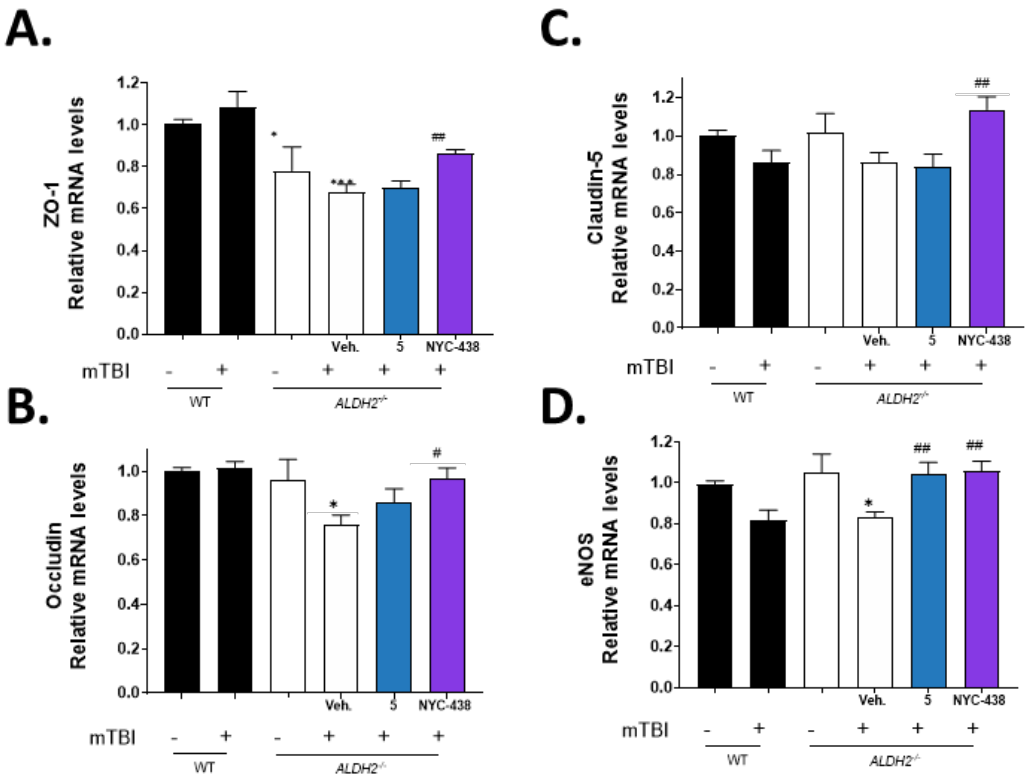

Figure 62. Treatment of NYC-438, not 5, attenuates decreased expression of TJs in *ALDH2*$^{-/-}$ mice with mTBI.

(A-D) mRNA levels of ZO-1 (A) Occludin (B), Claudin-5 (C), and eNOS (D) quantified by rt-qPCR. Data represents mean ± SEM of n=5-6 animals analyzed by One-Way ANOVA with or Tukey's multi-comparison analysis. All protein was normalized to the housekeeping protein, β-actin. 50µg of protein was loaded in each well. *p<.05, **p<.01, **p<.001 *v.* nontreated control. $^{\#}$p<.05, $^{\#}$p<.01, $^{\#}$p<.001 $^{\#}$p<.05 *v. ALDH2*$^{-/-}$ + mTBI

3.4 CONCLUSION

Recent studies have implicated BBB-dysfunction as an early feature in ADRD disease progression.[396] However, it has not been determined if this is a causative or consequential step of ADRD. Furthermore, there exists a significant lapse on studies focusing on the BBB, and in particular BECs. This research strongly advocates for understanding the therapeutic impact of ADRD pre-clinical strategies beyond neuroprotection.

Isolating primary cells directly from mouse models allowed us the ability to contrast effects of genetic states that mimic disorders to further define functional effects. BECs incorporating AD contributors (OS via the *ALDH2*$^{-/-}$ mouse model and APOE4 via the transgenic mice) had enhanced susceptibility to OGD-R insult. This further confirms and supports the necessity to test preclinical strategies on mitigating BBB damage, in particular BEC-dysfunction.

The *ALDH2*$^{-/-}$ + mTBI provided a subtle and applicable *in vivo* model to characterize efficacy of novel therapies in attenuating BBB-dysfunction. Moreover, it afforded an opportunity to disseminate the individual contributions of the individual "hits" (OS and mTBI) alone. While both "hits" are sufficient to induce subtle dysfunction of various BBB properties, the synergy produced significant BBB-dysfunction. This validates the theory that the combination of multiple hits (environmental, chemical, genetic, physical etc.) leads to exacerbated damage.

It was determined from the *in vitro* assays that inhibiting calpain-1 (whether selectively or nonselectively) is required for protecting BECs against OS-mediated damage, as the selective cathepsin B inhibitor had varying efficacy. However, *in vivo* studies provided no clear preference on selective or nonselective inhibition as they both attenuated BEC-dysfunction and mitigated the loss of essential BBB-associated proteins. Regardless, the results suggest that the CCH extends to the BBB, and may even be the causative step in neurodegeneration and exacerbation of secondary sequelae.

Examining eNOS levels provided valuable information. Just a single treatment of inhibition strategies administered 1 hour post-mTBI profoundly restored eNOS levels. This complemented previous literature that reported a significant increase in phosphorylated CREB following calpain-1 inhibition. We conclude that eNOS may be the upstream target for calpain-inhibitory efficacy in models of cognitive decline.

Brain ischemia and TBI induce acute BBB-dysfunction and OS, whereas chronic OS and BBB dysfunction contribute to MCI and ADRD. These findings suggest OS potentiates BBB-dysfunction, in particular BEC-dysfunction, via CCH, which can be mitigated by pharmacological CCH inhibition.

4. CONCLUSIONS

The path to ADRD therapeutics is long and strenuous. Currently, no therapies exist that stops, reverses or prevents disease progression. In tandem, numerous longitudinal clinical-pathological studies have disproven the idea that neuropathology directly correlates with cognitive decline and exposed the varying susceptibilities of individuals. Translational researchers have thus been forced to reevaluate ADRD as a complex, multifactorial set of diseases. The work presented here sought to contribute to ADRD drug discovery through target elucidation, mechanistic inclusion of the BBB (in particular BECs) in addition to neurons, and the characterization of a novel and relevant *in vivo* preclinical model with attenuated neural resilience.

Given the high clinical failure rates of AD therapeutics, it is apparent that alternative, new targets are urgently needed for drug discovery. However, there have also been countless validated targets with significant efficacy in preclinical studies that were abandoned prior to essential proof-of-concept clinical trials. The efficacy of small molecule CCH inhibitors in the numerous *in vitro* and *in vivo* studies presented here clearly demonstrate that calpain-1 and cathepsin B are valid targets for ADRD drug discovery. However, our studies did not provide sufficient evidence that selective calpain-1 inhibitors are superior to nonselective calpain-1 inhibitors, thus, the question remains: *is selectivity compulsory for therapeutic success?*

Moreover, we demonstrated that many purported selective calpain-1 inhibitors are actually more nonselective than reported in the literature (***E-64d, BDA-410, CAPN1XI***). Thus, literature must be carefully critiqued to determine what drives the observed efficacy. We acknowledge that efficacy in our studies may be controlled by another cysteine protease (deubiquitinases, caspases, etc). Thus, future studies should incorporate additional screens to fully characterize the small molecule inhibition profiles.

This research was at the crossroads of basic science and drug discovery (Figure 63); we sought to extend the understanding of CCH in ADRD while simultaneously providing a platform for target-based drug discovery. The enzyme assays provided a screen to establish small molecule inhibition profiles while the use of clinical biomarkers (SBDP, GFAP-BDP) afforded the ability to monitor specific inhibitory efficacy both *in vitro* and *in vivo*. For target-based drug discovery, it's imperative to confirm a target but translational scientists must go beyond and fully understand the pathway. This is necessary for when a small molecule reaches the clinic as drug-drug interactions can be more carefully monitored. Moreover, if resistance occurs, extensive pathway elucidation can lead development of second-line therapy. By expanding the CCH to the BBB, we further validated and categorized the CCH as a common, potentially wide-spread mechanism in ADRD.

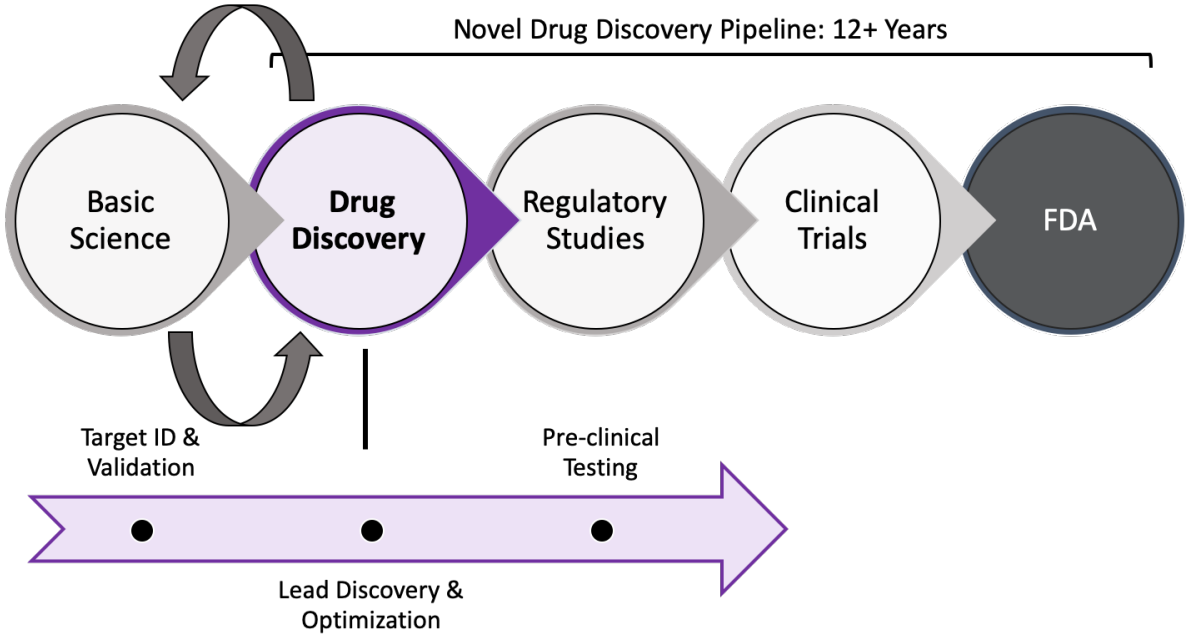

Figure 63. Schematic of the drug discovery process
Traditionally, basic science leads directly to the drug discovery. Successful development of a drug candidate can lead to regulatory studies, clinical trials, then eventual FDA-approval.

It is overwhelmingly acknowledged that for a neurodegenerative disease, protecting against neuronal death is a major a benefit for therapeutic strategies. However, given the multifaceted nature of ADRD, it is necessary to move beyond just neurons, and fully characterize mechanisms and/or targeting strategies on other features that are hypothesized to drive disease progression. In fact, a major issue in the ADRD therapeutic realm is the overwhelming possibility that we may be targeting the disease too late. Thus, by focusing on mitigating early features of ADRD progression, we may be able to target early-stage disease before the years of severe disability.

This research, among other literature reports, demonstrated that targeting the CCH is neuroprotective. However, this work is one of the first to demonstrate that CCH protect against BBB-dysfunction, as well as specific BEC-dysfunction, through numerous *in vitro* and *in vivo*, and in various treatment paradigms (Figure 64). Thus, we speculate that the CCH may be a primary driving force in neurovascular degeneration, and even wider, in ADRD. Calpain-1 inhibitors may be the causative step in not only neuroprotection, but also prevention of secondary sequelae post-neurotrauma.

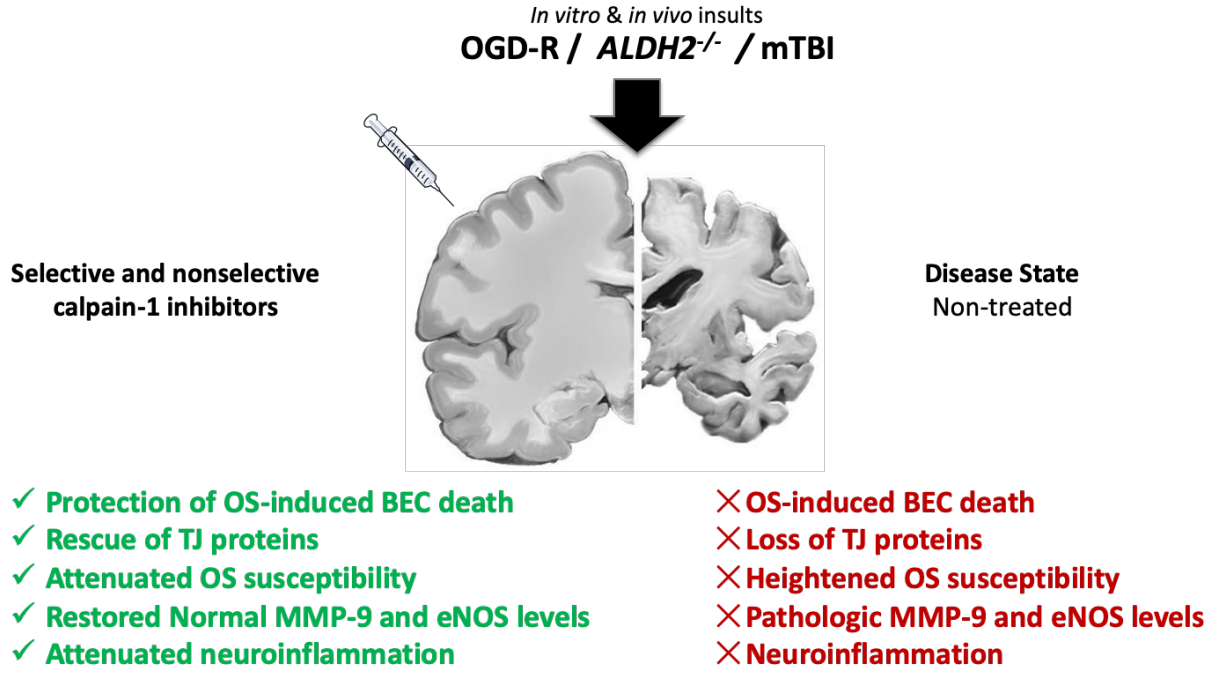

Figure 64. Efficacy of calpain-1 inhibitors in *in vitro* and *in vivo* models
The studies in this thesis utilized both *in vitro* and *in vivo* studies to reveal the multifactorial effect of CCH inhibitors.

A single administration of calpain-1 inhibitors profoundly restored levels of TJ proteins, a BEC-specific feature, both *in vitro* and *in vivo*. This suggested that BBB-permeability may be restored in the "2-hit" mice; however, more studies including calpain-1 inhibitors' effect on TEER and NaFl extravasation are required. Furthermore, in the *in vivo* studies, other essential BBB-associated proteins were significantly restored. This indicates that calpain-1 inhibition may be modifying BEC functionality beyond simple protection of BBB leakiness. Overall, these findings further incriminate calpain-1 hyper-activation as an upstream, early contributor to neurovascular damage.

This thesis also contributed to the further characterization of a preclinical *in vivo* model. Over the last 20 years, several novel transgenic murine models for age-related dementias have been developed. However, the majority encompass genetic mutations associated with fAD. While these are undoubtedly required, there exists a significant lack of models encompassing attenuated neural reserve.

This work demonstrated that *ALDH2*$^{-/-}$ mice have significantly attenuated BEC-dysfunction. Moreover, the *ALDH2*$^{-/-}$ exhibit significant BBB-dysfunction and provide an attractive model to test preclinical strategies both *in vitro* and *in vitro*. The "2-hit" mouse model of underlying OS and neurotrauma is a highly relevant, significant addition to the preclinical *in vivo* models.

To conclude, understanding cysteine proteases' imbalance plays a key role in further understanding the mechanism behind these devastating diseases. Proteases offer a viable drug target, providing varying avenues and approaches for possible therapies. Current preclinical research benefits neuroprotective and pro-cognitive agents that are successful in pre-clinical, pathologic hallmark-based animal models. However, with little clinical success, recharacterization of our preclinical strategies is imperative. Our studies support a role for oxidative stress and mTBI

in exacerbating CCH-mediated BBB damage and endorses further research into their pharmacological inhibition.

CITED LITERATURE

1. Marco-Contelles, J., Facts, Results, and Perspectives of the Current Alzheimer's Disease Research. *ACS Chem Neurosci* **2019,** *10* (3), 1127-1128.
2. Yamashima, T., Reconsider Alzheimer's disease by the 'calpain-cathepsin hypothesis'--a perspective review. *Prog Neurobiol* **2013,** *105*, 1-23.
3. Yamashima, T., Can 'calpain-cathepsin hypothesis' explain Alzheimer neuronal death? *Ageing Res Rev* **2016,** *32*, 169-179.
4. Siklos, M.; BenAissa, M.; Thatcher, G. R., Cysteine proteases as therapeutic targets: does selectivity matter? A systematic review of calpain and cathepsin inhibitors. *Acta Pharm Sin B* **2015,** *5* (6), 506-19.
5. Hook, G.; Jacobsen, J. S.; Grabstein, K.; Kindy, M.; Hook, V., Cathepsin B is a New Drug Target for Traumatic Brain Injury Therapeutics: Evidence for E64d as a Promising Lead Drug Candidate. *Front Neurol* **2015,** *6*, 178.
6. Ferreira, A., Calpain dysregulation in Alzheimer's disease. *ISRN Biochem* **2012,** *2012*, 728571.
7. Yin, Y.; Wang, Y.; Gao, D.; Ye, J.; Wang, X.; Fang, L.; Wu, D.; Pi, G.; Lu, C.; Zhou, X. W.; Yang, Y.; Wang, J. Z., Accumulation of human full-length tau induces degradation of nicotinic acetylcholine receptor alpha4 via activating calpain-2. *Sci Rep* **2016,** *6*, 27283.
8. Medeiros, R.; Kitazawa, M.; Chabrier, M. A.; Cheng, D.; Baglietto-Vargas, D.; Kling, A.; Moeller, A.; Green, K. N.; LaFerla, F. M., Calpain inhibitor A-705253 mitigates Alzheimer's disease-like pathology and cognitive decline in aged 3xTgAD mice. *Am J Pathol* **2012,** *181* (2), 616-25.
9. Fa, M.; Zhang, H.; Staniszewski, A.; Saeed, F.; Shen, L. W.; Schiefer, I. T.; Siklos, M. I.; Tapadar, S.; Litosh, V. A.; Libien, J.; Petukhov, P. A.; Teich, A. F.; Thatcher, G. R.; Arancio, O., Novel Selective Calpain 1 Inhibitors as Potential Therapeutics in Alzheimer's Disease. *J Alzheimers Dis* **2016,** *49* (3), 707-21.
10. Schiefer, I. T.; Tapadar, S.; Litosh, V.; Siklos, M.; Scism, R.; Wijewickrama, G. T.; Chandrasena, E. P.; Sinha, V.; Tavassoli, E.; Brunsteiner, M.; Fa, M.; Arancio, O.; Petukhov, P.; Thatcher, G. R., Design, synthesis, and optimization of novel epoxide incorporating peptidomimetics as selective calpain inhibitors. *J Med Chem* **2013,** *56* (15), 6054-68.
11. Lon, H. K.; Mendonca, N.; Goss, S.; Othman, A. A.; Locke, C.; Jin, Z.; Rendenbach-Mueller, B., Pharmacokinetics, Safety, Tolerability, and Pharmacodynamics of Alicapistat, a Selective Inhibitor of Human Calpains 1 and 2 for the Treatment of Alzheimer Disease: An Overview of Phase 1 Studies. *Clin Pharmacol Drug Dev* **2019,** *8* (3), 290-303.
12. Ikeda, K.; Akiyama, H.; Arai, T.; Oda, T.; Kato, M.; Iseki, E.; Kosaka, K.; Wakabayashi, K.; Takahashi, H., Clinical aspects of 'senile dementia of the tangle type'--a subset of dementia in the senium separable from late-onset Alzheimer's disease. *Dement Geriatr Cogn Disord* **1999,** *10* (1), 6-11.
13. Harman, D., The aging process: major risk factor for disease and death. *Proc Natl Acad Sci U S A* **1991,** *88* (12), 5360-3.

14. Bettcher, B. M.; Kramer, J. H., Inflammation and clinical presentation in neurodegenerative disease: a volatile relationship. *Neurocase* **2013,** *19* (2), 182-200.

15. Silberberg, D., The high impact of neurologic disorders in developing countries: the struggle for global recognition. *Neurology* **2011,** *77* (3), 307-8.

16. Pedro, A. V., Coping with Brain Disorders using Neurotechnology. *Malays J Med Sci* **2012,** *19* (1), 1-3.

17. Brady, S. T.; Morfini, G. A., Regulation of motor proteins, axonal transport deficits and adult-onset neurodegenerative diseases. *Neurobiol Dis* **2017,** *105*, 273-282.

18. Chung, C. G.; Lee, H.; Lee, S. B., Mechanisms of protein toxicity in neurodegenerative diseases. *Cell Mol Life Sci* **2018,** *75* (17), 3159-3180.

19. Sheng, M.; Sabatini, B. L.; Sudhof, T. C., Synapses and Alzheimer's disease. *Cold Spring Harb Perspect Biol* **2012,** *4* (5).

20. Gorman, A. M., Neuronal cell death in neurodegenerative diseases: recurring themes around protein handling. *J Cell Mol Med* **2008,** *12* (6A), 2263-80.

21. Katsuno, M.; Sahashi, K.; Iguchi, Y.; Hashizume, A., Preclinical progression of neurodegenerative diseases. *Nagoya J Med Sci* **2018,** *80* (3), 289-298.

22. Alzheimer's, A., 2016 Alzheimer's disease facts and figures. *Alzheimers Dement* **2016,** *12* (4), 459-509.

23. Berchtold, N. C.; Cotman, C. W., Evolution in the conceptualization of dementia and Alzheimer's disease: Greco-Roman period to the 1960s. *Neurobiol Aging* **1998,** *19* (3), 173-89.

24. Harada, C. N.; Natelson Love, M. C.; Triebel, K. L., Normal cognitive aging. *Clin Geriatr Med* **2013,** *29* (4), 737-52.

25. Murman, D. L., The Impact of Age on Cognition. *Semin Hear* **2015,** *36* (3), 111-21.

26. Hebert, L. E.; Weuve, J.; Scherr, P. A.; Evans, D. A., Alzheimer disease in the United States (2010-2050) estimated using the 2010 census. *Neurology* **2013,** *80* (19), 1778-83.

27. 2020 Alzheimer's disease facts and figures. *Alzheimers Dement* **2020**.

28. Hoff, P.; Hippius, H., [Alois Alzheimer 1864-1915. An overview of his life and work on the occasion of his 125th birthday]. *Nervenarzt* **1989,** *60* (6), 332-7.

29. Glenner, G. G.; Wong, C. W., Alzheimer's disease: initial report of the purification and characterization of a novel cerebrovascular amyloid protein. *Biochem Biophys Res Commun* **1984,** *120* (3), 885-90.

30. Grundke-Iqbal, I.; Iqbal, K.; Tung, Y. C.; Quinlan, M.; Wisniewski, H. M.; Binder, L. I., Abnormal phosphorylation of the microtubule-associated protein tau (tau) in Alzheimer cytoskeletal pathology. *Proc Natl Acad Sci U S A* **1986,** *83* (13), 4913-7.

31. Blennow, K.; de Leon, M. J.; Zetterberg, H., Alzheimer's disease. *Lancet* **2006,** *368* (9533), 387-403.

32. Riley, K. P.; Snowdon, D. A.; Markesbery, W. R., Alzheimer's neurofibrillary pathology and the spectrum of cognitive function: findings from the Nun Study. *Ann Neurol* **2002,** *51* (5), 567-77.

33. Davis, D. G.; Schmitt, F. A.; Wekstein, D. R.; Markesbery, W. R., Alzheimer neuropathologic alterations in aged cognitively normal subjects. *J Neuropathol Exp Neurol* **1999,** *58* (4), 376-88.

34. Katzman, R.; Terry, R.; DeTeresa, R.; Brown, T.; Davies, P.; Fuld, P.; Renbing, X.; Peck, A., Clinical, pathological, and neurochemical changes in dementia: a subgroup with preserved mental status and numerous neocortical plaques. *Ann Neurol* **1988,** *23* (2), 138-44.

35. Gold, G.; Bouras, C.; Kovari, E.; Canuto, A.; Glaria, B. G.; Malky, A.; Hof, P. R.; Michel, J. P.; Giannakopoulos, P., Clinical validity of Braak neuropathological staging in the oldest-old. *Acta Neuropathol* **2000,** *99* (5), 579-82; discussion 583-4.

36. Tucker, A. M.; Stern, Y., Cognitive reserve in aging. *Curr Alzheimer Res* **2011,** *8* (4), 354-60.

37. Stern, Y., Cognitive reserve in ageing and Alzheimer's disease. *Lancet Neurol* **2012,** *11* (11), 1006-12.

38. Schofield, P. W.; Logroscino, G.; Andrews, H. F.; Albert, S.; Stern, Y., An association between head circumference and Alzheimer's disease in a population-based study of aging and dementia. *Neurology* **1997,** *49* (1), 30-7.

39. Stern, Y., What is cognitive reserve? Theory and research application of the reserve concept. *J Int Neuropsychol Soc* **2002,** *8* (3), 448-60.

40. Stern, Y., Cognitive reserve. *Neuropsychologia* **2009,** *47* (10), 2015-28.

41. Bennett, D. A.; Wilson, R. S.; Arvanitakis, Z.; Boyle, P. A.; de Toledo-Morrell, L.; Schneider, J. A., Selected findings from the Religious Orders Study and Rush Memory and Aging Project. *J Alzheimers Dis* **2013,** *33 Suppl 1*, S397-403.

42. Boyle, P. A.; Wilson, R. S.; Yu, L.; Barr, A. M.; Honer, W. G.; Schneider, J. A.; Bennett, D. A., Much of late life cognitive decline is not due to common neurodegenerative pathologies. *Ann Neurol* **2013,** *74* (3), 478-89.

43. Langa, K. M.; Foster, N. L.; Larson, E. B., Mixed dementia: emerging concepts and therapeutic implications. *JAMA* **2004,** *292* (23), 2901-8.

44. Toledo, J. B.; Arnold, S. E.; Raible, K.; Brettschneider, J.; Xie, S. X.; Grossman, M.; Monsell, S. E.; Kukull, W. A.; Trojanowski, J. Q., Contribution of cerebrovascular disease in autopsy confirmed neurodegenerative disease cases in the National Alzheimer's Coordinating Centre. *Brain* **2013,** *136* (Pt 9), 2697-706.

45. Neuropathology Group. Medical Research Council Cognitive, F.; Aging, S., Pathological correlates of late-onset dementia in a multicentre, community-based population in England and Wales. Neuropathology Group of the Medical Research Council Cognitive Function and Ageing Study (MRC CFAS). *Lancet* **2001,** *357* (9251), 169-75.

46. Sonnen, J. A.; Larson, E. B.; Crane, P. K.; Haneuse, S.; Li, G.; Schellenberg, G. D.; Craft, S.; Leverenz, J. B.; Montine, T. J., Pathological correlates of dementia in a longitudinal, population-based sample of aging. *Ann Neurol* **2007,** *62* (4), 406-13.

47. White, L.; Small, B. J.; Petrovitch, H.; Ross, G. W.; Masaki, K.; Abbott, R. D.; Hardman, J.; Davis, D.; Nelson, J.; Markesbery, W., Recent clinical-pathologic research on the causes of dementia in late life: update from the Honolulu-Asia Aging Study. *J Geriatr Psychiatry Neurol* **2005,** *18* (4), 224-7.

48. Brenowitz, W. D.; Hubbard, R. A.; Keene, C. D.; Hawes, S. E.; Longstreth, W. T., Jr.; Woltjer, R. L.; Kukull, W. A., Mixed neuropathologies and associations with domain-specific cognitive decline. *Neurology* **2017,** *89* (17), 1773-1781.

49. Auld, D. S.; Kornecook, T. J.; Bastianetto, S.; Quirion, R., Alzheimer's disease and the basal forebrain cholinergic system: relations to beta-amyloid peptides, cognition, and treatment strategies. *Prog Neurobiol* **2002,** *68* (3), 209-45.

50. DeKosky, S. T.; Harbaugh, R. E.; Schmitt, F. A.; Bakay, R. A.; Chui, H. C.; Knopman, D. S.; Reeder, T. M.; Shetter, A. G.; Senter, H. J.; Markesbery, W. R., Cortical biopsy in Alzheimer's disease: diagnostic accuracy and neurochemical, neuropathological, and cognitive correlations. Intraventricular Bethanecol Study Group. *Ann Neurol* **1992,** *32* (5), 625-32.

51. Rafii, M. S.; Aisen, P. S., Recent developments in Alzheimer's disease therapeutics. *BMC Med* **2009,** *7*, 7.

52. Salloway, S.; Ferris, S.; Kluger, A.; Goldman, R.; Griesing, T.; Kumar, D.; Richardson, S.; Donepezil 401 Study, G., Efficacy of donepezil in mild cognitive impairment: a randomized placebo-controlled trial. *Neurology* **2004,** *63* (4), 651-7.

53. Feldman, H. H.; Ferris, S.; Winblad, B.; Sfikas, N.; Mancione, L.; He, Y.; Tekin, S.; Burns, A.; Cummings, J.; del Ser, T.; Inzitari, D.; Orgogozo, J. M.; Sauer, H.; Scheltens, P.; Scarpini, E.; Herrmann, N.; Farlow, M.; Potkin, S.; Charles, H. C.; Fox, N. C.; Lane, R., Effect of rivastigmine on delay to diagnosis of Alzheimer's disease from mild cognitive impairment: the InDDEx study. *Lancet Neurol* **2007,** *6* (6), 501-12.

54. Winblad, B.; Gauthier, S.; Scinto, L.; Feldman, H.; Wilcock, G. K.; Truyen, L.; Mayorga, A. J.; Wang, D.; Brashear, H. R.; Nye, J. S.; Group, G.-I.-S., Safety and efficacy of galantamine in subjects with mild cognitive impairment. *Neurology* **2008,** *70* (22), 2024-35.

55. Kabir, M. T.; Sufian, M. A.; Uddin, M. S.; Begum, M. M.; Akhter, S.; Islam, A.; Mathew, B.; Islam, M. S.; Amran, M. S.; Md Ashraf, G., NMDA Receptor Antagonists: Repositioning of Memantine as a Multitargeting Agent for Alzheimer's Therapy. *Curr Pharm Des* **2019,** *25* (33), 3506-3518.

56. Shimizu, E.; Tang, Y. P.; Rampon, C.; Tsien, J. Z., NMDA receptor-dependent synaptic reinforcement as a crucial process for memory consolidation. *Science* **2000,** *290* (5494), 1170-4.

57. Chen, R.; Chan, P. T.; Chu, H.; Lin, Y. C.; Chang, P. C.; Chen, C. Y.; Chou, K. R., Treatment effects between monotherapy of donepezil versus combination with memantine for Alzheimer disease: A meta-analysis. *PLoS One* **2017,** *12* (8), e0183586.

58. Cummings, J. L.; Morstorf, T.; Zhong, K., Alzheimer's disease drug-development pipeline: few candidates, frequent failures. *Alzheimers Res Ther* **2014,** *6* (4), 37.

59. Fawzi, A. A.; Weintraub, S.; Fawzi, W., Retinal Imaging in Alzheimer's Disease: In Search of the Holy Grail. *Ophthalmology* **2020,** *127* (1), 119-121.

60. Yaffe, K., Preclinical Alzheimer disease: Prevention Holy Grail or Pandora's Box?: Comment on "Heavy smoking in midlife and long-term risk of Alzheimer disease and vascular dementia". *Arch Intern Med* **2011,** *171* (4), 339-40.

61. Chuang, D. M.; Manji, H. K., In search of the Holy Grail for the treatment of neurodegenerative disorders: has a simple cation been overlooked? *Biol Psychiatry* **2007,** *62* (1), 4-6.

62. Hardy, J.; Selkoe, D. J., The amyloid hypothesis of Alzheimer's disease: progress and problems on the road to therapeutics. *Science* **2002,** *297* (5580), 353-6.

63. Hardy, J., Framing beta-amyloid. *Nat Genet* **1992,** *1* (4), 233-4.

64. Goate, A.; Chartier-Harlin, M. C.; Mullan, M.; Brown, J.; Crawford, F.; Fidani, L.; Giuffra, L.; Haynes, A.; Irving, N.; James, L.; et al., Segregation of a missense mutation in the amyloid precursor protein gene with familial Alzheimer's disease. *Nature* **1991,** *349* (6311), 704-6.

65. Rygiel, K., Novel strategies for Alzheimer's disease treatment: An overview of anti-amyloid beta monoclonal antibodies. *Indian J Pharmacol* **2016,** *48* (6), 629-636.

66. van Dyck, C. H., Anti-Amyloid-beta Monoclonal Antibodies for Alzheimer's Disease: Pitfalls and Promise. *Biol Psychiatry* **2018,** *83* (4), 311-319.

67. Congdon, E. E.; Sigurdsson, E. M., Tau-targeting therapies for Alzheimer disease. *Nat Rev Neurol* **2018,** *14* (7), 399-415.

68. Medina, M., An Overview on the Clinical Development of Tau-Based Therapeutics. *Int J Mol Sci* **2018,** *19* (4).

69. Choi, K. Y.; Swierczewska, M.; Lee, S.; Chen, X., Protease-activated drug development. *Theranostics* **2012,** *2* (2), 156-78.

70. Murachi, T.; Tanaka, K.; Hatanaka, M.; Murakami, T., Intracellular Ca2+-dependent protease (calpain) and its high-molecular-weight endogenous inhibitor (calpastatin). *Adv Enzyme Regul* **1980,** *19*, 407-24.

71. Guroff, G., A Neutral, Calcium-Activated Proteinase from the Soluble Fraction of Rat Brain. *J Biol Chem* **1964,** *239*, 149-55.

72. Ohno, S.; Emori, Y.; Imajoh, S.; Kawasaki, H.; Kisaragi, M.; Suzuki, K., Evolutionary origin of a calcium-dependent protease by fusion of genes for a thiol protease and a calcium-binding protein? *Nature* **1984,** *312* (5994), 566-70.

73. Ishiura, S.; Murofushi, H.; Suzuki, K.; Imahori, K., Studies of a calcium-activated neutral protease from chicken skeletal muscle. I. Purification and characterization. *J Biochem* **1978,** *84* (1), 225-30.

74. Croall, D. E.; Ersfeld, K., The calpains: modular designs and functional diversity. *Genome Biol* **2007,** *8* (6), 218.

75. Sorimachi, H.; Hata, S.; Ono, Y., Impact of genetic insights into calpain biology. *J Biochem* **2011,** *150* (1), 23-37.

76. Gan-Or, Z.; Bouslam, N.; Birouk, N.; Lissouba, A.; Chambers, D. B.; Veriepe, J.; Androschuk, A.; Laurent, S. B.; Rochefort, D.; Spiegelman, D.; Dionne-Laporte, A.; Szuto, A.; Liao, M.; Figlewicz, D. A.; Bouhouche, A.; Benomar, A.; Yahyaoui, M.; Ouazzani, R.; Yoon, G.; Dupre, N.; Suchowersky, O.; Bolduc, F. V.; Parker, J. A.; Dion, P. A.; Drapeau, P.; Rouleau, G. A.; Ouled Amar Bencheikh, B., Mutations in CAPN1 Cause Autosomal-Recessive Hereditary Spastic Paraplegia. *Am J Hum Genet* **2016,** *98* (5), 1038-1046.

77. Azam, M.; Andrabi, S. S.; Sahr, K. E.; Kamath, L.; Kuliopulos, A.; Chishti, A. H., Disruption of the mouse mu-calpain gene reveals an essential role in platelet function. *Mol Cell Biol* **2001,** *21* (6), 2213-20.

78. Forman, O. P.; De Risio, L.; Mellersh, C. S., Missense mutation in CAPN1 is associated with spinocerebellar ataxia in the Parson Russell Terrier dog breed. *PLoS One* **2013,** *8* (5), e64627.

79. Goll, D. E.; Thompson, V. F.; Li, H.; Wei, W.; Cong, J., The calpain system. *Physiol Rev* **2003,** *83* (3), 731-801.

80. Campbell, R. L.; Davies, P. L., Structure-function relationships in calpains. *Biochem J* **2012,** *447* (3), 335-51.

81. Ono, Y.; Saido, T. C.; Sorimachi, H., Calpain research for drug discovery: challenges and potential. *Nat Rev Drug Discov* **2016,** *15* (12), 854-876.

82. Moldoveanu, T.; Hosfield, C. M.; Lim, D.; Elce, J. S.; Jia, Z.; Davies, P. L., A Ca(2+) switch aligns the active site of calpain. *Cell* **2002,** *108* (5), 649-60.

83. De Tullio, R.; Averna, M.; Pedrazzi, M.; Sparatore, B.; Salamino, F.; Pontremoli, S.; Melloni, E., Differential regulation of the calpain-calpastatin complex by the L-domain of calpastatin. *Biochim Biophys Acta* **2014,** *1843* (11), 2583-91.

84. Baudry, M.; Chou, M. M.; Bi, X., Targeting calpain in synaptic plasticity. *Expert Opin Ther Targets* **2013,** *17* (5), 579-92.

85. Ray, S. K.; Banik, N. L., Calpain and its involvement in the pathophysiology of CNS injuries and diseases: therapeutic potential of calpain inhibitors for prevention of neurodegeneration. *Curr Drug Targets CNS Neurol Disord* **2003,** *2* (3), 173-89.

86. Conacci-Sorrell, M.; Eisenman, R. N., Post-translational control of Myc function during differentiation. *Cell Cycle* **2011,** *10* (4), 604-10.

87. Piatkov, K. I.; Oh, J. H.; Liu, Y.; Varshavsky, A., Calpain-generated natural protein fragments as short-lived substrates of the N-end rule pathway. *Proc Natl Acad Sci U S A* **2014,** *111* (9), E817-26.

88. Alzheimer's Association Calcium Hypothesis, W., Calcium Hypothesis of Alzheimer's disease and brain aging: A framework for integrating new evidence into a comprehensive theory of pathogenesis. *Alzheimers Dement* **2017,** *13* (2), 178-182 e17.

89. Wu, H. Y.; Hudry, E.; Hashimoto, T.; Kuchibhotla, K.; Rozkalne, A.; Fan, Z.; Spires-Jones, T.; Xie, H.; Arbel-Ornath, M.; Grosskreutz, C. L.; Bacskai, B. J.; Hyman, B. T.,

Amyloid beta induces the morphological neurodegenerative triad of spine loss, dendritic simplification, and neuritic dystrophies through calcineurin activation. *J Neurosci* **2010,** *30* (7), 2636-49.

90. Bezprozvanny, I.; Mattson, M. P., Neuronal calcium mishandling and the pathogenesis of Alzheimer's disease. *Trends Neurosci* **2008,** *31* (9), 454-63.

91. Nilsson, E.; Alafuzoff, I.; Blennow, K.; Blomgren, K.; Hall, C. M.; Janson, I.; Karlsson, I.; Wallin, A.; Gottfries, C. G.; Karlsson, J. O., Calpain and calpastatin in normal and Alzheimer-degenerated human brain tissue. *Neurobiol Aging* **1990,** *11* (4), 425-31.

92. Ma, M., Role of calpains in the injury-induced dysfunction and degeneration of the mammalian axon. *Neurobiol Dis* **2013,** *60*, 61-79.

93. Wang, Y.; Hersheson, J.; Lopez, D.; Hammer, M.; Liu, Y.; Lee, K. H.; Pinto, V.; Seinfeld, J.; Wiethoff, S.; Sun, J.; Amouri, R.; Hentati, F.; Baudry, N.; Tran, J.; Singleton, A. B.; Coutelier, M.; Brice, A.; Stevanin, G.; Durr, A.; Bi, X.; Houlden, H.; Baudry, M., Defects in the CAPN1 Gene Result in Alterations in Cerebellar Development and Cerebellar Ataxia in Mice and Humans. *Cell Rep* **2016,** *16* (1), 79-91.

94. Kurbatskaya, K.; Phillips, E. C.; Croft, C. L.; Dentoni, G.; Hughes, M. M.; Wade, M. A.; Al-Sarraj, S.; Troakes, C.; O'Neill, M. J.; Perez-Nievas, B. G.; Hanger, D. P.; Noble, W., Upregulation of calpain activity precedes tau phosphorylation and loss of synaptic proteins in Alzheimer's disease brain. *Acta Neuropathol Commun* **2016,** *4*, 34.

95. Braak, H.; Braak, E., Neuropathological stageing of Alzheimer-related changes. *Acta Neuropathol* **1991,** *82* (4), 239-59.

96. Taniguchi, S.; Fujita, Y.; Hayashi, S.; Kakita, A.; Takahashi, H.; Murayama, S.; Saido, T. C.; Hisanaga, S.; Iwatsubo, T.; Hasegawa, M., Calpain-mediated degradation of p35 to p25 in postmortem human and rat brains. *FEBS Lett* **2001,** *489* (1), 46-50.

97. Liang, B.; Duan, B. Y.; Zhou, X. P.; Gong, J. X.; Luo, Z. G., Calpain activation promotes BACE1 expression, amyloid precursor protein processing, and amyloid plaque formation in a transgenic mouse model of Alzheimer disease. *J Biol Chem* **2010,** *285* (36), 27737-44.

98. Baudry, M.; Bi, X., Calpain-1 and Calpain-2: The Yin and Yang of Synaptic Plasticity and Neurodegeneration. *Trends Neurosci* **2016,** *39* (4), 235-45.

99. Johnson, G. V.; Foley, V. G., Calpain-mediated proteolysis of microtubule-associated protein 2 (MAP-2) is inhibited by phosphorylation by cAMP-dependent protein kinase, but not by Ca2+/calmodulin-dependent protein kinase II. *J Neurosci Res* **1993,** *34* (6), 642-7.

100. Jin, N.; Yin, X.; Yu, D.; Cao, M.; Gong, C. X.; Iqbal, K.; Ding, F.; Gu, X.; Liu, F., Truncation and activation of GSK-3beta by calpain I: a molecular mechanism links to tau hyperphosphorylation in Alzheimer's disease. *Sci Rep* **2015,** *5*, 8187.

101. Fischer, I.; Romano-Clarke, G.; Grynspan, F., Calpain-mediated proteolysis of microtubule associated proteins MAP1B and MAP2 in developing brain. *Neurochem Res* **1991,** *16* (8), 891-8.

102. Sato, K.; Minegishi, S.; Takano, J.; Plattner, F.; Saito, T.; Asada, A.; Kawahara, H.; Iwata, N.; Saido, T. C.; Hisanaga, S., Calpastatin, an endogenous calpain-inhibitor protein,

regulates the cleavage of the Cdk5 activator p35 to p25. *J Neurochem* **2011,** *117* (3), 504-15.

103. Sahara, S.; Yamashima, T., Calpain-mediated Hsp70.1 cleavage in hippocampal CA1 neuronal death. *Biochem Biophys Res Commun* **2010,** *393* (4), 806-11.

104. Zhu, H.; Yoshimoto, T.; Yamashima, T., Heat shock protein 70.1 (Hsp70.1) affects neuronal cell fate by regulating lysosomal acid sphingomyelinase. *J Biol Chem* **2014,** *289* (40), 27432-43.

105. Kirkegaard, T.; Roth, A. G.; Petersen, N. H.; Mahalka, A. K.; Olsen, O. D.; Moilanen, I.; Zylicz, A.; Knudsen, J.; Sandhoff, K.; Arenz, C.; Kinnunen, P. K.; Nylandsted, J.; Jaattela, M., Hsp70 stabilizes lysosomes and reverts Niemann-Pick disease-associated lysosomal pathology. *Nature* **2010,** *463* (7280), 549-53.

106. Luo, C. L.; Chen, X. P.; Yang, R.; Sun, Y. X.; Li, Q. Q.; Bao, H. J.; Cao, Q. Q.; Ni, H.; Qin, Z. H.; Tao, L. Y., Cathepsin B contributes to traumatic brain injury-induced cell death through a mitochondria-mediated apoptotic pathway. *J Neurosci Res* **2010,** *88* (13), 2847-58.

107. Guicciardi, M. E.; Deussing, J.; Miyoshi, H.; Bronk, S. F.; Svingen, P. A.; Peters, C.; Kaufmann, S. H.; Gores, G. J., Cathepsin B contributes to TNF-alpha-mediated hepatocyte apoptosis by promoting mitochondrial release of cytochrome c. *J Clin Invest* **2000,** *106* (9), 1127-37.

108. Nakamura, Y.; Takeda, M.; Suzuki, H.; Hattori, H.; Tada, K.; Hariguchi, S.; Hashimoto, S.; Nishimura, T., Abnormal distribution of cathepsins in the brain of patients with Alzheimer's disease. *Neurosci Lett* **1991,** *130* (2), 195-8.

109. Otto, H. H.; Schirmeister, T., Cysteine Proteases and Their Inhibitors. *Chem Rev* **1997,** *97* (1), 133-172.

110. Turk, V.; Stoka, V.; Vasiljeva, O.; Renko, M.; Sun, T.; Turk, B.; Turk, D., Cysteine cathepsins: from structure, function and regulation to new frontiers. *Biochim Biophys Acta* **2012,** *1824* (1), 68-88.

111. Flannery, T.; Gibson, D.; Mirakhur, M.; McQuaid, S.; Greenan, C.; Trimble, A.; Walker, B.; McCormick, D.; Johnston, P. G., The clinical significance of cathepsin S expression in human astrocytomas. *Am J Pathol* **2003,** *163* (1), 175-82.

112. Sloane, B. F.; Honn, K. V.; Sadler, J. G.; Turner, W. A.; Kimpson, J. J.; Taylor, J. D., Cathepsin B activity in B16 melanoma cells: a possible marker for metastatic potential. *Cancer Res* **1982,** *42* (3), 980-6.

113. Krueger, S.; Kalinski, T.; Hundertmark, T.; Wex, T.; Kuster, D.; Peitz, U.; Ebert, M.; Nagler, D. K.; Kellner, U.; Malfertheiner, P.; Naumann, M.; Rocken, C.; Roessner, A., Up-regulation of cathepsin X in Helicobacter pylori gastritis and gastric cancer. *J Pathol* **2005,** *207* (1), 32-42.

114. Campo, E.; Munoz, J.; Miquel, R.; Palacin, A.; Cardesa, A.; Sloane, B. F.; Emmert-Buck, M. R., Cathepsin B expression in colorectal carcinomas correlates with tumor progression and shortened patient survival. *Am J Pathol* **1994,** *145* (2), 301-9.

115. Neurath, H., Evolution of proteolytic enzymes. *Science* **1984,** *224* (4647), 350-7.

116. Nilsson, E.; Bodolea, C.; Gordh, T.; Larsson, A., Cerebrospinal fluid cathepsin B and S. *Neurol Sci* **2013,** *34* (4), 445-8.

117. Lowry, J. R.; Klegeris, A., Emerging roles of microglial cathepsins in neurodegenerative disease. *Brain Res Bull* **2018,** *139*, 144-156.

118. Hook, G. R.; Yu, J.; Sipes, N.; Pierschbacher, M. D.; Hook, V.; Kindy, M. S., The cysteine protease cathepsin B is a key drug target and cysteine protease inhibitors are potential therapeutics for traumatic brain injury. *J Neurotrauma* **2014,** *31* (5), 515-29.

119. Assfalg-Machleidt, I.; Jochum, M.; Nast-Kolb, D.; Siebeck, M.; Billing, A.; Joka, T.; Rothe, G.; Valet, G.; Zauner, R.; Scheuber, H. P.; et al., Cathepsin B-indicator for the release of lysosomal cysteine proteinases in severe trauma and inflammation. *Biol Chem Hoppe Seyler* **1990,** *371 Suppl*, 211-22.

120. Bordi, M.; Berg, M. J.; Mohan, P. S.; Peterhoff, C. M.; Alldred, M. J.; Che, S.; Ginsberg, S. D.; Nixon, R. A., Autophagy flux in CA1 neurons of Alzheimer hippocampus: Increased induction overburdens failing lysosomes to propel neuritic dystrophy. *Autophagy* **2016,** *12* (12), 2467-2483.

121. Nixon, R. A.; Cataldo, A. M.; Mathews, P. M., The endosomal-lysosomal system of neurons in Alzheimer's disease pathogenesis: a review. *Neurochem Res* **2000,** *25* (9-10), 1161-72.

122. Quraishi, O.; Nagler, D. K.; Fox, T.; Sivaraman, J.; Cygler, M.; Mort, J. S.; Storer, A. C., The occluding loop in cathepsin B defines the pH dependence of inhibition by its propeptide. *Biochemistry* **1999,** *38* (16), 5017-23.

123. Mueller-Steiner, S.; Zhou, Y.; Arai, H.; Roberson, E. D.; Sun, B.; Chen, J.; Wang, X.; Yu, G.; Esposito, L.; Mucke, L.; Gan, L., Antiamyloidogenic and neuroprotective functions of cathepsin B: implications for Alzheimer's disease. *Neuron* **2006,** *51* (6), 703-14.

124. Sun, B.; Zhou, Y.; Halabisky, B.; Lo, I.; Cho, S. H.; Mueller-Steiner, S.; Devidze, N.; Wang, X.; Grubb, A.; Gan, L., Cystatin C-cathepsin B axis regulates amyloid beta levels and associated neuronal deficits in an animal model of Alzheimer's disease. *Neuron* **2008,** *60* (2), 247-57.

125. Mi, W.; Pawlik, M.; Sastre, M.; Jung, S. S.; Radvinsky, D. S.; Klein, A. M.; Sommer, J.; Schmidt, S. D.; Nixon, R. A.; Mathews, P. M.; Levy, E., Cystatin C inhibits amyloid-beta deposition in Alzheimer's disease mouse models. *Nat Genet* **2007,** *39* (12), 1440-2.

126. Wu, Z.; Sun, L.; Hashioka, S.; Yu, S.; Schwab, C.; Okada, R.; Hayashi, Y.; McGeer, P. L.; Nakanishi, H., Differential pathways for interleukin-1beta production activated by chromogranin A and amyloid beta in microglia. *Neurobiol Aging* **2013,** *34* (12), 2715-25.

127. Trinchese, F.; Fa, M.; Liu, S.; Zhang, H.; Hidalgo, A.; Schmidt, S. D.; Yamaguchi, H.; Yoshii, N.; Mathews, P. M.; Nixon, R. A.; Arancio, O., Inhibition of calpains improves memory and synaptic transmission in a mouse model of Alzheimer disease. *J Clin Invest* **2008,** *118* (8), 2796-807.

128. Tsubokawa, T.; Solaroglu, I.; Yatsushige, H.; Cahill, J.; Yata, K.; Zhang, J. H., Cathepsin and calpain inhibitor E64d attenuates matrix metalloproteinase-9 activity after focal cerebral ischemia in rats. *Stroke* **2006,** *37* (7), 1888-94.

129. Hasanbasic, S.; Jahic, A.; Karahmet, E.; Sejranic, A.; Prnjavorac, B., The Role of Cysteine Protease in Alzheimer Disease. *Mater Sociomed* **2016,** *28* (3), 235-8.

130. Fa, M.; Zhang, H.; Staniszewski, A.; Saeed, F.; Shen, L. W.; Schiefer, I. T.; Siklos, M. I.; Tapadar, S.; Litosh, V. A.; Libien, J.; Petukhov, P. A.; Teich, A. F.; Thatcher, G. R.; Arancio, O., Novel Selective Calpain 1 Inhibitors as Potential Therapeutics in Alzheimer's Disease. *J Alzheimers Dis* **2015,** *49* (3), 707-21.

131. Hook, V. Y.; Kindy, M.; Hook, G., Inhibitors of cathepsin B improve memory and reduce beta-amyloid in transgenic Alzheimer disease mice expressing the wild-type, but not the Swedish mutant, beta-secretase site of the amyloid precursor protein. *J Biol Chem* **2008,** *283* (12), 7745-53.

132. Chu, J.; Lauretti, E.; Pratico, D., Caspase-3-dependent cleavage of Akt modulates tau phosphorylation via GSK3beta kinase: implications for Alzheimer's disease. *Mol Psychiatry* **2017,** *22* (7), 1002-1008.

133. Rohn, T. T.; Head, E., Caspase activation in Alzheimer's disease: early to rise and late to bed. *Rev Neurosci* **2008,** *19* (6), 383-93.

134. Graham, R. K.; Ehrnhoefer, D. E.; Hayden, M. R., Caspase-6 and neurodegeneration. *Trends Neurosci* **2011,** *34* (12), 646-56.

135. Jantos, K.; Kling, A.; Mack, H.; Hornberger, W.; Moeller, A.; Nimmrich, V.; Lao, Y.; Nijsen, M., Discovery of ABT-957: 1-Benzyl-5-oxopyrrolidine-2-carboxamides as selective calpain inhibitors with enhanced metabolic stability. *Bioorg Med Chem Lett* **2019,** *29* (15), 1968-1973.

136. Medicine, N. L. o. Study to Evaluate the Safety, Tolerability, and Pharmacokinetics of ABT-957 in Subjects with Mild-to-Moderate Alzheimer's Disease on Stable Doses of Acetylcholinesterase Inhibitors. https://clinicaltrials.gov/ct2/show/NCT02220738.

137. Satoyoshi, E., Therapeutic trials on progressive muscular dystrophy. *Intern Med* **1992,** *31* (7), 841-6.

138. Weber, J. J.; Ortiz Rios, M. M.; Riess, O.; Clemens, L. E.; Nguyen, H. P., The calpain-suppressing effects of olesoxime in Huntington's disease. *Rare Dis* **2016,** *4* (1), e1153778.

139. Cruciani, M.; Malena, M., Combination dolutegravir-abacavir-lamivudine in the management of HIV/AIDS: clinical utility and patient considerations. *Patient Prefer Adherence* **2015,** *9*, 299-310.

140. Chen, D.; Frezza, M.; Schmitt, S.; Kanwar, J.; Dou, Q. P., Bortezomib as the first proteasome inhibitor anticancer drug: current status and future perspectives. *Curr Cancer Drug Targets* **2011,** *11* (3), 239-53.

141. Powers, B. J.; Coeytaux, R. R.; Dolor, R. J.; Hasselblad, V.; Patel, U. D.; Yancy, W. S., Jr.; Gray, R. N.; Irvine, R. J.; Kendrick, A. S.; Sanders, G. D., Updated report on comparative effectiveness of ACE inhibitors, ARBs, and direct renin inhibitors for patients with essential hypertension: much more data, little new information. *J Gen Intern Med* **2012,** *27* (6), 716-29.

142. Wan, F.; Letavernier, E.; Le Saux, C. J.; Houssaini, A.; Abid, S.; Czibik, G.; Sawaki, D.; Marcos, E.; Dubois-Rande, J. L.; Baud, L.; Adnot, S.; Derumeaux, G.; Gellen, B.,

Calpastatin overexpression impairs postinfarct scar healing in mice by compromising reparative immune cell recruitment and activation. *Am J Physiol Heart Circ Physiol* **2015,** *309* (11), H1883-93.

143. Kaneko, Y.; Murphy, C. R.; Day, M. L., Calpain 2 activity increases at the time of implantation in rat uterine luminal epithelial cells and administration of calpain inhibitor significantly reduces implantation sites. *Histochem Cell Biol* **2014,** *141* (4), 423-30.

144. Taneike, M.; Mizote, I.; Morita, T.; Watanabe, T.; Hikoso, S.; Yamaguchi, O.; Takeda, T.; Oka, T.; Tamai, T.; Oyabu, J.; Murakawa, T.; Nakayama, H.; Nishida, K.; Takeda, J.; Mochizuki, N.; Komuro, I.; Otsu, K., Calpain protects the heart from hemodynamic stress. *J Biol Chem* **2011,** *286* (37), 32170-7.

145. Fang, J.; Liu, X.; Bolanos, L.; Barker, B.; Rigolino, C.; Cortelezzi, A.; Oliva, E. N.; Cuzzola, M.; Grimes, H. L.; Fontanillo, C.; Komurov, K.; MacBeth, K.; Starczynowski, D. T., A calcium- and calpain-dependent pathway determines the response to lenalidomide in myelodysplastic syndromes. *Nat Med* **2016,** *22* (7), 727-34.

146. Tandon, R. K., Tropical pancreatitis. *J Gastroenterol* **2007,** *42 Suppl 17*, 141-7.

147. Dauth, S.; Sirbulescu, R. F.; Jordans, S.; Rehders, M.; Avena, L.; Oswald, J.; Lerchl, A.; Saftig, P.; Brix, K., Cathepsin K deficiency in mice induces structural and metabolic changes in the central nervous system that are associated with learning and memory deficits. *BMC Neurosci* **2011,** *12*, 74.

148. Chapurlat, R. D., Odanacatib: a review of its potential in the management of osteoporosis in postmenopausal women. *Ther Adv Musculoskelet Dis* **2015,** *7* (3), 103-9.

149. Gelb, B. D.; Shi, G. P.; Chapman, H. A.; Desnick, R. J., Pycnodysostosis, a lysosomal disease caused by cathepsin K deficiency. *Science* **1996,** *273* (5279), 1236-8.

150. Saftig, P.; Hunziker, E.; Wehmeyer, O.; Jones, S.; Boyde, A.; Rommerskirch, W.; Moritz, J. D.; Schu, P.; von Figura, K., Impaired osteoclastic bone resorption leads to osteopetrosis in cathepsin-K-deficient mice. *Proc Natl Acad Sci U S A* **1998,** *95* (23), 13453-8.

151. Stone, J. A.; McCrea, J. B.; Witter, R.; Zajic, S.; Stoch, S. A., Clinical and translational pharmacology of the cathepsin K inhibitor odanacatib studied for osteoporosis. *Br J Clin Pharmacol* **2019,** *85* (6), 1072-1083.

152. Mullard, A., Merck &Co. drops osteoporosis drug odanacatib. *Nat Rev Drug Discov* **2016,** *15* (10), 669.

153. Swallow, S., Fluorine in medicinal chemistry. *Prog Med Chem* **2015,** *54*, 65-133.

154. Clift, M. D.; Ji, H.; Deniau, G. P.; O'Hagan, D.; Silverman, R. B., Enantiomers of 4-amino-3-fluorobutanoic acid as substrates for gamma-aminobutyric acid aminotransferase. Conformational probes for GABA binding. *Biochemistry* **2007,** *46* (48), 13819-28.

155. Dalvit, C.; Vulpetti, A., Intermolecular and intramolecular hydrogen bonds involving fluorine atoms: implications for recognition, selectivity, and chemical properties. *ChemMedChem* **2012,** *7* (2), 262-72.

156. Brown, N., Bioisosteres and Scaffold Hopping in Medicinal Chemistry. *Mol Inform* **2014,** *33* (6-7), 458-62.

157. Zhang, L.; Lin, D.; Kusov, Y.; Nian, Y.; Ma, Q.; Wang, J.; von Brunn, A.; Leyssen, P.; Lanko, K.; Neyts, J.; de Wilde, A.; Snijder, E. J.; Liu, H.; Hilgenfeld, R., alpha-Ketoamides as Broad-Spectrum Inhibitors of Coronavirus and Enterovirus Replication: Structure-Based Design, Synthesis, and Activity Assessment. *J Med Chem* **2020,** *63* (9), 4562-4578.

158. Yan, X. X.; Jeromin, A.; Jeromin, A., Spectrin Breakdown Products (SBDPs) as Potential Biomarkers for Neurodegenerative Diseases. *Curr Transl Geriatr Exp Gerontol Rep* **2012,** *1* (2), 85-93.

159. Pineda, J. A.; Lewis, S. B.; Valadka, A. B.; Papa, L.; Hannay, H. J.; Heaton, S. C.; Demery, J. A.; Liu, M. C.; Aikman, J. M.; Akle, V.; Brophy, G. M.; Tepas, J. J.; Wang, K. K.; Robertson, C. S.; Hayes, R. L., Clinical significance of alphaII-spectrin breakdown products in cerebrospinal fluid after severe traumatic brain injury. *J Neurotrauma* **2007,** *24* (2), 354-66.

160. Weiss, E. S.; Wang, K. K.; Allen, J. G.; Blue, M. E.; Nwakanma, L. U.; Liu, M. C.; Lange, M. S.; Berrong, J.; Wilson, M. A.; Gott, V. L.; Troncoso, J. C.; Hayes, R. L.; Johnston, M. V.; Baumgartner, W. A., Alpha II-spectrin breakdown products serve as novel markers of brain injury severity in a canine model of hypothermic circulatory arrest. *Ann Thorac Surg* **2009,** *88* (2), 543-50.

161. Marchesi, V. T.; Steers, E., Jr., Selective solubilization of a protein component of the red cell membrane. *Science* **1968,** *159* (3811), 203-4.

162. Bennett, V.; Lambert, S., The spectrin skeleton: from red cells to brain. *J Clin Invest* **1991,** *87* (5), 1483-9.

163. Baines, A. J., Evolution of spectrin function in cytoskeletal and membrane networks. *Biochem Soc Trans* **2009,** *37* (Pt 4), 796-803.

164. Siman, R.; Baudry, M.; Lynch, G., Brain fodrin: substrate for calpain I, an endogenous calcium-activated protease. *Proc Natl Acad Sci U S A* **1984,** *81* (11), 3572-6.

165. Nixon, R. A., Fodrin degradation by calcium-activated neutral proteinase (CANP) in retinal ganglion cell neurons and optic glia: preferential localization of CANP activities in neurons. *J Neurosci* **1986,** *6* (5), 1264-71.

166. Peterson, C.; Vanderklish, P.; Seubert, P.; Cotman, C.; Lynch, G., Increased spectrin proteolysis in fibroblasts from aged and Alzheimer donors. *Neurosci Lett* **1991,** *121* (1-2), 239-43.

167. Masliah, E.; Iimoto, D. S.; Saitoh, T.; Hansen, L. A.; Terry, R. D., Increased immunoreactivity of brain spectrin in Alzheimer disease: a marker for synapse loss? *Brain Res* **1990,** *531* (1-2), 36-44.

168. Czogalla, A.; Sikorski, A. F., Spectrin and calpain: a 'target' and a 'sniper' in the pathology of neuronal cells. *Cell Mol Life Sci* **2005,** *62* (17), 1913-24.

169. Wu, S.; Sangerman, J.; Li, M.; Brough, G. H.; Goodman, S. R.; Stevens, T., Essential control of an endothelial cell ISOC by the spectrin membrane skeleton. *J Cell Biol* **2001,** *154* (6), 1225-33.

170. Newcomb-Fernandez, J. K.; Zhao, X.; Pike, B. R.; Wang, K. K.; Kampfl, A.; Beer, R.; DeFord, S. M.; Hayes, R. L., Concurrent assessment of calpain and caspase-3 activation after oxygen-glucose deprivation in primary septo-hippocampal cultures. *J Cereb Blood Flow Metab* **2001,** *21* (11), 1281-94.

171. Yamaguchi, T.; Yoneyama, M.; Hinoi, E.; Ogita, K., Involvement of calpain in 4-hydroxynonenal-induced disruption of gap junction-mediated intercellular communication among fibrocytes in primary cultures derived from the cochlear spiral ligament. *J Pharmacol Sci* **2015,** *129* (2), 127-34.

172. Zhang, Z.; Larner, S. F.; Liu, M. C.; Zheng, W.; Hayes, R. L.; Wang, K. K., Multiple alphaII-spectrin breakdown products distinguish calpain and caspase dominated necrotic and apoptotic cell death pathways. *Apoptosis* **2009,** *14* (11), 1289-98.

173. Billger, M.; Wallin, M.; Karlsson, J. O., Proteolysis of tubulin and microtubule-associated proteins 1 and 2 by calpain I and II. Difference in sensitivity of assembled and disassembled microtubules. *Cell Calcium* **1988,** *9* (1), 33-44.

174. de Leon, M. J.; Pirraglia, E.; Osorio, R. S.; Glodzik, L.; Saint-Louis, L.; Kim, H. J.; Fortea, J.; Fossati, S.; Laska, E.; Siegel, C.; Butler, T.; Li, Y.; Rusinek, H.; Zetterberg, H.; Blennow, K.; Alzheimer's Disease Neuroimaging, I.; National Alzheimer's Coordinating, C., The nonlinear relationship between cerebrospinal fluid Abeta42 and tau in preclinical Alzheimer's disease. *PLoS One* **2018,** *13* (2), e0191240.

175. Carreiras, M. C.; Mendes, E.; Perry, M. J.; Francisco, A. P.; Marco-Contelles, J., The multifactorial nature of Alzheimer's disease for developing potential therapeutics. *Curr Top Med Chem* **2013,** *13* (15), 1745-70.

176. Bennett, D. A.; Launer, L. J., Longitudinal epidemiologic clinical-pathologic studies of aging and Alzheimer's disease. *Curr Alzheimer Res* **2012,** *9* (6), 617-20.

177. O'Brien, R. J.; Resnick, S. M.; Zonderman, A. B.; Ferrucci, L.; Crain, B. J.; Pletnikova, O.; Rudow, G.; Iacono, D.; Riudavets, M. A.; Driscoll, I.; Price, D. L.; Martin, L. J.; Troncoso, J. C., Neuropathologic studies of the Baltimore Longitudinal Study of Aging (BLSA). *J Alzheimers Dis* **2009,** *18* (3), 665-75.

178. Wang, D.; Schultz, T.; Novak, G. P.; Baker, S.; Bennett, D. A.; Narayan, V. A., Longitudinal Modeling of Functional Decline Associated with Pathologic Alzheimer's Disease in Older Persons without Cognitive Impairment. *J Alzheimers Dis* **2018,** *62* (2), 855-865.

179. LaFerla, F. M.; Green, K. N., Animal models of Alzheimer disease. *Cold Spring Harb Perspect Med* **2012,** *2* (11).

180. Mori, C.; Spooner, E. T.; Wisniewsk, K. E.; Wisniewski, T. M.; Yamaguch, H.; Saido, T. C.; Tolan, D. R.; Selkoe, D. J.; Lemere, C. A., Intraneuronal Abeta42 accumulation in Down syndrome brain. *Amyloid* **2002,** *9* (2), 88-102.

181. Tractenberg, R. E.; Pietrzak, R. H., Intra-individual variability in Alzheimer's disease and cognitive aging: definitions, context, and effect sizes. *PLoS One* **2011,** *6* (4), e16973.

182. Ferreira, D.; Machado, A.; Molina, Y.; Nieto, A.; Correia, R.; Westman, E.; Barroso, J., Cognitive Variability during Middle-Age: Possible Association with Neurodegeneration and Cognitive Reserve. *Front Aging Neurosci* **2017,** *9*, 188.

183. Krishnamurthy, K.; Laskowitz, D. T., Cellular and Molecular Mechanisms of Secondary Neuronal Injury following Traumatic Brain Injury. In *Translational Research in Traumatic Brain Injury*, Laskowitz, D.; Grant, G., Eds. Boca Raton (FL), 2016.

184. Dawson, T. M.; Golde, T. E.; Lagier-Tourenne, C., Animal models of neurodegenerative diseases. *Nat Neurosci* **2018,** *21* (10), 1370-1379.

185. Desmond, D. W.; Moroney, J. T.; Sano, M.; Stern, Y., Incidence of dementia after ischemic stroke: results of a longitudinal study. *Stroke* **2002,** *33* (9), 2254-60.

186. Battistin, L.; Cagnin, A., Vascular cognitive disorder. A biological and clinical overview. *Neurochem Res* **2010,** *35* (12), 1933-8.

187. Ruitenberg, A.; den Heijer, T.; Bakker, S. L.; van Swieten, J. C.; Koudstaal, P. J.; Hofman, A.; Breteler, M. M., Cerebral hypoperfusion and clinical onset of dementia: the Rotterdam Study. *Ann Neurol* **2005,** *57* (6), 789-94.

188. de la Tremblaye, P. B.; Plamondon, H., Impaired conditioned emotional response and object recognition are concomitant to neuronal damage in the amygdala and perirhinal cortex in middle-aged ischemic rats. *Behav Brain Res* **2011,** *219* (2), 227-33.

189. Pluta, R.; Ulamek-Koziol, M.; Januszewski, S.; Czuczwar, S. J., Tau Protein Dysfunction after Brain Ischemia. *J Alzheimers Dis* **2018,** *66* (2), 429-437.

190. Pluta, R.; Ulamek-Koziol, M.; Januszewski, S.; Czuczwar, S., Amyloid pathology in the brain after ischemia. *Folia Neuropathol* **2019,** *57* (3), 220-226.

191. Pluta, R.; Ulamek, M.; Jablonski, M., Alzheimer's mechanisms in ischemic brain degeneration. *Anat Rec (Hoboken)* **2009,** *292* (12), 1863-81.

192. Urabe, T., [Molecular mechanism and new protective strategy for ischemic white matter damages]. *Rinsho Shinkeigaku* **2012,** *52* (11), 908-10.

193. Mark, R. J.; Lovell, M. A.; Markesbery, W. R.; Uchida, K.; Mattson, M. P., A role for 4-hydroxynonenal, an aldehydic product of lipid peroxidation, in disruption of ion homeostasis and neuronal death induced by amyloid beta-peptide. *J Neurochem* **1997,** *68* (1), 255-64.

194. Shringarpure, R.; Grune T Fau - Sitte, N.; Sitte N Fau - Davies, K. J.; Davies, K. J., 4-Hydroxynonenal-modified amyloid-beta peptide inhibits the proteasome: possible importance in Alzheimer's disease. (1420-682X (Print)).

195. Morel, P.; Tallineau, C.; Pontcharraud, R.; Piriou, A.; Huguet, F., Effects of 4-hydroxynonenal, a lipid peroxidation product, on dopamine transport and Na+/K+ ATPase in rat striatal synaptosomes. *Neurochemistry International* **1998,** *33* (6), 531-540.

196. Jenner, P., Oxidative stress in Parkinson's disease. *Ann Neurol* **2003,** *53 Suppl 3*, S26-36; discussion S36-8.

197. Butterfield, D. A.; Reed, T.; Perluigi, M.; De Marco, C.; Coccia, R.; Cini, C.; Sultana, R., Elevated protein-bound levels of the lipid peroxidation product, 4-hydroxy-2-nonenal, in brain from persons with mild cognitive impairment. *Neurosci Lett* **2006,** *397* (3), 170-3.

198. Pratico, D.; Sung, S., Lipid peroxidation and oxidative imbalance: early functional events in Alzheimer's disease. *J Alzheimers Dis* **2004,** *6* (2), 171-5.

199. Nunomura, A.; Perry, G.; Aliev, G.; Hirai, K.; Takeda, A.; Balraj, E. K.; Jones, P. K.; Ghanbari, H.; Wataya, T.; Shimohama, S.; Chiba, S.; Atwood, C. S.; Petersen, R. B.; Smith, M. A., Oxidative damage is the earliest event in Alzheimer disease. *J Neuropathol Exp Neurol* **2001,** *60* (8), 759-67.

200. Cebak, J. E.; Singh, I. N.; Hill, R. L.; Wang, J. A.; Hall, E. D., Phenelzine Protects Brain Mitochondrial Function In Vitro and In Vivo following Traumatic Brain Injury by Scavenging the Reactive Carbonyls 4-Hydroxynonenal and Acrolein Leading to Cortical Histological Neuroprotection. *J Neurotrauma* **2017,** *34* (7), 1302-1317.

201. Hall, E. D.; Vaishnav, R. A.; Mustafa, A. G., Antioxidant therapies for traumatic brain injury. *Neurotherapeutics* **2010,** *7* (1), 51-61.

202. Shao, C.; Roberts, K. N.; Markesbery, W. R.; Scheff, S. W.; Lovell, M. A., Oxidative stress in head trauma in aging. *Free Radic Biol Med* **2006,** *41* (1), 77-85.

203. Gemma, C.; Vila, J.; Bachstetter, A.; Bickford, P. C., Oxidative Stress and the Aging Brain: From Theory to Prevention. In *Brain Aging: Models, Methods, and Mechanisms*, Riddle, D. R., Ed. Boca Raton (FL), 2007.

204. Pratico, D., Oxidative stress hypothesis in Alzheimer's disease: a reappraisal. *Trends Pharmacol Sci* **2008,** *29* (12), 609-15.

205. Butterfield, D. A.; Perluigi, M.; Sultana, R., Oxidative stress in Alzheimer's disease brain: new insights from redox proteomics. *Eur J Pharmacol* **2006,** *545* (1), 39-50.

206. Zhao, Y.; Zhao, B., Oxidative stress and the pathogenesis of Alzheimer's disease. *Oxid Med Cell Longev* **2013,** *2013*, 316523.

207. Sultana, R.; Robinson, R. A.; Lange, M. B.; Fiorini, A.; Galvan, V.; Fombonne, J.; Baker, A.; Gorostiza, O.; Zhang, J.; Cai, J.; Pierce, W. M.; Bredesen, D. E.; Butterfield, D. A., Do proteomics analyses provide insights into reduced oxidative stress in the brain of an Alzheimer disease transgenic mouse model with an M631L amyloid precursor protein substitution and thereby the importance of amyloid-beta-resident methionine 35 in Alzheimer disease pathogenesis? *Antioxid Redox Signal* **2012,** *17* (11), 1507-14.

208. Butterfield, D. A., Amyloid beta-peptide (1-42)-induced oxidative stress and neurotoxicity: implications for neurodegeneration in Alzheimer's disease brain. A review. *Free Radic Res* **2002,** *36* (12), 1307-13.

209. Pizzimenti, S.; Ciamporcero, E.; Daga, M.; Pettazzoni, P.; Arcaro, A.; Cetrangolo, G.; Minelli, R.; Dianzani, C.; Lepore, A.; Gentile, F.; Barrera, G., Interaction of aldehydes derived from lipid peroxidation and membrane proteins. *Frontiers in Physiology* **2013,** *4*, 242.

210. Nam, T.-g., Lipid Peroxidation and Its Toxicological Implications. *Toxicological Research* **2011,** *27* (1), 1-6.

211. Chen, C. H.; Ferreira, J. C.; Gross, E. R.; Mochly-Rosen, D., Targeting aldehyde dehydrogenase 2: new therapeutic opportunities. *Physiol Rev* **2014,** *94* (1), 1-34.

212. Markesbery, W. R.; Kryscio, R. J.; Lovell, M. A.; Morrow, J. D., Lipid peroxidation is an early event in the brain in amnestic mild cognitive impairment. *Ann Neurol* **2005,** *58* (5), 730-5.

213. Markesbery, W. R.; Lovell, M. A., Four-hydroxynonenal, a product of lipid peroxidation, is increased in the brain in Alzheimer's disease. *Neurobiol Aging* **1998,** *19* (1), 33-6.

214. Reed, T. T.; Pierce, W. M.; Markesbery, W. R.; Butterfield, D. A., Proteomic identification of HNE-bound proteins in early Alzheimer disease: Insights into the role of lipid peroxidation in the progression of AD. *Brain Res* **2009,** *1274*, 66-76.

215. Reed, T.; Perluigi, M.; Sultana, R.; Pierce, W. M.; Klein, J. B.; Turner, D. M.; Coccia, R.; Markesbery, W. R.; Butterfield, D. A., Redox proteomic identification of 4-hydroxy-2-nonenal-modified brain proteins in amnestic mild cognitive impairment: insight into the role of lipid peroxidation in the progression and pathogenesis of Alzheimer's disease. *Neurobiol Dis* **2008,** *30* (1), 107-20.

216. Lorente, L.; Martin, M. M.; Abreu-Gonzalez, P.; Ramos, L.; Argueso, M.; Caceres, J. J.; Sole-Violan, J.; Lorenzo, J. M.; Molina, I.; Jimenez, A., Association between serum malondialdehyde levels and mortality in patients with severe brain trauma injury. *J Neurotrauma* **2015,** *32* (1), 1-6.

217. Cristofori, L.; Tavazzi, B.; Gambin, R.; Vagnozzi, R.; Vivenza, C.; Amorini, A. M.; Di Pierro, D.; Fazzina, G.; Lazzarino, G., Early onset of lipid peroxidation after human traumatic brain injury: a fatal limitation for the free radical scavenger pharmacological therapy? *J Investig Med* **2001,** *49* (5), 450-8.

218. Al Nimer, F.; Strom, M.; Lindblom, R.; Aeinehband, S.; Bellander, B. M.; Nyengaard, J. R.; Lidman, O.; Piehl, F., Naturally occurring variation in the Glutathione-S-Transferase 4 gene determines neurodegeneration after traumatic brain injury. *Antioxid Redox Signal* **2013,** *18* (7), 784-94.

219. Di Domenico, F.; Tramutola, A.; Butterfield, D. A., Role of 4-hydroxy-2-nonenal (HNE) in the pathogenesis of alzheimer disease and other selected age-related neurodegenerative disorders. *Free Radic Biol Med* **2017,** *111*, 253-261.

220. Pizzimenti, S.; Ciamporcero, E.; Daga, M.; Pettazzoni, P.; Arcaro, A.; Cetrangolo, G.; Minelli, R.; Dianzani, C.; Lepore, A.; Gentile, F.; Barrera, G., Interaction of aldehydes derived from lipid peroxidation and membrane proteins. *Front Physiol* **2013,** *4*, 242.

221. Benedetti, E.; D'Angelo, B.; Cristiano, L.; Di Giacomo, E.; Fanelli, F.; Moreno, S.; Cecconi, F.; Fidoamore, A.; Antonosante, A.; Falcone, R.; Ippoliti, R.; Giordano, A.; Cimini, A., Involvement of peroxisome proliferator-activated receptor beta/delta (PPAR beta/delta) in BDNF signaling during aging and in Alzheimer disease: possible role of 4-hydroxynonenal (4-HNE). *Cell Cycle* **2014,** *13* (8), 1335-44.

222. Kitagawa, K.; Kawamoto, T.; Kunugita, N.; Tsukiyama, T.; Okamoto, K.; Yoshida, A.; Nakayama, K., Aldehyde dehydrogenase (ALDH) 2 associates with oxidation of methoxyacetaldehyde; in vitro analysis with liver subcellular fraction derived from human and Aldh2 gene targeting mouse. *FEBS Lett* **2000,** *476* (3), 306-11.

223. Luo, J.; Lee, S. H.; VandeVrede, L.; Qin, Z.; Ben Aissa, M.; Larson, J.; Teich, A. F.; Arancio, O.; D'Souza, Y.; Elharram, A.; Koster, K.; Tai, L. M.; LaDu, M. J.; Bennett, B. M.; Thatcher, G. R., A multifunctional therapeutic approach to disease modification in multiple familial mouse models and a novel sporadic model of Alzheimer's disease. *Mol Neurodegener* **2016,** *11* (1), 35.

224. D'Souza, Y.; Elharram, A.; Soon-Shiong, R.; Andrew, R. D.; Bennett, B. M., Characterization of Aldh2 (-/-) mice as an age-related model of cognitive impairment and Alzheimer's disease. *Mol Brain* **2015,** *8* (1), 27.

225. Ohta, S.; Ohsawa, I., Dysfunction of mitochondria and oxidative stress in the pathogenesis of Alzheimer's disease: on defects in the cytochrome c oxidase complex and aldehyde detoxification. *J Alzheimers Dis* **2006,** *9* (2), 155-66.

226. Ohta, S.; Ohsawa, I.; Kamino, K.; Ando, F.; Shimokata, H., Mitochondrial ALDH2 deficiency as an oxidative stress. *Ann N Y Acad Sci* **2004,** *1011*, 36-44.

227. Kamino, K.; Nagasaka, K.; Imagawa, M.; Yamamoto, H.; Yoneda, H.; Ueki, A.; Kitamura, S.; Namekata, K.; Miki, T.; Ohta, S., Deficiency in Mitochondrial Aldehyde Dehydrogenase Increases the Risk for Late-Onset Alzheimer's Disease in the Japanese Population. *Biochemical and Biophysical Research Communications* **2000,** *273* (1), 192-196.

228. Yu, R.-L.; Tan, C.-H.; Lu, Y.-C.; Wu, R.-M., Aldehyde dehydrogenase 2 is associated with cognitive functions in patients with Parkinson's disease. *Scientific Reports* **2016,** *6*, 30424.

229. Ohta, S.; Ohsawa, I., Dysfunction of mitochondria and oxidative stress in the pathogenesis of Alzheimer's disease: on defects in the cytochrome c oxidase complex and aldehyde detoxification. (1387-2877 (Print)).

230. Ohsawa, I.; Nishimaki, K.; Murakami, Y.; Suzuki, Y.; Ishikawa, M.; Ohta, S., Age-dependent neurodegeneration accompanying memory loss in transgenic mice defective in mitochondrial aldehyde dehydrogenase 2 activity. *J Neurosci* **2008,** *28* (24), 6239-49.

231. Wey, M. C.-Y.; Fernandez, E.; Martinez, P. A.; Sullivan, P.; Goldstein, D. S.; Strong, R., Neurodegeneration and Motor Dysfunction in Mice Lacking Cytosolic and Mitochondrial Aldehyde Dehydrogenases: Implications for Parkinson's Disease. *PLOS ONE* **2012,** *7* (2), e31522.

232. Gardner, R. C.; Yaffe, K., Epidemiology of mild traumatic brain injury and neurodegenerative disease. *Mol Cell Neurosci* **2015,** *66* (Pt B), 75-80.

233. Shively, S.; Scher, A. I.; Perl, D. P.; Diaz-Arrastia, R., Dementia resulting from traumatic brain injury: what is the pathology? *Arch Neurol* **2012,** *69* (10), 1245-51.

234. Fleminger, S.; Oliver, D. L.; Lovestone, S.; Rabe-Hesketh, S.; Giora, A., Head injury as a risk factor for Alzheimer's disease: the evidence 10 years on; a partial replication. *J Neurol Neurosurg Psychiatry* **2003,** *74* (7), 857-62.

235. Plassman, B. L.; Havlik, R. J.; Steffens, D. C.; Helms, M. J.; Newman, T. N.; Drosdick, D.; Phillips, C.; Gau, B. A.; Welsh-Bohmer, K. A.; Burke, J. R.; Guralnik, J. M.; Breitner, J. C., Documented head injury in early adulthood and risk of Alzheimer's disease and other dementias. *Neurology* **2000,** *55* (8), 1158-66.

236. Weber, J. T., Experimental models of repetitive brain injuries. *Prog Brain Res* **2007,** *161*, 253-61.

237. Kanayama, G.; Takeda, M.; Niigawa, H.; Ikura, Y.; Tamii, H.; Taniguchi, N.; Kudo, T.; Miyamae, Y.; Morihara, T.; Nishimura, T., The effects of repetitive mild brain injury

on cytoskeletal protein and behavior. *Methods Find Exp Clin Pharmacol* **1996,** *18* (2), 105-15.

238. Conte, V.; Uryu, K.; Fujimoto, S.; Yao, Y.; Rokach, J.; Longhi, L.; Trojanowski, J. Q.; Lee, V. M.; McIntosh, T. K.; Pratico, D., Vitamin E reduces amyloidosis and improves cognitive function in Tg2576 mice following repetitive concussive brain injury. *J Neurochem* **2004,** *90* (3), 758-64.

239. Kaur, P.; Sharma, S., Recent Advances in Pathophysiology of Traumatic Brain Injury. *Curr Neuropharmacol* **2018,** *16* (8), 1224-1238.

240. Bolouri, H.; Zetterberg, H., Animal Models for Concussion: Molecular and Cognitive Assessments-Relevance to Sport and Military Concussions. In *Brain Neurotrauma: Molecular, Neuropsychological, and Rehabilitation Aspects*, Kobeissy, F. H., Ed. Boca Raton (FL), 2015.

241. Khalin, I.; Jamari, N. L.; Razak, N. B.; Hasain, Z. B.; Nor, M. A.; Zainudin, M. H.; Omar, A. B.; Alyautdin, R., A mouse model of weight-drop closed head injury: emphasis on cognitive and neurological deficiency. *Neural Regen Res* **2016,** *11* (4), 630-5.

242. Osier, N.; Dixon, C. E., The Controlled Cortical Impact Model of Experimental Brain Trauma: Overview, Research Applications, and Protocol. *Methods Mol Biol* **2016,** *1462*, 177-92.

243. Kabadi, S. V.; Hilton, G. D.; Stoica, B. A.; Zapple, D. N.; Faden, A. I., Fluid-percussion-induced traumatic brain injury model in rats. *Nat Protoc* **2010,** *5* (9), 1552-63.

244. Koliatsos, V. E.; Cernak, I.; Xu, L.; Song, Y.; Savonenko, A.; Crain, B. J.; Eberhart, C. G.; Frangakis, C. E.; Melnikova, T.; Kim, H.; Lee, D., A mouse model of blast injury to brain: initial pathological, neuropathological, and behavioral characterization. *J Neuropathol Exp Neurol* **2011,** *70* (5), 399-416.

245. Cernak, I.; Wing, I. D.; Davidsson, J.; Plantman, S., A novel mouse model of penetrating brain injury. *Front Neurol* **2014,** *5*, 209.

246. Feeney, D. M.; Boyeson, M. G.; Linn, R. T.; Murray, H. M.; Dail, W. G., Responses to cortical injury: I. Methodology and local effects of contusions in the rat. *Brain Res* **1981,** *211* (1), 67-77.

247. Amorini, A. M.; Dunbar, J. G.; Marmarou, A., Modulation of aquaporin-4 water transport in a model of TBI. *Acta Neurochir Suppl* **2003,** *86*, 261-3.

248. Marmarou, A.; Foda Ma Fau - van den Brink, W.; van den Brink W Fau - Campbell, J.; Campbell J Fau - Kita, H.; Kita H Fau - Demetriadou, K.; Demetriadou, K., A new model of diffuse brain injury in rats. Part I: Pathophysiology and biomechanics. **1994,** (0022-3085 (Print)).

249. Rush, D. K., Scopolamine amnesia of passive avoidance: a deficit of information acquisition. *Behav Neural Biol* **1988,** *50* (3), 255-74.

250. Abdul-Hay, S.; Schiefer, I. T.; Chandrasena, R. E.; Li, M.; Abdelhamid, R.; Wang, Y. T.; Tavassoli, E.; Michalsen, B.; Asghodom, R. T.; Luo, J.; Thatcher, G. R., NO-SSRIs: Nitric Oxide Chimera Drugs Incorporating a Selective Serotonin Reuptake Inhibitor. *ACS Med Chem Lett* **2011,** *2* (9), 656-661.

251. Zohar, O.; Schreiber, S.; Getslev, V.; Schwartz, J. P.; Mullins, P. G.; Pick, C. G., Closed-head minimal traumatic brain injury produces long-term cognitive deficits in mice. *Neuroscience* **2003,** *118* (4), 949-55.

252. Tasca, C. I.; Dal-Cim, T.; Cimarosti, H., In vitro oxygen-glucose deprivation to study ischemic cell death. *Methods Mol Biol* **2015,** *1254*, 197-210.

253. de Vries, D. K.; Kortekaas, K. A.; Tsikas, D.; Wijermars, L. G.; van Noorden, C. J.; Suchy, M. T.; Cobbaert, C. M.; Klautz, R. J.; Schaapherder, A. F.; Lindeman, J. H., Oxidative damage in clinical ischemia/reperfusion injury: a reappraisal. *Antioxid Redox Signal* **2013,** *19* (6), 535-45.

254. Abdelhamid, R.; Luo, J.; Vandevrede, L.; Kundu, I.; Michalsen, B.; Litosh, V. A.; Schiefer, I. T.; Gherezghiher, T.; Yao, P.; Qin, Z.; Thatcher, G. R., Benzothiophene Selective Estrogen Receptor Modulators Provide Neuroprotection by a novel GPR30-dependent Mechanism. *ACS Chem Neurosci* **2011,** *2* (5), 256-268.

255. Gordon, J.; Amini, S.; White, M. K., General overview of neuronal cell culture. *Methods Mol Biol* **2013,** *1078*, 1-8.

256. Frederick, J. R.; Chen, Z.; Bevers, M. B.; Ingleton, L. P.; Ma, M.; Neumar, R. W., Neuroprotection with delayed calpain inhibition after transient forebrain ischemia. *Crit Care Med* **2008,** *36* (11 Suppl), S481-5.

257. Bartus, R. T.; Hayward, N. J.; Elliott, P. J.; Sawyer, S. D.; Baker, K. L.; Dean, R. L.; Akiyama, A.; Straub, J. A.; Harbeson, S. L.; Li, Z.; et al., Calpain inhibitor AK295 protects neurons from focal brain ischemia. Effects of postocclusion intra-arterial administration. *Stroke* **1994,** *25* (11), 2265-70.

258. Kling, A.; Jantos, K.; Mack, H.; Hornberger, W.; Drescher, K.; Nimmrich, V.; Relo, A.; Wicke, K.; Hutchins, C. W.; Lao, Y.; Marsh, K.; Moeller, A., Discovery of Novel and Highly Selective Inhibitors of Calpain for the Treatment of Alzheimer's Disease: 2-(3-Phenyl-1H-pyrazol-1-yl)-nicotinamides. *J Med Chem* **2017,** *60* (16), 7123-7138.

259. Thatcher, G. R.; Bennett, B. M.; Reynolds, J. N., Nitric oxide mimetic molecules as therapeutic agents in Alzheimer's disease. *Curr Alzheimer Res* **2005,** *2* (2), 171-82.

260. Thatcher, G. R.; Bennett, B. M.; Reynolds, J. N., NO chimeras as therapeutic agents in Alzheimer's disease. *Curr Alzheimer Res* **2006,** *3* (3), 237-45.

261. Thatcher, G. R.; Bennett, B. M.; Dringenberg, H. C.; Reynolds, J. N., Novel nitrates as NO mimetics directed at Alzheimer's disease. *J Alzheimers Dis* **2004,** *6* (6 Suppl), S75-84.

262. Ji, J.; Su, L.; Liu, Z., Critical role of calpain in inflammation. *Biomed Rep* **2016,** *5* (6), 647-652.

263. Abarikwu, S. O.; Pant, A. B.; Farombi, E. O., 4-Hydroxynonenal induces mitochondrial-mediated apoptosis and oxidative stress in SH-SY5Y human neuronal cells. *Basic Clin Pharmacol Toxicol* **2012,** *110* (5), 441-8.

264. Guiotto, A.; Calderan A Fau - Ruzza, P.; Ruzza P Fau - Osler, A.; Osler A Fau - Rubini, C.; Rubini C Fau - Jo, D.-G.; Jo Dg Fau - Mattson, M. P.; Mattson Mp Fau - Borin, G.; Borin, G., Synthesis and evaluation of neuroprotective alpha,beta-unsaturated aldehyde scavenger histidyl-containing analogues of carnosine. (0022-2623 (Print)).

265. Tang, S. C.; Arumugam Thiruma, V.; Cutler Roy, G.; Jo, D. G.; Magnus, T.; Chan Sic, L.; Mughal Mohamed, R.; Telljohann Richard, S.; Nassar, M.; Ouyang, X.; Calderan, A.; Ruzza, P.; Guiotto, A.; Mattson Mark, P., Neuroprotective actions of a histidine analogue in models of ischemic stroke. *Journal of Neurochemistry* **2006,** *101* (3), 729-736.

266. Olivieri, G.; Baysang G Fau - Meier, F.; Meier F Fau - Muller-Spahn, F.; Muller-Spahn F Fau - Stahelin, H. B.; Stahelin Hb Fau - Brockhaus, M.; Brockhaus M Fau - Brack, C.; Brack, C., N-acetyl-L-cysteine protects SHSY5Y neuroblastoma cells from oxidative stress and cell cytotoxicity: effects on beta-amyloid secretion and tau phosphorylation. (0022-3042 (Print)).

267. Bennett, D. A., Mixed pathologies and neural reserve: Implications of complexity for Alzheimer disease drug discovery. *PLOS Medicine* **2017,** *14* (3), e1002256.

268. Werner, C.; Engelhard, K., Pathophysiology of traumatic brain injury. *Br J Anaesth* **2007,** *99* (1), 4-9.

269. Knopp, R. C.; Lee, S. H.; Hollas, M.; Nepomuceno, E.; Gonzalez, D.; Tam, K.; Aamir, D.; Wang, Y.; Pierce, E.; BenAissa, M.; Thatcher, G. R. J., Interaction of oxidative stress and neurotrauma in ALDH2(-/-) mice causes significant and persistent behavioral and pro-inflammatory effects in a tractable model of mild traumatic brain injury. *Redox Biol* **2020,** *32*, 101486.

270. Dodson, M.; Wani, W. Y.; Redmann, M.; Benavides, G. A.; Johnson, M. S.; Ouyang, X.; Cofield, S. S.; Mitra, K.; Darley-Usmar, V.; Zhang, J., Regulation of autophagy, mitochondrial dynamics, and cellular bioenergetics by 4-hydroxynonenal in primary neurons. *Autophagy* **2017,** *13* (11), 1828-1840.

271. Sun, L.; Wu, Z.; Hayashi, Y.; Peters, C.; Tsuda, M.; Inoue, K.; Nakanishi, H., Microglial cathepsin B contributes to the initiation of peripheral inflammation-induced chronic pain. *J Neurosci* **2012,** *32* (33), 11330-42.

272. Lee, Y. B.; Du, S.; Rhim, H.; Lee, E. B.; Markelonis, G. J.; Oh, T. H., Rapid increase in immunoreactivity to GFAP in astrocytes in vitro induced by acidic pH is mediated by calcium influx and calpain I. *Brain Res* **2000,** *864* (2), 220-9.

273. Zoltewicz, J. S.; Scharf, D.; Yang, B.; Chawla, A.; Newsom, K. J.; Fang, L., Characterization of Antibodies that Detect Human GFAP after Traumatic Brain Injury. *Biomark Insights* **2012,** *7*, 71-9.

274. Papa, L.; Rosenthal, K.; Silvestri, F.; Axley, J. C.; Kelly, J. M.; Lewis, S. B., Evaluation of alpha-II-spectrin breakdown products as potential biomarkers for early recognition and severity of aneurysmal subarachnoid hemorrhage. *Sci Rep* **2018,** *8* (1), 13308.

275. Daneman, R.; Prat, A., The blood-brain barrier. *Cold Spring Harb Perspect Biol* **2015,** *7* (1), a020412.

276. Weerasuriya, A.; Mizisin, A. P., The blood-nerve barrier: structure and functional significance. *Methods Mol Biol* **2011,** *686*, 149-73.

277. Campbell, M.; Humphries, P., The blood-retina barrier: tight junctions and barrier modulation. *Adv Exp Med Biol* **2012,** *763*, 70-84.

278. Juhn, S. K.; Hunter, B. A.; Odland, R. M., Blood-labyrinth barrier and fluid dynamics of the inner ear. *Int Tinnitus J* **2001,** *7* (2), 72-83.

279. Redzic, Z., Molecular biology of the blood-brain and the blood-cerebrospinal fluid barriers: similarities and differences. *Fluids Barriers CNS* **2011,** *8* (1), 3.

280. Iadecola, C., The pathobiology of vascular dementia. *Neuron* **2013,** *80* (4), 844-66.

281. Iadecola, C., The Neurovascular Unit Coming of Age: A Journey through Neurovascular Coupling in Health and Disease. *Neuron* **2017,** *96* (1), 17-42.

282. Abbott, N. J.; Patabendige, A. A.; Dolman, D. E.; Yusof, S. R.; Begley, D. J., Structure and function of the blood-brain barrier. *Neurobiol Dis* **2010,** *37* (1), 13-25.

283. Coomber, B. L.; Stewart, P. A., Morphometric analysis of CNS microvascular endothelium. *Microvasc Res* **1985,** *30* (1), 99-115.

284. Coomber, B. L.; Stewart, P. A., Three-dimensional reconstruction of vesicles in endothelium of blood-brain barrier versus highly permeable microvessels. *Anat Rec* **1986,** *215* (3), 256-61.

285. Sweeney, M. D.; Sagare, A. P.; Zlokovic, B. V., Blood-brain barrier breakdown in Alzheimer disease and other neurodegenerative disorders. *Nat Rev Neurol* **2018,** *14* (3), 133-150.

286. Gonzalez-Mariscal, L.; Betanzos, A.; Nava, P.; Jaramillo, B. E., Tight junction proteins. *Prog Biophys Mol Biol* **2003,** *81* (1), 1-44.

287. Zlokovic, B. V., Neurovascular pathways to neurodegeneration in Alzheimer's disease and other disorders. *Nat Rev Neurosci* **2011,** *12* (12), 723-38.

288. Erickson, M. A.; Banks, W. A., Age-Associated Changes in the Immune System and Blood(-)Brain Barrier Functions. *Int J Mol Sci* **2019,** *20* (7).

289. Andreone, B. J.; Chow, B. W.; Tata, A.; Lacoste, B.; Ben-Zvi, A.; Bullock, K.; Deik, A. A.; Ginty, D. D.; Clish, C. B.; Gu, C., Blood-Brain Barrier Permeability Is Regulated by Lipid Transport-Dependent Suppression of Caveolae-Mediated Transcytosis. *Neuron* **2017,** *94* (3), 581-594 e5.

290. Ben-Zvi, A.; Lacoste, B.; Kur, E.; Andreone, B. J.; Mayshar, Y.; Yan, H.; Gu, C., Mfsd2a is critical for the formation and function of the blood-brain barrier. *Nature* **2014,** *509* (7501), 507-11.

291. Pardridge, W. M., Blood-brain barrier endogenous transporters as therapeutic targets: a new model for small molecule CNS drug discovery. *Expert Opin Ther Targets* **2015,** *19* (8), 1059-72.

292. O'Kane, R. L.; Hawkins, R. A., Na+-dependent transport of large neutral amino acids occurs at the abluminal membrane of the blood-brain barrier. *Am J Physiol Endocrinol Metab* **2003,** *285* (6), E1167-73.

293. Mann, G. E.; Yudilevich, D. L.; Sobrevia, L., Regulation of amino acid and glucose transporters in endothelial and smooth muscle cells. *Physiol Rev* **2003,** *83* (1), 183-252.

294. Mayerl, S.; Muller, J.; Bauer, R.; Richert, S.; Kassmann, C. M.; Darras, V. M.; Buder, K.; Boelen, A.; Visser, T. J.; Heuer, H., Transporters MCT8 and OATP1C1 maintain murine brain thyroid hormone homeostasis. *J Clin Invest* **2014,** *124* (5), 1987-99.

295. Mitchell, R. W.; On, N. H.; Del Bigio, M. R.; Miller, D. W.; Hatch, G. M., Fatty acid transport protein expression in human brain and potential role in fatty acid transport across human brain microvessel endothelial cells. *J Neurochem* **2011,** *117* (4), 735-46.

296. Cass, C. E.; Young, J. D.; Baldwin, S. A., Recent advances in the molecular biology of nucleoside transporters of mammalian cells. *Biochem Cell Biol* **1998,** *76* (5), 761-70.

297. Gao, B.; Vavricka, S. R.; Meier, P. J.; Stieger, B., Differential cellular expression of organic anion transporting peptides OATP1A2 and OATP2B1 in the human retina and brain: implications for carrier-mediated transport of neuropeptides and neurosteriods in the CNS. *Pflugers Arch* **2015,** *467* (7), 1481-1493.

298. Ganapathy, M. E.; Huang, W.; Rajan, D. P.; Carter, A. L.; Sugawara, M.; Iseki, K.; Leibach, F. H.; Ganapathy, V., beta-lactam antibiotics as substrates for OCTN2, an organic cation/carnitine transporter. *J Biol Chem* **2000,** *275* (3), 1699-707.

299. Bray, N., Biologics: Transferrin' bispecific antibodies across the blood-brain barrier. *Nat Rev Drug Discov* **2015,** *14* (1), 14-5.

300. Deane, R.; Du Yan, S.; Submamaryan, R. K.; LaRue, B.; Jovanovic, S.; Hogg, E.; Welch, D.; Manness, L.; Lin, C.; Yu, J.; Zhu, H.; Ghiso, J.; Frangione, B.; Stern, A.; Schmidt, A. M.; Armstrong, D. L.; Arnold, B.; Liliensiek, B.; Nawroth, P.; Hofman, F.; Kindy, M.; Stern, D.; Zlokovic, B., RAGE mediates amyloid-beta peptide transport across the blood-brain barrier and accumulation in brain. *Nat Med* **2003,** *9* (7), 907-13.

301. Deane, R.; Wu, Z.; Sagare, A.; Davis, J.; Du Yan, S.; Hamm, K.; Xu, F.; Parisi, M.; LaRue, B.; Hu, H. W.; Spijkers, P.; Guo, H.; Song, X.; Lenting, P. J.; Van Nostrand, W. E.; Zlokovic, B. V., LRP/amyloid beta-peptide interaction mediates differential brain efflux of Abeta isoforms. *Neuron* **2004,** *43* (3), 333-44.

302. Zlokovic, B. V.; Jovanovic, S.; Miao, W.; Samara, S.; Verma, S.; Farrell, C. L., Differential regulation of leptin transport by the choroid plexus and blood-brain barrier and high affinity transport systems for entry into hypothalamus and across the blood-cerebrospinal fluid barrier. *Endocrinology* **2000,** *141* (4), 1434-41.

303. Silverman, J. A., Multidrug-resistance transporters. *Pharm Biotechnol* **1999,** *12*, 353-86.

304. Fromm, M. F., P-glycoprotein: a defense mechanism limiting oral bioavailability and CNS accumulation of drugs. *Int J Clin Pharmacol Ther* **2000,** *38* (2), 69-74.

305. Funck, V. R.; Ribeiro, L. R.; Pereira, L. M.; de Oliveira, C. V.; Grigoletto, J.; Della-Pace, I. D.; Fighera, M. R.; Royes, L. F.; Furian, A. F.; Larrick, J. W.; Oliveira, M. S., Contrasting effects of Na+, K+-ATPase activation on seizure activity in acute versus chronic models. *Neuroscience* **2015,** *298*, 171-9.

306. Kisler, K.; Nelson, A. R.; Montagne, A.; Zlokovic, B. V., Cerebral blood flow regulation and neurovascular dysfunction in Alzheimer disease. *Nat Rev Neurosci* **2017,** *18* (7), 419-434.

307. Millar, I. D.; Wang, S.; Brown, P. D.; Barrand, M. A.; Hladky, S. B., Kv1 and Kir2 potassium channels are expressed in rat brain endothelial cells. *Pflugers Arch* **2008,** *456* (2), 379-91.

308. Foroutan, S.; Brillault, J.; Forbush, B.; O'Donnell, M. E., Moderate-to-severe ischemic conditions increase activity and phosphorylation of the cerebral microvascular endothelial cell Na+-K+-Cl- cotransporter. *Am J Physiol Cell Physiol* **2005,** *289* (6), C1492-501.

309. Taylor, C. J.; Nicola, P. A.; Wang, S.; Barrand, M. A.; Hladky, S. B., Transporters involved in regulation of intracellular pH in primary cultured rat brain endothelial cells. *J Physiol* **2006,** *576* (Pt 3), 769-85.

310. Sweeney, M. D.; Ayyadurai, S.; Zlokovic, B. V., Pericytes of the neurovascular unit: key functions and signaling pathways. *Nat Neurosci* **2016,** *19* (6), 771-83.

311. Abbott, N. J.; Ronnback, L.; Hansson, E., Astrocyte-endothelial interactions at the blood-brain barrier. *Nat Rev Neurosci* **2006,** *7* (1), 41-53.

312. Erickson, M. A.; Banks, W. A., Blood-brain barrier dysfunction as a cause and consequence of Alzheimer's disease. *J Cereb Blood Flow Metab* **2013,** *33* (10), 1500-13.

313. Chen, R. L., Is it appropriate to use albumin CSF/plasma ratio to assess blood brain barrier permeability? *Neurobiol Aging* **2011,** *32* (7), 1338-9.

314. Chen, R. L.; Kassem, N. A.; Redzic, Z. B.; Chen, C. P.; Segal, M. B.; Preston, J. E., Age-related changes in choroid plexus and blood-cerebrospinal fluid barrier function in the sheep. *Exp Gerontol* **2009,** *44* (4), 289-96.

315. Montagne, A.; Barnes, S. R.; Sweeney, M. D.; Halliday, M. R.; Sagare, A. P.; Zhao, Z.; Toga, A. W.; Jacobs, R. E.; Liu, C. Y.; Amezcua, L.; Harrington, M. G.; Chui, H. C.; Law, M.; Zlokovic, B. V., Blood-brain barrier breakdown in the aging human hippocampus. *Neuron* **2015,** *85* (2), 296-302.

316. Elahy, M.; Jackaman, C.; Mamo, J. C.; Lam, V.; Dhaliwal, S. S.; Giles, C.; Nelson, D.; Takechi, R., Blood-brain barrier dysfunction developed during normal aging is associated with inflammation and loss of tight junctions but not with leukocyte recruitment. *Immun Ageing* **2015,** *12*, 2.

317. Stamatovic, S. M.; Martinez-Revollar, G.; Hu, A.; Choi, J.; Keep, R. F.; Andjelkovic, A. V., Decline in Sirtuin-1 expression and activity plays a critical role in blood-brain barrier permeability in aging. *Neurobiol Dis* **2019,** *126*, 105-116.

318. Bonte, S.; Vandemaele, P.; Verleden, S.; Audenaert, K.; Deblaere, K.; Goethals, I.; Van Holen, R., Healthy brain ageing assessed with 18F-FDG PET and age-dependent recovery factors after partial volume effect correction. *Eur J Nucl Med Mol Imaging* **2017,** *44* (5), 838-849.

319. Shibata, M.; Yamada, S.; Kumar, S. R.; Calero, M.; Bading, J.; Frangione, B.; Holtzman, D. M.; Miller, C. A.; Strickland, D. K.; Ghiso, J.; Zlokovic, B. V., Clearance of Alzheimer's amyloid-ss(1-40) peptide from brain by LDL receptor-related protein-1 at the blood-brain barrier. *J Clin Invest* **2000,** *106* (12), 1489-99.

320. Ramanathan, A.; Nelson, A. R.; Sagare, A. P.; Zlokovic, B. V., Impaired vascular-mediated clearance of brain amyloid beta in Alzheimer's disease: the role, regulation and restoration of LRP1. *Front Aging Neurosci* **2015,** *7*, 136.

321. Toornvliet, R.; van Berckel, B. N.; Luurtsema, G.; Lubberink, M.; Geldof, A. A.; Bosch, T. M.; Oerlemans, R.; Lammertsma, A. A.; Franssen, E. J., Effect of age on functional P-glycoprotein in the blood-brain barrier measured by use of (R)-[(11)C]verapamil and positron emission tomography. *Clin Pharmacol Ther* **2006,** *79* (6), 540-8.

322. van Assema, D. M.; Lubberink, M.; Boellaard, R.; Schuit, R. C.; Windhorst, A. D.; Scheltens, P.; Lammertsma, A. A.; van Berckel, B. N., P-glycoprotein function at the blood-brain barrier: effects of age and gender. *Mol Imaging Biol* **2012,** *14* (6), 771-6.

323. Chiu, C.; Miller, M. C.; Monahan, R.; Osgood, D. P.; Stopa, E. G.; Silverberg, G. D., P-glycoprotein expression and amyloid accumulation in human aging and Alzheimer's disease: preliminary observations. *Neurobiol Aging* **2015,** *36* (9), 2475-82.

324. Sartorius, T.; Peter, A.; Heni, M.; Maetzler, W.; Fritsche, A.; Haring, H. U.; Hennige, A. M., The brain response to peripheral insulin declines with age: a contribution of the blood-brain barrier? *PLoS One* **2015,** *10* (5), e0126804.

325. Frolich, L.; Blum-Degen, D.; Bernstein, H. G.; Engelsberger, S.; Humrich, J.; Laufer, S.; Muschner, D.; Thalheimer, A.; Turk, A.; Hoyer, S.; Zochling, R.; Boissl, K. W.; Jellinger, K.; Riederer, P., Brain insulin and insulin receptors in aging and sporadic Alzheimer's disease. *J Neural Transm (Vienna)* **1998,** *105* (4-5), 423-38.

326. Park, M. H.; Lee, J. Y.; Park, K. H.; Jung, I. K.; Kim, K. T.; Lee, Y. S.; Ryu, H. H.; Jeong, Y.; Kang, M.; Schwaninger, M.; Gulbins, E.; Reichel, M.; Kornhuber, J.; Yamaguchi, T.; Kim, H. J.; Kim, S. H.; Schuchman, E. H.; Jin, H. K.; Bae, J. S., Vascular and Neurogenic Rejuvenation in Aging Mice by Modulation of ASM. *Neuron* **2018,** *100* (1), 167-182 e9.

327. Doolittle, N. D.; Muldoon, L. L.; Culp, A. Y.; Neuwelt, E. A., Delivery of chemotherapeutics across the blood-brain barrier: challenges and advances. *Adv Pharmacol* **2014,** *71*, 203-43.

328. Lipsman, N.; Meng, Y.; Bethune, A. J.; Huang, Y.; Lam, B.; Masellis, M.; Herrmann, N.; Heyn, C.; Aubert, I.; Boutet, A.; Smith, G. S.; Hynynen, K.; Black, S. E., Blood-brain barrier opening in Alzheimer's disease using MR-guided focused ultrasound. *Nat Commun* **2018,** *9* (1), 2336.

329. Sweeney, M. D.; Zhao, Z.; Montagne, A.; Nelson, A. R.; Zlokovic, B. V., Blood-Brain Barrier: From Physiology to Disease and Back. *Physiol Rev* **2019,** *99* (1), 21-78.

330. Nation, D. A.; Sweeney, M. D.; Montagne, A.; Sagare, A. P.; D'Orazio, L. M.; Pachicano, M.; Sepehrband, F.; Nelson, A. R.; Buennagel, D. P.; Harrington, M. G.; Benzinger, T. L. S.; Fagan, A. M.; Ringman, J. M.; Schneider, L. S.; Morris, J. C.; Chui, H. C.; Law, M.; Toga, A. W.; Zlokovic, B. V., Blood-brain barrier breakdown is an early biomarker of human cognitive dysfunction. *Nat Med* **2019,** *25* (2), 270-276.

331. Arvanitakis, Z.; Capuano, A. W.; Leurgans, S. E.; Bennett, D. A.; Schneider, J. A., Relation of cerebral vessel disease to Alzheimer's disease dementia and cognitive function in elderly people: a cross-sectional study. *Lancet Neurol* **2016,** *15* (9), 934-943.

332. Iturria-Medina, Y.; Sotero, R. C.; Toussaint, P. J.; Mateos-Perez, J. M.; Evans, A. C.; Alzheimer's Disease Neuroimaging, I., Early role of vascular dysregulation on late-onset Alzheimer's disease based on multifactorial data-driven analysis. *Nat Commun* **2016,** *7*, 11934.

333. Takechi, R.; Lam, V.; Brook, E.; Giles, C.; Fimognari, N.; Mooranian, A.; Al-Salami, H.; Coulson, S. H.; Nesbit, M.; Mamo, J. C. L., Blood-Brain Barrier Dysfunction Precedes Cognitive Decline and Neurodegeneration in Diabetic Insulin Resistant Mouse Model: An Implication for Causal Link. *Front Aging Neurosci* **2017,** *9*, 399.

334. Zlokovic, B. V., The blood-brain barrier in health and chronic neurodegenerative disorders. *Neuron* **2008,** *57* (2), 178-201.

335. Shi, Y.; Zhang, L.; Pu, H.; Mao, L.; Hu, X.; Jiang, X.; Xu, N.; Stetler, R. A.; Zhang, F.; Liu, X.; Leak, R. K.; Keep, R. F.; Ji, X.; Chen, J., Rapid endothelial cytoskeletal reorganization enables early blood-brain barrier disruption and long-term ischaemic reperfusion brain injury. *Nat Commun* **2016,** *7*, 10523.

336. Basun, H.; Bogdanovic, N.; Ingelsson, M.; Almkvist, O.; Naslund, J.; Axelman, K.; Bird, T. D.; Nochlin, D.; Schellenberg, G. D.; Wahlund, L. O.; Lannfelt, L., Clinical and neuropathological features of the arctic APP gene mutation causing early-onset Alzheimer disease. *Arch Neurol* **2008,** *65* (4), 499-505.

337. Genin, E.; Hannequin, D.; Wallon, D.; Sleegers, K.; Hiltunen, M.; Combarros, O.; Bullido, M. J.; Engelborghs, S.; De Deyn, P.; Berr, C.; Pasquier, F.; Dubois, B.; Tognoni, G.; Fievet, N.; Brouwers, N.; Bettens, K.; Arosio, B.; Coto, E.; Del Zompo, M.; Mateo, I.; Epelbaum, J.; Frank-Garcia, A.; Helisalmi, S.; Porcellini, E.; Pilotto, A.; Forti, P.; Ferri, R.; Scarpini, E.; Siciliano, G.; Solfrizzi, V.; Sorbi, S.; Spalletta, G.; Valdivieso, F.; Vepsalainen, S.; Alvarez, V.; Bosco, P.; Mancuso, M.; Panza, F.; Nacmias, B.; Bossu, P.; Hanon, O.; Piccardi, P.; Annoni, G.; Seripa, D.; Galimberti, D.; Licastro, F.; Soininen, H.; Dartigues, J. F.; Kamboh, M. I.; Van Broeckhoven, C.; Lambert, J. C.; Amouyel, P.; Campion, D., APOE and Alzheimer disease: a major gene with semi-dominant inheritance. *Mol Psychiatry* **2011,** *16* (9), 903-7.

338. Liu, C. C.; Liu, C. C.; Kanekiyo, T.; Xu, H.; Bu, G., Apolipoprotein E and Alzheimer disease: risk, mechanisms and therapy. *Nat Rev Neurol* **2013,** *9* (2), 106-18.

339. Tanzi, R. E., The genetics of Alzheimer disease. *Cold Spring Harb Perspect Med* **2012,** *2* (10).

340. Halliday, M. R.; Rege, S. V.; Ma, Q.; Zhao, Z.; Miller, C. A.; Winkler, E. A.; Zlokovic, B. V., Accelerated pericyte degeneration and blood-brain barrier breakdown in apolipoprotein E4 carriers with Alzheimer's disease. *J Cereb Blood Flow Metab* **2016,** *36* (1), 216-27.

341. Sheline, Y. I.; Morris, J. C.; Snyder, A. Z.; Price, J. L.; Yan, Z.; D'Angelo, G.; Liu, C.; Dixit, S.; Benzinger, T.; Fagan, A.; Goate, A.; Mintun, M. A., APOE4 allele disrupts resting state fMRI connectivity in the absence of amyloid plaques or decreased CSF Abeta42. *J Neurosci* **2010,** *30* (50), 17035-40.

342. Suri, S.; Mackay, C. E.; Kelly, M. E.; Germuska, M.; Tunbridge, E. M.; Frisoni, G. B.; Matthews, P. M.; Ebmeier, K. P.; Bulte, D. P.; Filippini, N., Reduced cerebrovascular

reactivity in young adults carrying the APOE epsilon4 allele. *Alzheimers Dement* **2015,** *11* (6), 648-57 e1.

343. Carrasquillo, M. M.; Belbin, O.; Hunter, T. A.; Ma, L.; Bisceglio, G. D.; Zou, F.; Crook, J. E.; Pankratz, V. S.; Dickson, D. W.; Graff-Radford, N. R.; Petersen, R. C.; Morgan, K.; Younkin, S. G., Replication of CLU, CR1, and PICALM associations with alzheimer disease. *Arch Neurol* **2010,** *67* (8), 961-4.

344. Zhao, Z.; Sagare, A. P.; Ma, Q.; Halliday, M. R.; Kong, P.; Kisler, K.; Winkler, E. A.; Ramanathan, A.; Kanekiyo, T.; Bu, G.; Owens, N. C.; Rege, S. V.; Si, G.; Ahuja, A.; Zhu, D.; Miller, C. A.; Schneider, J. A.; Maeda, M.; Maeda, T.; Sugawara, T.; Ichida, J. K.; Zlokovic, B. V., Central role for PICALM in amyloid-beta blood-brain barrier transcytosis and clearance. *Nat Neurosci* **2015,** *18* (7), 978-87.

345. Yates, P. A.; Desmond, P. M.; Phal, P. M.; Steward, C.; Szoeke, C.; Salvado, O.; Ellis, K. A.; Martins, R. N.; Masters, C. L.; Ames, D.; Villemagne, V. L.; Rowe, C. C.; Group, A. R., Incidence of cerebral microbleeds in preclinical Alzheimer disease. *Neurology* **2014,** *82* (14), 1266-73.

346. Halliday, M. R.; Pomara, N.; Sagare, A. P.; Mack, W. J.; Frangione, B.; Zlokovic, B. V., Relationship between cyclophilin a levels and matrix metalloproteinase 9 activity in cerebrospinal fluid of cognitively normal apolipoprotein e4 carriers and blood-brain barrier breakdown. *JAMA Neurol* **2013,** *70* (9), 1198-200.

347. Cortes-Canteli, M.; Paul, J.; Norris, E. H.; Bronstein, R.; Ahn, H. J.; Zamolodchikov, D.; Bhuvanendran, S.; Fenz, K. M.; Strickland, S., Fibrinogen and beta-amyloid association alters thrombosis and fibrinolysis: a possible contributing factor to Alzheimer's disease. *Neuron* **2010,** *66* (5), 695-709.

348. Cullen, K. M.; Kocsi, Z.; Stone, J., Pericapillary haem-rich deposits: evidence for microhaemorrhages in aging human cerebral cortex. *J Cereb Blood Flow Metab* **2005,** *25* (12), 1656-67.

349. Bailey, T. L.; Rivara, C. B.; Rocher, A. B.; Hof, P. R., The nature and effects of cortical microvascular pathology in aging and Alzheimer's disease. *Neurol Res* **2004,** *26* (5), 573-8.

350. Sengillo, J. D.; Winkler, E. A.; Walker, C. T.; Sullivan, J. S.; Johnson, M.; Zlokovic, B. V., Deficiency in mural vascular cells coincides with blood-brain barrier disruption in Alzheimer's disease. *Brain Pathol* **2013,** *23* (3), 303-10.

351. O'Driscoll, M. C.; Daly, S. B.; Urquhart, J. E.; Black, G. C.; Pilz, D. T.; Brockmann, K.; McEntagart, M.; Abdel-Salam, G.; Zaki, M.; Wolf, N. I.; Ladda, R. L.; Sell, S.; D'Arrigo, S.; Squier, W.; Dobyns, W. B.; Livingston, J. H.; Crow, Y. J., Recessive mutations in the gene encoding the tight junction protein occludin cause band-like calcification with simplified gyration and polymicrogyria. *Am J Hum Genet* **2010,** *87* (3), 354-64.

352. Miyazaki, T.; Koya, T.; Kigawa, Y.; Oguchi, T.; Lei, X. F.; Kim-Kaneyama, J. R.; Miyazaki, A., Calpain and atherosclerosis. *J Atheroscler Thromb* **2013,** *20* (3), 228-37.

353. Gonscherowski, V.; Becker, B. F.; Moroder, L.; Motrescu, E.; Gil-Parrado, S.; Gloe, T.; Keller, M.; Zahler, S., Calpains: a physiological regulator of the endothelial barrier? *Am J Physiol Heart Circ Physiol* **2006,** *290* (5), H2035-42.

354. Youn, J. Y.; Wang, T.; Cai, H., An ezrin/calpain/PI3K/AMPK/eNOSs1179 signaling cascade mediating VEGF-dependent endothelial nitric oxide production. *Circ Res* **2009,** *104* (1), 50-9.

355. Zhang, Y.; Liu, N. M.; Wang, Y.; Youn, J. Y.; Cai, H., Endothelial cell calpain as a critical modulator of angiogenesis. *Biochim Biophys Acta Mol Basis Dis* **2017,** *1863* (6), 1326-1335.

356. Nassar, D.; Letavernier, E.; Baud, L.; Aractingi, S.; Khosrotehrani, K., Calpain activity is essential in skin wound healing and contributes to scar formation. *PLoS One* **2012,** *7* (5), e37084.

357. Rami, A.; Krieglstein, J., Protective effects of calpain inhibitors against neuronal damage caused by cytotoxic hypoxia in vitro and ischemia in vivo. *Brain Res* **1993,** *609* (1-2), 67-70.

358. McDonald, M. C.; Mota-Filipe, H.; Paul, A.; Cuzzocrea, S.; Abdelrahman, M.; Harwood, S.; Plevin, R.; Chatterjee, P. K.; Yaqoob, M. M.; Thiemermann, C., Calpain inhibitor I reduces the activation of nuclear factor-kappaB and organ injury/dysfunction in hemorrhagic shock. *FASEB J* **2001,** *15* (1), 171-186.

359. Stalker, T. J.; Gong, Y.; Scalia, R., The calcium-dependent protease calpain causes endothelial dysfunction in type 2 diabetes. *Diabetes* **2005,** *54* (4), 1132-40.

360. Ikeda, Y.; Young, L. H.; Lefer, A. M., Attenuation of neutrophil-mediated myocardial ischemia-reperfusion injury by a calpain inhibitor. *Am J Physiol Heart Circ Physiol* **2002,** *282* (4), H1421-6.

361. Bralić, M.; Stemberga, V., Calpain expression in the brain cortex after traumatic brain injury. *Coll Antropol* **2012,** *36* (4), 1319-23.

362. Alluri, H.; Grimsley, M.; Anasooya Shaji, C.; Varghese, K. P.; Zhang, S. L.; Peddaboina, C.; Robinson, B.; Beeram, M. R.; Huang, J. H.; Tharakan, B., Attenuation of Blood-Brain Barrier Breakdown and Hyperpermeability by Calpain Inhibition. *J Biol Chem* **2016,** *291* (53), 26958-26969.

363. Wang, T.; Wang, L.; Moreno-Vinasco, L.; Lang, G. D.; Siegler, J. H.; Mathew, B.; Usatyuk, P. V.; Samet, J. M.; Geyh, A. S.; Breysse, P. N.; Natarajan, V.; Garcia, J. G., Particulate matter air pollution disrupts endothelial cell barrier via calpain-mediated tight junction protein degradation. *Part Fibre Toxicol* **2012,** *9*, 35.

364. Miyoshi, Y.; Tanabe, S.; Suzuki, T., Cellular zinc is required for intestinal epithelial barrier maintenance via the regulation of claudin-3 and occludin expression. *Am J Physiol Gastrointest Liver Physiol* **2016,** *311* (1), G105-16.

365. Chun, J.; Prince, A., TLR2-induced calpain cleavage of epithelial junctional proteins facilitates leukocyte transmigration. *Cell Host Microbe* **2009,** *5* (1), 47-58.

366. Zhang, Y.; Chen, Y.; Zhang, Y.; Li, P. L.; Li, X., Contribution of cathepsin B-dependent Nlrp3 inflammasome activation to nicotine-induced endothelial barrier dysfunction. *Eur J Pharmacol* **2019,** *865*, 172795.

367. Asahi, M.; Wang, X.; Mori, T.; Sumii, T.; Jung, J. C.; Moskowitz, M. A.; Fini, M. E.; Lo, E. H., Effects of matrix metalloproteinase-9 gene knock-out on the proteolysis of blood-brain barrier and white matter components after cerebral ischemia. *J Neurosci* **2001,** *21* (19), 7724-32.

368. Weekman, E. M.; Wilcock, D. M., Matrix Metalloproteinase in Blood-Brain Barrier Breakdown in Dementia. *J Alzheimers Dis* **2016,** *49* (4), 893-903.

369. Pijet, B.; Stefaniuk, M.; Kostrzewska-Ksiezyk, A.; Tsilibary, P. E.; Tzinia, A.; Kaczmarek, L., Elevation of MMP-9 Levels Promotes Epileptogenesis After Traumatic Brain Injury. *Mol Neurobiol* **2018,** *55* (12), 9294-9306.

370. Freeman, L. R.; Keller, J. N., Oxidative stress and cerebral endothelial cells: regulation of the blood-brain-barrier and antioxidant based interventions. *Biochim Biophys Acta* **2012,** *1822* (5), 822-9.

371. Horstmann, S.; Budig, L.; Gardner, H.; Koziol, J.; Deuschle, M.; Schilling, C.; Wagner, S., Matrix metalloproteinases in peripheral blood and cerebrospinal fluid in patients with Alzheimer's disease. *Int Psychogeriatr* **2010,** *22* (6), 966-72.

372. Lorenzl, S.; Albers, D. S.; Relkin, N.; Ngyuen, T.; Hilgenberg, S. L.; Chirichigno, J.; Cudkowicz, M. E.; Beal, M. F., Increased plasma levels of matrix metalloproteinase-9 in patients with Alzheimer's disease. *Neurochem Int* **2003,** *43* (3), 191-6.

373. Zhang, H.; Adwanikar, H.; Werb, Z.; Noble-Haeusslein, L. J., Matrix metalloproteinases and neurotrauma: evolving roles in injury and reparative processes. *Neuroscientist* **2010,** *16* (2), 156-70.

374. Popp, O.; Heidinger, M.; Ruiz-Heinrich, L.; Ries, C.; Jochum, M.; Gil-Parrado, S., The calpastatin-derived calpain inhibitor CP1B reduces mRNA expression of matrix metalloproteinase-2 and -9 and invasion by leukemic THP-1 cells. *Biol Chem* **2003,** *384* (6), 951-8.

375. Yanamandra, N.; Gumidyala, K. V.; Waldron, K. G.; Gujrati, M.; Olivero, W. C.; Dinh, D. H.; Rao, J. S.; Mohanam, S., Blockade of cathepsin B expression in human glioblastoma cells is associated with suppression of angiogenesis. *Oncogene* **2004,** *23* (12), 2224-30.

376. Kamat, P. K.; Swarnkar, S.; Rai, S.; Kumar, V.; Tyagi, N., Astrocyte mediated MMP-9 activation in the synapse dysfunction: An implication in Alzheimer disease. *Ther Targets Neurol Dis* **2014,** *1* (1).

377. Zozulya, A.; Weidenfeller, C.; Galla, H. J., Pericyte-endothelial cell interaction increases MMP-9 secretion at the blood-brain barrier in vitro. *Brain Res* **2008,** *1189*, 1-11.

378. Takata, F.; Dohgu, S.; Matsumoto, J.; Takahashi, H.; Machida, T.; Wakigawa, T.; Harada, E.; Miyaji, H.; Koga, M.; Nishioku, T.; Yamauchi, A.; Kataoka, Y., Brain pericytes among cells constituting the blood-brain barrier are highly sensitive to tumor necrosis factor-alpha, releasing matrix metalloproteinase-9 and migrating in vitro. *J Neuroinflammation* **2011,** *8*, 106.

379. Kotecki, M.; Zeiger, A. S.; Van Vliet, K. J.; Herman, I. M., Calpain- and talin-dependent control of microvascular pericyte contractility and cellular stiffness. *Microvasc Res* **2010,** *80* (3), 339-48.

380. Kubes, P.; Kurose, I.; Granger, D. N., NO donors prevent integrin-induced leukocyte adhesion but not P-selectin-dependent rolling in postischemic venules. *Am J Physiol* **1994,** *267* (3 Pt 2), H931-7.

381. Dimmeler, S.; Zeiher, A. M., Nitric oxide-an endothelial cell survival factor. *Cell Death Differ* **1999,** *6* (10), 964-8.

382. Austin, S. A.; Santhanam, A. V.; Hinton, D. J.; Choi, D. S.; Katusic, Z. S., Endothelial nitric oxide deficiency promotes Alzheimer's disease pathology. *J Neurochem* **2013,** *127* (5), 691-700.

383. Tan, X. L.; Xue, Y. Q.; Ma, T.; Wang, X.; Li, J. J.; Lan, L.; Malik, K. U.; McDonald, M. P.; Dopico, A. M.; Liao, F. F., Partial eNOS deficiency causes spontaneous thrombotic cerebral infarction, amyloid angiopathy and cognitive impairment. *Mol Neurodegener* **2015,** *10*, 24.

384. Daiber, A.; Xia, N.; Steven, S.; Oelze, M.; Hanf, A.; Kroller-Schon, S.; Munzel, T.; Li, H., New Therapeutic Implications of Endothelial Nitric Oxide Synthase (eNOS) Function/Dysfunction in Cardiovascular Disease. *Int J Mol Sci* **2019,** *20* (1).

385. Bhuiyan, M. S.; Shioda, N.; Fukunaga, K., Chronic beta-AR activation-induced calpain activation and impaired eNOS-Akt signaling mediates cardiac injury in ovariectomized female rats. *Expert Opin Ther Targets* **2009,** *13* (3), 275-86.

386. Smith, I. J.; Dodd, S. L., Calpain activation causes a proteasome-dependent increase in protein degradation and inhibits the Akt signalling pathway in rat diaphragm muscle. *Exp Physiol* **2007,** *92* (3), 561-73.

387. Stalker, T. J.; Skvarka, C. B.; Scalia, R., A novel role for calpains in the endothelial dysfunction of hyperglycemia. *FASEB J* **2003,** *17* (11), 1511-3.

388. Dong, Y.; Wu, Y.; Wu, M.; Wang, S.; Zhang, J.; Xie, Z.; Xu, J.; Song, P.; Wilson, K.; Zhao, Z.; Lyons, T.; Zou, M. H., Activation of protease calpain by oxidized and glycated LDL increases the degradation of endothelial nitric oxide synthase. *J Cell Mol Med* **2009,** *13* (9A), 2899-910.

389. Chen, M.; Ren, L.; Meng, Y.; Shi, L.; Chen, L.; Yu, B.; Wu, Q.; Qi, G., The protease inhibitor E64d improves ox-LDL-induced endothelial dysfunction in human aortic endothelial cells. *Can J Physiol Pharmacol* **2018,** *96* (2), 120-127.

390. Yu, L.; Yin, M.; Yang, X.; Lu, M.; Tang, F.; Wang, H., Calpain inhibitor I attenuates atherosclerosis and inflammation in atherosclerotic rats through eNOS/NO/NF-kappaB pathway. *Can J Physiol Pharmacol* **2018,** *96* (1), 60-67.

391. Pugazhenthi, S.; Wang, M.; Pham, S.; Sze, C. I.; Eckman, C. B., Downregulation of CREB expression in Alzheimer's brain and in Abeta-treated rat hippocampal neurons. *Mol Neurodegener* **2011,** *6*, 60.

392. Yamamoto-Sasaki, M.; Ozawa, H.; Saito, T.; Rosler, M.; Riederer, P., Impaired phosphorylation of cyclic AMP response element binding protein in the hippocampus of dementia of the Alzheimer type. *Brain Res* **1999,** *824* (2), 300-3.

393. Puzzo, D.; Vitolo, O.; Trinchese, F.; Jacob, J. P.; Palmeri, A.; Arancio, O., Amyloid-beta peptide inhibits activation of the nitric oxide/cGMP/cAMP-responsive element-binding protein pathway during hippocampal synaptic plasticity. *J Neurosci* **2005,** *25* (29), 6887-97.

394. Love, S.; Miners, J. S., Cerebrovascular disease in ageing and Alzheimer's disease. *Acta Neuropathol* **2016,** *131* (5), 645-58.

395. Tosto, G.; Bird, T. D.; Bennett, D. A.; Boeve, B. F.; Brickman, A. M.; Cruchaga, C.; Faber, K.; Foroud, T. M.; Farlow, M.; Goate, A. M.; Graff-Radford, N. R.; Lantigua, R.; Manly, J.; Ottman, R.; Rosenberg, R.; Schaid, D. J.; Schupf, N.; Stern, Y.; Sweet, R. A.; Mayeux, R.; National Institute on Aging Late-Onset Alzheimer Disease/National Cell Repository for Alzheimer Disease Family Study, G., The Role of Cardiovascular Risk Factors and Stroke in Familial Alzheimer Disease. *JAMA Neurol* **2016,** *73* (10), 1231-1237.

396. Nelson, A. R.; Sweeney, M. D.; Sagare, A. P.; Zlokovic, B. V., Neurovascular dysfunction and neurodegeneration in dementia and Alzheimer's disease. *Biochim Biophys Acta* **2016,** *1862* (5), 887-900.

397. Maiuolo, J.; Gliozzi, M.; Musolino, V.; Scicchitano, M.; Carresi, C.; Scarano, F.; Bosco, F.; Nucera, S.; Ruga, S.; Zito, M. C.; Mollace, R.; Palma, E.; Fini, M.; Muscoli, C.; Mollace, V., The "Frail" Brain Blood Barrier in Neurodegenerative Diseases: Role of Early Disruption of Endothelial Cell-to-Cell Connections. *Int J Mol Sci* **2018,** *19* (9).

398. Youmans, K. L.; Tai, L. M.; Nwabuisi-Heath, E.; Jungbauer, L.; Kanekiyo, T.; Gan, M.; Kim, J.; Eimer, W. A.; Estus, S.; Rebeck, G. W.; Weeber, E. J.; Bu, G.; Yu, C.; Ladu, M. J., APOE4-specific changes in Abeta accumulation in a new transgenic mouse model of Alzheimer disease. *J Biol Chem* **2012,** *287* (50), 41774-86.

399. Yamazaki, Y.; Shinohara, M.; Shinohara, M.; Yamazaki, A.; Murray, M. E.; Liesinger, A. M.; Heckman, M. G.; Lesser, E. R.; Parisi, J. E.; Petersen, R. C.; Dickson, D. W.; Kanekiyo, T.; Bu, G., Selective loss of cortical endothelial tight junction proteins during Alzheimer's disease progression. *Brain* **2019,** *142* (4), 1077-1092.

400. Stamatovic, S. M.; Johnson, A. M.; Keep, R. F.; Andjelkovic, A. V., Junctional proteins of the blood-brain barrier: New insights into function and dysfunction. *Tissue Barriers* **2016,** *4* (1), e1154641.

401. Solito, R.; Corti, F.; Chen, C. H.; Mochly-Rosen, D.; Giachetti, A.; Ziche, M.; Donnini, S., Mitochondrial aldehyde dehydrogenase-2 activation prevents beta-amyloid-induced endothelial cell dysfunction and restores angiogenesis. *J Cell Sci* **2013,** *126* (Pt 9), 1952-61.

402. Safieh, M.; Korczyn, A. D.; Michaelson, D. M., ApoE4: an emerging therapeutic target for Alzheimer's disease. *BMC Med* **2019,** *17* (1), 64.

403. Mahley, R. W.; Rall, S. C., Jr., Apolipoprotein E: far more than a lipid transport protein. *Annu Rev Genomics Hum Genet* **2000,** *1*, 507-37.

404. Lahoz, C.; Schaefer, E. J.; Cupples, L. A.; Wilson, P. W.; Levy, D.; Osgood, D.; Parpos, S.; Pedro-Botet, J.; Daly, J. A.; Ordovas, J. M., Apolipoprotein E genotype and cardiovascular disease in the Framingham Heart Study. *Atherosclerosis* **2001,** *154* (3), 529-37.

405. Liu, D. S.; Pan, X. D.; Zhang, J.; Shen, H.; Collins, N. C.; Cole, A. M.; Koster, K. P.; Ben Aissa, M.; Dai, X. M.; Zhou, M.; Tai, L. M.; Zhu, Y. G.; LaDu, M.; Chen, X. C., APOE4 enhances age-dependent decline in cognitive function by down-regulating an NMDA receptor pathway in EFAD-Tg mice. *Mol Neurodegener* **2015,** *10*, 7.

406. Tai, L. M.; Mehra, S.; Shete, V.; Estus, S.; Rebeck, G. W.; Bu, G.; LaDu, M. J., Soluble apoE/Abeta complex: mechanism and therapeutic target for APOE4-induced AD risk. *Mol Neurodegener* **2014,** *9*, 2.

407. Thomas, R.; Morris, A. W. J.; Tai, L. M., Epidermal growth factor prevents APOE4-induced cognitive and cerebrovascular deficits in female mice. *Heliyon* **2017,** *3* (6), e00319.

408. Kaya, M.; Ahishali, B., Assessment of permeability in barrier type of endothelium in brain using tracers: Evans blue, sodium fluorescein, and horseradish peroxidase. *Methods Mol Biol* **2011,** *763*, 369-82.

409. Wang, F.; Cao, Y.; Ma, L.; Pei, H.; Rausch, W. D.; Li, H., Dysfunction of Cerebrovascular Endothelial Cells: Prelude to Vascular Dementia. *Front Aging Neurosci* **2018,** *10*, 376.

410. Wang, L.; Chen, Y.; Li, X.; Zhang, Y.; Gulbins, E.; Zhang, Y., Enhancement of endothelial permeability by free fatty acid through lysosomal cathepsin B-mediated Nlrp3 inflammasome activation. *Oncotarget* **2016,** *7* (45), 73229-73241.

411. Villalba, N.; Sonkusare, S. K.; Longden, T. A.; Tran, T. L.; Sackheim, A. M.; Nelson, M. T.; Wellman, G. C.; Freeman, K., Traumatic brain injury disrupts cerebrovascular tone through endothelial inducible nitric oxide synthase expression and nitric oxide gain of function. *J Am Heart Assoc* **2014,** *3* (6), e001474.

412. Aguilar Diaz De Leon, J.; Borges, C. R., Evaluation of Oxidative Stress in Biological Samples Using the Thiobarbituric Acid Reactive Substances Assay. *J Vis Exp* **2020,** (159).

413. de Castro, M. A.; Bunt, G.; Wouters, F. S., Cathepsin B launches an apoptotic exit effort upon cell death-associated disruption of lysosomes. *Cell Death Discov* **2016,** *2*, 16012.

414. Singh, G. P.; Nigam, R.; Tomar, G. S.; Monisha, M.; Bhoi, S. K.; S, A.; Sengar, K.; Akula, D.; Panta, P.; Anindya, R., Early and rapid detection of UCHL1 in the serum of brain-trauma patients: a novel gold nanoparticle-based method for diagnosing the severity of brain injury. *Analyst* **2018,** *143* (14), 3366-3373.

415. Walker, G.; Pfeilschifter, J.; Otten, U.; Kunz, D., Proteolytic cleavage of inducible nitric oxide synthase (iNOS) by calpain I. *Biochim Biophys Acta* **2001,** *1568* (3), 216-24.

APPENDICES

The work presented below is select data that supports the results but is either superfluous or did not fit with the story above. Some of this work is preliminary and requires further replicates to confirm. Appendix I contains the statement of authors rights from Elsevier publishing group. Appendix J contains animal approval forms.

APPENDIX A: Neuroprotective Profiles of All Inhibitors

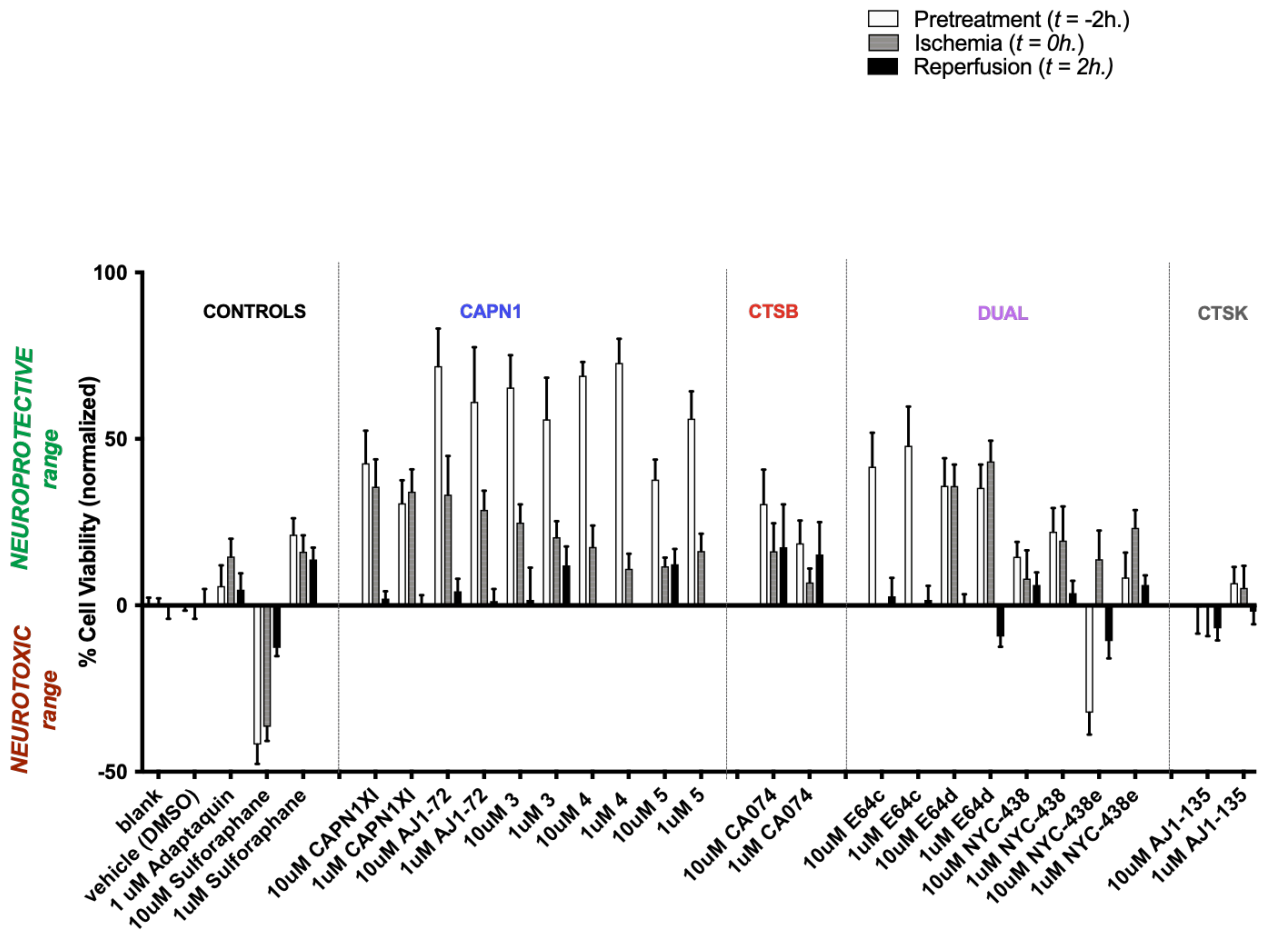

Figure 65. Neuroprotective profiles of all inhibitors
For the sake of simplicity, only some of this data was presented in the main thesis text. Data represent at least one replicate, Mean ± SEM

APPENDIX B: Optimization of TBARS Assay to Monitor LPPs *In Vitro* and *In Vivo*

The TBARS (Thiobarbituric Acid Reactive Substances) assay is a method to detect LPPs in a sample (cell or tissue homogenate).[412] We optimized the assay to be run in house. However, it was not used for any studies in this thesis.

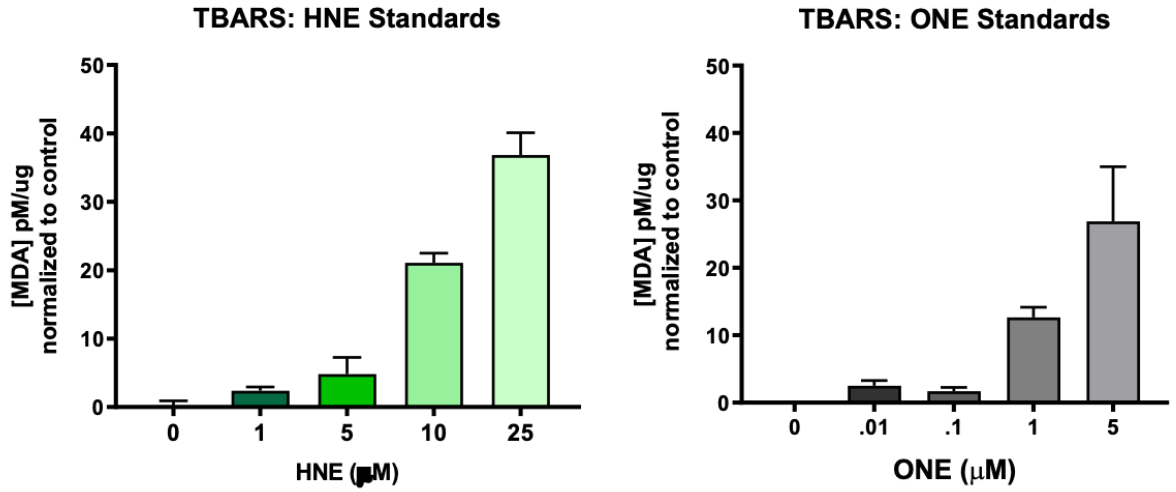

Figure 66. Optimization of the TBARS assay.
SHSY-5Y cells were treated with 0-25μM HNE or ONE for 24 hours, and quantified for LPPs using an MDA standard curve.

Methodology: TBAR solution (0.375% w/v thiobarbituric acid, 15% v/v trichloroacetic acid, and 25% v/v 1M HCl) was added to cell lysates (2:1) then heated for 15 minutes at 96-100 degrees Celsius. Samples were subsequently equilibrated to room temperature, and centrifuged at 9,000g for 10 minutes. Absorbance measurements at 530nm were measured using the SynergyH4 Hybrid Microplate reader, and standardized using an MDA standard curve (0-50uM MDA).

APPENDIX C: Validation of LPP-mediated BEC-degeneration

LDH release confirmed that HNE and ONE induce concentration-dependent cell death of BECs. This data was superfluous and not needed in the main body of this dissertation.

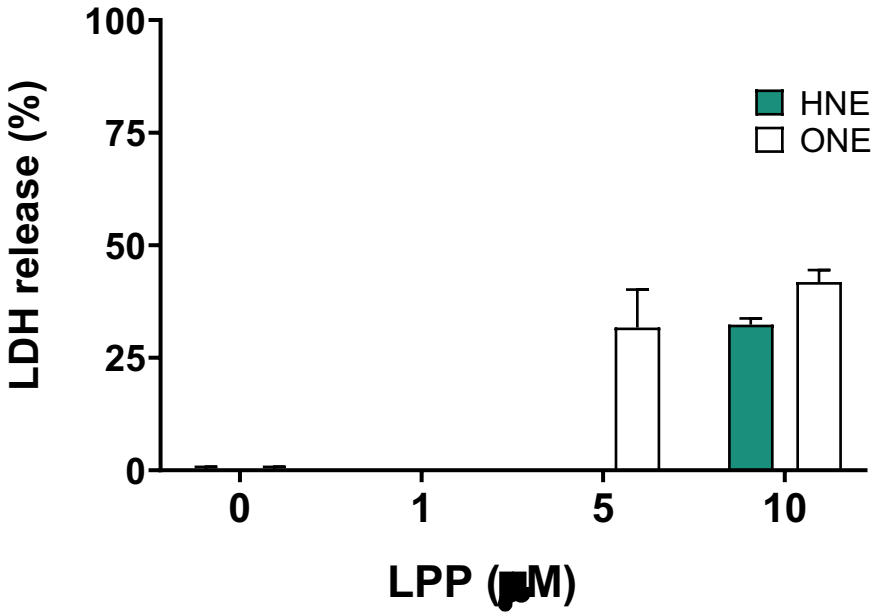

Figure 67. HNE and ONE induce concentration-dependent increase in LDH release in BECs.
Cell death quantified by LDH release of BECs following 24 hour treatment of the lipid peroxidation products HNE or ONE at various concentrations. Data represents mean ± SEM of at least n=3 in 3 separate isolations

APPENDIX D: Characterization of BID (BH3 interacting-domain death agonist) levels on BECs following OGD-R

ALDH2$^{-/-}$ BECs were more susceptible to an increase in BID (a pro-apoptotic protein) following OGD-R. Reports indicate cathepsin B inhibitors mitigate increases in BID.[413] ***CA-074*** mitigated the levels which demonstrated specific inhibitory efficacy and that cathepsin B is contributing to the exacerbated BID levels.

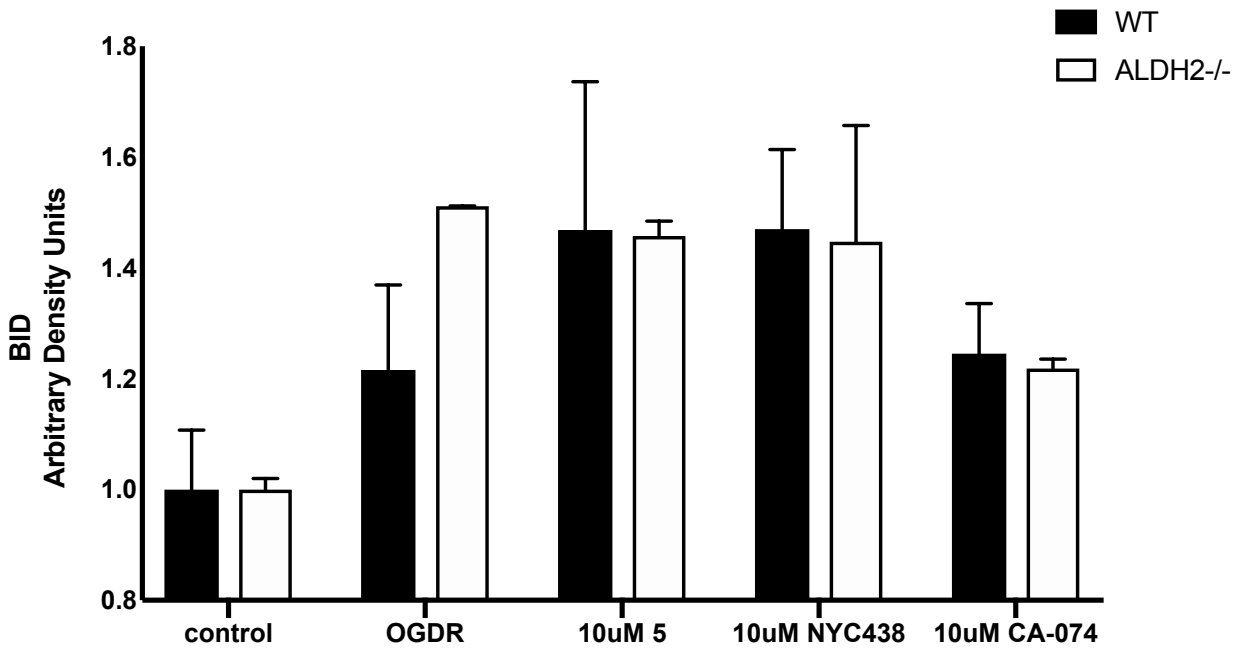

Figure 68. Examining BID (BH3 interacting-domain death agonist) on BECs following OGD-R

Quantification of western blots of BECs co-treated with 10μM inhibitors and 1 hour OGD-R, probed with BID Ab. All protein was normalized to the housekeeping protein, actin. Equal protein amounts were loaded in all lanes of immunoblots. Data represent at least n=5, Mean ± SEM

APPENDIX E: Characterization of UCHL1 and ALDH2 levels following one or two mTBIs

UCHL1 (Ubiquitin C-Terminal Hydrolase) is a deubiquitinating enzyme, and found elevated following TBI.[414] Levels of UCHL1 were elevated in the ipsilateral hemispheres of WT and *ALDH2*$^{-/-}$ mice 24 hours after the administration of two back-to-back mTBIs. These levels were restored to baseline after 1 week and sustained up to a month.

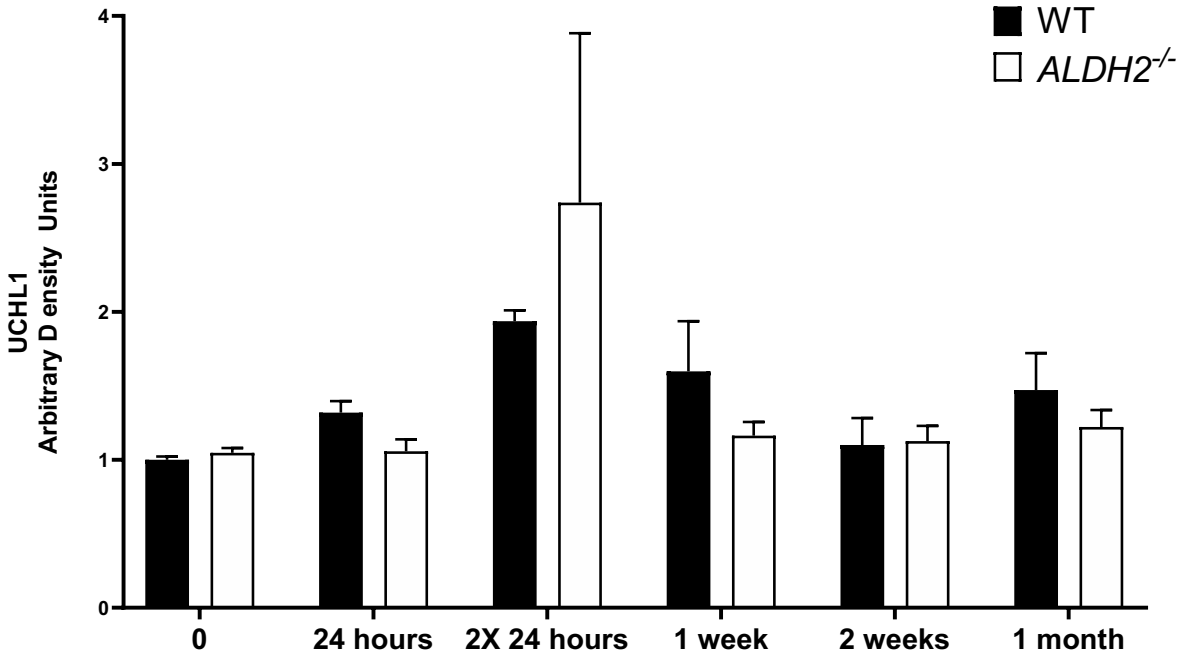

Figure 69. Changes in UCHL1 following 1 or 2 mTBIs
Quantitative analysis of ipsilateral hemispheres of WT and *ALDH2*$^{-/-}$ mice hit with one or two mTBIs back-to-back (2X), and sacrificed either 24 hours, 1 week, 2 weeks or 1 month post-neurotrauma. Data represent at least n=3, Mean ± SEM

Levels of Aldh2 were elevated following 24 hours post-mTBI, and significantly reduced post 1-week, then restored to baseline levels following one month. Intriguingly after two mTBIs (back-to-back), Aldh2 levels were elevated over 2-fold, then reduced back to baseline following one month.

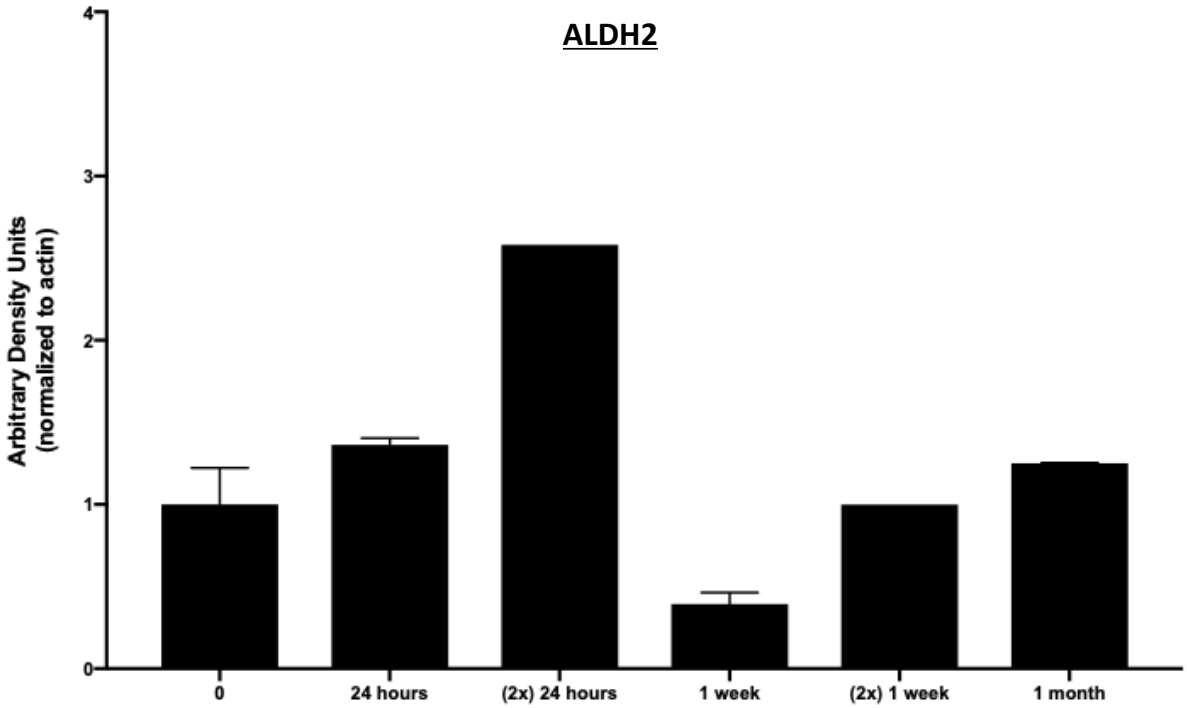

Figure 70. Levels of Aldh2 following one or two mTBIs
Quantitative analysis of ipsilateral hemispheres of WT mice with one or two (2x) mTBIs probed with Aldh2 Ab. Mice were sacrified and analyzed at 0, 24 hours, 1 week, and 1 month post-trauma. Data represent at least one replicate, Mean ± SEM

Following the significant protein changes observed with one or two mTBIs 24 hours post-trauma, mRNA levels of ALDH2 were analyzed. A single mTBI did not elicit significant increase in ALDH2. However, two mTBIs administered back-to-back induced significant elevation in levels. This further validates that the mTBI model is subtle, and that multiple hits exacerbate the neuro-response.

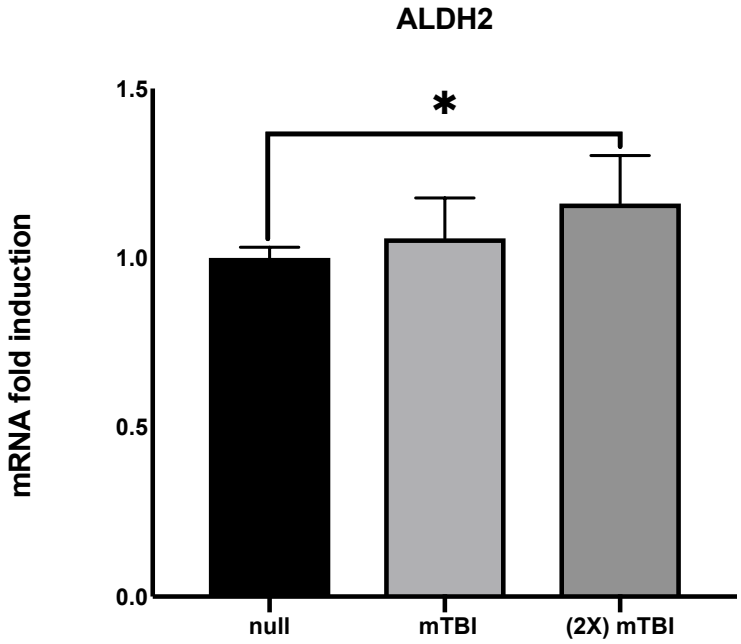

Figure 71. Gene expression of ALDH2 24 hours following one or two mTBIs
Quantitative mRNA analysis of WT mice following one or two mTBIs and sacrificed 24 hours post-trauma. Data represent at least n=5, Mean ± SEM

APPENDIX F: Calpain-1 Inhibitors minimally attenuate iNOS (inducible NOS) mRNA levels in *ALDH2*$^{-/-}$ following mTBI.

iNOS (inducible NOS) is a known substrate of calpain.[415] We theorized levels would be significantly restores following treatment. However, both selective and nonselective inhibitors only minimally attenuated iNOS levels following mTBI in *ALDH2*$^{-/-}$ mice.

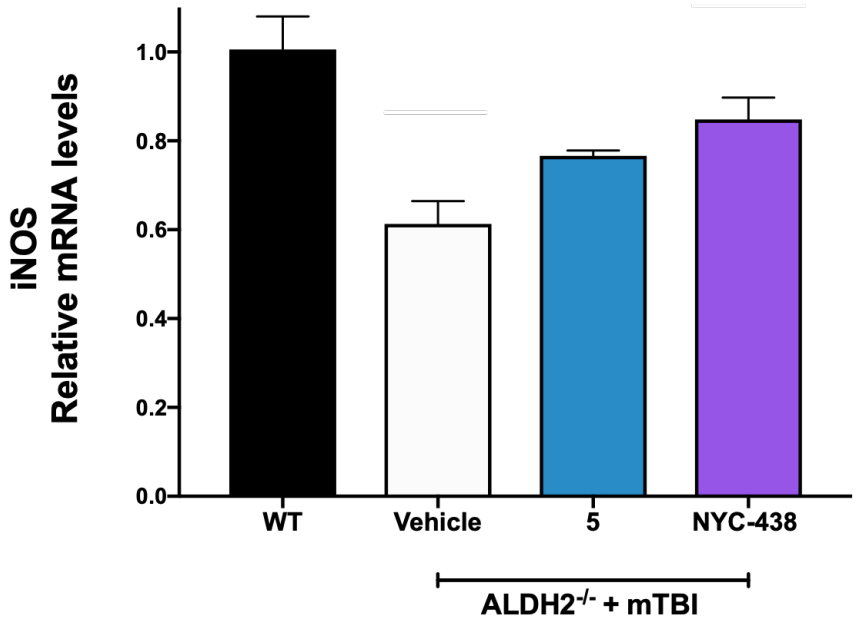

Figure 72. *5* and *NYC-438* minimally attenuate mRNA expression of iNOS in *ALDH2*$^{-/-}$ mice following mTBI.
Quantitative mRNA analysis of iNOS levels in ipsilateral hemispheres of WT and *ALDH2*$^{-/-}$ mice with or without mTBI, treated with 10mg/kg ***5*** or ***NYC-438*** and sacrificed 24 hours post-trauma. Data represent at least n=5, Mean ± SEM

APPENDIX G: Inhibitors do not cause HepG2 spheroidal death.

HepG2 liver cells were grown in 3D cell culture and utilized in this study to identify off-target effects and toxicity. No significant antiproliferative activity was observed.

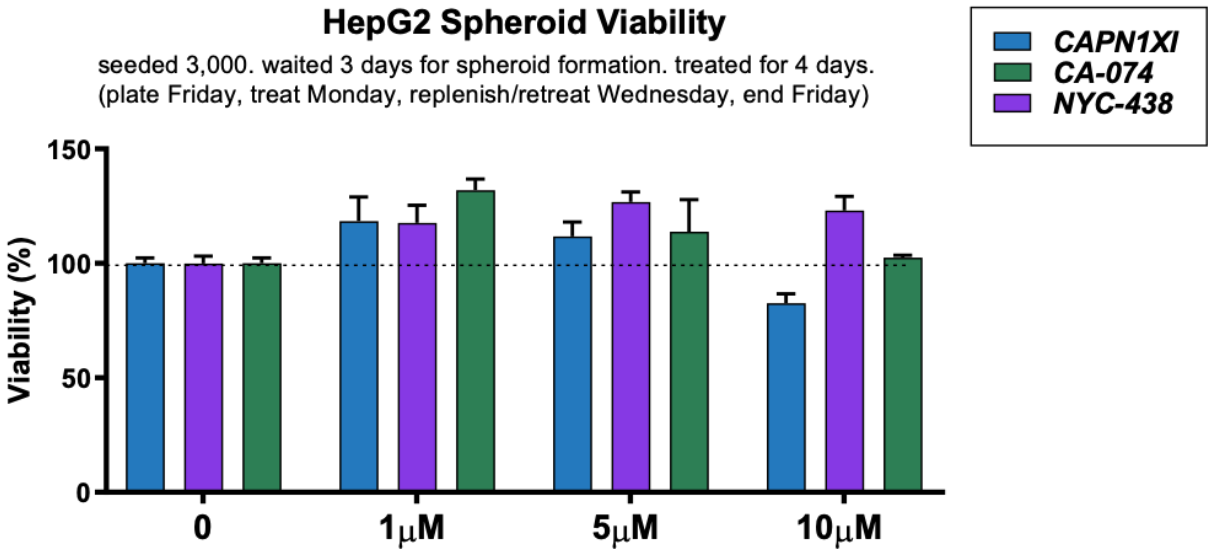

Figure 73. CCH inhibitors do not induce HepG2 spheroidal death
Cell viability of HepG2 spheroids following 4 days of treatment. Data represent at least n=5, Mean ± SEM

APPENDIX H: LAMP2 Levels Restored with Cathepsin B Inhibitors

LAMP2 (lysosomal-associated membrane glycoprotein 2) is a protein on the lysosomal membrane, and used as a marker for non-permeabilized lysosomes. Following ionomycin treatment in HT22 cells, LAMP2 levels were slightly decreased. Treatment with cathepsin B inhibitors, not selective calpain-1 inhibitors, significantly and profoundly increased levels over baseline.

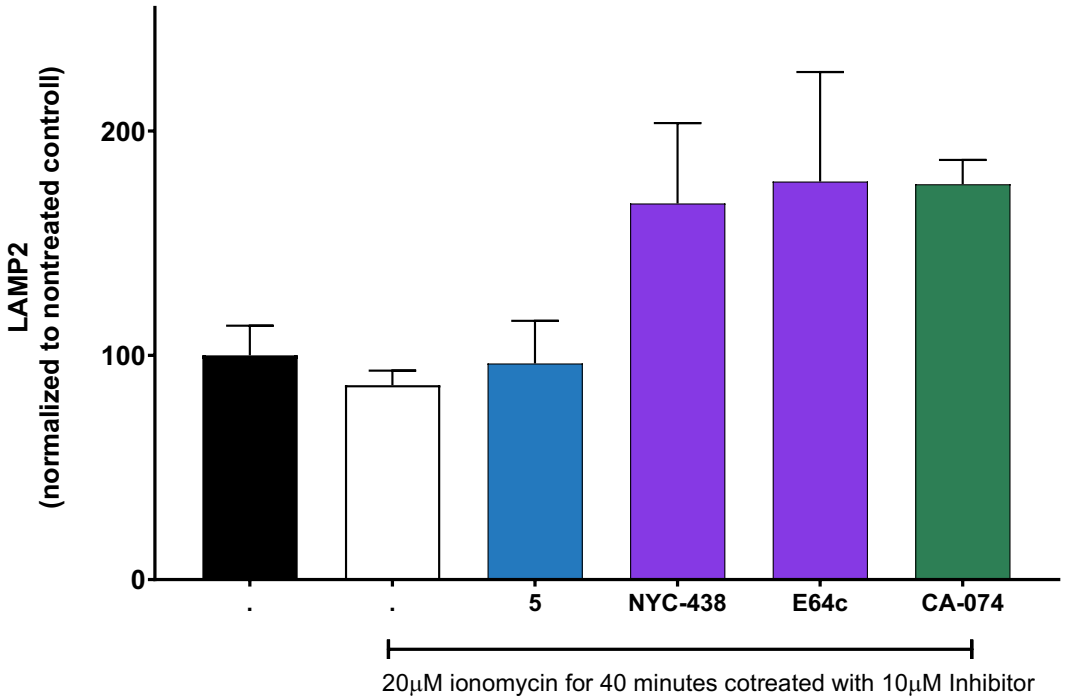

Figure 74. Cathepsin B inhibitors attenuate LAMP2 levels
Quantification of western blots of HT22 cells co-treated with 10μM inhibitors and 20μM ionomycin for 40 minutes and probed with LAMP2 Ab. All protein was normalized to the housekeeping protein, actin. Equal protein amounts were loaded in all lanes of immunoblots. Data represent at least n=5, Mean ± SEM

APPENDIX I: Elsevier Statement of Author Rights

ELSEVIER (https://www.elsevier.com) (https://global-checkout.elsevier.com)

Home (https://w... › About (https:/... › Policies (https... › Copyright (htt...

Copyright

Describes the rights related to the publication and distribution of research. It governs how authors (as well as their employers or funders), publishers and the wider general public can use, publish and distribute articles or books.

Journal author rights | Government employees | Elsevier's rights | Protecting aut

Journal author rights

In order for Elsevier to publish and disseminate research articles, we need publishing rights. This is determined by a publishing agreement between the author and Elsevier. This agreement deals with the transfer or license of the copyright to Elsevier and authors retain significant rights to use and share their own published articles. Elsevier supports the need for authors to share, disseminate and maximize the impact of their research and these rights, in Elsevier proprietary journals* are defined below:

For subscription articles	For open access articles
Authors transfer copyright to the publisher as part of a journal publishing agreement, but have the right to: • Share their article for Personal Use (https://www.elsevier.com/about/policies/copyright#personaluse), Internal Institutional Use (https://www.elsevier.com/about/policies/copyright#internaluse) and Scholarly Sharing (https://www.elsevier.com/about/policies/sharing) purposes, with a DOI link to the version of record on ScienceDirect (and with the Creative Commons CC-BY-NC- ND license for author manuscript versions) • Retain patent, trademark and other intellectual property rights (including research data),	Authors sign an exclusive license agreement, where authors have copyright but license exclusive rights in their article to the publisher**. In this case authors have the right to: • Share their article in the same ways permitted to third parties under the relevant user license (together with Personal Use (https://www.elsevier.com/about/policies/copyright#personaluse) rights) so long as it contains a CrossMark logo (https://www.elsevier.com/about/policies/crossmark), the end user license (https://www.elsevier.com/about/policies/open-access-licenses), and a DOI link to the version of record on ScienceDirect. • Retain patent, trademark and other

• Proper attribution and credit for the published work.	intellectual property rights (including research data). • Proper attribution and credit for the published work.

***Please note that society or third party owned journals may have different publishing agreements. Please see the journal's guide for authors for journal specific copyright information.**

****This includes the right for the publisher to make and authorize commercial use (https://www.elsevier.com/about/policies/copyright#CU), please see "Rights granted to Elsevier (https://www.elsevier.com/about/policies/copyright#Elsevier%20rights)" for more details.**

Help and Support

- Download a sample publishing agreement for subscription articles in ↓ English and ↓ French.
- Download a sample publishing agreement for open access articles for authors choosing a ↓ commercial user license and ↓ non-commercial user license.
- For authors who wish to self-archive see our sharing guidelines (https://www.elsevier.com/about/policies/sharing)
- See our author pages (https://www.elsevier.com/authors) for further details about how to promote your article.
- For use of Elsevier material not defined below please see our permissions page (https://www.elsevier.com/about/policies/copyright/permissions) or visit the Permissions Support Center (https://service.elsevier.com/app/contact/supporthub/permissions-helpdesk/) .

Government employees

Elsevier has specific publishing agreements with certain government and inter-governmental organizations for their employee authors. These agreements enable authors to retain substantially the same rights as detailed in the "Author Rights section (https://www.elsevier.com/about/policies/copyright#author%20rights)" but are specifically tailored for employees from the relevant organizations, including:

- World Bank
- World Health Organization
- For US government employees, works created within the scope of their employment are considered to be public domain and Elsevier's publishing

agreements do not require a transfer or license of rights for such works.

- In the UK and certain commonwealth countries, a work created by a government employee is copyrightable but the government may own the copyright (Crown copyright). Click here (https://www.elsevier.com/about/open-science/open-access/agreements/uk-national-archives) for information about UK government employees publishing open access

Rights granted to Elsevier

For both subscription and open access articles, published in proprietary titles, Elsevier is granted the following rights:

- The exclusive right to publish and distribute an article, and to grant rights to others, including for commercial purposes.
- For open access articles, Elsevier will apply the relevant third party user license (https://www.elsevier.com/about/policies/open-access-licenses) where Elsevier publishes the article on its online platforms.
- The right to provide the article in all forms and media so the article can be used on the latest technology even after publication.
- The authority to enforce the rights in the article, on behalf of an author, against third parties, for example in the case of plagiarism or copyright infringement.

Protecting author rights

Copyright aims to protect the specific way the article has been written to describe an experiment and the results. Elsevier is committed to its authors to protect and defend their work and their reputation and takes allegations of infringement, plagiarism, ethic disputes and fraud very seriously.

If an author becomes aware of a possible plagiarism, fraud or infringement we recommend contacting their Elsevier publishing contact who can then liaise with our in-house legal department. Note that certain open access user licenses may permit quite broad re-use (https://www.elsevier.com/about/policies/open-access-licenses) that might otherwise be counted as copyright infringement. For details about how to seek permission to use an article see our permission page (https://www.elsevier.com/about/policies/copyright/permissions).

Open access

How copyright works with open access licenses

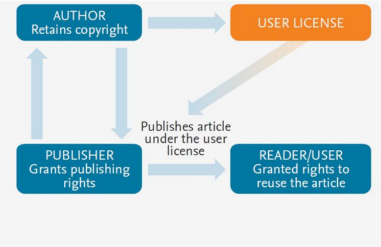

For Elsevier proprietary journals the following steps apply:

1. Authors sign a publishing agreement where they will have copyright but grant broad publishing and distribution rights to the publisher, including the right to publish the article on Elsevier's online platforms.
2. The author chooses an end user license (https://www.elsevier.com/about/policies/open-access-licenses) under which readers can use and share the article.
3. The publisher makes the article available online with the author's choice of end user license.

Quick definitions

Personal use

Authors can use their articles, in full or in part, for a wide range of scholarly, non-commercial purposes as outlined below:

- Use by an author in the author's classroom teaching (including distribution of copies, paper or electronic)
- Distribution of copies (including through e-mail) to known research colleagues for their personal use (but not for Commercial Use)
- Inclusion in a thesis or dissertation (provided that this is not to be published commercially)
- Use in a subsequent compilation of the author's works
- Extending the Article to book-length form
- Preparation of other derivative works (but not for Commercial Use)
- Otherwise using or re-using portions or excerpts in other works

These rights apply for all Elsevier authors who publish their article as either a subscription article or an open access article. In all cases we require that all Elsevier authors always include a full acknowledgement and, if appropriate, a link to the final published version hosted on Science Direct.

Commercial use

This is defined as the use or posting of articles:

- **For commercial gain without a formal agreement with the publisher.**
  - For example by associating advertising with the full-text of the article, by providing hosting services to other repositories or to other organizations (including where an otherwise non-commercial site or repository provides a service to other organizations or agencies), or charging fees for document delivery or access
- **To substitute for the services provided directly by the journal.**
  - For example article aggregation, systematic distribution of articles via e-mail lists or share buttons, posting, indexing, or linking for promotional/marketing activities, by commercial companies for use by customers and intended target audiences of such companies (e.g. pharmaceutical companies and healthcare professionals/physician-prescribers).

If you would like information on how to obtain permission for such uses click here (https://www.elsevier.com/about/policies/copyright/permissions) or if you would like to make commercial use of the article please visit the Permissions Support Center (https://service.elsevier.com/app/contact/supporthub/permissions-helpdesk/) .

Internal institutional use

- Use by the author's institution for classroom teaching at the institution and for internal training purposes (including distribution of copies, paper or electronic, and use in coursepacks and courseware programs, but not in Massive Open Online Courses)
- Inclusion of the Article in applications for grant funding
- For authors employed by companies, the use by that company for internal training purposes

APPENDIX J. Animal Protocol Approval Forms.

UIC UNIVERSITY OF ILLINOIS AT CHICAGO

Office of Animal Care and
Institutional Biosafety Committees (MC 672)
Office of the Vice Chancellor for Research
206 Administrative Office Building
1737 West Polk Street
Chicago, Illinois 60612-7227

June 4, 2018

Gregory Thatcher
Medicinal Chemistry & Pharmacognosy
M/C 781

Dear Dr. Thatcher:

The protocol indicated below was reviewed at a convened ACC meeting in accordance with the Animal Care Policies of the University of Illinois at Chicago on **4/17/2018**. *The protocol was not initiated until final clarifications were reviewed and approved on* **6/4/2018**. *The protocol is approved for a period of 3* years with annual continuation.

Title of Application: Testing NO-methylthiazole compounds in prevention and treatment of mild traumatic brain injury murine model

ACC Number: 18-034

Initial Approval Period: 6/4/2018 to 4/17/2019

Current Funding: ***Portions of this protocol are supported by the funding sources indicated in the table below.***
Number of funding sources: 1

Funding Agency	**Funding Title**			**Portion of Proposal Matched**
NIH via subcontract from	*Nomethiazoles harnessing GABA and NO mimetic activity for Alzheimer's therapy ((Institutional #00332735)*			*Other* *Linked to 17-029*
Funding Number	**Current Status**	**UIC PAF NO.**	**Performance Site**	**Funding PI**
R42 AG044024	*Funded*	*201503328*	*UIC* *Subcontract from Revivo Therapeutics*	*Yueting Wang (for UIC subcontract)*

This institution has Animal Welfare Assurance Number A3460.01 on file with the Office of Laboratory Animal Welfare (OLAW), NIH. **This letter may only be provided as proof of IACUC approval for those specific funding sources listed above in which all portions of the funding proposal are matched to this ACC protocol.**

In addition, all investigators are responsible for ensuring compliance with all federal and institutional policies and regulations related to use of animals under this protocol and the funding sources listed on this protocol. Please use OLAW's "*What Investigators Need to Know about the*

Use of Animals" (http://grants.nih.gov/grants/olaw/InvestigatorsNeed2Know.pdf) as a reference guide. Thank you for complying with the Animal Care Policies and Procedures of UIC.

Sincerely yours,

Timothy J. Koh, PhD
Chair, Animal Care Committee
TJK /*mbb*
cc: BRL, ACC File, Oleksii Dubrovskyi

UIC UNIVERSITY OF ILLINOIS AT CHICAGO

Office of Animal Care and Institutional
Biosafety Committee (OACIB) (M/C 672)
Office of the Vice Chancellor for Research
206 Administrative Office Building
1737 West Polk Street
Chicago, Illinois 60612

4/17/2020

Gregory Thatcher
Medicinal Chemistry & Pharmacognosy
M/C 781

Dear Dr. Thatcher:

The protocol indicated below was reviewed in accordance with the Animal Care Policies and Procedures of the University of Illinois at Chicago and **renewed on 4/17/2020.**

Title of Application: Testing NO-methylthiazole Compounds in Prevention and Treatment of Mild Traumatic Brain Injury Murine Model
ACC NO: 18-034
Original Protocol Approval: 6/4/2018 **(3 year approval with annual continuation required).**
Current Approval Period: 4/17/2020 **to** 4/17/2021

Funding: ***Portions of this protocol are supported by the funding sources indicated in the table below.***
Number of funding sources: 1

Funding Agency	**Funding Title**			**Portion of Funding Matched**
NIH via subcontract from	*Nomethiazoles harnessing GABA and NO mimetic activity for Alzheimer's therapy (Institutional #00332735)*			*Other: Linked to 17-029*
Funding Number	**Current Status**	**UIC PAF NO.**	**Performance Site**	**Funding PI**
R42 AG044024	*Funded*	*2015-03328*	*UIC Subcontract from Revivo Therapeutics*	*Yueting Wang (for UIC subcontract)*

This institution has Animal Welfare Assurance Number A3460.01 on file with the Office of Laboratory Animal Welfare, NIH. **This letter may only be provided as proof of IACUC approval for those specific funding sources listed above in which all portions of the grant are matched to this ACC protocol.**

Thank you for complying with the Animal Care Policies and Procedures of the UIC.

Sincerely,

Amy Lasek

Amy Lasek, PhD
Chair, Animal Care Committee
AL/*kg*
cc: BRL, ACC File, Oleksii Dubrovskyi

VITA

RACHEL KNOPP

(206) 948 – 5002 • rachel.knopp@comcast.net

EDUCATION

Doctor of Philosophy in Medicinal Chemistry & Pharmacognosy Anticipated July 2020
University of Illinois at Chicago, School of Pharmacy

Bachelor of Arts in Chemistry (Biochemistry Emphasis)
Spring 2014
Willamette University, Salem, OR

RESEARCH INTERESTS

Cysteine proteases, brain endothelial cells, drug discovery, neurodegeneration

EXPERIENCE

Graduate Research Fellow, University of Illinois at Chicago (UIC) Chicago, IL
2015-current

- My graduate studies encompass two main projects: (1) characterization of cysteine proteases as therapeutic targets for neurodegeneration with an emphasis in the BBB; and (2) development of a tractable model of mild traumatic brain injury with underlying oxidative-stress
- Advisor: Professor Gregory R.J. Thatcher, Ph.D.

Summer Intern, Eli Lilly and Company Indianapolis, IN
Neurodegeneration Clinical Team June 2019

- Short summer internship in the early clinical development neurodegeneration clinical team
- Participated in meetings investigating early clinical development and safety of Alzheimer's disease therapies, resulting in a presentation of a literature-based research project
- Preceptor: Jennifer Zimmer M.D.

Undergraduate Research Project, Willamette University Salem, OR
2013-2014

- My undergraduate studies focused on synthesis of a redox-and pH-sensitive fluorescent probe for a novel ruthenium-centered antineoplastic drug, NAMI-A.
- Advisor: Professor James Hoobler, Ph.D.

FELLOWSHIPS, HONORS & AWARDS

Best Oral Presentation, Chicago Neurovascular Meeting	2020
Predoctoral Fellow, ADRD Training Program (T32AG057468 PI: Orly Lazarov)	2018 - 2020
Alzheimer's Drug Discovery Foundation Young Investigator Scholarship	2019
Chancellor's Student Service and Leadership Award	2019
AbbVie Award for Excellence in Research, COPRD 2018	2018
W.E. van Doren Scholar	2017
Professor Ludwig Bauer Scholarship	2016
Paul M. Duel Memorial Scholarship	2013

PUBLICATIONS

1. **Knopp, R.**; Jastinah, A.; Dubrovskyi, O.; Gaisina, I.; Izar, I.; Tai, L.;Thatcher, G.R.J. Calpain Inhibition Attenuates BBB-Dysfunction in *ALDH2*$^{-/-}$ mice with mTBI. *In Preparation*
2. Jastinah, A.; Gaisina, I.; **Knopp, R.;** Thatcher, G.R.J. Synthesis of α-Ketoamide-based Stereoselective Calpain-1 Inhibitors as Neuroprotective Agents. *In Submission*

3. **Knopp, R.**.; Lee, S.H.; Hollas, M;, Neomuceno, E.; Gonzalez, D.; Tam, K.T.; Aamir, D.; Wang, Y,; Pierce, E.; BenAissa, M.; Thatcher, G.R.J. Interaction of oxidative stress and neurotrauma causes significant and persistent behavioral and pro-inflammatory effects in a tractable model of mild traumatic brain injury. *Redox Biology*, 2020, *32*, 101486
4. Taha, T. Y.; Aboukhatwa, S. M.; **Knopp, R.**.; Ikegaki, N.; Abdelkarim, H.; Neerasa, J.; Lu, Y.; Neelarapu, R.; Hanigan, T. W.; Thatcher, G. R. J. R.; et al. Design, Synthesis, and Biological Evaluation of Tetrahydroisoquinoline-Based Histone Deacetylase 8 Selective Inhibitors. *ACS Med Chem Lett,* **2017,** *8*, 824–829.
5. Kent, C.; Bryja, M.; Gustafson, J.; Kawarski, M.; Lenti, G; Pierce, E.; **Knopp, R**.; Ceja, V.; Pati, B.; Walters, E.; Karver, C. Variation of the aryl substituent on the piperazine ring within the 4-(piperazin-1-yl)-2.6-di(pyrrolindin-1-yl)pyramidine scaffold unveils potent, noncompetive inhibitors of the inflammatory caspases. *Bioorg Med Chem Lett* **2016**, *26* (26), 5476-80.

CONFERENCE PRESENTATIONS

ORAL PRESENTATIONS

Knopp, R., Jastaniah A, Dubrovskyi, O., Lee, Sue., Tai, L, Thatcher, G. (2020, June). *Nonselective Calpain Inhibition Attenuates Neuroinflammation in an Oxidative Stress-Based mTBI mouse Model.* Anatomy & Cell Biology Seminar Series, Chicago, IL

Knopp, R., Jastaniah A, Dubrovskyi, O., Lee, Sue., Tai, L, Thatcher, G. (2020, February). *Nonselective Calpain/Cathepsin Inhibition Attenuates Neuroinflammation in an Oxidative Stress-Based mTBI Model.* Chicago Neurovascular Meeting, Chicago, IL

Knopp, R., Jastaniah A, Dubrovskyi, O., Lee, Sue., Tai, L, Thatcher, G. (2019, October). *Evidence for Attenuation of BBB-dysfunction via Calpain-cathepsin Inhibition Strategies Relevant to TBI and AD.* Society for Neuroscience, Nanosymposium, Chicago, IL

Knopp, R., Jastaniah A, Dubrovskyi, O., Lee, Sue., Tai, L, Thatcher, G. (2019, April). *Evidence for Attenuation of BBB-dysfunction via Calpain-cathepsin Inhibition Strategies Relevant to TBI and AD.* G.H. Miller Research Day. Anatomy and Cell Biology Department. University of Illinois at Chicago. Chicago, IL

POSTER PRESENTATIONS

Knopp, R., Jastaniah A, Dubrovskyi, O., Lee, Sue., Tai, L, Thatcher, G. (2019, September). *Calpain-1 Inhibition in ADRD & TBI: Evidence for Attenuation of BBB-Dysfunction.* Alzheimer's Drug Discovery Foundation International Conference, Jersey City, NJ.

Knopp, R., Jastaniah A, Dubrovskyi, O., Lee, Sue., Tai, L, Thatcher, G. (2019, July). *Calpain-1 Inhibition in ADRD & TBI: Evidence for Attenuation of BBB-Dysfunction.* Alzheimer's Association International Conference, Los Angeles, CA.

Knopp, R., Jastaniah A, Dubrovskyi, O., Lee, Sue., Tai, L, Thatcher, G. (2019, April). *Cysteine Proteases in Neurodegeneration: Evaluating the Therapeutic Efficacy of Selective vs. Dual Calpain 1 and Cathepsin B Inhibitors*. Meeting-in-Miniature on Medicinal Chemistry, MIKI, Lawrence, KS.

Knopp, R., Jastaniah A, Dubrovskyi, O., Lee, Sue., Tai, L, Thatcher, G. (2019, March). *Cysteine Proteases in Neurodegeneration: Evaluating the Therapeutic Efficacy of Selective vs. Dual Calpain 1 and Cathepsin B Inhibitors*. The 14th International Conference on Alzheimer's & Parkinson's Diseases, Lisbon, Portugal.

Knopp, R., Ben Aissa, M., Lee, S., Jastaniah A, Izar, R., Thatcher, G. (2018, July). *Selective Calpain-1 Versus Calpain/Cathepsin-B Dual Inhibition As A Therapeutic Approach to Neurodegeneration*. Alzheimer's Association International Conference, Chicago, IL.

Knopp, R., Ben Aissa, M. Jastinah, A., Lee, S.,Izar, R., Thatcher, G. (2018, June). *Selective Calpain-1 Versus Calpain/Cathepsin-B Dual Inhibition As A Therapeutic Approach to Neurodegeneration*. International Conference on Molecular Neurodegeneration, Stockholm, Sweden.

Knopp, R., Ben Aissa, M. Jastinah, A., Lee, S.,Izar, R., Thatcher, G. (2018, February). *Selective Calpain-1 Versus Calpain/Cathepsin-B Dual Inhibition As A Therapeutic Approach to Neurodegeneration*. Brain Research Foundation's 2018 Neuroscience Day, Northwestern University, Chicago, IL.

Knopp, R., Ben Aissa, M. Jastinah, A., Izar, R., Thatcher, G. (2017, October). *Evaluating Calpain-1 and Cathepsin B as Therapeutic Targets for Neurodeneration*. Chicago Biomedical Consortium, Chicago, IL.

Knopp, R., Ben Aissa, M., Jastinah, A., Pierce, E., Thatcher, G. (2017, April). *Investigating the Role of Cysteine Protease Inhibition as a Therapeutic Target in Neurodegeneration.* Meeting-in-Miniature on Medicinal Chemistry, MIKI, Minneapolis, MN.

Knopp, R., Lee, S., Thatcher, G. (2017, February*). Inhibition of Lipid Peroxidation In Vitro as a Model for Neuroprotection in Alzheimer's Disease and Related Dementia*. College of Pharmacy Research Day, University of Illinois at Chicago, Chicago, IL.

UNIVERSITY SERVICE

President, Graduate Student Council	2018-2019
Co-Chair Graduate Student Council	2017-2018
MIKI 2018 Organizing Committee	2017-2018
Your Future in Science Seminar Series, Committee Member	2017-2020
Webster-Sibilsky Lectureship Chair	2016-2017
Willamette Emergency Medical Service	2011-2014

TEACHING & ADVISING

Teaching Assistantships, University of Illinois at Chicago, Chicago, IL.

PHAR 408: Principles of Drug Action and Therapeutics VIII	2018-2019
PHAR 423: Biomedicinal Chemistry	2017
PHAR 422: Fundamentals of Drug Action	2016
PHAR 353: Fundamentals of Drug Action II	2016
PHAR 353: Experimental III – IPPE	2015

Organic Chemistry Class Tutor – Willamette University, Salem, OR. 2013-2014

COMMUNITY ENGAGEMENTS

Ronald McDonald House near Lurie Children's, Ongoing Monthly Volunteer	2016-current
Judge at Chicago Public Schools Science Fair	2017, 2018